Cruise Report

Cruise No. NBP 25-01

Tominaga/Panter

11 February 2025 – 16 April 2025

Christchurch (New Zealand) – Christchurch (New Zealand)

Chief Scientist: Masako Tominaga

Project Principal Investigators: Masako Tominaga, Kurt Panter

Cruise Report Coordinator & Chief Editor: Jonas Preine

Acknowledgments

We extend our sincere thanks to Captain John Souza and the entire crew of the RV Nathaniel B. Palmer for their enthusiastic and unwavering support throughout the cruise. Their professionalism and dedication were key in the success of this expedition. We are particularly grateful to the bridge officers team—Rob Potter, Luke Zeller, and Trevor Webb—for skillfully navigating the vessel through challenging ice conditions and adapting to the evolving demands of our science program.

A special thanks goes to the Marine Technicians—Ken Block, Andrew Micks, Chet Balding, Emma Hayward, and Hila Shooter—for their tireless long hours of work and reliability under often extreme conditions on deck.

We also thank Marine Project Coordinator Leila Harris, Marine Laboratory Technician Jamee Johnson, Electronics Technicians Thea Rae and Krystian Kopka, and Information Technicians Lilly Petersen and Isaac Treaster for their valuable support throughout the cruise.

Our appreciation goes to Chief Engineer Fabriel Ferrell, 1st Engineer Gilbert Taylor, 2nd Engineer Rowan Jurgens Manthei, and 3rd Engineer Jason Cheng for their behind-the-scenes efforts, which were vital to the smooth operation of the vessel.

We further thank the Able-Bodied Seamen Louie Andrada, Bienvenido Aaron, Ronnie Carpio, and Fernando Naraga, as well as the Oilers Ric Tamayo, Rodel Labatos, and “OG” Pagdanganan, for their hard work and dedication.

Last but certainly not least, we are deeply grateful to the galley team—Chad Cavalier, Gerry Simeon, Gernie Dela Cruz, and Akashia James—for providing excellent meals and all day-to-day services that kept morale high during our time at sea.

Table of Contents

Summary

The Tominaga-Panter Team of Expedition NBP25-01 (February 11 to April 16, 2025) set out to investigate the distribution of heat source and flux due to modern tectonic and magmatic evolution of the Terror Rift and adjacent areas in the western Ross Sea, Antarctica. The goal was to map volcanic and tectonic structures, sample volcanic and sedimentary rocks, and collect seafloor image, chemical and magnetic, and heat flow data to gain a better understanding of the geodynamics and glacio-volcanology of this region of West Antarctica.

Mobilization for the 65-day voyage began in Lyttelton, New Zealand, where the science team prepared the R/V Nathaniel B. Palmer. After completing safety training, equipment setup, and initial system checks, the vessel departed on February 11. As the ship made its way south out of New Zealand's EEZ, the team established a 24/7 watch schedule and initiated a range of underway geophysical and geological investigations, including high-resolution multibeam mapping, chirp sub-bottom profiling, and magnetic and gravity measurements.

Upon arrival in the study area on February 20, the team began an intensive program of fieldwork in the western Ross Sea, focusing on volcanic seamounts and the Terror Rift Basin. This included dredging, TowCam deployments, heat flow measurements, gravity coring, and Smith-Mac bottom grab sampling, carried out between the western Terror Rift in the west until Franklin Island in the east. Despite increasingly severe ice conditions and weather, the team remained agile, adapting the cruise's route and schedule as needed through close coordination and careful planning.

The science program in the western Ross Sea concluded on April 02, after which the vessel began a return journey back to port, continuing to collect geophysical data along the way until reaching New Zealand's EEZ. By the end of the cruise on April 16, the expedition had completed 50 successful dredge hauls, performed 17 TowCam dives, 29 Heat Flow Probe measurements, 8 Smith Mac casts, 22 XBT casts, and acquired 3,264 km^2 in the western Ross. The resulting dataset will significantly enhance our understanding of rift dynamics, magmatism, and tectonic processes that have affected ice evolution in this part of Antarctica.

1. Roster

1.1 Principal Investigators

Name	Institution
Masako Tominaga	Woods Hole Oceanographic Institution
Kurt Panther	Bowlin Green State University

1.2 Geological Sampling

Name	Institution
Carole Berthod	Paris Institute of Earth Physics
Jacquelyn Kalemba	Bowlin Green State University
Katherine Shanks	Bowlin Green State University
Daniel Wildrick	Oregon State University

1.3 Geophysics

Name	Institution
Jonas Preine	Woods Hole Oceanographic Institution

1.4 MISO Tow Cam

Name	Institution
Eric Hayden	Woods Hole Oceanographic Institution
Marissa Small	Woods Hole Oceanographic Institution
Mathilde Cannat	Institut de physique du globe de Paris

1.5 Heat Flow Probe

Name	Institution
Florian Neumann	MARUM – Center for Marine Environmental Sciences, University of Bremen
Jyun-Nai Wu	Woods Hole Oceanographic Institution

2. Cruise Objectives

Kurt Panter

Understanding the origins and nature of heat available at the base of the cryosphere is essential in deciphering the extent and residence timeseries of the ice in Antarctica and its oceans Constraints on parameters that control ice sheet stability, response of the crust to ice loading and unloading, and the effects of volcanism and heat from Earth's interior on overlying ice is of broad interest to the global climate change community. The goal of this study is to identify and to document the distribution of heat source and heat flux within the seafloor of the southwestern Ross Sea. Detailed interpretations on the seafloor glacial landforms in the western Ross Sea has enabled us to decipher ice-sea-lithosphere dynamics since the Last Glacial Maximum (LGM). These seafloor observations made it then possible to establish timeseries views of Antarctic ice sheet evolution over the Holocene into Plio-Pleistocene (e.g. Anderson et al., 2014; Naish et al., 2009; McKay et al., 2016; Halberstadt et al., 2016; Greenwood et al., 2018). Despite such advancement in reconstructing cryosphere timeseries in Antarctica and its oceans, however, there has been little investigation made in the Ross Sea to date on how lithospheric heat flux – heat generated by deep interior and tectono-magmatic activities within lithosphere, which overall accounts ~75% of Earth's heat loss by various seafloor processes – has contributed to the cryosphere dynamics over time.

The western Ross Sea lithosphere encompasses active volcanism and major magmatic centers within the Terror Rift (**Fig. 2.1**). The Terror Rift, which represents the youngest phase of extension within the West Antarctic Rift System, is one of the world's largest rifts and the only one covered by continental ice sheets. The thinned western Ross Sea lithosphere and Terror Rift encompasses active volcanism that range from 5 million years to present-day, suggesting that Pliocene-Quaternary fault movement and dynamic changes in ice sheet extent and thickness over this period are concurrent with magmatic activities (**Figs. 2.1B** and **2.2**). The local, short-term scale heat flux, such as volcanism and associated hydrothermal circulation in the crust, contributes to instantaneous melting of ice whereas a much longer-term scale heat flux, such as geothermal gradient radiating from magmatism, contributes to systematic background heat source within lithosphere that likely control overall ice flow dynamics (e.g. Goldsby and Kohlstedt, 2001; Schäfer et al., 2014; MacGregor et al., 2016). Accurately documenting the origins and nature of heat available at the base of the cryosphere is

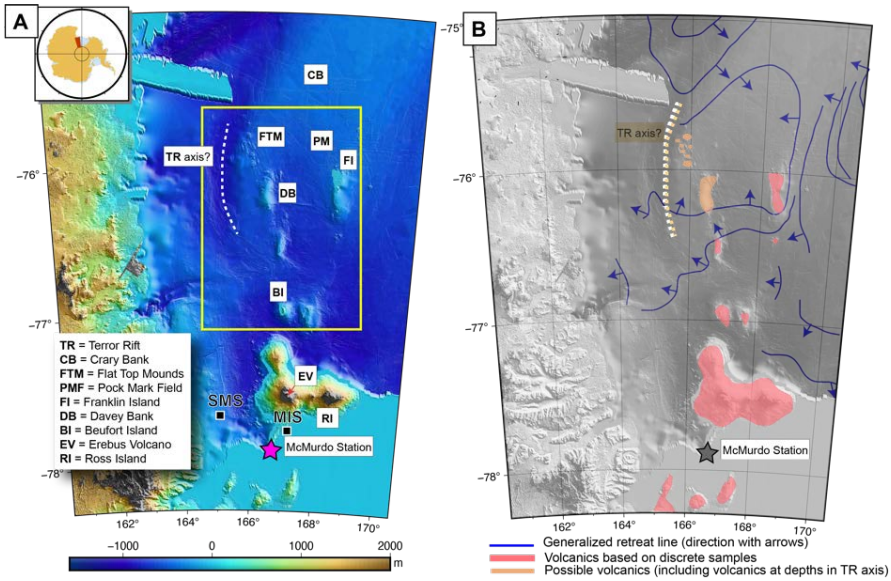

Figure 2.1. (A) A topographic map of the western Ross Sea with major volcanic features adjacent to the Terror Rift (TR) with study area outlined by the yellow box. Terror Rift axis is approximated based on Hall et al. (2007). (B) Gray-scaled, same bathymetry to the left panel with generalized ice retreat lines (e.g. Lee et al., 2017; Greenwood et al., 2018) and volcanics identified.

essential in deciphering the extent and residence timeseries of the ice in Antarctica and its oceans.

Our overarching hypothesis is that magmatic intrusion and volcanism in the western Ross Sea is the primary lithospheric heat source, and their locations and resulting heat flux have impacted lithosphere processes, such as evolution of geothermal (long-term, crustal scale) and seafloor hydrothermal (short-term, local) activities, which in turn, have influenced the dynamics of the ocean-cryosphere system in this region. Under this hypothesis, we tackle specific science questions: Are there systematic and/or systemic heat flow distributions with rifting and volcanism emerged in the western Ross Sea lithosphere? What are the age and origins of minimally explored, volcanic features? Are the distributions of fluid-flow associated seafloor features related to both inferred (sub-)seafloor architecture and distribution of heat source? Do the volumes, morphologies, timing and composition of volcanic constructs and other seafloor features suggest any links between the heat source and associated heat flux to glacial cycles?

Two Late Miocene-to-today's magmatic systems of the Erebus Volcanic Province (**Fig. 2.3**) that encapsulate the lithosphere dynamics within western Ross Sea are: Ross Island Volcanic Field (RIVF - Mounts Bird, Terror, Erebus, Hut Point Peninsula) and a group of volcanic edifices arranged en echelon adjacent to the Terror Rift (Terror Rift Volcanic Field - TRVF) (Smellie and Rocchi, 2021). Heat generated from these recently-to-currently active systems most likely impact seafloor processes and ecosystem as observed in other thickly sedimented active rift basins, e.g. Guaymus Basin (Fisher and Becker, 1991; Teske et al., 2016). Seafloor evidence of hydrothermal activities (e.g., pockmarks, mounds, etc.) and volcanism have been documented in the western Ross Sea; yet the origins and relationship among these features remain enigmatic (e.g. MaGee et al., 2010; Lee et al., 2015; Busetti et al., 2023). Multichannel seismic (MCS) reflection campaigns highlighted subsurface structures that might have fed some of these features (ANTOSTRAT Project, 1995; Salvini et al., 1997; Busetti et al., 2023); yet how these relate to deeper magmatic processes, and ultimately, how they have been impacted by ice has barely been investigated.

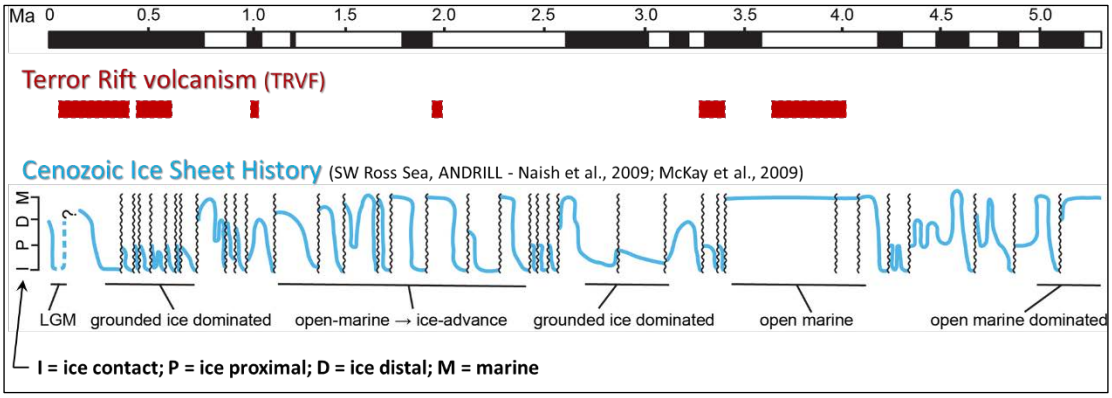

Figure 2.2: (Top) Geomagnetic Polarity Time Scale (Gradstein et al., 2020), (Middle) Relative to age of volcanism in Terror Rift (Rilling et al., 2009; Lee et al., 2015), (Bottom) Glacial proximity to the ANDRILL MIS site for 38 glacimarine cycles in upper 600 m of core (Naish et al., 2009; McKay et al., 2009).

Our study centers within the Terror Rift Volcanic Field (**Figs. 2.1A** and **2.3**), a c. 200 x 150 km area that includes two islands: Beaufort and Franklin, and three large seamounts with areas greater than 50 km^2 each and bases as deep as c. 600 meters below sea level (mbsl) with summit depths of less than 200 mbsl. Numerous smaller seamounts are found near Beaufort and Franklin islands as well as in isolated clusters, most notably a field of small and round (c. ≤ 4 km across

and ≤ 100 m high) flat-topped features at depths of c. 500 mbsl that lie approximately 20 km northwest of Davey Bank (**Fig. 2.1A**). The volcanology, geochronology and petrology of seafloor volcanics have received limited attention compared to the extensively studied subaerial deposits within the East Volcanic Province (Smellie and Martin, 2021 and references therein). Sparse rock sampling by dredge hauls have recovered volcanic materials from a total of ten sites within the Terror Rift Volcanic Field during two ice breaker campaigns; R/V *Palmer* cruise (NBP-0401) in 2004 (Rilling et al., 2009) and the South Korean R/V *Araon* cruise in 2010-2011 (Lee et al., 2015). Most of the dredge sites are within 23 km of Franklin Island (**Fig. 2.3**). A more complete and systematic sampling campaign of submarine basalts within the Terror Rift with their age and composition will fill geographic gaps in the marine data set, enabling us to further understand magma origins and tectono-magmatic process in this region of the WARS, which will in turn, to constrain the region's geothermal heat source.

Seafloor processes and their geological architecture observed in the western Ross Sea represent not only cryosphere interactions with the seafloor but also underlying tectono-magmatic activities. Marine geological interpretations have mostly been derived from a multi-scale bathymetry data compilation grid (GMRT v.3.9, Ryan et al., 2009), including the data from strategic multibeam mapping during 2004 R/V Palmer cruises NBP04-01 (Hall, 2006; Hall et al., 2007; Magee et al., 2012; Wilson et al., 2004; Lawver et al., 2007; Magee et al., 2010; Greenwood et al., 2018; Lee et al., 2017) and NBP1502 (e.g. Halberstadt , 2016, Halberstadt et al., 2016), and a later 2007 R/V Araon cruise(Lawver et al., 2012; Lee et al., 2015). There remains, however, large data gaps to be filled in and those gaps hinder the accuracy of tracing the linearity, distribution, origin and nature of seafloor morphology.

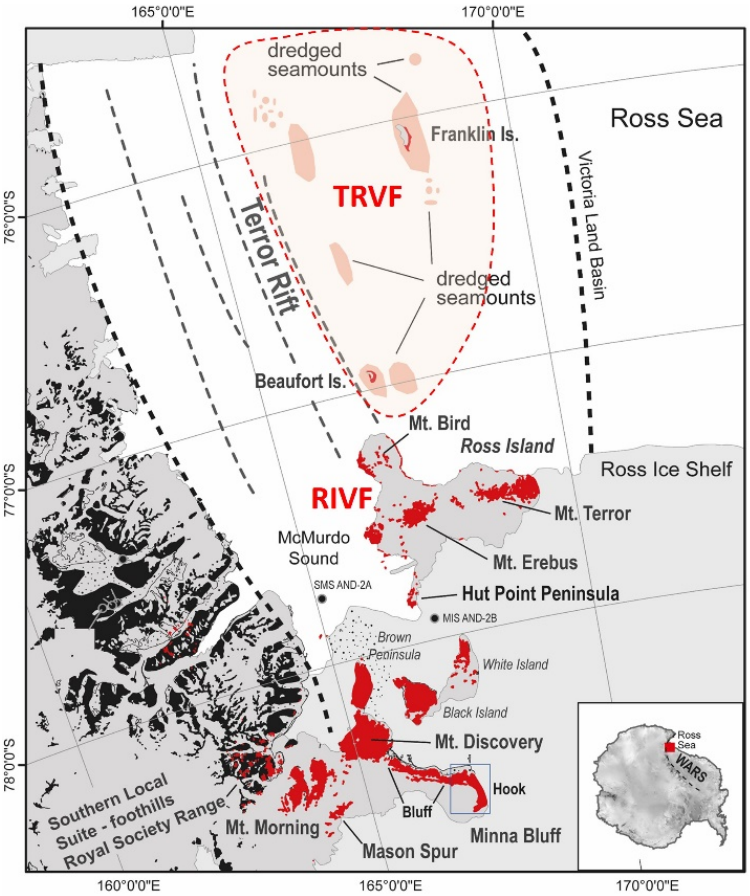

Figure 2.3. Map showing Erebus Volcanic Province modified from Martin et al. (2021). Areas highlighted in red are exposed volcanic deposits. Areas of previous dredging campaigns in the TRVF (Rilling et al., 2009; Lee et al., 2015) are indicated.

Heat flow measurements in Antarctica have traditionally been conducted on land, providing invaluable ground-truths to calibrate geophysics inversion- or water-temperature derived heat flow models (e.g. An et al., 2015; Martos et al., 2017; Giustiniani et al., 2017). However, in the western Ross Sea area (**Fig. 2.4**), there have only been a handful of studies were this has been conducted and reported (Blackman et al., 1987; Della Vedova et al., 1992). ANDRILL-1B and -2A holes provide two heat flow measurements (Morin, 2010; Schröder et al., 2011) (MIS and SMS sites, **Figs. 2.1** and **2.3**), which are currently not archived at International Heat Flow Commission database. The values of 87-118 mW/m^2 were measured in Terror Rift axial area by Blackman et al. (1987). However, the

implication of these values provides little insight because there is no spatial coverage provided by the data. Although a geothermal gradient is predicted based on thermobarometry of minerals in granulite xenoliths found in terrestrial volcanics (Berg et al., 1989), there is virtually no heat flow data within the seafloor and this precludes us from predicting a basic crustal scale geothermal state of the western Ross Sea lithosphere (i.e. conductive cooling), let alone local heat transfer by various seafloor processes (i.e. convective heat transfer via fluid flow) (e.g. Davis and Elderfield, 2005, and references therein).

Our shipboard multi-technology, multi-scale, strategic survey of the western Ross Sea seafloor/Terror Rift Volcanic Field will advance our understanding of the parameters that control ice sheet flows and responses of the crust to, and the effects of volcanism and heat from Earth's interior on overlying ice. Data has been collected via geophysics, seafloor heatflow/conductivity measurements, *in situ* real-time seafloor visualization, water-column hydrothermal signal acquisition and rock sampling via dredging and coring. The compilation of all the data will enable us to test hypotheses that magmatic intrusion and volcanism in the western Ross Sea is the primary lithospheric heat source that has influenced the dynamics of the ocean-cryosphere system in this region. Data collected will also allow us to refine current timeseries and geodynamics that drive one of the world's major continental rift systems. Deliverables from this project will be new geospatial information data, including all the underway geophysics grids of the area, publicly available via NSF funded data repositories. Core samples will be archived at the Oregon State University-Marine Geology Repository. After acquiring geochemistry and geochronology at Bowling Green State University, the remaining rock samples will be archived at the Polar Rock Repository, Byrd Polar and Climate Research Center.

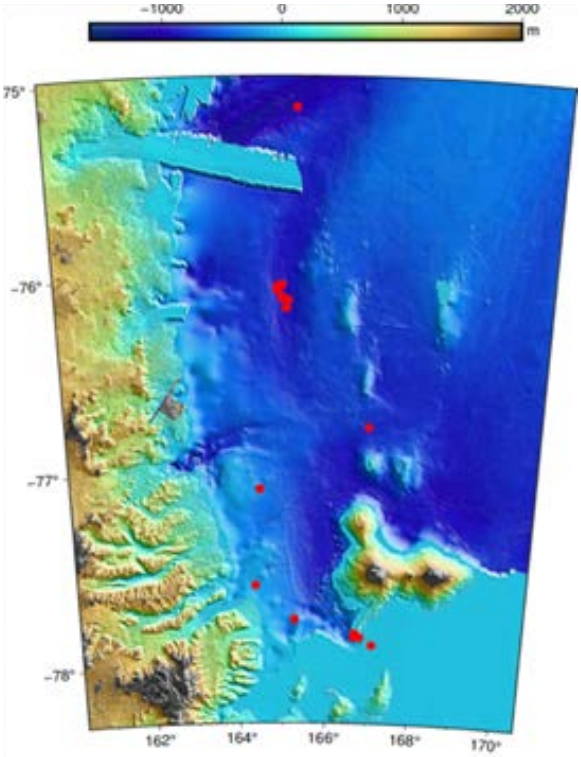

Figure 2.4. Locations of heat flow measurements (red dots) (Blackman et al., 1987; Della Vedova et al., 1992).

3. Cruise Narrative

Jonas Preine & Masako Tominaga

3.1 Science Operations Summary

Tominaga-Panter team-centric narrative

Mobilization for Expedition NBP25-01 began on February 6 in Lyttelton, New Zealand. Most of the science party arrived in Christchurch on February 7. On February 9, the full team embarked on the 63-day expedition aboard the research vessel Nathaniel B. Palmer. Onboard preparations included safety training, vessel orientation, introductions to laboratory and IT systems, and the distribution of Extreme Cold Weather (ECW) gear.

The vessel departed Lyttelton on February 11. The first stop was just outside the port, where tests of the Ultra-Short Baseline (USBL) positioning system and the MISO TowCam were conducted. The purpose of this earlier test was two-fold: (1) all the MTs and ETs who would be involved in the USBL and MISO TowCam deployment and recovery will be able to experience the operations together before they switch to their 12hrs shift; and (2) expected calm sea near Lyttleton so that the crane operation could bring up the assembled USBL pole to helo deck to be secured. During the initial transit, the science team continued laboratory setup, familiarized themselves with onboard procedures, and adjusted to life at sea. An evening science lecture series was launched, fostering interdisciplinary exchange. On Day 3, daily shift crossover meetings were initiated at noon, a routine that continued throughout the expedition. The MISO TowCam team also began daily dry-run rehearsals to optimize deployment coordination and timing.

On Day 4, the vessel exited the New Zealand Exclusive Economic Zone (EEZ), marking the start of geophysical data acquisition (**Fig. 3.1**). This included activation of the EM122 multibeam sonar, Knudsen Chirp echosounder, and the marine gravimeter. A surface-towed magnetometer was deployed astern and we initiated the 24/7 watch schedule involving both USAP ETs/MTs and the Tominaga-Panter team. On Day 7, the first iceberg was sighted, indicating arrival in Antarctic waters. By Day 8, most research teams had settled into their shift schedules.

On Day 10, the vessel reached the groups' nominal study area (**Fig. 3.2**) and began high-resolution multibeam mapping in a largely ice-free region. Two expendable bathythermographs (XBTs) were deployed, followed by a dedicated magnetometer profile crossing the Terror Rift, along with 14 additional XBTs. On Day 12, the vessel transited to the Nordenskjöld Ice Tongue for deck reconfiguration for science operations. The USBL pole was then calibrated with the ship maneuvering figure-8. Heaves (no active heave compensation winch onboard NB Palmer) due to the adverse weather prevented heat flow probe operations, prompting the start of the dredging program. Four successful dredges (DR01–DR04) were completed in the Flapjack Seamount Field. This was followed by the first MISO TowCam deployment (TC01) and the first Epibenthic Sled (EBS) deployment, marking a full day of aft deck-based science. The next day included TC02 and another stop at Nordenskjöld for further deck reconfiguration (**Fig. 3.1**).

On the evening of Day 14, the Coffin-Pecher team began their scientific program, including chirp sub-bottom profiling, gravity and piston coring, and heat flow measurements. These activities continued through Day 17. Later on Day 17, the Tow Cam (TC03) was deployed in the central Terror Rift and recovered the next day, followed by an EBS and three more dredges (DR05–DR08).

During the dredge operations DR05, the vessel encountered an iceberg to avoid; hence the dredge was hauled in immediately and redeployed as soon as the vessel was in a safe operation environment (Feb. 27th 17:33 UTC). The Coffin-Pecher team continued with heat flow transects and gravity coring through Day 18.

On Day 20, the vessel transited south toward Lewis Bay while strategically conducting multibeam mapping along the way in minimizing a "dead-head" transit (**Fig. 3.3**). Upon arrival on Day 21, a Knudsen chirp survey helped identify gravity coring sites for the Tominaga-Panter team. Two gravity cores (GC01 and GC02) and a heat flow transect for the Tominaga-Panter team were completed. These cores were immediately curated and stowed in 4°C refrigerator onboard Palmer so that the cores will be measured on MST as well as CT-scanned upon arrival at Oregon State University core repository. Following another EBS deployment, the vessel transited northeast of Beaufort Island, deployed TC04, and began a dredging sequence (DR08–DR10) that continued into Day 22. This was followed by mapping at Davey Bank. South of Franklin Island, the team conducted multibeam mapping and deployed TC05, followed by dredges DR11–DR14 at a nearby seamount chain through Day 23. TC06 was deployed, and the vessel transited west for additional heat flow work for Tominaga-Panter team, continuing into Day 25. Overnight, a multibeam survey was carried out at southern Davey Bank (**Fig. 3.4**).

On Day 26, EBS and Coffin-Pecher team's gravity coring attempts were interrupted by strong Southerly winds, which were funneling through both the eastern and western sides of Ross Island and became a weather pattern for the rest of this Expedition. Tominaga-Panter team moved the ship and mapped north of Davey Bank (**Fig. 3.2**) and deployed three dredges (DR15–DR17) and another EBS where wind speed was minimal in between the strong funneling winds. The dredge DR17 suffered from unforeseen strengthening of the wind with vortex directions of both wind and current over a shallow bank. Strong winds again delayed coring on Day 28, so an EBS was deployed, followed by more mapping. In the afternoon, coring resumed at previous Pecher-Coffin sites but was again disrupted by worsening weather. Another EBS was deployed in the western survey area.

The vessel transited north of the flat-topped seamount field to deploy TC07 and TC08 without USBL due to ice (i.e. TC006 was the last TowCam deployment with USBL as ice condition interacting with the pole worsened over time). A multibeam survey and dredge (DR18) were completed at an isolated seamount further north. Day 30 began with an EBS and deck reconfiguration for aft-based coring operations because the starboard coring operations were determined far too risky for both the ship and techs due to the worsening ice conditions. Coffin-Pecher teams' coring resumed at aft deck, but was again interrupted by wind on Day 31, prompting a westward transit. Mapping in the southern flat-topped seamount area continued into Day 32 (**Fig. 3.2**). Day 33 included Coffin-Pecher team's gravity and piston coring and an evening EBS. Days 34 and 35 focused entirely on Coffin-Pecher team's coring.

On Day 36, after nighttime coring, the vessel transited east for further mapping of flapjack field was attempted; but it was forced to abort due to heavy ice. The transit continued eastward to cover easternmost proposed area of Tominaga-Pecher team. On Day 37, two dredges (DR19 and DR20) were completed at northern Davey Bank and at Attenuator Smt **(Fig. 3.2**), followed by a transit north of Franklin Island. An attempted XBT transect failed due to severe ice. Upon arrival at the northern tip of Franklin Island, dredges DR21–DR23 were deployed.

Day 38 began with a Tow Cam deployment (TC09) and multibeam mapping north of Franklin Island (**Fig. 3.5**). The team then returned west to deploy a dredge (DR24), followed by mapping a central peak at Davey Bank, which required icebreaking. Hereafter, the acquisition of quality multibeam data entailed icebreaking a path and double-back mapping the path with slower (2-4kts) in mitigating ice noise to the hull. The Tow Cam was deployed on this small peak (Mt. Petite) in the evening (TC11). Day 39 included six dredges (DR25–DR30), a CTD, and an EBS at Davey Bank from south to north.

On Day 40, the vessel transited north to Vagabond Seamount (**Fig. 3.1, 3.2**), deployed DR31, and conducted multibeam mapping. Mapping continued into Day 41. To bring back the vessel to the final coring operations for Coffin-Pecher team, the team then transited west and attempted to cross the Terror Rift axis to the west. This was the first time the vessel could not make further progress (i.e. being beset due to ice), hence the turn-around and chose to map the eastern flank heading south. Subsequently, Coffin-Pecher team's coring was resumed and continued through Day 42. Overnight, smaller mapping sequences were conducted amid worsening ice conditions while optimizing science missions. Day 43 was occupied with coring followed by nighttime mapping. Day 44 marked the final day of Coffin-Pecher team's coring; an EBS deployed afterward was lost due to ice. The aft deck was switched from the coring mode to heatflow probe mode.

On Day 45, the Pecher-Coffin team completed a final round of heat flow measurements in extremely calm sea without motions of ices. Subsequently, Tominaga-Pecher team took over the heatflow measurements aiming in the basin in between the Davey Bank and Franklin island. Ice conditions prevented further deployments west of Franklin Island, so the vessel continued southeast to deploy dredges (DR32 and DR33) at Baby Banksy Baby Bank and Weasley Smt both located east of Franklin Island (**Fig. 3.5**), along with heat flow probe, multibeam mapping and another EBS.

On Day 47, the team transited back west to Feathertop Seamount and deployed two CTDs, TC12, three Smith-Mac ("Smith-McIntyer Benthic Grab Sampler") (SM01–SM03), and one dredge (DR34). Day 48 focused on gap-filling multibeam mapping through the ice and included dredges DR35–DR37, TowCams TC13 and TC14, and a Smith-Mac (SM04) (**Fig. 3.2**).

On Day 49, densification/thickening of ice prevented even "icy-multibeam" mode of bathymetry mapping as previously created channels closed and almost beset. The vessel moved northeast to Vagabond Seamount, where SM05, DR37, and TC15 were deployed. Given the conditions, the TowCam drifted with the ice rather than being towed. The vessel then transited further northeast, deploying SM06 and DR38 at a seamount north of Franklin Island (**Fig. 3.5**).

Day 50 began with DR39 east of Franklin Island, followed by mapping and another Smith-Mac deployment. Additional dredges (DR40–DR42), TC16, and SM07 followed. Day 51 included more mapping and three dredges (DR43–DR45), plus the final TowCam dive (TC17).

Day 52 marked the final day of dredging, with DR46–DR50 at seamounts north of Franklin Island. Sampling operations concluded with SM08 (**Fig. 3.5**).

On Day 53, cargo holder was packed away and secured, the lab was packed away and secured, and the deck was reconfigured for the return transit, including USBL pole disassembled and

palletized on helo deck. On Day 54, two final EBS deployments were completed to the north, concluding scientific operations aside from ongoing underway data collection.

Following the final scientific deployments, Expedition NBP25-01 began its northbound transit to Lyttelton, New Zealand. Days 55 through 61 were marked by a gradual shift from challenging ice and stormy seas to calmer waters and warming temperatures. The vessel encountered severe weather on Days 55 and 56, with winds exceeding 70 knots, but conditions steadily improved, allowing for smoother sailing. Wildlife sightings increased, signaling the approach to more temperate zones. Throughout the transit, the science team remained engaged—monitoring underway systems, finalizing the cruise report, and preparing data. On Day 59, the RV Nathaniel B. Palmer entered New Zealand's Exclusive Economic Zone, officially ending scientific operations and data collection for the expedition. We reached our Anchorage point off Lyttleton on Day 61 and entered the port on Day 63. Demobilization of the vessel started immediately and commenced during Day 64. On Day 65, the science team left the ship in the morning, concluding Expedition NBP25-01.

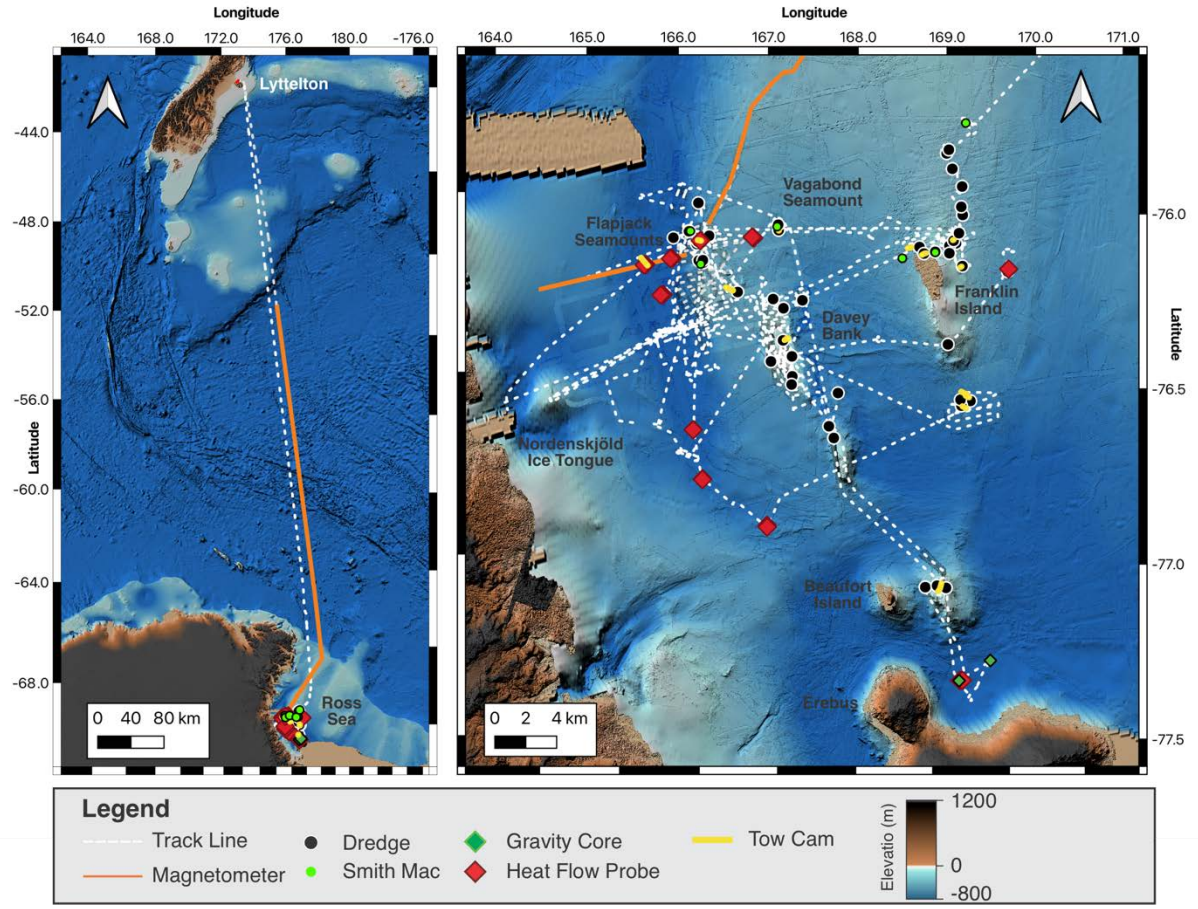

Figure 3.1: Overview of the track line of Expedition NBP25-01 and the Tominaga-Panter Science Operations.

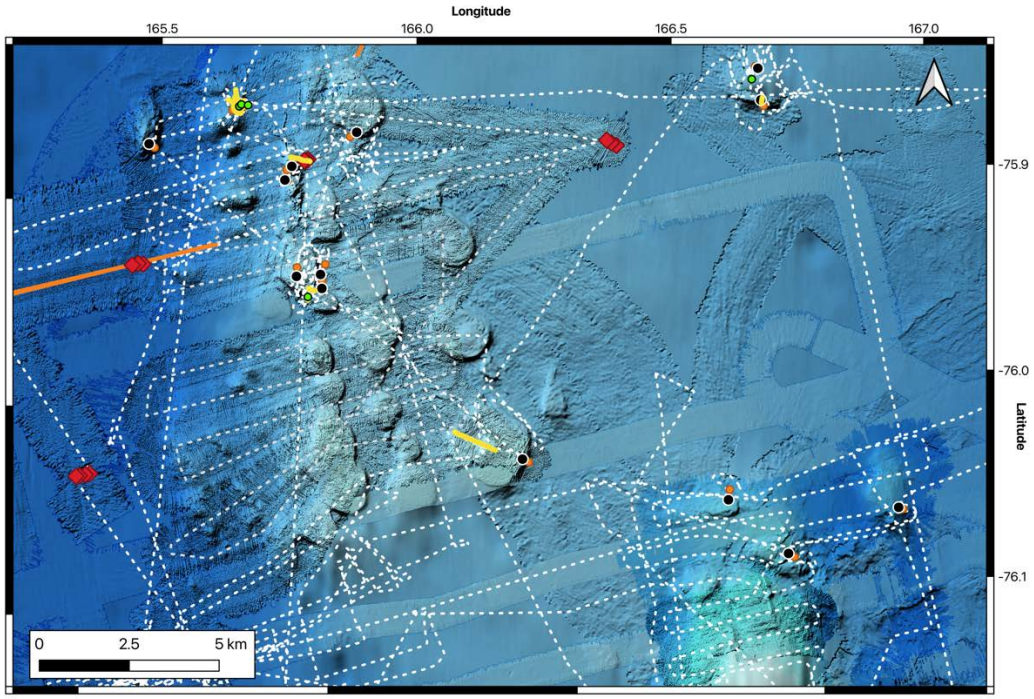

Figure 3.2: Map of the Flapjack Seamount area with the cruise track and science operations from the Tominaga-Panter team. Legend as in **Figure 3.1.**

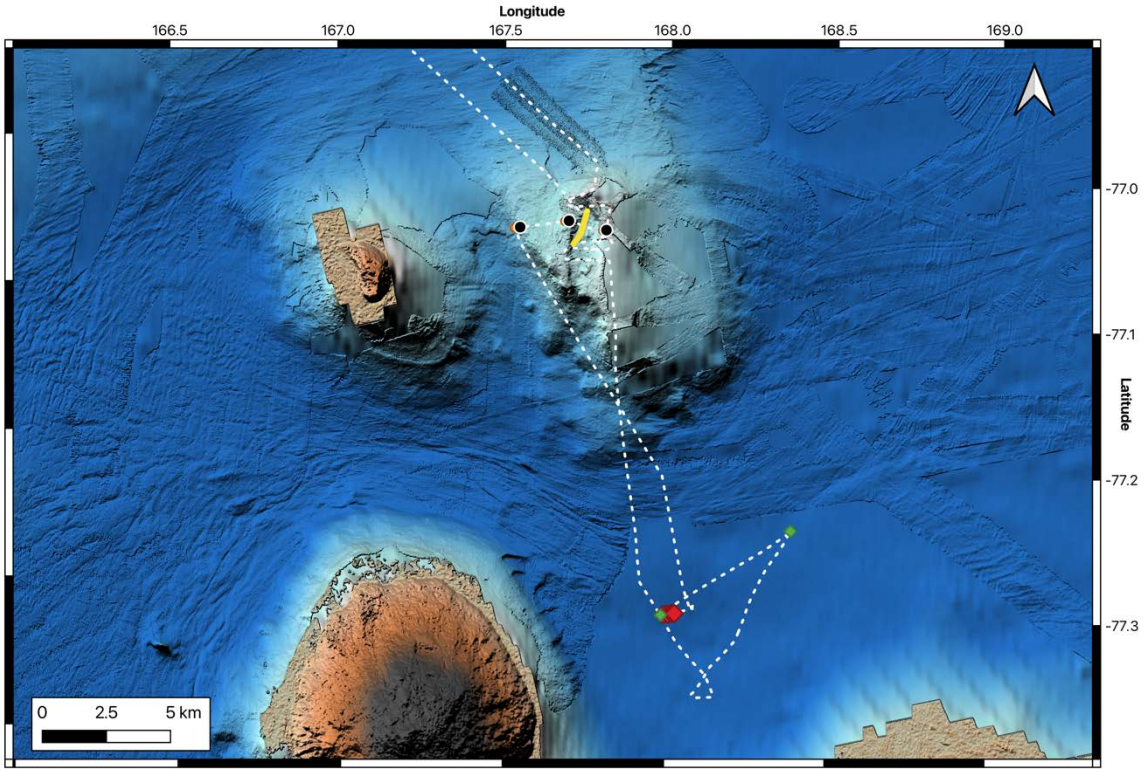

Figure 3.3: Map of the Lewis Bay the cruise track and science operations from the Tominaga-Panter team. Legend as in **Figure 3.1.**

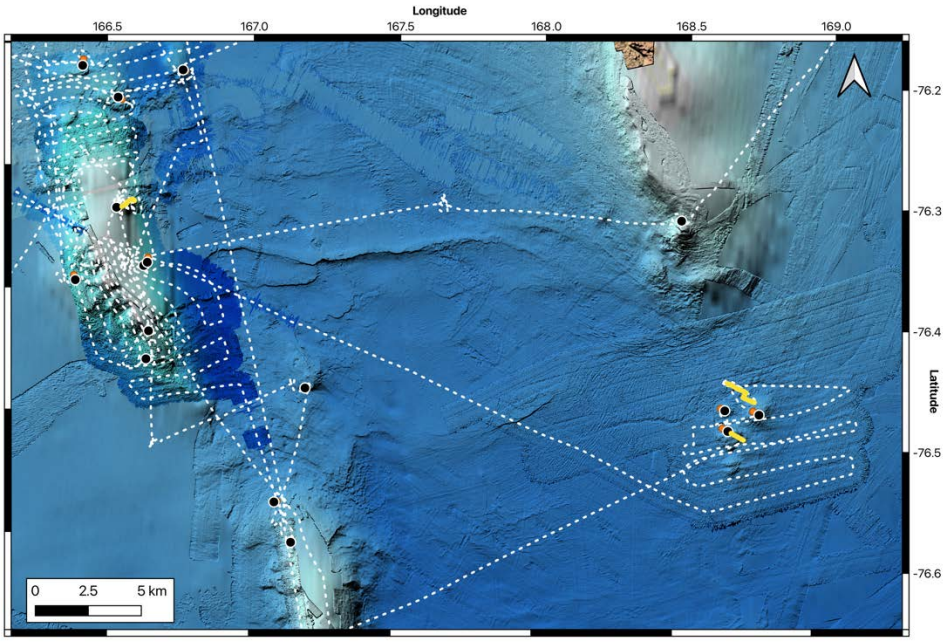

Figure 3.4: Map of the area around Davey Bank and south of Franklin island with the cruise track and science operations from the Tominaga-Panter team. Legend as in **Figure 3.1.**

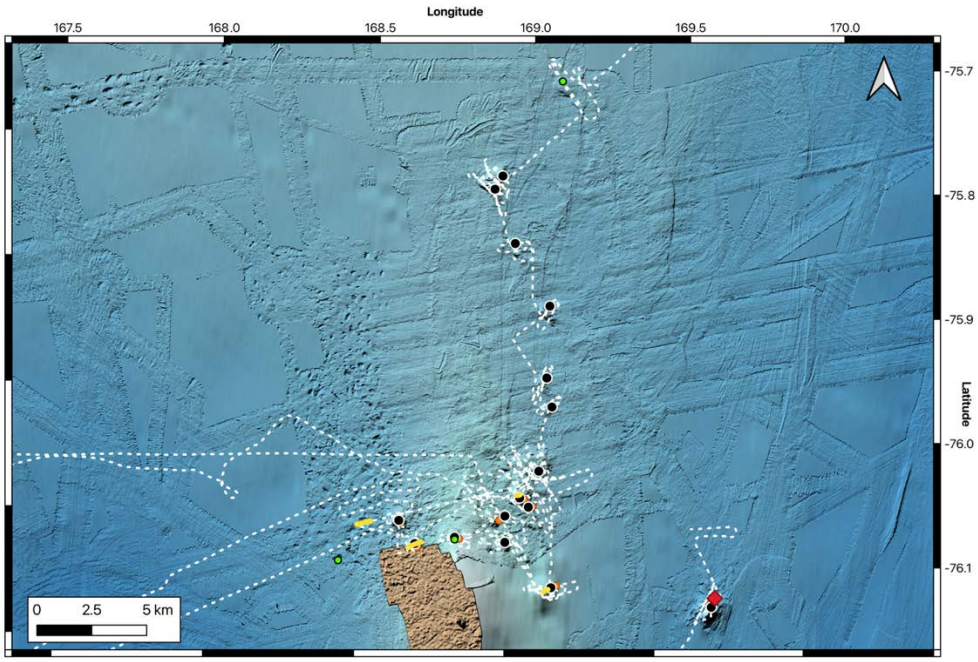

Figure 3.5: Map of the area north of Franklin Island with the cruise track and science operations from the Tominaga-Panter team. Legend as in **Figure 3.1.**

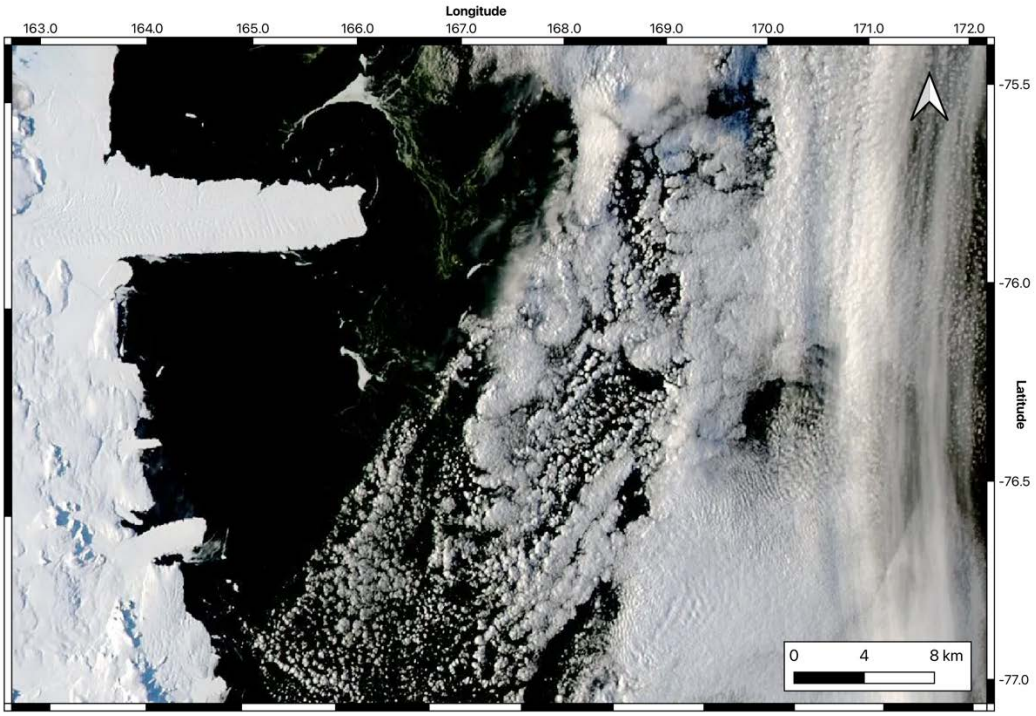

Figure 3.6: Satellite image of our study area from the beginning of our expedition (February 17th)**.**

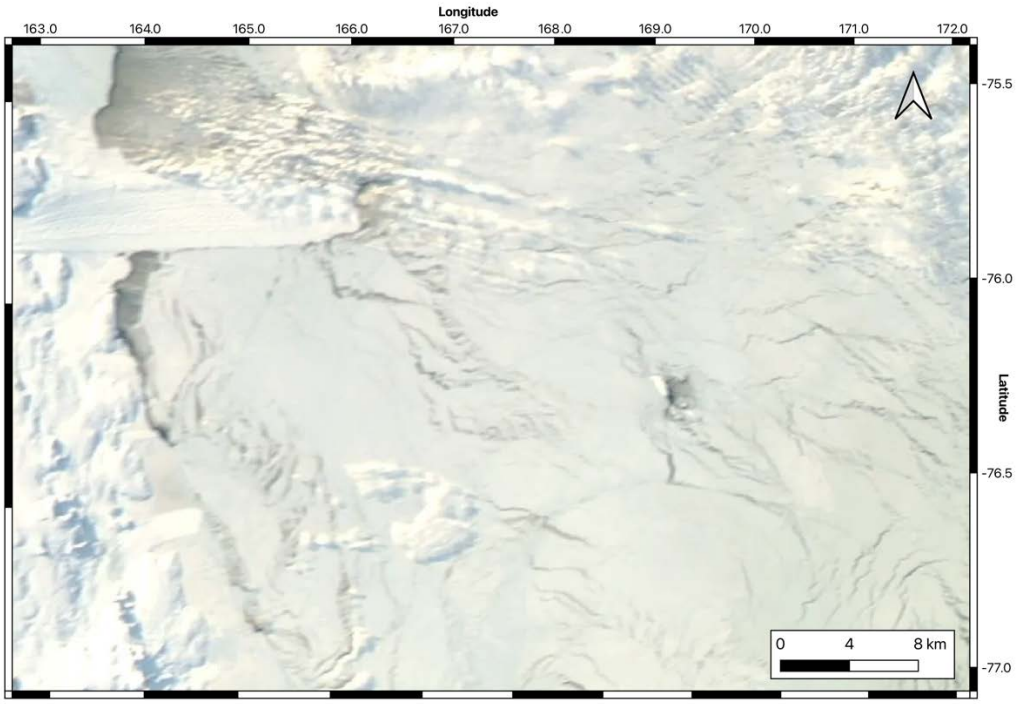

Figure 3.7: Satellite image of our study area from the end of our expedition (April 4^{h})**.**

Figure 3.8: Group photo of the science party of Expedition NBP25-01.

3.2 Cruise Statistics

M. Tominaga

Multi-disciplinary, multi-instrumentations science operation was planned iteratively throughout the NBP25-01 Expedition. Carefully considered in the effort of interweaving various science missions were: site-to-site transit time, ship maneuverability due to the sea/ice/weather state, balancing MTs laboring intensity, and distribution of the funded hours for each of the science teams at "fare-share" basis (**Fig. 3.9, 3.10**).

Gerken_Kocot team's requested "cadence" of benthic sampling (24-36hrs in between sampling with geographical sparseness) had been accommodated as much as other science operations can at opportunistic basis, totaling 23 casts. Due to the lengthy gas analyses on the recovered cores, the Coffin_Pecher team's operations needed to be finalized first. Jeffrey's CTD operations included both proposed ones along the coring site as well as a few opportunistic casts, totaling 21 CTD casts. Gerken_Kocot team's operations became the last one to be conducted for their final sampling sites located on the way to the Voyage North, 70-90 nm from our nominal area during this Expedition.

Final numbers for the cumulative consumption of funded days are:

- Tominaga_Panter (94 % i.e. 22.61 days)
- Gerken_Kocot (91% i.e. 5.46 days)
- Coffin_Pecher (99%, i.e. 14.85 days)
- Jeffrey (105%, i.e. 1.05 day)

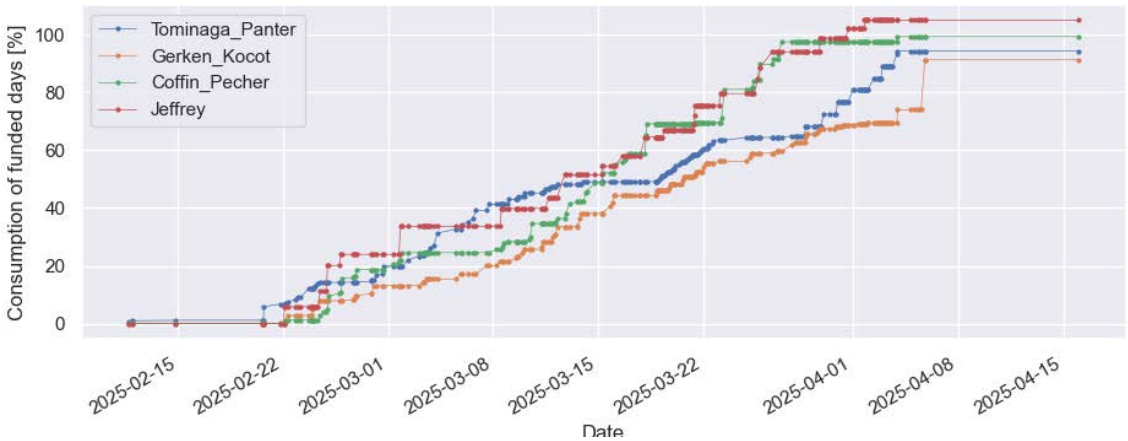

Figure 3.9: Cumulative consumption of funded days in % over the course of the entire cruise.

Note for our transit voyage from/to Lyttleton, NZ, is that 9 days was spent for the outbound voyage south (i.e. total duration from Lyttleton to deck configuration minus USBL pole test and underway magnetometer deployment/recovery time). Transit inbound, the voyage north totals 10 days and 5 hrs, including X hours at the anchorage point due to early departure to duck from the ice breaking and the Southern Ocean crossing with 50-70kts wind/10-30 ft waves.

Shared time among all the teams included: deck (re)configurations, some of the .916 wire switch (stbd to/from aft), from/to Lyttleton transit, aloft (aft A-frame block fixing), and coring cradle repair. Other non-science businesses, such as winch control room maintenance, were readily

compensated by science-mission multibeam survey for Tominaga_Panter team. Welding (and re-painting the stbd coring cradle) was completed in total 7 hrs (2/26/2025 08:39-15:36 local) with the generous effort of the Engine Room.

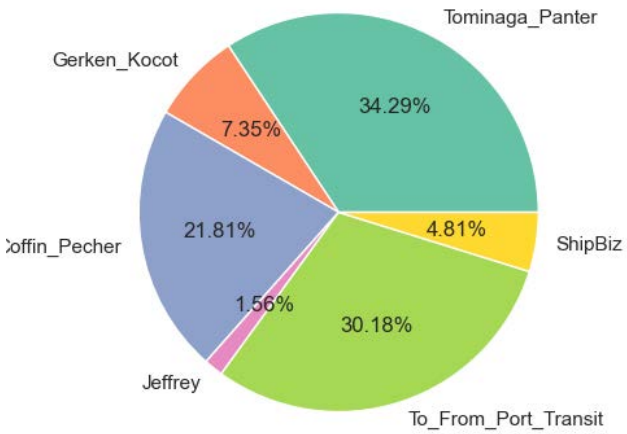

Figure 3.10: Percentage of activities during this cruise. Total science operations spent (minus shared "ship business") was 65.01% whereas Ship's transit time from/to Lyttleton was 30.18%. Only 4.81 % was spent for ship-related business, including the aloft, cradle repair, and deck (re)configuration. All the site-to-site transit, which is a part of science planning, is included in the science.

3.3 Cruise Statistics

Table 3.1: Summary of science operations (numbers of casts and sampling)

Tominaga_Panter	**Jeffrey**	***Gerken-Kocot***	***Coffin_Pecher***
2 Gravity Cores 29 HFP measurements 50 Dredges (49 successful) 17 TowCam deployments (7 with USBL pole deployed) 22 XBT casts 8 Smith Mac sampling 3264 km^2 of high quality multibeam (fully processed, targeted seamounts are 2233 km^2)	21 CTD cast 1 C-prop cast 3 Smith-Mac sampling	23 Epibenthic Sled casts 7 Smith-Mac sampling	42 HFP measure-ments 64 Cores (inc. both PC and GC, standard (2.5") and jumbo (4")) yielded 98.6m cored materials.

143 km of high-quality chirp sonar			

Table 3.2: Science Operations Time Monitoring

1	Setting sail	-43.607	172.719	2/11/25 15:47	TP/IW/SG
2	USBL/TC dunk test site arrival, and deployment practicen with all MTs/Ets, then secure main deck. The hfp rig up to helo deck 21:20 - 22:18 (TP/IW share), then all deck was secured go move on underway to the end of NZ EEZ.	-43.52	172.847	2/11/25 17:04	TP/IW
3	At the end of NZ EEZ, at the magnetometer deployment point	-54.535	173.714	2/11/25 22:18	TP
4	SOL mag_1, payout at 3 kts, the mag, secure deck. (MTs shift starts for 24/7 watch; so did underway geophysics watch)	-54.644	173.711	2/14/25 19:24	Tp
	mag_1 EOL due to ice interacting with cable	-75.658	166.286	2/20/25 15:03	TP
	XBT01(2/20/25 16:12-:45)	-75.772	165.879	2/20/25 16:12	TP
5	MB1 SOL (with multiple way points) , flat top mounds, the IT90R-65 with 8 XBT profiles	-75.777	165.733	2/20/25 16:45	TP
6	Mag_2 SOL	-75.848	165.457	2/21/25 19:27	TP
5	MB1 EOL (note after WPT24, ship made great effort filling in MB gaps due to ice - hence out of original WPTs locations. But we keep the original MB1 EOL WP number to continue. Aso Mag_2 EOL.	-75.835	163.794	2/22/25 01:01	TP
7	CTD_1 and/or C-props (can be independent location from CTD, ideally at high noon but could be done 10am-3pm)	-75.833	163.777	2/22/25 01:35	W
8	Looked into possible locations on bridge (2:31-2:58) and ship transiting to the deck reconfig position, went N, then went S.	-75.832	163.785	2/22/25 02:58	TP/SG/IW
9	NBP reconfigures the deck for science, completed by 17:30, then hold station for cleaning/sorting the deck and dinner	-76.135	162.971	2/22/25 07:34	TP/SG/IW
10	Transit to USBL cal location, USBL cal	-76.092	163.001	2/22/25 19:04	TP
11	Transit to Heat Flow Station 1, after the arrival, MTs, PIs assessed the sea state, much heave due to the sea state/gust, postpone the heat flow ops. for the night.	-75.839	164.198	2/23/25 00:06	TP
12	Transit to dredge site DR_01, some wire tension display glitch due to the data system switch at some point	-75.796	165.874	2/23/25 03:31	TP
13	Dredge at Flat Top/Rift Zone	-75.785	165.777		TP
14	TC_1, fiber connection took 1 hr or so extra. Launch: 17:58	-75.877	165.762	2/23/25 16:00	TP
	EOL TC_1	-75.819	165.795	2/23/25 20:49	TP
14'	.916 reterm (out of sequence, so the "prime")	-75.818	165.716	2/23/25 21:31	TP/SG/IW

15	EBS_1_SOL	-75.818	165.716	2/23/25 23:00	SG
	EBS_1_EOL	-75.819	165.731	2/24/25 00:35	SG
16	Transit to SOL of TC_2	-75.845	164.973		TP
17	SOL of TC_2 (3 nm total, 6 hrs; if no anomalies, then kill it at 3 hrs)	-75.823	164.996	2/24/25 01:59	TP
	EOL of TC_2 (3 nm total, 6 hrs; if no anomalies, then kill it at 3 hrs)	-75.85	165.046	2/24/25 07:24	TP
18	Transit to do aloft site	-76.135	162.971		TP/SG/IW
19	C prop (11:37-11:56) at the aloft site then .916/block fix and PC set up (3 hrs for PC set up after Chet was aloft 14:20 local, the fastest!!)	-76.135	162.971	2/24/25 11:25	IW
20	Transit to coring site (given the 3 hrs for the PC set up and 20 min. C-prop, technically IW ops. Started 14:00)	-76.073	163.074	2/24/25 17:21	IW
	Chirp survey SOL while transit (reduced speed)	-76.048	165.294	2/24/25 21:13	IW
21	CTD_2 (at Chirp survey EOL)	-76.047	164.914	2/24/25 22:46	IW
22	Coring Site 1 reference site. GC x2 (00:34-6:10), PC x1 (10:00-17:12)	-76.048	164.928	2/25/25 00:34	IW
23	Securing deck, then transit to Coring Site 2	-76.048	165.029	2/25/25 17:12	IW
24	CTD_3 at the west side of coring sequence	-76.048	165.029	2/25/25 20:49	IW
25	Coring Site 2 transect, preparation, GC (2/26/25 02:39:54 failed attempt to deploy the GC),Coring cradle fix (completed from 08:39-15:36)	-76.05	165.095	2/25/25 21:44	IW
26	transit (waiting for next event wihle doing CTD_4+ usbl test)	-76.051	165.095	2/26/25 15:36	TP/IW/SG
27	.916 wire switch and aft deck reconfig., including the EBS fix	-76.064	164.885	2/26/25 17:28	TP/IW/SG
28	EBS_2	-76.065	164.885	2/26/25 19:20	SG
29	Transit (directly north by 1 nm) and HFP at Ingo 1A-a	-76.067	164.913	2/26/25 21:38	IW
30	Transit/MB to Flat Top	-75.981	165.955	2/27/25 20:00	TP
31	TC_3	-75.968	165.883	2/27/25 21:38	TP
32	EBS_3	-75.977	165.935	2/28/25 01:42	SG
33	transit filling MB and Dredge 5,6,&7 (Dredge 5 lost 1 hr, due to ice berg dodging)	-75.991	166.002	2/28/25 05:36	TP
34	Reconfig the deck and transit to Heatflow site	-75.849	166.343	2/28/25 14:50	TP
35	JW HFP Rift magmatism (Stations 12-1, the lat lon here are for Statino 6) and with XBTs transect	-75.846	165.031	2/28/25 17:00	TP
36	Ingo heat flow	-76.067	164.913	3/1/25 08:08	IW
37	Transit to Ingo's Site 2Da	-76.048	165.127	3/1/25 16:00	IW
38	.916 switch, standard GC assembly	-76.048	165.127	3/1/25 17:06	IW
39	CTD_4 (the on deck 19:45 to rad van clearance took until 21:50)	-76.048	165.127	3/1/25 19:30	W
40	Coring Site 2 contd. And the 07:44 is the end of coring.	-76.048	165.127	3/1/25 21:50	IW
41	Transit to south, inc. Davy Bank and Beaufort isd MB survey with 3 XBT, MB/Chirp survey for the coring transect	-76.037	166.511	3/2/25 08:00	TP
	MB/Chirp survey for the coring transect	-77.07	167.616		TP
42	Coring for Lewis Bay tephra layers	-77.277	167.719	3/3/25 01:25	TP

43	As soon as the coring done, .916 switch, deck reconfig.	-77.231	167.592	3/3/25 06:33	SG/TP
44	CTD_5 during deck config	-77.231	167.599	3/3/25 08:27	W
45	HFP deck to deck 4hrs including 4 pogos	-77.231	167.599	3/3/25 09:48	TP
46	EBS_4	-77.232	167.68	3/3/25 13:14	SG
47	USBL cal (figure-8 for 18/34 system)	-77.231	167.68	3/3/25 15:53	TP
48	transit to beaufort isd	-76.945	167.404	3/3/25 17:18	TP
49	Dredge 8,9,10 Beaufort Is.	-76.977	167.503	3/3/25 19:24	TP
50	TC_4 with .68 switch	-76.977	167.503	3/4/25 01:00	TP
51	Transit with MB to Coco seamounts, south of Franklin Is/channel and MB	-76.447	168	3/4/25 06:37	TP
52	TC_5	-76.434	168.462	3/5/25 12:04	TP
53	EBS_5	-76.412	168.362	3/5/25 19:32	SG
54	transit and Dregde (DR11, 12, and 13)	-76.38	166.691	3/5/25 22:00	TP
55	TC_6	-76.463	168.396	3/6/25 08:30	TP
56	Transit to JW Heat Flow Station Must Do, Lovely, Really Appreciated. And Will be Great.	-76.664	165.655	3/6/25 15:13	TP
57	Station Must Do, Lovely, Really Appreciated. And Will be Great.	-76.664	165.602	3/6/25 20:15	TP
58	Transit and EBS_6	-76.101	166.01	3/7/25 13:12	SG
59	MB Davey Bank	-75.982	165.972	3/7/25 17:00	TP
60	Site survey over the Lindsay's 9Aa	-76.428	165.039	3/8/25 05:02	IW
61	EBS_6	-76.433	165.034	3/8/25 11:28	SG
62	CTD_6	-76.431	165.001	3/8/25 12:51	W
63	More transit to Lindasy's 9Ad, wire switch, setting up	-76.4	164.898	3/8/25 14:20	IW
64	Gravity coring for Lindsay 9Ad then more survey for GC	-75.982	165.972	3/8/25 17:00	IW
65	Transit to Site 3 to try the better weather - weathered out for 40 kts wind	-76.051	165.71	3/8/25 23:00	IW
66	DavyBank north map; wire switch was already completed during the transit. The greatest thank to MTs.	-76.07	166.317	3/9/25 01:18	TP
67	Transit to EBS	-76.208	166.375	3/9/25 12:35	SG
68	EBS_7	-76.047	165.545	3/9/25 14:06	TP
69	Transit to Dredge_15	-76.047	165.545	3/9/25 14:51	TP
70	Dredge_15,16,and 17 Davey Bank; (unpredictable) bad weather for DR17	-76.2	166.133	3/9/25 16:41	TP
71	Transit to sled	-75.964	166.314	3/9/25 23:05	SG
72	EBS_8	-75.976	166.377	3/10/25 01:10	SG
73	.916 switch for GC ready while transit with MB	-76.142	166.294	3/10/25 02:38	TP
74	transit to Site 3	-76.048	165.263	3/10/25 09:24	IW
75	CTD_7 while assessing sea state	-75.849	165.982	3/10/25 11:07	IW
76	Site 3 GC	-76.056	165.25	3/10/25 13:55	IW
77	switch .916 to aft	-76.049	165.128	3/11/25 06:22	TP/IW/SG
78	Transit to EBS	-76.049	165.128	3/11/25 06:22	SG
79	EBS_9	-75.928	165.192	3/11/25 07:47	SG
80	Transit to TowCam site	-75.784	165.623	3/11/25 09:55	TP

81	TC_7 without USBL pole/ then TC_8	-75.782	165.63	3/11/25 11:05	TP
82	CTD_8	-75.784	165.623	3/11/25 17:07	W
83	Transit with MB to northernmost flattop	-75.702	165.829	3/11/25 18:01	TP
84	Dredge_18	-75.712	165.809	3/11/25 20:56	TP
85	Transit to Sled	-76.025	165.838	3/11/25 23:51	SG
86	EBS_10	-76.023	165.852	3/12/25 02:27	SG
87	Transit to coring Site 1	-76.023	165.852	3/12/25 03:49	IW
88	Deck reconfig all for aft	-76.048	164.926	3/12/25 06:09	TP/IW/SG
89	CTD_9	-76.048	164.927	3/12/25 18:09	W
90	Site 1 GC	-76.048	164.927	3/12/25 20:02	IW
91	PC set up, assessing weather (with MB to the east, then back to Site 1)	-76.052	164.677	3/13/25 02:05	IW
92	Transit back to Site 1, then assessing the core-ability	-76.048	164.922	3/13/25 14:30	IW
93	Transit to EBS_11	-76.147	163.49	3/13/25 15:13	SG
94	EBS_11	-76.154	163.506	3/13/25 18:31	SG
95	Transit back to MB site	-76.042	165.419	3/13/25 19:24	SG
96	MB on south side of flapjack field	-75.99	165.734	3/13/25 23:23	TP
97	Transit back to Site 1, then assessing the core-ability	-76.048	164.928	3/14/25 04:29	IW
98	PC at Site 1-2	-76.048	164.998	3/14/25 05:31	IW
99	Transit to Site 3 hoping to switch to GC while troubleshooting the barrel/liner issues	-76.048	165.265	3/14/25 17:52	IW
100	Transit back to Site 2	-76.048	165.266	3/15/25 05:31	IW
101	CTD_10	-76.049	165.129	3/15/25 06:14	W
102	PC at Site 2 (with 1.5 barrel, then loose piston?)	-76.048	165.266	3/15/25 06:58	IW
103	Transit to EBS	-76.145	163.506	3/15/25 19:23	SG
104	EBS_12	-76.139	163.558	3/15/25 23:01	SG
105	Transit back to Site 3	-76.048	165.266	3/16/25 00:41	SG
106	Coring at Site 3	-76.047	165.243	3/16/25 04:02	IW
107	CTD_11 (14:29-15:19)	-76.047	165.246	3/16/25 14:29	IW
108	Transit to Site 9D	-76.306	164.658	3/16/25 18:10	IW
109	GC at Site 9Da, 9Db	-76.26	164.217	3/16/25 21:27	IW
110	Transit back to Site 1Aa	-76.135	164.594	3/17/25 00:39	IW
111	PC at Site 1Aa	-76.045	164.926	3/17/25 05:26	IW
112	Post coring work (900m/.916 re-termination)	-76.044	164.926	3/17/25 09:46	IW
113	Transit to Site 8 (near Site 2)	-76.049	165.408	3/17/25 18:30	IW
114	GC at Site 8	-76.047	165.354	3/17/25 19:10	IW
115	CTD_12	-76.05	165.411	3/18/25 02:58	W
116	Transit back to Site 2	-76.048	165.158	3/18/25 04:32	IW
117	PC at Site 2	-76.048	165.158	3/18/25 05:15	IW
118	Transit to MB site	-76.05	165.084	3/18/25 19:31	TP
119	MB at the south of Flapjack Field a bit (due to ice, no way)	-76.041	165.524	3/18/25 20:30	TP
120	Transit to EBS site	-76.011	166.134	3/18/25 21:00	SG
121	EBS_13	-76.012	166.16	3/18/25 22:33	SG

122	Transit to Flat Top Davey Bank	-76.06	166.451	3/18/25 23:50	TP
123	Dredge_19 at flat top DB (with prep time for 45 min or so?)	-76.054	166.733	3/19/25 00:55	TP
124	Transit to the Attenuator	-76.058	166.743	3/19/25 03:23	TP
125	Dredge_20 at the Attenuator	-76.054	166.733	3/19/25 05:06	TP
126	Transit to Franklin Isd	-76.051	166.77	3/19/25 06:33	TP
127	CTD_13	-75.985	168.25	3/19/25 10:21	W
128	Dredge_21 (basically started at the same place with CTD)	-75.979	168.237	3/19/25 11:07	TP
129	Dredge_22	-76.001	168.275	3/19/25 13:01	TP
130	Dredge_23 (inc. transit to)	-75.99	168.677	3/19/25 14:58	TP
131	Transit to SLED site	-75.97	168.881	3/19/25 18:19	SG
132	EBS_14	-75.97	168.879	3/19/25 19:25	SG
133	Transit to TC	-75.971	168.852	3/19/25 21:15	TP
134	TC_9	-75.975	168.146	3/19/25 22:32	TP
135	Transit to TC	-76	168.3	3/20/25 00:55	TP
136	TC_10	-76.003	168.252	3/20/25 01:41	TP
137	Multibeam N. Franklin Island w/o transit	-75.947	168.096	3/20/25 03:30	TP
138	Transit to dredge site	-76.027	166.422	3/20/25 09:06	TP
139	Dredge_24	-75.978	166.396	3/20/25 12:48	TP
140	Transit to SLED site	-76.009	166.122	3/20/25 15:31	SG
141	EBS_15	-76.02	166.131	3/20/25 16:29	SG
142	Transit to Mt. Petit	-76.149	166.443	3/20/25 18:23	Tp
143	MB at Mt. Petit	-76.159	166.433	3/20/25 19:43	Tp
144	TC_11 at Mt. Petit	-76.154	166.462	3/20/25 23:06	Tp
145	Dredge_25 at Mt. Petit	-76.157	166.388	3/21/25 00:55	Tp
146	Transit to Southern Peak of the Davey Bank	-76.265	166.396	3/21/25 02:27	Tp
147	Dredge_26	-76.263	166.406	3/21/25 04:57	Tp
148	Transit to the southern tip of the Davey Bank	-76.286	166.372	3/21/25 05:46	Tp
149	Dredge_27	-76.285	166.387	3/21/25 07:15	TP
150	Transit to CTD/SLED	-76.297	166.382	3/21/25 09:06	SG/W
151	CTD_14	-76.358	166.309	3/21/25 10:04	W
	Ops. meeting/ lunch/x-over	-76.358	166.309	3/21/25 10:43	IW
152	EBS_16	-76.356	166.323	3/21/25 12:27	SG
153	Transit to dredge	-76.335	166.858	3/21/25 14:02	TP
154	Dredge_28 @ conquest Smt	-76.342	166.897	3/21/25 15:51	TP
155	Transit to dredge	-76.338	166.915	3/21/25 17:50	TP
156	Dredge_29 @ N. tip of Endurance Bank	-76.462	166.734	3/21/25 19:34	TP
157	Transit to dredge	-76.432	166.728	3/21/25 21:19	TP
158	Dredge_30 @ E. tip of Endurance Bank	-76.438	166.711	3/21/25 22:09	TP
159	Transit to EBS/dredge (35nm)	-76.438	166.711	3/21/25 23:43	SG/TP
160	EBS_17	-75.843	166.774	3/22/25 05:05	SG
161	Transit to dredge (5 nm)	-75.846	166.654	3/22/25 06:35	TP
162	Dredge_31 @ Vagabond	-75.842	166.649	3/22/25 07:22	TP
163	MB @Vagabond	-75.841	166.65	3/22/25 08:26	TP

164	Transit to N. rift zone	-75.666	165.769	3/22/25 13:40	TP
165	MB @ Niemand, attempted original Jemand on the west side of the ridge but unabled by ice, then switch the name of Jemand to the smt right south of the Niemand, start MB	-75.653	165.654	3/22/25 16:14	TP
166	Transit to CTD site/coring site	-75.796	165.123	3/23/25 01:00	TP/IW/SG
167	CTD_15	-76.046	165.131	3/23/25 04:00	W
168	deck config for coring	-76.048	165.16	3/23/25 05:08	IW
169	Coring and the extrusion has occurred	-76.048	165.198	3/23/25 10:14	IW
170	MB on southwest side of flapjack field during winch control panel maintenance (0000-0231)	-76.033	165.713	3/24/25 21:58	TP
171	Transit to EBS site	-76.072	165.806	3/25/25 03:10	SG
172	EBS_18	-76.06	164.995	3/25/25 05:17	SG
173	Transit to Coring site	-75.796	165.806	3/25/25 07:12	IW
174	Coring Site 2 and 3	-76.048	165.275	3/25/25 09:44	IW
175	Transit to Site 5	-75.796	165.806	3/25/25 15:27	IW/W
176	CTD_16	-76.203	165.2	3/25/25 17:56	W
177	Site 4GC	-76.187	165.165	3/25/25 18:52	IW
178	CTD_17	-76.19	165.555	3/26/25 14:35	W
179	Site 5 JGC final/deck secured	-76.187	165.224	3/26/25 15:52	IW
180	Transit to EBS site	-76.183	165.117	3/26/25 22:40	SG
181	EBS_19 - didn't happen due to ice took down the sled to abyss	-76.182	165.114	3/26/25 23:39	SG
182	Deck config for HFP, bridge mtg (0515: the Capt was cautious as "do not push to the extreme", per Luke, the ice has been moving 0.05-0.08 kts. Cannot exeeding the 30m wire pay out)	-76.182	165.114	3/26/25 23:40	IW
183	Ingo's HFP	-76.184	165.511	3/27/25 06:15	IW
184	Transit to SLED/HFP site	-76.22	167.53	3/27/25 20:56	SG/TP
185	EBS_20	-75.796	165.806	3/28/25 02:50	SG
186	Transit to HEP site	-76.215	167.525	3/28/25 04:28	TP
187	Heat flow (cancelled two sites west of the Franklin Isd. after assessing the sea state)	-75.796	165.806		TP
188	Transit to Dredge	-76.215	167.525		TP
189	Dredge_32 at Baby Banksy Baby Bank (actually in the water at 09:16 due to setting up Hila Special)	-76.272	168.334	3/28/25 07:27	TP
190	Transit to Dredge	-75.796	165.806	3/28/25 10:24	TP
191	Dredge_33 at Weasley Smt	-76.096	169.219	3/28/25 15:28	TP
192	Heatflow at Weasley Smt	-76.092	169.236	3/28/25 18:11	TP
193	Transit to SLED	-76.043	169.293	3/28/25 19:56	SG
194	EBS_21	-76.044	169.28	3/28/25 20:52	SG
195	Transit to west (56 nm) for FeatherTop	-75.783	165.632	3/28/25 22:17	TP
196	CTD_18_driftow_yo	-75.779	165.607	3/29/25 09:51	W
197	TC_12 FeatherTop (on deck by 1347, then config. Til 14:45)	-75.78	165.602	3/29/25 10:56	TP
198	SmithMac_1 crest	-75.783	165.615	3/29/25 14:45	TP/SG

199	SmithMac_2 w flank	-75.783	165.616	3/29/25 16:04	TP/SG
200	SmithMac_3 e flank/CTD anomalies	-75.784	165.638	3/29/25 17:46	TP/SG
201	CTD_19	-75.784	165.634	3/29/25 19:18	W
202	Dredge_34 at FeatherTop (transit and situating ship 20:33-dredge in water at 21:42)	-75.781	165.619	3/29/25 20:33	TP
203	IcyMultibeam	-75.83	166.002	3/30/25 00:55	TP
204	Dredge_35, 36, and 37 at Pfankuchen, including 17:00-18:48 ship/ET fixing the mast	-75.875	165.695	3/30/25 09:29	TP
205	TowCam_13	-75.885	165.659	3/30/25 18:48	TP
206	Smith Mac_4	-75.884	165.659	3/30/25 20:27	TP
207	TowCam_14	-75.88	165.665	3/30/25 23:09	TP
208	Transit to IcyMapping	-75.886	165.674	3/31/25 00:44	TP
209	IcyMapping - shortly after impeded by formedable ice. tried to stabilize ship for Smith Mac...but too much pressure from the ice... Have to move to north/east to find better ice"	-75.973	166.031	3/31/25 03:20	TP
210	Transit to Vagabond	-75.972	165.941	3/31/25 05:55	TP
211	IcyMapping - shortly after impeded by formedable ice sheet, tabled	-75.944	166		TP
212	SmithMac_5	-75.825	166.667	3/31/25 08:29	TP
213	Dredge_38	-75.828	166.643	3/31/25 10:32	TP
214	TC_15	-75.845	166.651	3/31/25 12:29	TP
215	CTD_20	-75.84	166.657	3/31/25 15:36	W
216	Transit to La Pleiad "Merope" smt	-75.837	166.656	3/31/25 16:26	TP
217	Dredge_39 at Merope smt	-76.058	168.716	3/31/25 23:01	TP
218	icy multibeam on La Pleiad	-76.003	168.407	4/1/25 01:44	TP
219	SmithMac_6	-76.005	168.419	4/1/25 08:35	TP/SG
220	Dredge_40 at "Electra" Smt	-76.004	168.426	4/1/25 10:05	TP
221	Dredge_41 at Celaine smt	-75.996	168.571	4/1/25 13:19	TP
222	Transit to Alcyone smt	-76.018	168.586	4/1/25 14:16	TP
223	Dredge_42_at_Alcyone smt	-76.014	168.575	4/1/25 17:48	TP
224	CTD_21 - the last one!, including making a hole (18:12~, then CTD 1902)	-76.008	168.558	4/1/25 18:12	TP
225	Transit to Merope smt	-76.007	168.57	4/1/25 19:43	TP
226	TC_16 at Merope smt	-76.061	168.662	4/1/25 20:34	TP
227	Smith Mac_7	-76.059	168.703	4/1/25 22:53	TP/SG
228	Transit to Taygeta and Asterope	-75.982	168.695	4/1/25 23:31	TP
229	IcyMultibeam for Taygeta and Asterope	-75.982	168.653		TP
230	Dredge_43 at Taygeta	-75.959	168.585	4/2/25 09:20	TP
231	Could not approach Maia or Atlas. Transit to another dredge site due to ice ridges preventing us from re-dredge DR22 and Maia then to Asterope"	-75.963	168.735	4/2/25 10:23	TP
232	Dredge_44 at Asterope	-75.96	168.724	4/2/25 14:43	TP
233	MB survey filling gap at Taygeta smt	-75.985	168.686	4/2/25 16:29	TP

234	DriftCam TC_17	-75.979	168.658	4/2/25 18:36	TP
235	Transit	-75.915	168.807	4/2/25 19:25	TP
236	Dredge_45 at Alpha_Centauri_A, including ice breaking and situating the vessel (dredge in water at 21:38, on deck 22:46)	-75.914	168.82	4/2/25 20:26	TP
237	Transit (including breaking ice path 23:33-00:29)	-75.889	168.807	4/2/25 23:02	TP
238	Dredge_46 at Alpha Centauri_B	-75.892	168.809	4/3/25 00:29	TP
239	Transit, including breaking ice	-75.832	168.878	4/3/25 01:49	TP
240	Dredge_47 at Proxima Centauri	-75.836	168.869	4/3/25 04:46	TP
241	Transit, including breaking ice	-75.777	168.806	4/3/25 06:01	TP
242	Dredge_48 at End_Is_Near Peak	-75.777	168.789	4/3/25 08:25	TP
243	Transit	-75.73	168.775	4/3/25 09:32	TP
244	Dredge_49 at Potter Peak	-75.727	168.766	4/3/25 11:20	TP
245	Dredge_50 at _Potter Peak	-75.717	168.804	4/3/25 13:49	TP
246	Icy Multibeam at Potter Peak	-75.717	168.803	4/3/25 15:00	TP
247	Transit	-75.668	169.135		TP
248	IcyMultibeam and Smith_Mac_8 for rock people at Smith_Mac smt (smith Mac 22:29-23:07)	-75.654	169.063	4/3/25 22:09	TP
249	Deck reconfig (was almost done by noon ish), then science needed to work on "transit/demob prep" including cleaning deck gears/ECW, packing cargo, secure items in the lab, packaway items in helo deck, and clean the lab.	-75.654	169.063	4/3/25 23:07	TP/IW/SG
250	Transit to SLED site	-75.239	171.456	4/4/25 19:40	SG
251	SLED attempt 1 with , Ice breaking and MB, ice channel asessment at the launcing pt - no go.	-75.239	171.456	4/5/25 01:41	SG
252	Transit to SLED	-74.875	171.79		SG
253	SLED attempt 2 with Ice breaking and MB, ice channel asessment at the launcing pt - aborted.	-74.823	171.867	4/5/25 07:33	SG
254	Transit to further north	-74.735	171.936	4/5/25 09:59	SG
255	Ice breaking	-74.735	171.997		SG
256	Multibeam	-74.725	171.983		SG
257	SLED attempt 3 with drift assessment, ice breaking, MB, then ice channel asessment at the launcing pt - success EBS_23	-74.719	171.997	4/5/25 12:45	SG
258	SLED attempt 4 with drift assessment, ice breaking, MB, then ice channel asessment at the launcing pt - EBS_23: All science ops. Completed.	-74.456	172.263	4/5/25 18:41	SG
259	Voyage North (Leave the ice, enter EEZ)	-74.46	172.251	4/5/25 19:58	TP/IW/SG
260	Arrive in Lyttleton	-45.017	170.159	4/16/25 01:00	TP/IW/SG

3.4 Tominaga-Panter Team Organization

Name	Shift Time	Responsibilities
M. Tominaga	Floating, On call 24/7	Chief Scientist for Expedition NBP25-01 and PI of Tominaga-Panter Group
K. Panter	6 am to 6 pm, floating during dredging operations	PI of Tominaga-Panter Group, Lead of Dredge Operations
J.-N. Wu	12 am to 12 pm, floating during heat flow probe operations	Head of Heat Flow Probe Operations, Cruise Management, Science Lead of Tow Cam Operations
J. Preine	12 pm to 12 am	Cruise Management, Chief Editor and Coordinator of Cruise Report and Daily Reports, Science Lead of Tow Cam Operations, Weather and Ice Reports
C. Berthod	12 am to 12 pm, floating during dredge and coring operations	Head of Dredging and Coring Operations
M. Cannat	12 am to 12 pm	Watch standing, Science Support for Dredge and Tow Cam operations
E. Hayden	Floating, on call for tow cam operations	MISO Tow Cam Operator, Support for Dredge operations
M. Small	20-24 during transit, on call for tow cam operations	MISO Tow Cam operator, Watch standing
F. Neumann	Floating, on call for heat flow probe operations	Heat Flow Probe Measurements, Support for Dredge operations
J. Kalemba	12 pm to 12 am	Watch standing, Multibeam processing, Dredge operations
K. Shanks	12 am to 12 pm	Watch standing, Multibeam processing, Dredge operations
D. Wildrick	8-12 am during transit. On call for dredge operations.	MARSSAM Technical Lead of Dredging Operations, Watch standing

4. Multibeam Bathymetry

Jyun-Nai Wu

4.1 Overview

Bathymetric data during Expedition NBP25-01 was collected with Kongsberg EM 122 multibeam system at 12 kHz. The EM 122 sonar system transmitted a sound source and used a fan of narrow acoustic beams to create a map of seafloor by travel time of soundings. Data were collected throughout the entire cruise except for the area within New Zealand's Economic Exclusion Zone (EEZ), as well as during TowCam dive 003 for USBL system test, and rebooting sonar system for maintenance. Resolution of gridded product range from 10 to 30 m in surveying area depending on data quality, vessel speed and depth. Sound speed profiles were obtained by the nearest CTD cast or XBT cast conducted during this cruise. The mapped area extended from -77° to -75.5° S and from 163° to 169.5° E (**Fig. 4.1**). The newly mapped area extends over ~3,264 km^2, which covers ~2,233 km^2 of targeted seamounts where most area (~1,597 km^2) are gridded in 10 m and the rest of the area (~636 km^2) are grided in 20 m due to deeper depth.

4.2 Operation Strategy

Aims of mapping were to survey seamounts for morphological studies and providing information for other operations such as MISO TowCam and dredge. The survey route was first simply designed to have optimal coverage of mapping targets (**Fig. 4.2**). Once the ice condition became too severe to achieve quality multibeam data, our strategy was to first use the vessel to break ice along the survey line and return along the same path of broken ice for multibeam (**Fig. 4.3**). The mapping data quality depended on the routes which were optimized by assessing ice movement with ship drifting direction.

4.3 Processing

Multibeam data was processed with MB System, an open-source package managed by MBARI. Kongsberg EM122 system generated ".all" raw files which contain ship navigation, sound speed profile, tidal model, sounding travel time, and sounding distribution derived from information above. MB system reads and converts these raw files via *mbpreprocess* into MB System files (.mb59). Once the MB System files were generated, we manually edited the noise out of sounding distribution (i.e., sounding cloud) based on geological assesments. Noise sources were mostly from the sound of breaking ice, interference of Kundsen chirp sonar system, which ran at 3.5 kHz, and the heave of ship.

Besides noise of soundings, we also noticed angular misalignments during processing of overlapping patches of sounding from differently oriented angles. Angular misalignments are the disagreements between sonar system and ship motion reference unit (MRU), which can be corrected by applying attitude bias on roll, pitch, and heading of ship (e.g., Gueriot et al., 2000). We used grid search to find the optimal fitting in the overlapping patch (i.e., minimum misfit between soundings from different looking angle), and determined a roll bias of ~0.6 degree in certain areas (**Fig 4.4**).

Once editing processes done, we gridded with beam footprint slope algorithm (-F5 in *mbgrid* function). This algorithm first grids the raw data with lower resolution (twice the final grid size) and with a simple mean filtering to determine slope for each cell in final grid. Then based on local slope and sonar altitude above seafloor, the footprint of the beam and the weight of each

sounding in the footprint was determined. This approach allowed us to grid the raw data with optimal resolution.

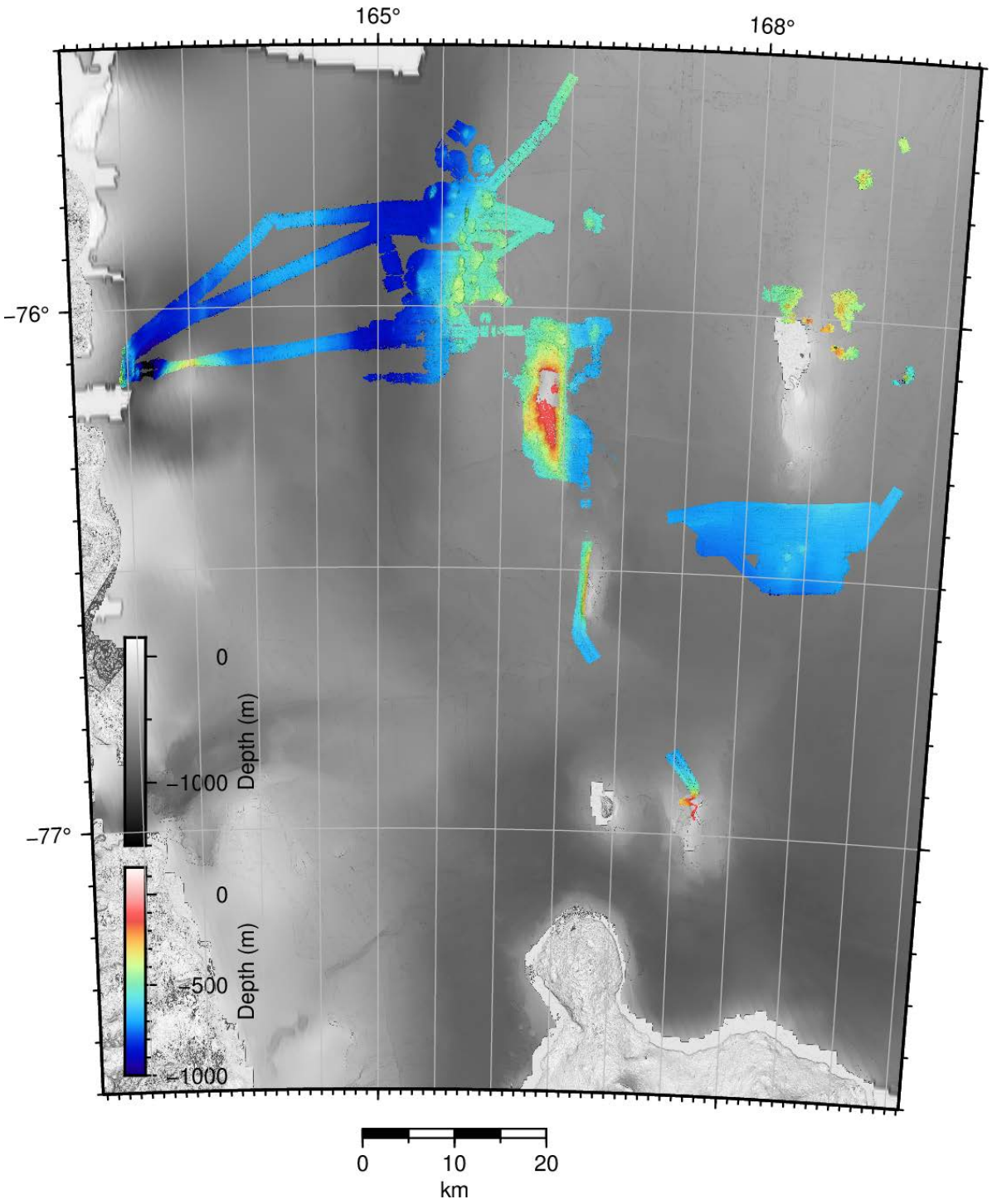

Figure 4.1: Bathymetric data coverage map. Previous data are shown in grayscale and newly added data are shown in colorscale. Noted that the grid around -76.5°, 168° is combined grid with NBP1502 data downloaded via Rolling deck to Repository (R2R).

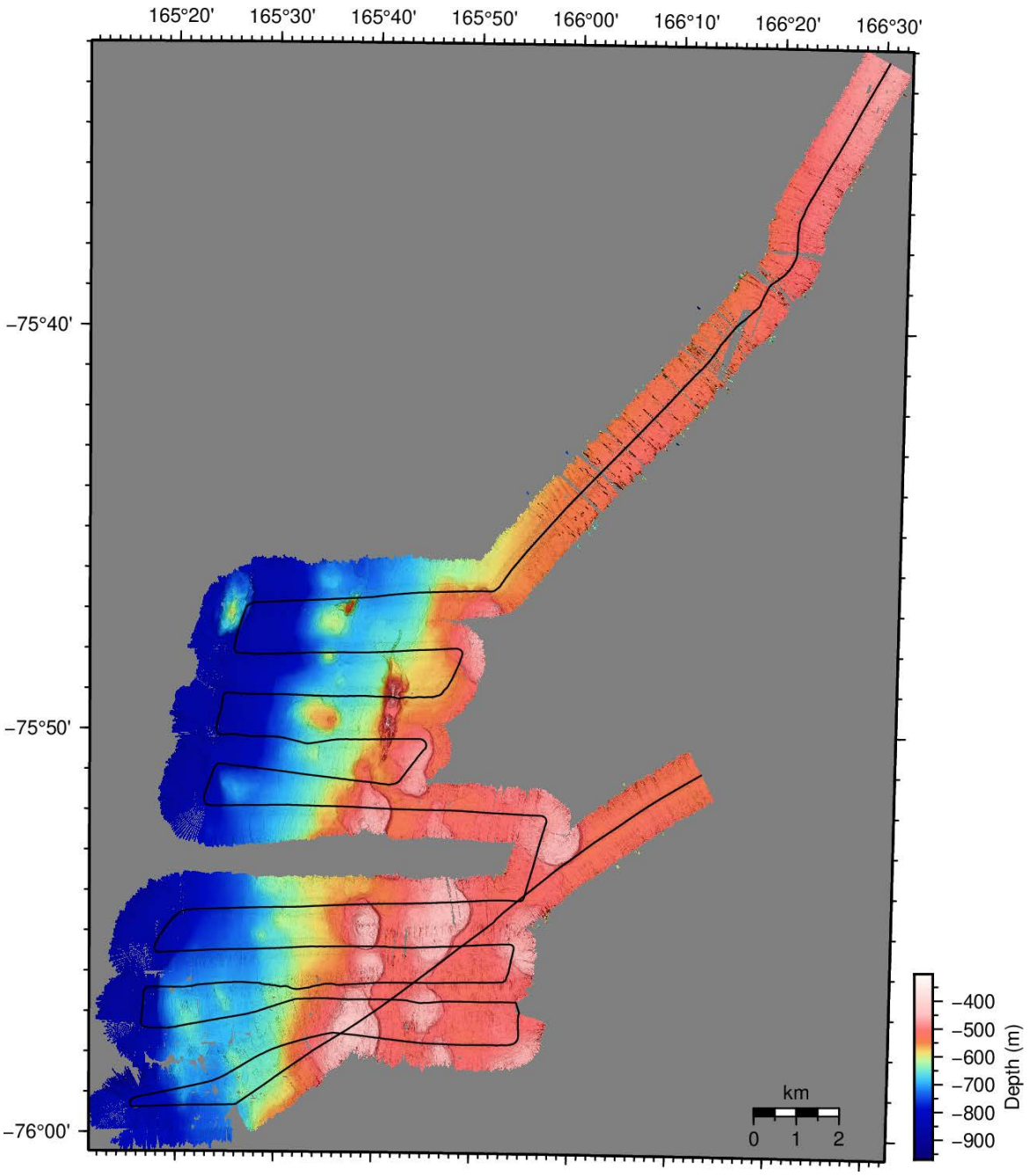

Figure 4.2: Mapping routes (black line) in the flat-topped seamount area that were designed to optimize the coverage. These lines were recorded in largely ice-free conditions.

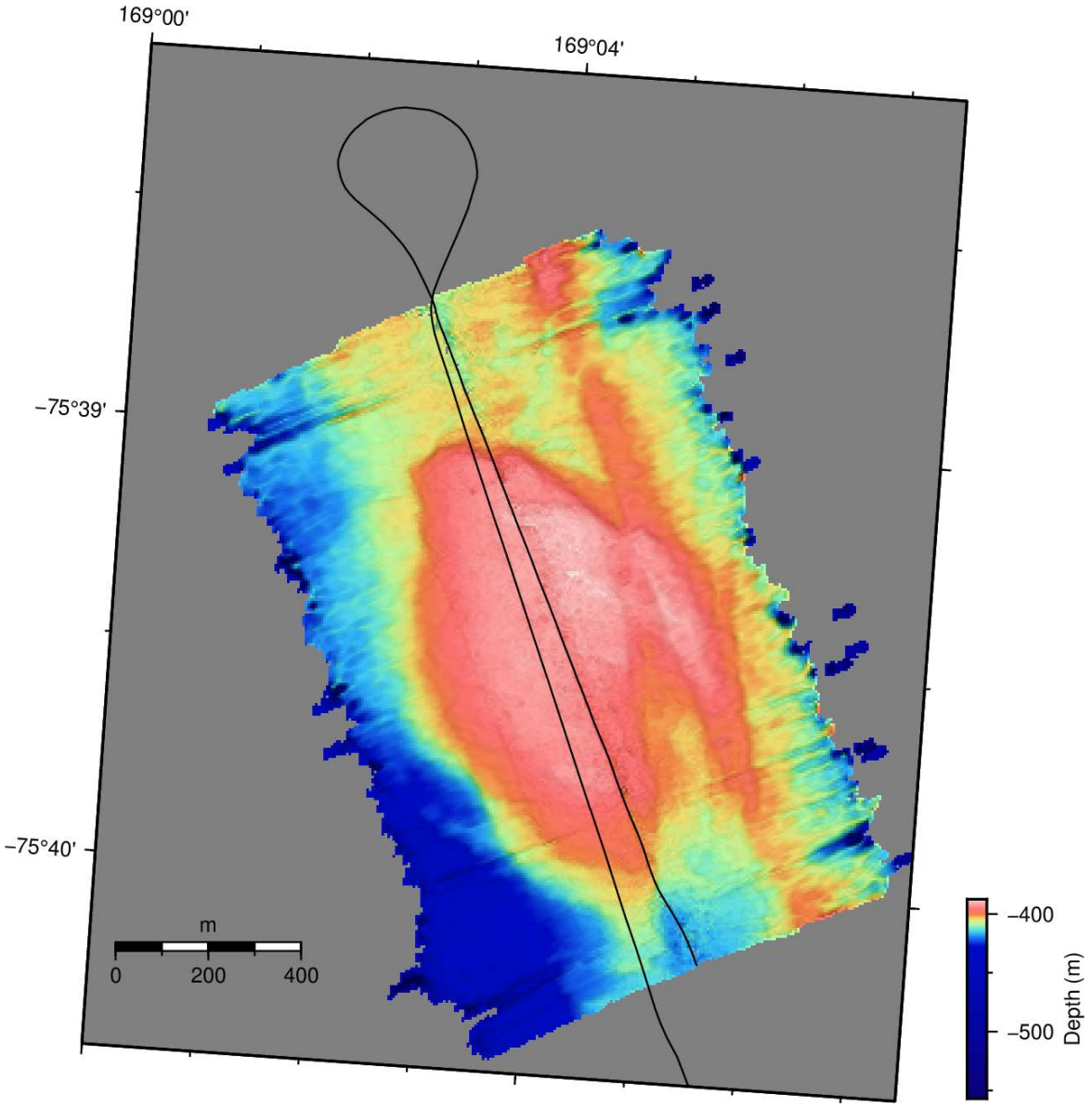

Figure 4.3: Mapping routes (black line) that were designed to break the ice and conduct survey. Northwest-bound route was the ice breaking path and southeast-bound is the mapping path along the broken track. Note the deviation of both paths due to the ice drift.

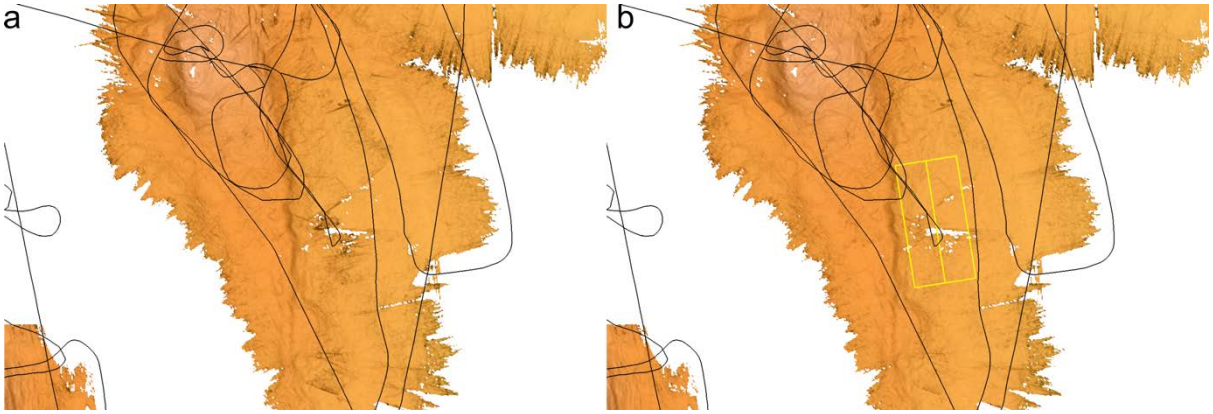

Figure 4.4: Example maps before and after applying roll bias of 0.6 degree. a) Original data gridded with 10 m resolution. b) Corrected data gridded with 10 m resolution, yellow box show the overlapping patch used to determine the bias.

5. Chirp Echosounder

Jonas Preine

5.1 Overview

The Knudsen Chirp Echosounder is a sub-bottom profiling system that emits frequency-modulated acoustic pulses (chirps) into the water column. These pulses penetrate the seafloor and reflect off subsurface layers with varying acoustic impedance. The system records the returning echoes, which are processed to generate high-resolution images of the uppermost subsurface structure.

Besides using the subsurface imagery for geological interpretations, we used the Knudsen Chirp Echosounder during Expedition NBP25-01 for determining the most promising locations for heat flow probe and coring deployments.

Data acquisition commenced upon exiting New Zealand's Exclusive Economic Zone (EEZ) and continued until re-entering it. Recording was occasionally interrupted when conducting dedicated multibeam mapping, as we observed intermittent interference between the two systems.

5.2 Operation Principles

The system operates by:

Transmitting a chirp signal: The echosounder emits a swept-frequency pulse, typically ranging from 2 to 12 kHz, which enhances resolution and penetration compared to single-frequency pingers. In our case, we operated the chirp with a frequency of 3.5 kHz.

Signal propagation and reflection: The acoustic signal propagates through the water column and penetrates the seafloor. At boundaries between different sediment layers, some of the energy is reflected back to the receiver.

Receiving and processing echoes: The transducer detects the returning signals, which are then amplified, digitized, and processed to construct an acoustic profile of the seafloor and shallow subsurface.

This method allows for the identification of stratigraphic layers, sedimentary structures, and potential coring and heat flow probe sites by providing continuous subsurface imaging along the survey track.

5.3 Acquisition Parameters

During the transit, we performed a dedicated parameter testing to ensure the best data quality for our purposes. For the system operated onboard RVIB Nathaniel B. Palmer we determined the following acquisition parameters as the most important ones:

- **Tx Pulse**: The length of the frequency-modulated sweep. Typically set to 8 ms. Depending on the water depth and sea/ice state it was varied between 4 and 16 ms.
- **Tx Power**: The power level of the transmitted acoustic signal. Adjusted based on survey conditions, typically set to 1 ms. In great water depths and more difficult sea/ice states, we set it to up to 3 ms.

- **Gain Value**: Amplification applied to the returning pulse to enhance signal detectability. Typically set to 28 dB.
- **TVG Mode**: Time-varying gain (TVG) was applied as a standard post-processing step rather than during data acquisition. Generally set to *None*.
- **Process Shift**: Display gain adjustments only for visualization. Does not affect recorded data. Generally set to 0.
- **Global TX**:
- *On*: Both 3.5 and 12 kHz signals transmitted. Will significantly degrade the 3.5 kHz signal.
- *Off*: Both frequencies disabled.
- *Mixed*: Either 3.5 or 12 kHz transmitted; we used only the 3.5 kHz configuration.
- **Range**: Defined the recording window length, where a larger range resulted in lower resolution due to constant sampling across the window. Typically set to 100 ms for high-resolution surveying, otherwise set to 200-500 ms during transit.
- **Phase**: Controls the minimum and maxium length of the recording window – signals outside this window were not recorded.

Data were initially recorded in .keb and .kea formats and subsequently converted to SEGY using the conversion utilities in Knudsen Post Survey Software. For onboard data visualization, we used the SeisPhro software developed by the Institute of Marine Sciences of the National Research Council of Italy (CNR-ISMAR), as well as SeisSee (**Fig. 5.1**).

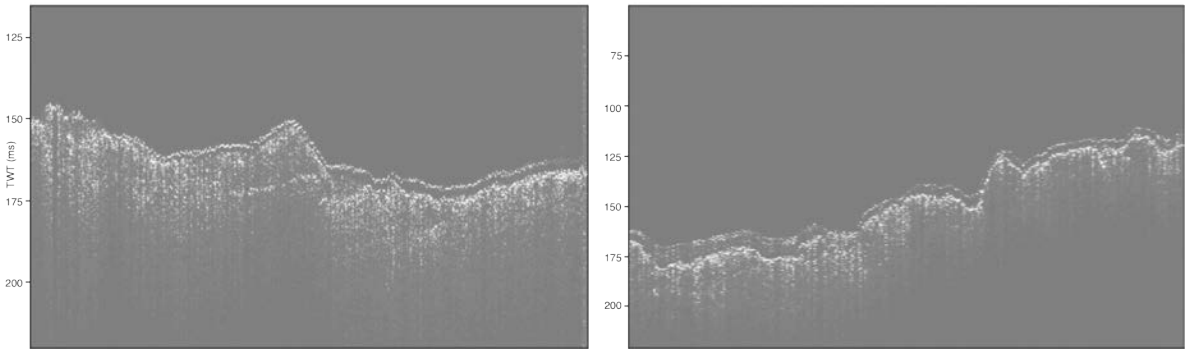

Figure 5.1: Data examples of the Knudsen Chirp Echosounder in the Ross Sea. TWT: Two-way travel time.

6. MISO Tow Cam

Eric Hayden, Marissa Small, Mathilde Cannat

6.1 Overview

The MISO (Multidisciplinary Instrumentation in Support of Oceanography) TowCam system prepared for NBP25-01 provided high quality live seafloor imaging along with complementary environmental data.

Figure 6.1: TowCam being deployed off the stern of the Palmer during NBP25-01.

On NBP25-01, most TowCam operations were performed in conjunction with dredging operations. With high quality imagery from the TowCam complementing the physical samples obtained from dredging, a robust characterization of the seafloor geology was achieved. To this end, the TowCam was usually deployed either 1) before a dredge to inform decisions on upcoming dredge location or 2) after a dredge to visually confirm

bottom characteristics. The TowCam was deployed 17 times between February 23rd and April 2nd at the locations shown in **Figure 6.2**.

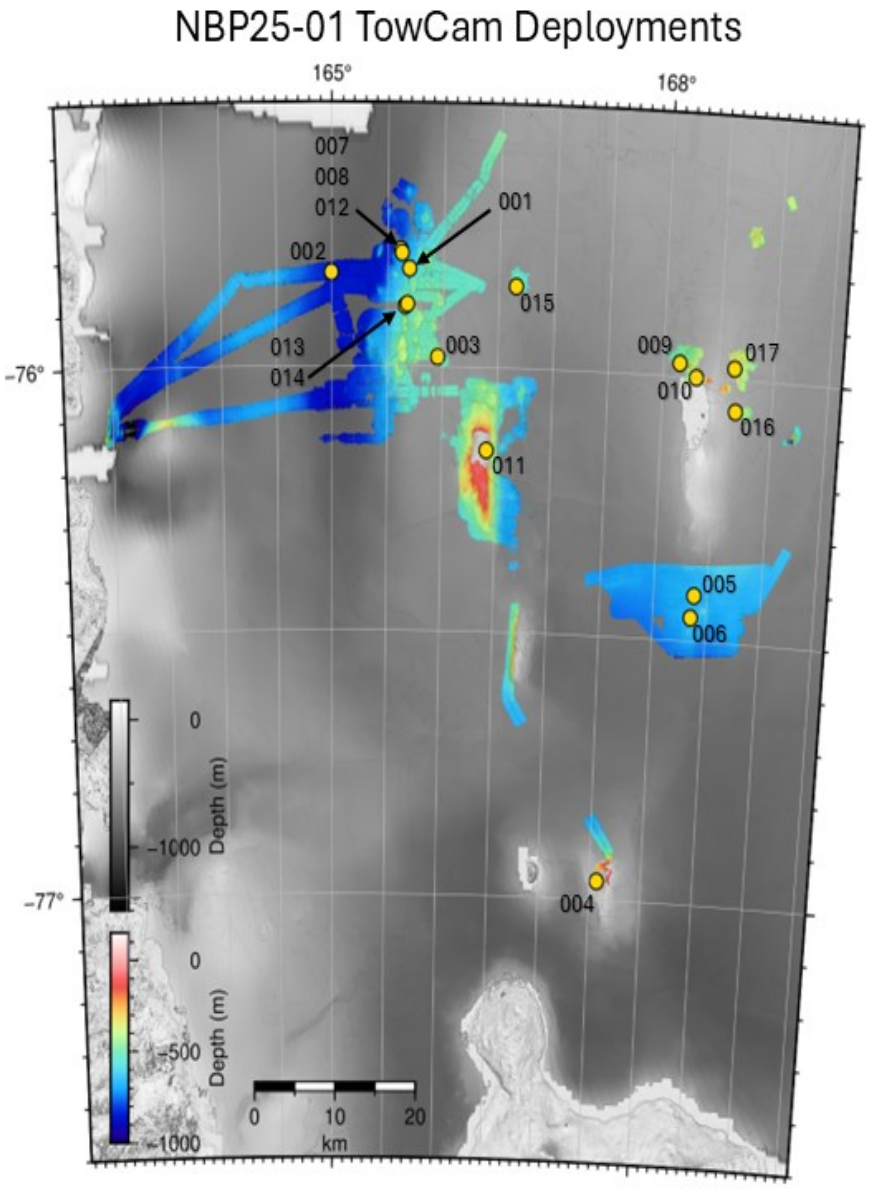

Figure 6.2: Map of all TowCam deployment locations during NBP25-01.

The TowCam system consisted of the following instrumentation mounted on a towable frame (**Fig. 6.1**):

- MISO DataLink telemetry system - serial and ethernet I/O
- MISO Fiber to Ethernet telemetry system
- OIS-24MP (MegaPixel) camera and 300 watt/s strobe

- MISO GoPro 5.3k cinematic video, self-recording camera lit by ~9000 lumen DSPL SeaLite LED subsea light
- DSPL IP Seacam HD video camera lit by DSPL LED SeaLite, recording continuously via screen recording on the Mac laptop used to view the video stream
- RBR CTD with O2 sensor
- NOAA Miniature Autonomous Plume Recorder (MAPR)
- MISO scaling green lights - 19.7cm apart
- 2 WHOI magnetometers (for high resolution near-bottom magnetic gradiometry)
- USBL acoustic positioning beacon
- VA500P depth/altitude sensor
- VA500 range altimeter mounted forward-facing for obstacle avoidance

The TowCam was deployed off the stern of the Palmer and lowered on the ship's .680 cable to an altitude that allowed for good imagery (roughly 2-6m off the bottom). It was then towed along a predetermined trackline at a speed of < .5 knots while maintaining acceptable altitude. Later in the cruise, ice conditions prohibited active towing. However, the ship was able to drift with surrounding ice sheets with the TowCam deployed, so surveys were still possible at speeds of ~.3 knots. For more detail about operating in ice, see Section 6.8. The trackline (or point of interest for drifting) was determined in advance of deployment by the science party, with input from the TowCam engineers to ensure optimal imagery and timing, and that the trackline did not pose any operational hazards. General slope of the trackline (uphill or downhill), extremity of seafloor features (outcrops, spires), vertical heave from sea state and towing speed were all factors that introduced various levels of risk of grounding the TowCam. The response to any increased risk was to appropriately increase towing altitude, ensuring system safety at the temporary expense of image quality.

During each tow, the following can be viewed in real time from the topside through a fiber optic connection to the system (**Fig. 6.3**):

- Video from the IP SeaCam
- Low-resolution stills every 10 seconds from the OIS camera
- Depth, altitude and range from the Valeport altimeters
- Magnetometer data (x, y, z axes, and total field)

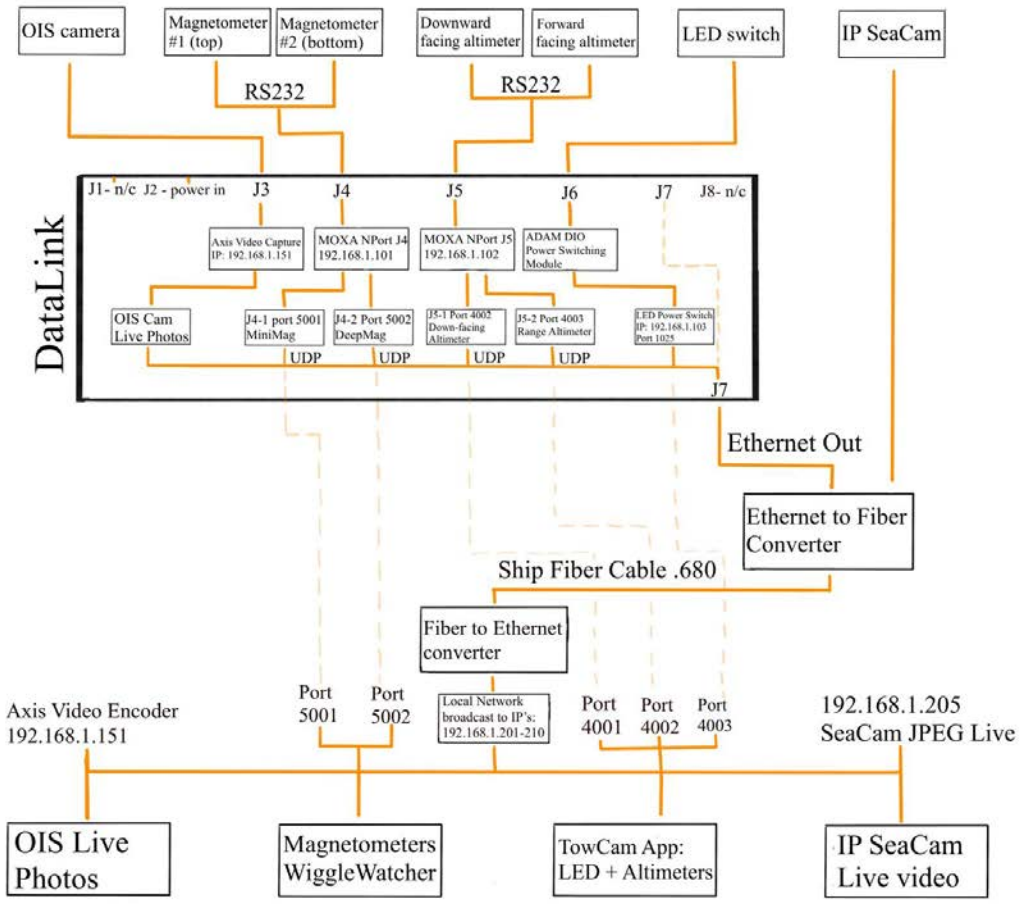

Figure 6.3: Overview of TowCam live data transmission over fiber-optic cabling.

The complete data set collected on each tow consisted of the following:

- 24MP still images from OIS camera every 10 seconds
- Continuous 5.3k GoPro video
- Continuous 1080p video (screen recording of DSPL IP Multi SeaCam)
- TowCam altitude and depth recorded at 1Hz
- Heading (including raw accel/mag data) and temperature recorded at 1/60Hz (MAT-1 Logger)

- Light-backscattering, oxidation-reduction potential, temperature and pressure recorded at 1/5Hz (MAPR)
- Conductivity, pressure, depth and optical dissolved oxygen recorded at 1Hz throughout deployment (CTD)
- Magnetic data collected throughout deployment at 6.8Hz (APS1540 Magnetometers)
- Ship navigation data collected throughout deployment (Seapath 380 GPS)
- USBL (EvoLogics 18/34 system) navigation data

6.2 Positioning

The positioning of the TowCam was determined by an Evologics USBL (Ultra-Short Baseline) acoustic underwater positioning system. The USBL transducer head was mounted on the end of an 11.6 meter pole loaned by the Sentry program which could pivot between horizontal (stowed) and vertical (deployed) positions (**Fig. 6.4**). The USBL beacon was mounted on the TowCam frame. The pole was lengthened for this particular cruise so that when deployed, the transducer head was positioned well below (~1.4 meters) the lowest point of the Palmer's hull. This ensured that there was no physical acoustic shadowing between the head and the beacon. The USBL transducer head was attached to a power and comms cable that ran up the inside of the pole to the aft control room providing a live view of the positioning data. The Evologics SiNAPS software was used to view the live position data, and log the positions into a database file.

We began the cruise with a USBL system that used frequencies from 7-17Hz, and were unsuccessful in establishing communication between the beacon and the head. After communication, noise, and temperature testing, we determined that ship noise had resulted in the transducer head not being able to distinguish the signal from the beacon, and switched to a USBL system using frequencies from 18-34Hz which was successful. Due to ice conditions, it was not always possible to deploy the USBL transducer pole. In these cases, TowCam position was determined with the ship SeaPath 380 GPS data, by calculating the offset of the TowCam tow point from the ship GPS. This was only possible since it was noted that the winch's "wire out" value consistently matched TowCam depth within 1-2 meters. Based on the proximity of these values, it was inferred that the TowCam was positioned almost directly beneath the tow point on the A-frame.

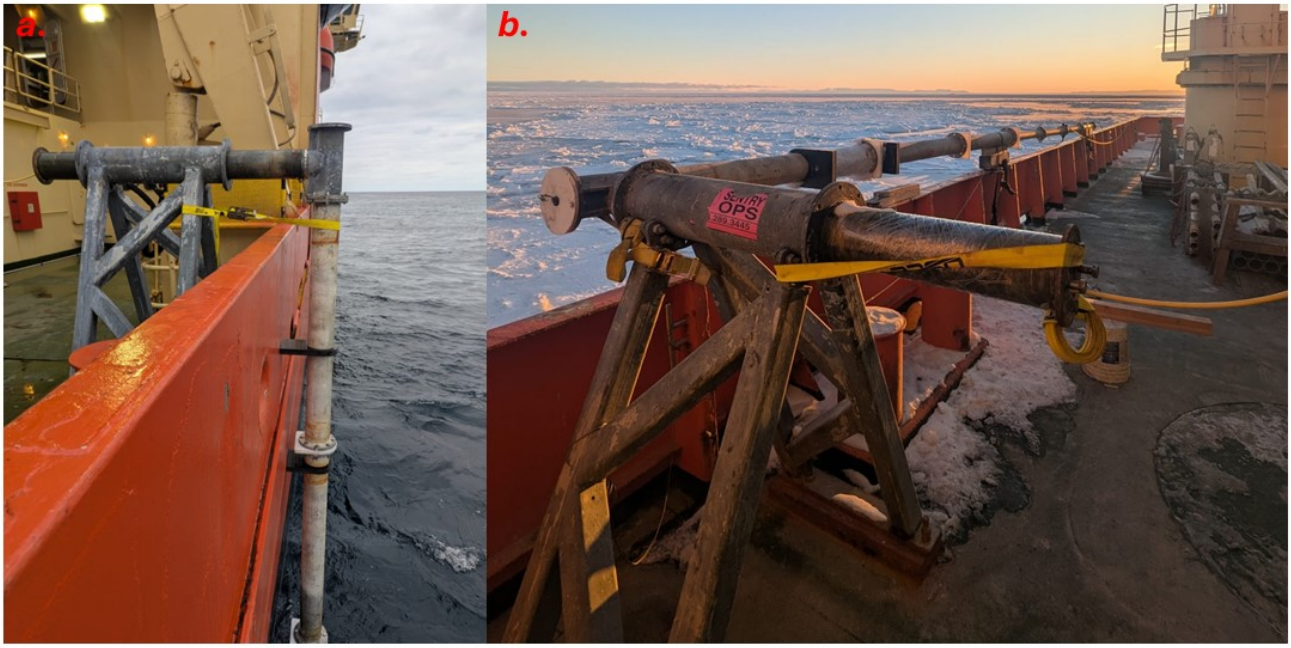

Figure 6.4: USBL Pole set up on the deck of the RVIB Palmer for NBP2025-01 in deployed **(a)** and stowed **(b)** positions.

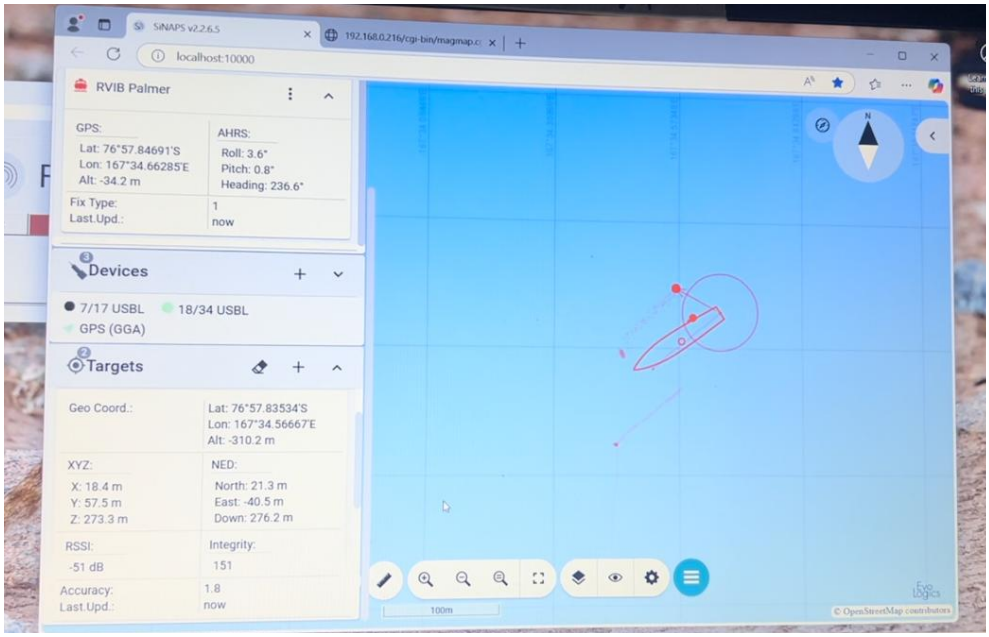

Figure 6.5: SiNAPS Software displaying location data of the TowCam during TC005, shifted -90° off in the yaw axis due to offset mounting of the USBL head. This offset was fixed in post-processing for accurate positioning data.

6.3 Imagery

The MISO TowCam has three main imaging instruments. The MISO GoPro, the OIS (Ocean Imaging Systems) Digital Still Camera, and the DSPL (DeepSea Power and

Light) IP SeaCam. The MISO GoPro provides high resolution video footage downloaded post-dive, while both the OIS Camera (stills) and the IP SeaCam (video) are viewed live during the tow.

The MISO GoPro is a fixed focus camera system consisting of a 6,000 m rated housing with a dome port optimized to correct for image distortion and yield a depth of field which extends from ~ .5 m to infinity. Inside the housing is a GoPro HERO11 camera module with a 5.4 mm non-distortion lens, axially aligned with the corrector and dome optics. The MISO GoPro records internally to a 1TB SD card that is downloaded after recovery of the TowCam. The GoPro records continuous 5.3k video at 30fps (frames per second), set to auto exposure with max 800 ISO, min 400. The MISO GoPro was mounted on the TowCam frame facing directly downward, capturing continuous footage throughout the dive. Illumination for the MISO GoPro is provided by a ~9000 lumen LED SeaLite made by DSPL.

The OIS (Ocean Imaging Systems) Digital Still Camera consists of a 24MP (megapixel) Nikon D3300 DSLR camera inside a 6,000 m pressure rated housing. The OIS camera points directly downwards, and captures still images at regular time intervals, set to every 10 seconds during NBP2025-01. The photos are illuminated with a 300 W/S strobe that is set to trigger simultaneously as the photos are captured. The strobe is wired in conjunction with the OIS Camera through a power junction box (Jbox). The OIS Camera's F-stop and ISO are set before each dive, and were set to 400 ISO (light sensitivity) and 6.3 F-stop (aperture) for each tow. The photos are viewable live at a reduced resolution, through an Axis M7001 Video Encoder capture box. The low resolution photos are transmitted through the DataLink telemetry system in conjunction with the fiber optic cable, and available on the local TowCam network.

The IP SeaCam, designed by DeepSea Power and Light is a fixed focus dome port camera that streams 1080 p video at 30 fps. It has a wide field of view, 105° H x 60° V, which supports its use to 'pilot' the TowCam during operations. The wide field of view also captures a larger swath of the seafloor topography. The IP SeaCam is mounted on the fin of the TowCam facing down and forwards. The depth of field extends from ~100mm to infinity. The IP SeaCam video is transmitted through the .680 ship fiber cable to the topside local network, where it is recorded via a screen recording. Like the GoPro, its lighting is provided by the DSPL LED light.

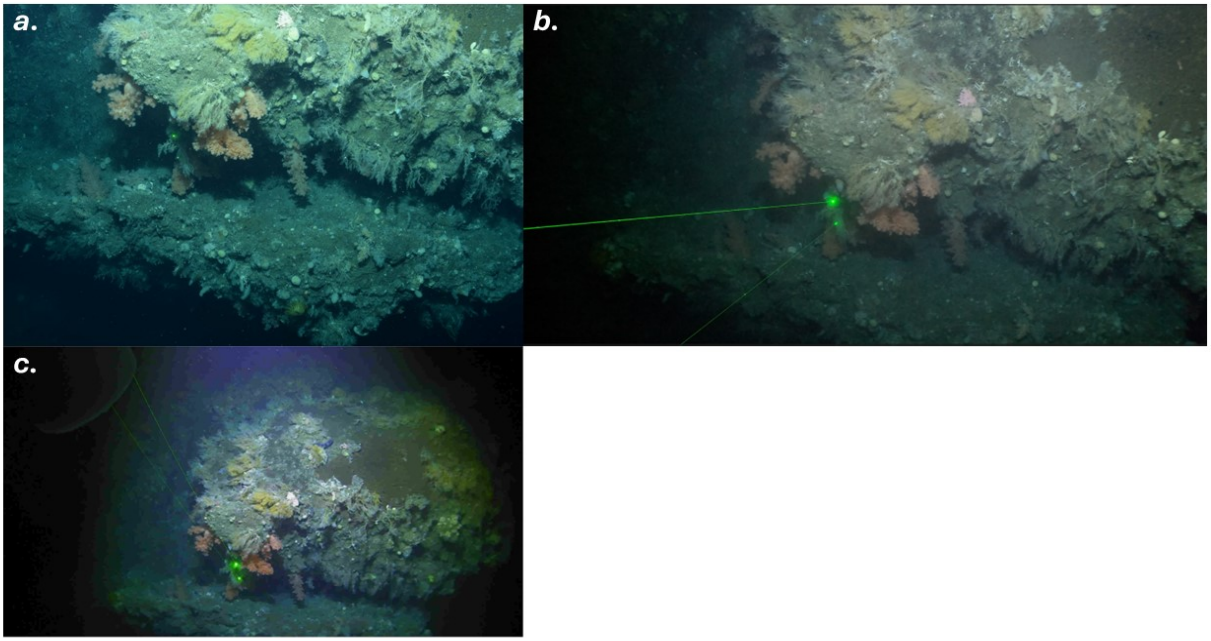

Figure 6.5: Simultaneous imagery from **a.** OIS camera, **b.** GoPro, and **c.** IP SeaCam, from TowCam007 (Feathertop seamount). Images taken at 23:17:38, Altitude 3.25m, Depth 508.30m

6.4 Magnetometers

To gather high resolution magnetometry data of the seafloor we utilized two APS1540 24-bit 3-Axis Fluxgate magnetometers, one titled “MiniMag” (top of fin) and the other “DeepMag” (bottom of fin). The magnetometers were mounted on the plastic tail fin of the TowCam, spaced .5 meters apart vertically to provide a measurement gradient (**Fig. 6.7**). Magnetic field data was measured in Gauss (G) units, with a precision of ±0.65G down to the threshold of the system noise level, 5 x 10^{-6} G. The magnetometers each contain three ring core fluxgate sensors that measure the magnetic field, and analog processing electronics that produce analog output voltages proportional to the measured magnetic field. The analog output voltage data provides measurements of the magnetic field in the x, y, and z axes, at a sampling rate of ~6.8Hz, which is then converted into a digital format with three 24-bit A/D converters. The magnetic data is corrected according to the calibration loaded onto the system microprocessor. The magnetometers also measure temperature in degrees C.

The 24-bit corrected serial data is transmitted through an RS232 interface to an NPort MOXA in the TowCam DataLink ethernet telemetry system, converted to fiber optic transmission up the ship’s .680 cable, and then converted back to ethernet on the topside, which makes the serial data transmittable on the local TowCam network. On the topside, serial data from the APS1540 magnetometers is viewed live and recorded by the WiggleWatcher app, designed by Zac Berkowitz (**Fig. 6.7**). WiggleWatcher logs the time, temperature, magnetic field x-component, magnetic

field y-component, and magnetic field z-component as an ASCII text format log file. WiggleWatcher also calculates the total field measurement and plots this data live, but this data is not recorded in the log. Each magnetometer produces one ASCII text format log, and they are divided into 1 hour partitions.

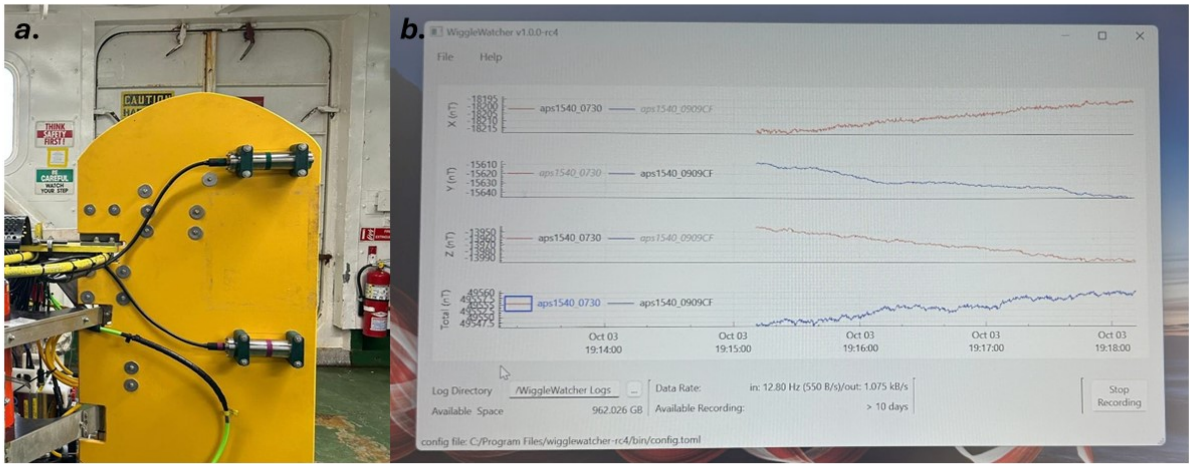

Figure 6.7: (a) APS1540 magnetometers mounted on the TowCam fin, .5 m apart and **(b)** WiggleWatcher App displaying live magnetometry data for x, y, and z axes, and total field measurement

6.5 CTD

To acquire physical oceanographic information, the TowCam was equipped with a Ruskin RBR-multichannel concerto^3 CTD. The CTD was set to sample in 1 Hz and measure temperature, salinity, pressure, oxygen, and conductivity, and derived sound speed profile (**Table 6.1**). The CTD is self-recording and powered by 8 lithium AA batteries that allows >2 weeks recording, and was mounted on the port side of top of the frame (**Figure 6.8**). Data was read by RBR software, while it was also possible to stream via modified cabling. During dive TowCam 012, we tested streaming the CTD data over the DataLink system and succeeded. All data were stored as raw data (.rsk), excel, and ASCII file format.

Table 6.1: Specification of RBR-multichannel sensors

Sensors	Resolution

Temperature	< $5*10^{-5}$ °C
Conductivity	0.0001 mS/cm
Pressure	0.001 dbar
Dissolved Oxygen	1% of saturation

6.6 MAPR

To detect potential hydrothermal-related signals, we mounted a NOAA Miniature Autonomous Plume Recorder (MAPR) onto the TowCam. MAPR is a self-recording device with 4 alkaline 9V batteries which was mounted on the starboard side of top of the frame (**Figure 6.8**). In the later dives (after dive TowCam 010), we mounted a second MAPR on the wire to test its functionality. MAPR was set to sample in 0.2 Hz and measure oxidation-reduction potential (ORP), turbidity, temperature, and pressure. The basic principle is that as heated and buoyant fluid in crust flow out and mix with seawater, mineral precipitate to form warm, particle-rich plumes that contain abundant reduced chemical compounds (e.g., Tivey, 2007) leading to detectable anomalies in temperature, turbidity and ORP (e.g., German et al., 2008). Among most dives, all three measurements remain relatively stable throughout the dive. Several dives on top of seamounts show drops of ORP but we consider these drops too sparse to be statistically significant.

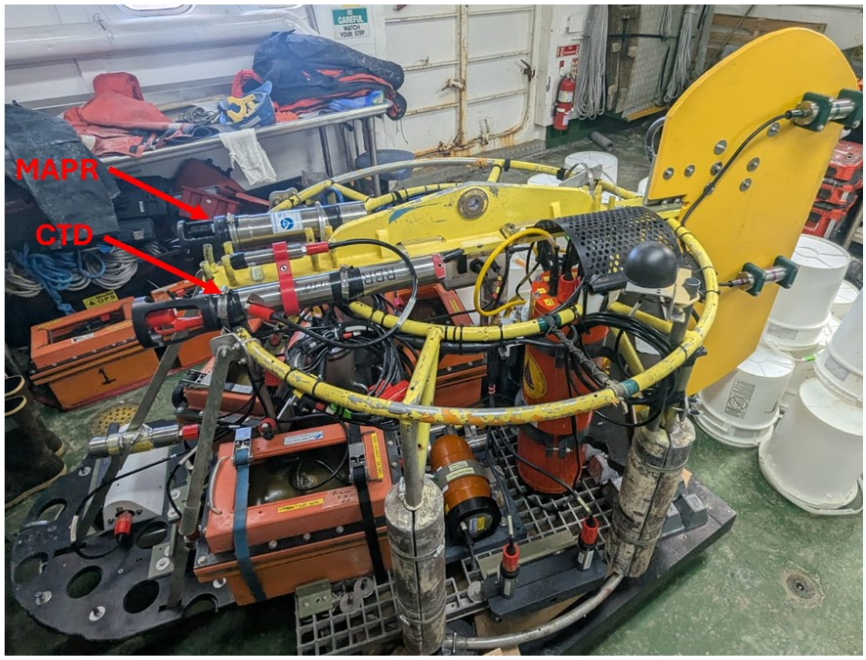

Figure 6.8: MAPR and CTD mounted on the TowCam in forward-facing positions

6.7 Dive Overview, Examples

Typically, a TowCam deployment would proceed as follows:

Three hours before intended launch time, the predive preparation would be started by TowCam engineer Marissa Small. This consisted of checking battery voltages, ensuring all clocks are set to UTC, preparing all cameras and verifying their settings, starting the compass recording, and starting MAPR and CTD recording (the latter normally done by scientists Jyun-Nai Wu or Jonas Preine). Once all instruments were set up and mounted on the TowCam frame, the TowCam is considered 40 minutes to being ready for deployment. At this point system functionality and comms checks would be performed between the TowCam system and the topside, connected by an optical fiber running from the wet lab (TowCam staging area) up to the aft control room (topside location). As the instruments on the TowCam were physically activated by one person in the Wet Lab, another person would make sure that all expected data was appearing on the topside laptops. Communication between these two engineers was over radio. This process included confirming that the LED light could be triggered remotely from the topside, as well as confirming live streaming of altitude, depth, forward range, magnetometers, IPSeaCam, and OIS camera stills.

At some point preferably prior to- but often during the predive process, the intended trackline would be decided upon by science, with input from the TowCam engineers, marine techs, and bridge; after science identified the area of interest, the approach would be discussed taking into consideration weather, ice conditions (passive drifting vs active towing), and bathymetry.

Once the ship was on station, ready for deployment, a brief standup meeting would be held in the wet lab with two TowCam engineers, USAP marine techs, and a member of the science party present. The purpose of this meeting was to summarize operations and timing before beginning the deployment so that everyone was on the same page. After this meeting, the TowCam was moved out onto the back deck and hooked up to the .680 cable by MT's and TowCam deckside engineer, while topside personnel (TowCam topside engineer, AB winch operator, and scientist) took their positions in the aft control room. After connecting to the ship's cable, system functionality and topside connectivity were re-confirmed and camera strobe and scalars were enabled directly before launch.

Launch and recovery deck ops were directed and conducted by USAP MT's and ship's AB controlling the winch and A-frame. "Off deck" and "in water" times were noted in the TowCam engineering log, and the winch was zeroed as the TowCam touched the surface. The winch operator was instructed to pay out wire to ~50 m less than water depth at a speed of 30m/min. During the first 50m of pay out, system functionality was continually monitored and tested by turning the LED light on and off. After 50 m depth, the topside engineer radioed the deck engineer that the system was functional and the deployment would proceed. At this point, the deck crew

could stand down.

On NB Palmer, each tow required four people to be present at the topside:

1. Ship's AB to operate the winch
2. TowCam engineer to dictate winch operations and keep engineering log
3. Science party representative to observe, take notes and make operational requests
4. USAP Marine Tech to communicate with the bridge as needed for ship maneuvering

Within 50 m altitude the TowCam engineer directed a bottom approach, watching altitude and live feed from the downward facing IP SeaCam, and taking into account any heave from the ship. Once a clear bottom image was achieved, altitude and image quality was confirmed as acceptable to the topside scientist, and the survey was commenced (if towing, ship was directed to move along trackline at .5 knt; if drifting, no action was required). During the survey, live video and altimeter values were used to actively "pilot" the TowCam by paying wire in and out to adjust the altitude of the system to optimize imagery and avoid obstacles. An engineering log was kept at ~10 minute intervals, and for any notable event.

On NBP25-01, most surveys (bottom time) lasted less than two hours. When the survey was completed, either due to direction from the science party or operational time constraints, the AB was instructed to pay in at 40m/min, bringing the TowCam back to the surface for recovery. The LED light was turned off before reaching the surface. Recovery operations were directed and conducted only by USAP MT's and ship's AB controlling the winch and A-frame. "On surface" and "on deck" times were noted in the TowCam engineering log. Once secure on deck, the TowCam was disconnected from the ship's cable, strobe and scalars were disabled, and the entire system was rinsed with fresh water before being moved inside to the wet lab.

Upon arriving in the wet lab and being strapped down, the TowCam was usually covered in ice. Individual instruments (GoPro, OIS Camera, MAPR(s), CTD, and compass) were removed from the tow frame and thawed under lukewarm water. Special care was taken not to expose the glass domes of the camera housings to warm water before they had thawed sufficiently in air. Once the ice covering each instrument had been melted, the instrument was dried and brought into the dry lab to begin the data offload process. Post-deployment battery voltages were noted and batteries were put on charge.

6.8 Operations in Ice

As the season transitioned from summer to winter, worsening ice conditions presented challenges to TowCam operations. By the time of TowCam007 (March 10), it was deemed too hazardous to deploy the USBL pole. There was concern that ice

would build up in front of the pole during a tow and cause extreme stress to the system. There was also concern that passing ice would abrade the forward stay as it pinched the line against the hull, and potentially cause it to weaken or part. Both of these concerns were related to equipment and personnel safety. See **Figure 6.9** for photo of ice conditions prohibiting use of the pole.

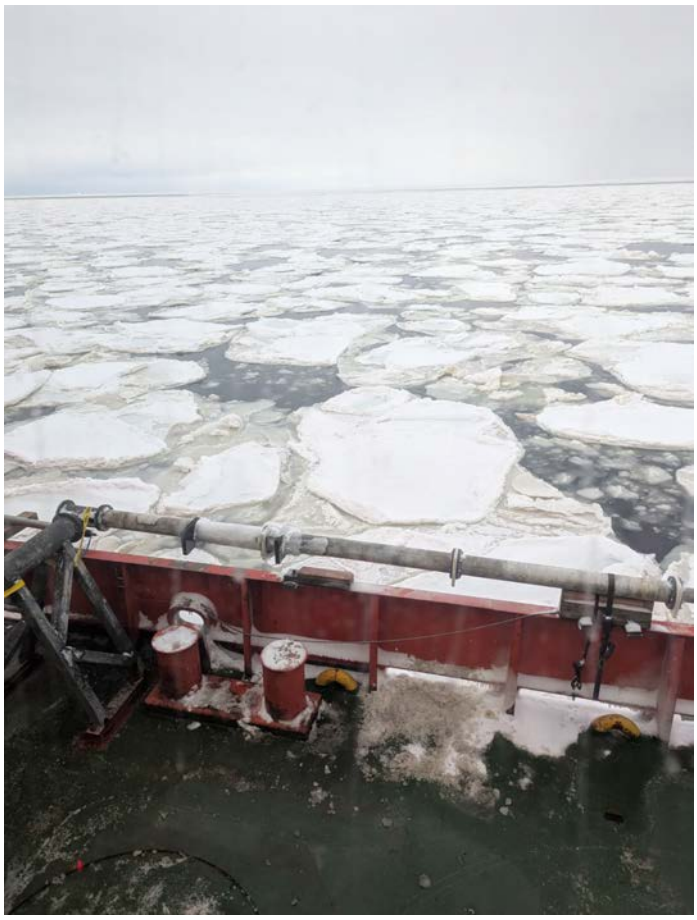

Figure 6.9: Ice conditions on March 10, when USBL pole deployments were discontinued.

As previously stated, in the absence of USBL positioning, the TowCam's position was inferred to be directly below the tow point due to its reported depth being within 2 meters of the wire payout value (if there was any wire angle due to kiting, these values would have been more significantly different). Therefore the TowCam position could be determined as a consistent offset from the ship's GPS.

By the time of TowCam012 (March 28), the ship was no longer able to reliably tow the TowCam at the requested speed of .5 knt along a predetermined trackline, while breaking ice. However, the ice itself was drifting at a fairly predictable speed and heading and the ship was able to drift with the ice. By predicting the ship/ice drift (particularly speed and direction), TowCam surveys could still be achieved with sufficient planning. Trackline direction was now dictated by environmental

conditions, but the ship could still be positioned so that it would pass over a specific target during the survey. “Drift” deployments proceeded as follows:

1. Target of interest was identified by science
2. The ship positioned itself on top of the target and drifted with the ice to quantify speed and direction of drift
3. Based on this information, a deployment location was identified at a distance and heading that would allow for the TowCam to reach the bottom before passing over the target of interest
4. Ship positioned itself at the deployment location, and created an opening in the ice large enough to deploy the TowCam
5. Ship began drifting as TowCam was deployed and lowered to the bottom.
6. If drift predictions were accurate, the TowCam would complete a survey including the point of interest.

This method was used, largely successfully, for tows 012-017 (final six deployments of the cruise). Drift speeds were normally ~.3 knots.

6.9 Geological Overview

Mathiled Cannat, Kurt Panter, Carole Berthod, Jacquelyn Kalemba, Katherine Shanks

This preliminary geological analysis was conducted based only on the OIS camera photographs, guided by notes taken by observers during each of the cruise's 17 TowCam dives. Representative photographs were selected and commented, and a short summary paragraph was drafted for each dive. This report provides a summary of these observations.

Selected observations were also relocated on the dives navigation and exported as a single shapefile (TOWCAMgeologicalfeatures) for the 17 dives.

6.9.1 TOWCAM dive NBP25-1-01

February 23, 2025 / Top and east slopes of Squid Ridge

Clear outcrops of a rubbly material (volcanic breccia?) at start of dive, with an upper surface that is smooth, with a scaly foliation and rusty to black stains. Rubbly material under is not stained. Then just under the top surface of the ridge, in the steeper slopes underneath, outcrops of the dark gravel formation, with rocky-rubbly ledges, grey fine grained patches (ash?), and angular loose rock fragments. This dark gravel formation is present, as outcrops or degraded, and locally under up to a few decimeters of mud, from top to bottom of the ridge... and even on the flat surface that forms the base of Squid Ridge.. There, however, we see smooth rusty stained surfaces again.

Top of Squid Ridge, eastern edge of corrugated upper platform	Just under the edge of the platform, outcrop of the dark gravel and rubbly ledges volcanic formation

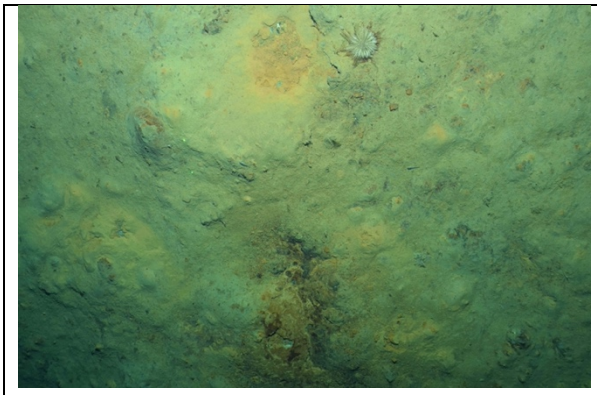	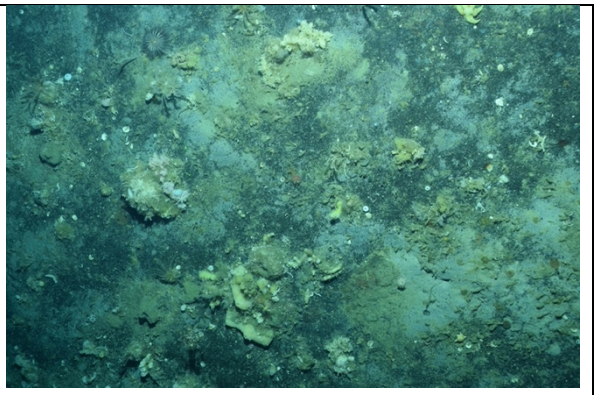
054934 breccia formation, no dark gravel in view, surface clearly smoothed, with rusty to black stains	055224 dark gravels are back, with patches of grey (ash?) and few rubbly ledges

Figure 6.10: Example photos of TowCam Dive NBP25-1-01.

6.9.2 TOWCAM dive NBP25-1-02

February 23, 2025 / Bottom of Terror Rift

No outcrop. Mud all the way. Little biology (sea pigglets).

6.9.3 TOWCAM dive NBP25-1-03

February 27, 2025 / Flapjack area, west flank Hoto Keiki flat top

These gentle slopes expose muddy seafloor with patches of dark gravel but no clear outcrop. Surficial mud, locally with piles of loose rocks and pebbles commonly subrounded, probably glacial deposits. Also isolated IRD boulders.

Top of flat top	about midway, in gentle westward slope
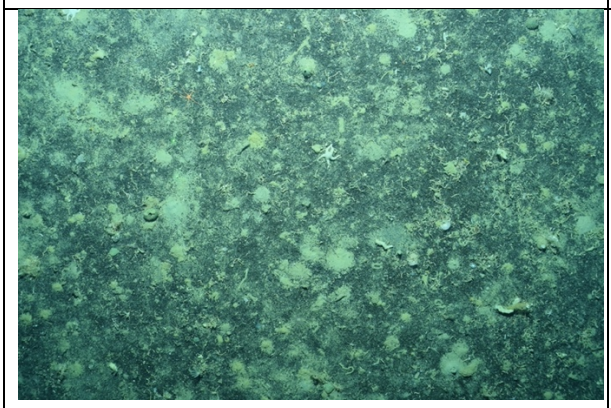	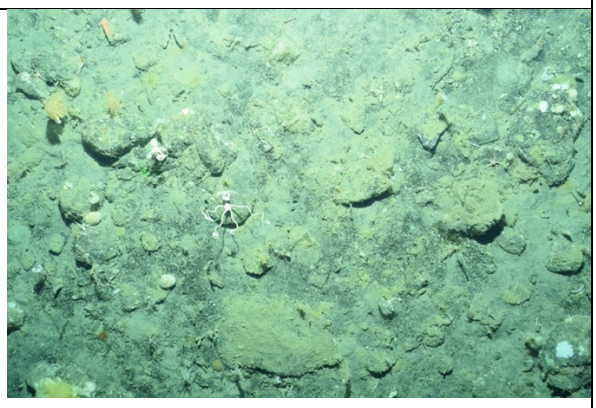
095228 mud and dark gravel patches	110118 lots of loose rocks in mud, flattish to subrounded

Figure 6.11: Example photos of TowCam Dive NBP25-1-03.

6.9.4 TOWCAM dive NBP25-1-04

March 3 2025 / Beaufort Bank, in summit depression

Rubbly outcrops and/or loose pebbles in mud most of the way to the end, locally with grey fine grained patches (ash?) and ledges of more rubbly material. Several instances of ~ slope parallel layering, in semi-consolidated surficial mud, but once with slabby material sticking out. Also at least one big IRD. Lots of nice biology.

6.9.5 TOWCAM dive NBP25-1-05

March 5, 2025 / Coco Seamounts

Mud and rubbly mud with occasional larger rocks (IRD), dark gravel patches in surficial mud toward the end, possible outcrops (?). Lots of bioturbations, life mostly on rubbly rocky domains, interesting linear ridges or furrows and fresh furrow in rubbly mud on south flank of glacial channel (made by large animal? seal? whale?).

6.9.6 TOWCAM dive NBP25-1-06

March 6 and 5, 2025 / Coco Seamounts

Mud and rubbly mud with bioturbations. Clear outcrops of beige rubbly formation, layers visible at several locations, dark gravel locally present. Occasional big rocks on mud (IRD).

Top of flat top	near base of flat top
	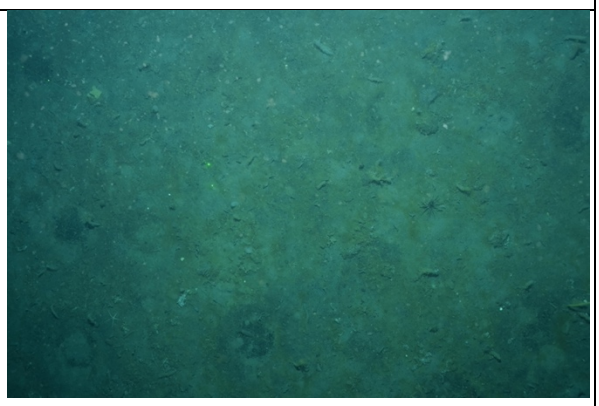
005136 clearly layered rubbly outcrop with life, beige, no dark gravel in sight	013316 muddy rubbly with dark gravel in fish holes

Figure 6.12: Example photos of TowCam Dive NBP25-1-06.

6.9.7 TOWCAM dive NBP25-1-07

March 10 and 11, 2025 / Flat top area, SE flank of Feathertop ridge.

The ridge is made of layered volcanic formation with beige finely layered more rocky intervals, discontinuous, irregular and up to a few meters-thick, in a more finely grained material with

dark gravel. Luxuriant life on the rocky ledges. Slopes are steep, with erosional gullies and recent talus. The rocky intervals form ledges sticking out of slope, and erosion locally produces the appearance of pillars. This upper volcanic formation rests unconformably on a pale beige fine grained and also layered volcanic formation with more gravel-rich intervals and spectacular iron-oxide veins and stains. This lower formation forms the top of the flat top. Contact around 650 m depth, consistent with slope break in bathymetry.

Top of ridge, start of dive	toward the base of the ridge
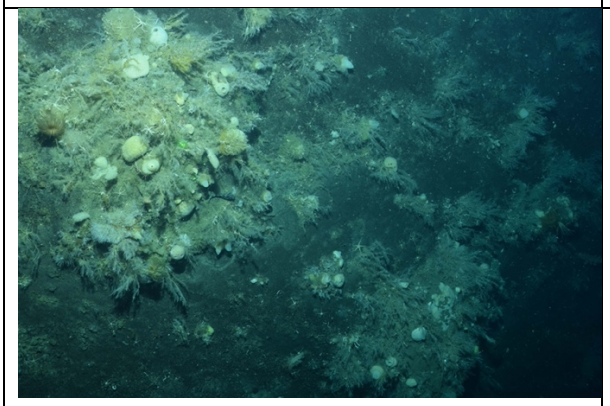	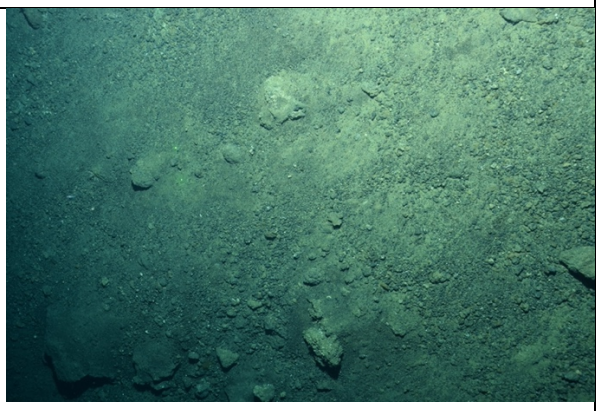
231216 start, rocky ledges with life stick out of darker gravel seafloor, strong slope	235026 talus again, recent, blocks of the rocky ledges formation

Figure 6.13: Example photos of TowCam Dive NBP25-1-07.

6.9.8 TOWCAM dive NBP25-1-08

March 11 2025 / Flat top area, NW flank of Feathertop ridge

Same geological succession as observed during dive 7. The ridge is made of layered volcanic formation with beige finely layered more rocky intervals, discontinuous, irregular and up to a few meters-thick, in a more finely grained material with dark gravel. Luxuriant life on the rocky ledges. Slopes are steep, with erosional gullies and recent talus. The rocky intervals form ledges sticking out of slope, and erosion locally produces the appearance of pillars.

This upper volcanic formation rests unconformably on a pale beige fine grained and also layered volcanic formation with more gravel-rich intervals and iron-oxide veins and stains. This lower formation forms the top of the flat top. Contact around 605 m depth, consistent with slope break in bathymetry.

Smooth upper surface of flat top with rusty and dark stains	just above the rusty stained smooth surface
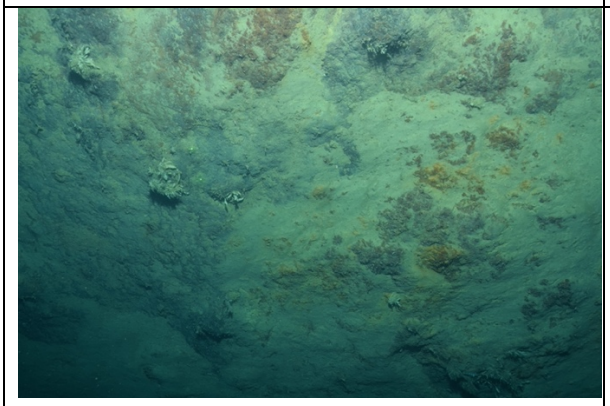	
021636 rock surface, dark crust with red stains	021756 small rocky ledges and dark gravel formation, downslope trails of gravel indicate erosion

Figure 6.14: Example photos of TowCam Dive NBP25-1-08.

6.9.9 TOWCAM dive NBP25-1-09
March 19, 2025 / North of Franklin Island

Giant pockmark or depression formed under stationary block of ice during the ice sheet's retreat ?

Mud, bumpy with bioturbations, sea pigs paradise, locally less bumpy and more fixed life. A few loose large IRDs on and in mud.

6.9.10 TOWCAM dive NBP25-1-10
March 19, 2025 / North Franklin area, seamount

Muddy rubbly beige formation with surficial mud. A few clear layered outcrops. More gravel-rich beige meter-sized patches of surficial mud contain subrounded pebbles and have more fixed life. Locally patches of darker gravel are visible. Also IRD boulders and loose pebbles on mud here and there.

east flank of seamount, start of dive	west flank of seamount
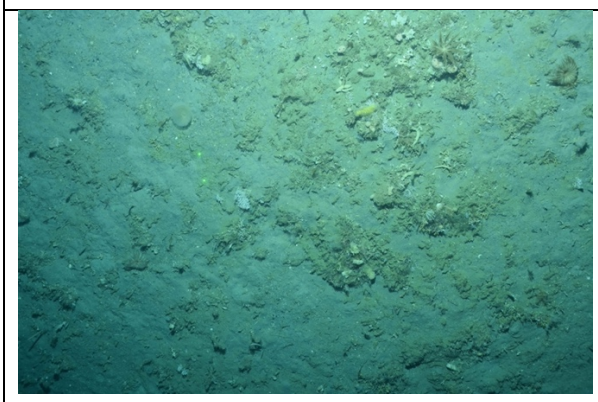	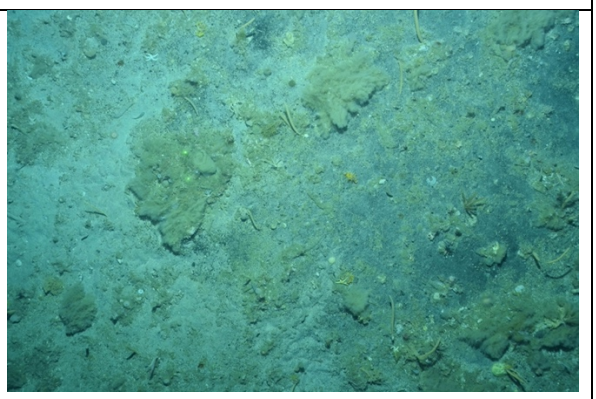
125052 on bottom muddy rubbly (outcrop?) with beige patches of fixed life	135034 patches of darker gravel visible under surficial muddy-rubbly discontinuous formation, with rounded pebbles

Figure 6.15: Example photos of TowCam Dive NBP25-1-10.

6.9.11 TOWCAM dive NBP25-1-11

March 20, 2025 / Top of Davey Bank (formerly known as "Mont Petit")

Muddy rubbly surficial formation with more rubbly patches including flattish-roundish pebbles and boulders (IRD) and more of less circular fish holes and patches exposing the underlying dark gravel and angular grey lava pebbles. This loose volcanic formation is seen in erosion scars in the middle (and steeper) part of the dive (10:55-11:26).

top of seamount	mid-way downslope on east flank of seamount
	
104544 more rocky, gravels and rounded boulders, still dark gravel in circular depressions	112654 downslope erosion showing lighter grey fine grained levels under the dark gravel

Figure 6.15: Example photos of TowCam Dive NBP25-1-11.

6.9.12 TOWCAM dive NBP25-1-12

March 28 and 29, 2025 / Flat top area, from east to west across Feathertop ridge

The geological sequences encountered are the same as in dives 7 and 8. The dive starts quite way up on the eastern slopes of Feathertop summit. After just a few tens of meters upslope in a muddy rubbly beige outcrop with coherent ledges and faint foliation, and no dark patches, but with a NNE-trending dike that resisted erosion, and a few pillar-like erosional features, there is a few meters-high quite linear NS cliff and we get into the layered volcanic formation with beige discontinuous finely layered more rocky intervals with fixed life in a more finely grained material with dark gravel. This goes on to the summit, with no conspicuous erosion. Going down the western slopes, this upper volcanic formation rests unconformably on a pale beige fine grained and also layered volcanic formation (similar to the eroded beige formation on the eastern slope?). Then there is a SW to S-facing cliff, TowCam is far from bottom for a bit, and when it gets near again, it is the flat fine-grained tuff ? formation with iron-oxide crusts and stains, with meter-sized bumps made of more gravel-rich rusty intervals with fixed life.

midway up east flank of ridge	mid-way downslope on west flank of ridge, less than 100m east of the contact on the rusty stained smooth surface
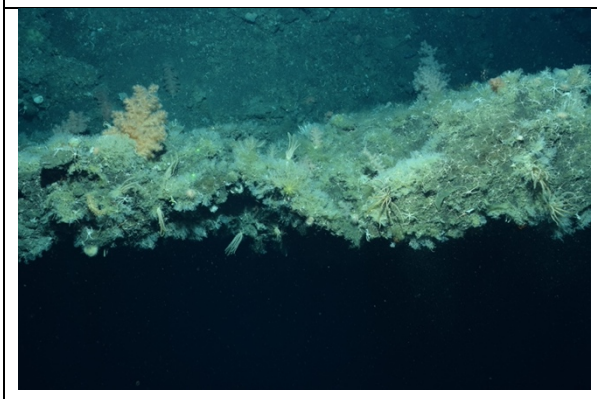	
231012 vertical scarp is likely a dike, 60-80 cm-wide, subvertical, almost perp. to N315 course	000702 a bit muddy, no dark graveel patches, small ledges with life outline trace of layering

Figure 6.16: Example photos of TowCam Dive NBP25-1-12.

6.9.13 TOWCAM dive NBP25-1-13

March 30, 2025 / Flat top area, flat top below Pfannkuchen

Short dive meant to explore successively the two superposed flat tops… but ice drift made progression so slow a decision was made to interrupt dive 13 and explore the upper flat top in dive 14. Muddy pebbly seafloor with local darker patches we have come to recognize as probably patches of volcanic gravel.

6.9.14 TOWCAM dive NBP25-1-14

March 30, 2025 / Flat top area, southeast flank of Pfannkuchen

Upper flat top (the edge of the lower one was explored during dive 13). Muddy formation, beige with patches of darker gravel we have come to recognize as volcanic gravel. Locally this formation appears weakly layered or foliated, apparently sub parallel to slope, with small flatty ledges (with fixed life) sticking out and in one location, meter-sized beige and more pebbly

patches over the muddy pebbly-gravely formation.. or part of it? Not clear... It might also be an upper coating of rubbly mud... The abundance of IRD blocks makes this dive special among all others made during the cruise. Locally these blocks emerge from the muddy gravely seafloor.

near base of seamount	near top of seamount
	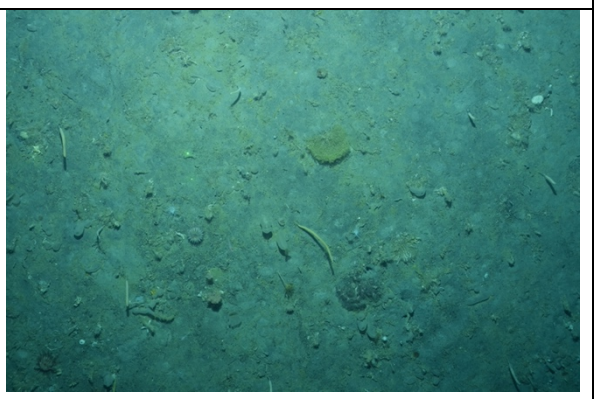
104518 more blocks, emerging from mud, maybe faint slope parallel foliation in mud.. and faint darker patches suggesting mud is surficial	112848 same, distinct dark gravel in circular fish hole

Figure 6.17: Example photos of TowCam Dive NBP25-1-14.

6.9.15 TOWCAM dive NBP25-1-15

March 31, 2025 / top of Vagabond flat top seamount

Dive planned for the southern scarp of the isolated Vagabond flat top. Due to ice conditions and drift, explored the top of the seamount instead. Dark gravel volcanic formation with angular pebbles and possibly very small local rocky ledges is covered by mud and rubble and revealed as patches, commonly associated to bioturbation. In two intervals the surface mud contains a lot of blocks, all sizes, with loose flattish to rounded IRDs. These could be small moraines. Life is beautiful throughout.

near start of dive	near top of seamount
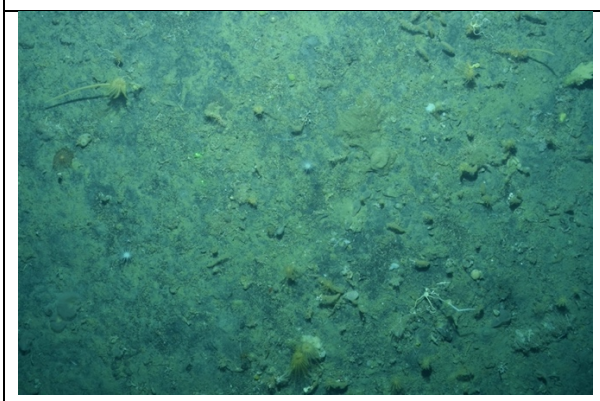	
005638 beige muddy formation is thin and on top of dark gravel formation	011118 more rocky, muddy formation with flatty and rounded pebbles, and isolated IRDs... a moraine?

Figure 6.18: Example photos of TowCam Dive NBP25-1-15.

6.9.16 TOWCAM dive NBP25-1-16

April 1, 2025 / East flank of Merope seamount, NE Franklin

Starting from up on the slope, the dive encounters the now usual volcanic dark gravel formation, under a thin cover of mud, muddy rubble and locally muddy piles of pebbles (IRDs). In steeper sections, patches of more rubbly or rocky material (breccia?) locally stick out as decimeter to pluri-decimeter-thick discontinuous ledges in the gravel formation. Life is very nice and at 090540, the mystery of the circular patches of dark gravels is solved: a fish is caught in the act!

in steeper portion of the dive	toward base of seamount
	
081940 (heading 189) outcrop: here muddy rubbly levels clearly form more rocky discontinuous ledges in dark gravel formation	085040 pile of muddy pebbles and blocks sitting on dark gravel formation, lots of life

Figure 6.16: Example photos of TowCam Dive NBP25-1-16.

6.9.17 TOWCAM dive NBP25-1-17

April 2, 2025 / Taygeta Seamount, NE of Franklin

The dive explores the top and uppermost western slopes of the seamount and encounters the now usual volcanic dark gravel formation, under a thin cover of mud and muddy rubble. In steeper sections, patches of more rubbly or rocky material locally stick out as decimeter to pluri-decimeter-thick discontinuous ledges in the gravel formation. At 055620 the photo shows clearly how the thin muddy-pebbly surficial formation sits on the dark gravel volcanic formation with its more rocky ledges. Life is very nice.

near top of seamount	a bit downslope
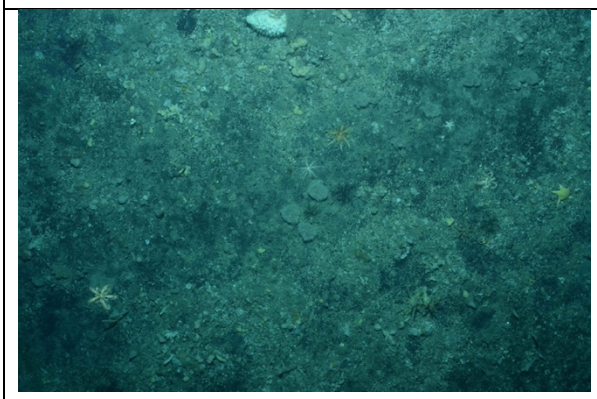	
054420 mud is locally semi consolidated with scaly slope parallel foliation, numerous patches of dark gravel	055040 muddy pebbly patch clearly sitting on dark gravel formation

Figure 6.17: Example photos of TowCam Dive NBP25-1-17.

Table 6.2: NBP25-01 TowCam dives. Summary of preliminary geological observations and highlights

dive #	Location	outcrops	"dark gravel and breccia" formation	rusty stains	IRDs on seafloor	IRD-looking blocks in mud	contact(s) observed	active erosion scarps	others and comments	dredge(s) nearby #
1	Flapjack region, top to base of east flank of Squid Ridge	yes	yes	yes	no	no	yes	no	corrugated flat summit region and flat basal surface both are smooth and bear rusty stains	DR2, DR3 west flank of ridge
2	bottom of Terror Rift	no	no	no	no	no	no	no	mud all the way	
3	Flapjack region, west (less steep)	no?	yes	no	yes	yes	no	no	mud and local piles of rubble and boulder in mud, on top of dark gravel formation	DR5 east (steep) flank of flat top

	flank of Hoto Keiki flat top									
4	Beaufort Bank in "caldeira"?	yes?	yes but grey not dark	no	yes	no	no	no	outcrops are probable, not spectacular	DR8 west flank base of bank, DR9 top of knoll to the west
5	Coco seamounts, across glacial channel and up flat top #5	yes???	yes?	no	yes	no	no	no	outcrops are not clear... very muddy	DR11 on top of flat top
6	Coco seamounts, Mademoiselle seamount, east flank	yes	yes	no	yes	no	no	no	beige more rocky-rubbly (breccia) formation is clearly layered in places, dark gravel is not prevalent	DR13 on western flank of seamount
7	Flapjack region, south east flank of Feathertop ridge	yes	yes	yes	no	no	yes	yes	spectacular outcrops of layered dark gravel and beige breccia formation, basal contact to smooth and rusty stained top of flat top	DR7 (eastern flank) and DR4 (south western flank) and DR34 western flank of Feathertop ridge
8	Flapjack region, west flank of Feathertop ridge	yes	yes	yes	no	no	yes	yes	spectacular outcrops of layered dark gravel and beige breccia formation, basal contact to smooth and rusty stained top of flat top	DR7 (eastern flank) and DR4 (south western flank) and DR34 western flank of Feathertop ridge
9	"Pockmarks" north of	no	no	no	yes	yes	no	no	muddy all the way, bioturbations	none

	Franklin Island									
10	across seamount north of Franklin Island	yes	yes but dark gravel not that common	no	yes	yes	no	no	a few outcrops of the beige rubbly (breccia) formation, not much dark gravel	DR22 on south east flank of seamount
dive #	**Location**	**outcrops**	**"dark gravel and breccia" formation**	**rusty stains**	**IRDs on seafloor**	**IRD-looking blocks in mud**	**contact(s) observed**	**active erosion scarps**	**others and comments**	**dredge(s) nearby #**
11	Top of Davey Bank ("Mt Petit"), east flank	yes?	yes	no	yes	yes	no	yes a little	in middle and steeper part of dive, dark gravel is everywhere under surficial mud	DR25 on top
12	Flapjack region, east to west across Feathertop ridge	yes	yes	yes	no	no	yes	yes	spectacular outcrops of layered dark gravel and beige breccia formation, dike and basal contact to smooth and rusty stained top of flat top	DR7 (eastern flank) and DR4 (south western flank) and DR34 western flank of Feathertop ridge
13	Flapjack region, southwest flank of lower flat top south of Pfannkü chen	?	yes	no	no	no	no	no	short dive, drifting Towcam mode. Muddy pebbly seafloor with local darker patches	DR36, north flank of same flat top, DR37 basal surface of flapjack seamounts
14	Flapjack region, southwest flank of Pfannkü chen flat top	?	yes	no	yes	yes	no	no	The abundance of IRD blocks makes this dive special among all others made during the cruise.	DR35, top of same flat top, DR37 basal surface of flapjack seamounts

15	top of Vagabond seamount	yes?	yes	no	yes	yes	no	no	In two intervals the surface mud contains a lot of blocks, all sizes, with loose flattish to rounded IRDs.	DR31, southern flank of Vagabond seamount
16	East flank of Merope seamount, NE Franklin	yes	yes	no	yes	yes	no	no	volcanic dark gravel formation, locally with rubbly ledges, under thin cover of mud, and locally muddy piles of IRDs	DR39, lower on east flank of Merope seamount
17	west flank of Taygeta seamount, NE Flanklin	yes	yes	no	yes?	no	no	no	muddy-pebbly surficial formation clearly seen on dark gravel and rocky ledges volcanic formation	DR43 upper slopes of same seamount

7. Heat Flow Measurements

F. Neumann

7.1 Overview

During cruise NBP-25-01, we deployed the 6-meter-long Giant Heat Flow Probe (GHF) from CICESE, Ensenada (**Fig. 7.1a, b**). The probe operates in a pogo-style mode and is capable of deployment in water depths of up to 6000 meters. Its design follows the classical “violin bow” configuration (Hyndman et al., 1979; Hartmann and Villinger, 2002), featuring 22 thermistors distributed along an active length of 5.25 meters at 0.25-meter intervals. These thermistors are housed within an oil-filled hydraulic tube (outer diameter: 14 mm), which is attached to the strength member (outer diameter: 130 mm).

The sensor tube is also equipped with a heater wire capable of generating high-energy heat pulses, typically delivering 1100 J/m. This setup allows for in-situ thermal conductivity measurements based on the pulsed needle probe method (Lister, 1979). The data acquisition unit, including the power supply (Sea & Sun, Germany), is enclosed in a single titanium pressure case (outer diameter: 110 mm, length: 300 mm) and is mounted inside the probe’s weight stand. A second pressure case houses the battery pack used to generate the heat pulses. For this cruise, we used data acquisition unit #951 and sensor string #T86 and #T82.

The temperature sensors measure signals with a resolution of 20 bits at a sampling rate of 1 second, achieving a final temperature resolution of better than 1 mK under ambient seafloor conditions. A calibrated PT-100 seawater sensor is included for calibrating the sensor string relative to deep-water temperatures. Additionally, the probe is equipped with inclination and acceleration sensors to monitor its penetration into the sediment.

The probe was deployed using an 18 mm trawl wire and operated in autonomous mode, with internal data storage and automatic heat pulse triggering throughout the cruise. The winch speed during probe penetration was maintained at 0.8 m/s at all sites. The probe was initially lowered to approximately 100 meters above the seafloor, followed by penetration into the sediment, indicated by a rise in temperature due to frictional heating (**Fig. 7.1c**). After penetration, the probe was left to equilibrate with in-situ temperatures for 10 minutes, followed by another 10 minutes to observe heat pulse decay (**Fig. 7.1c**). Once measurements were completed, the probe was pulled out of the sediment to 100 m above seafloor, and the system was moved to the next station, continuing in “pogo mode.” In order to save time, heat pulse was only fired every second station or in the case of three penetration per station once.

Figure 7.1c shows a typical temperature vs. time record during a measurement, highlighting the different measurement stages. The colored lines correspond to the 22 thermistors (15 in this example). Heat flow was estimated using the thermal resistance vs. temperature method (Bullard plot), where the slope of the plot indicates the surface heat flow.

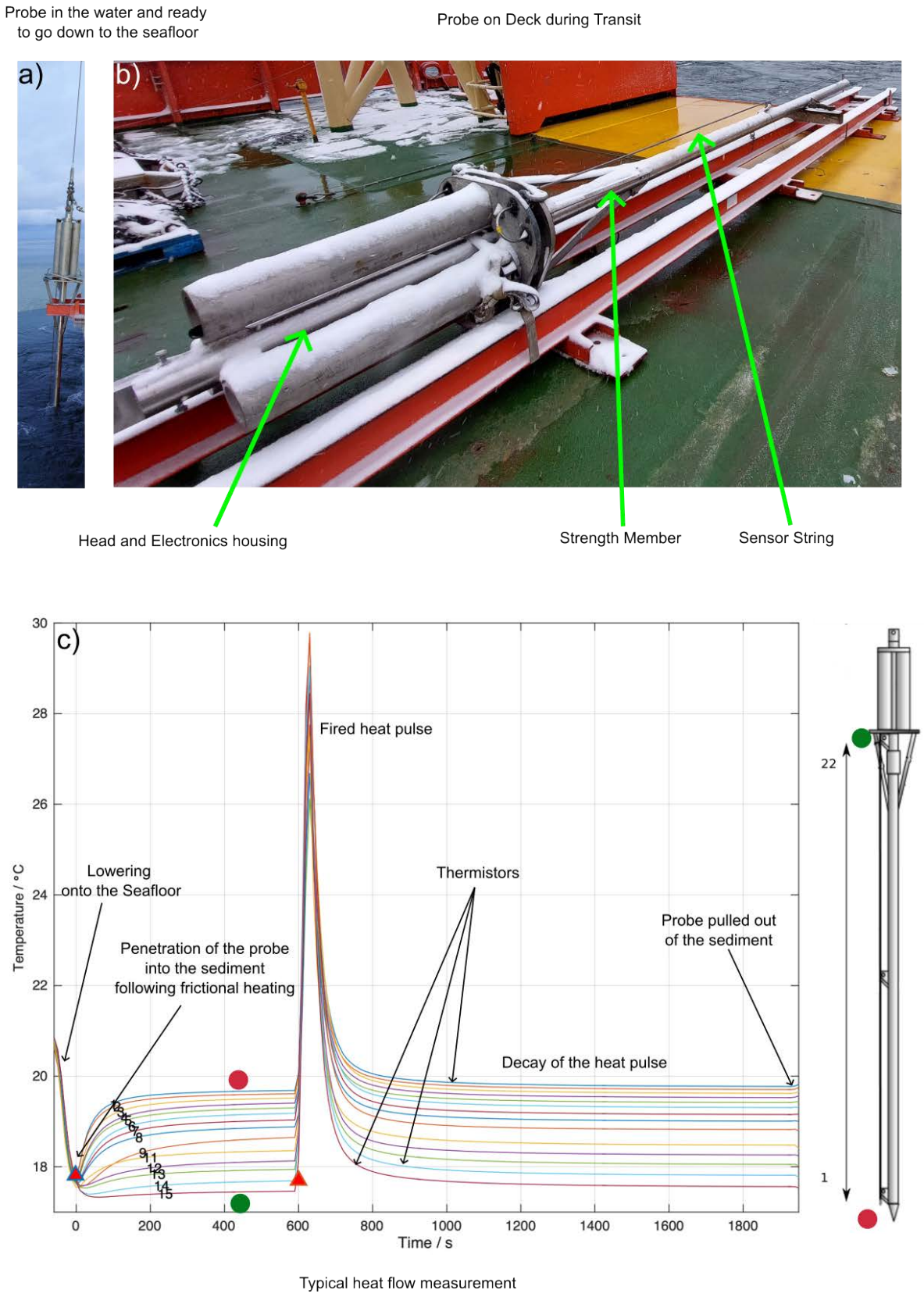

Figure 7.1: a) Heat flow probe in vertical position on the back deck. b) The probe stored during transit on the coring rail. c) Typical stages of the probe recording temperature over time, highlighting the key phases of measurement.

7.2 Preliminary Results

A total of 29 positions were successfully penetrated across 10 stations (**Fig. 7.2, Table 7.1**). Penetration was not achieved at ten sites, resulting in a success rate of 90%. Measurements were taken at depths ranging from 520 m to 930 m below sea level, with the number of penetrations per site varying between three and six.

The calculated temperature gradients ranged from 51.82 K/km to 260.19 K/km, with some sites exhibiting significant variability. Mean thermal conductivity values ranged from 0.67 to 1.30 W/m·K, with uncertainties typically between 0.05 and 0.26 W/m·K. Thermal conductivity was successfully measured at 34 positions, yielding a total of 364 measurements and an average value of 0.96 ± 0.18 W/m·K.

Heat flow values were determined for most stations, ranging from 56.1 mW/m^2 to 260.2 mW/m^2, with a mean of 99.8 ± 29.8 mW/m^2. The highest heat flow, 260.2 mW/m^2, was recorded to the east near Franklin Island. Penetration depths varied from 0.9 m to 4.6 m, with most penetrations being less than 3 m due to the presence of stiffer sediment. This stiffer sediment may also contribute to large temperature errors, as water could be trapped between the sediment and the probe.

For successful penetrations, probe tilt ranged from 0.5° to 7.7°. However, measurement failures occurred at some sites (e.g., HF08Pen03, HF10Pen02, and HF13Pen03), primarily due to an inability to penetrate the sediment. Additionally, some measurements (e.g., HF02Pen02, HF03Pen05) relied on thermal conductivity values from nearby stations due to missing heat pulse data. The overall heat flow distribution is consistent with previous measurements in the region (Blackmann et al., 1987; Della Vedova et al., 1992).

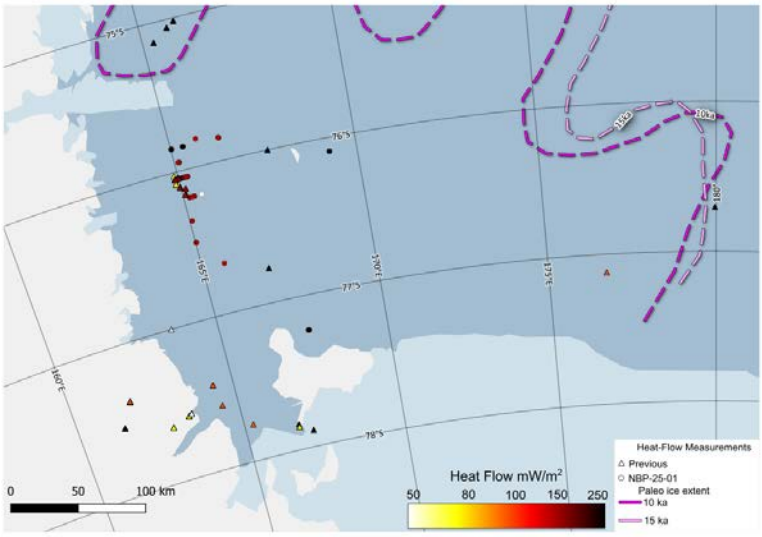

Figure 7.2: Overview Map of the study area including previous (triangles) and heat flow measurements during NBP-25-01 (circles). Paleo ice extent is shown as dashed lines.

Table 7.1: Summary of Heat flow Survey in the Ross Sea NBP-25-01.

Site Name	Lat	Lon	Elevation	Calculated or inferred temperature gradient	Heat Flow Value	General Comments
HF04Pen01	-75.8485	166.3438	-527	92.81	92.6	
HF04Pen02	-75.8467	166.3353	-524	95.46	100.4	
HF04Pen03	-75.8448	166.3272	-525	87.98	93.5	
HF05Pen01	-75.8482	165.3508	-871	101.69	97	
HF05Pen02	-75.8473	165.341	-876	98.91	98.9	TC assumed from nearby
HF05Pen03	-75.8473	165.3288	-868	113.24	113.2	TC assumed from nearby
HF06Pen01	-75.846	165.031	-850	122.64	84.9	
HF06Pen02	-75.8457	165.0203	-850	110.77	88.6	TC assumed from nearby
HF06Pen03	-75.8457	165.0092	-851	110.97	116.2	
HF07Pen01	-75.9423	165.1362	-856	77.78	83.4	
HF07Pen02	-75.9422	165.1269	-849	138.66	124.8	TC assumed from nearby
HF07Pen03	-75.942	165.1146	-851	91.7	82.5	TC assumed from nearby
HF07Pen04	-75.9418	165.1076	-857	83.25	86.4	
HF09Pen01	-77.2313	167.5985	-929	125.27	92.9	
HF09Pen02	-77.2317	167.6127	-924	101.34	101.3	TC assumed from nearby
HF09Pen03	-77.2318	167.6245	-930	120.91	120.9	TC assumed from nearby
HF09Pen04	-77.2322	167.6327	-930	105.18	105.2	TC assumed from nearby
HF10Pen01	-76.664	165.6552	-679	51.82	65.3	
HF10Pen02	-76.6667	165.6527	-675			failed
HF10Pen03	-76.6693	165.6502	-683	71.86	71.9	TC assumed from nearby
HF11Pen01	-76.4865	165.0233	-765	73.92	97.2	
HF11Pen02	-76.489	165.0185	-752	58.86	75.3	TC assumed from nearby
HF12Pen01	-76.3422	165.0676	-814	61.79	89.6	
HF12Pen02	-76.343	165.0664	-816	73.95	96.1	TC assumed from nearby

HF13Pen01	-75.8183	165.7283	-570			failed
HF13Pen02	-75.8185	165.7245	-570	94.43	94.4	TC assumed from nearby
HF13Pen03	-75.8183	165.7207	-520			failed
HF19Pen02	-76.0923	169.2361	-530	260.19	260.2	TC assumed from nearby
HF19Pen03	-76.0923	169.2359	-530	234.56	234.6	TC assumed from nearby

8. Shipboard Gravity

Jyun-Nai Wu

Gravity data during Expedition NBP25-01 were acquired using a DgS gravimeter (model AT1M), sampling at 1 Hz. The goal was to detect small variations in the local gravity field by measuring the current required to maintain a constant spring length in a Lorentz force actuator system, which is stabilized by a position detector. The resulting measurements represent relative gravity values in milligals (mGal). To reference these data to an absolute gravity framework, gravity ties were conducted before and after the cruise—both at the port of Lyttleton and at a land-based absolute gravity station in Christchurch. Data acquisition commenced upon exiting the Exclusive Economic Zone (EEZ) on February 14, 2025, and concluded upon re-entry into the EEZ (**Fig. 8.1**). Three notable spikes in the data were identified, likely associated with abrupt ship motions caused by various factors such as sea state or operational activities (**Fig. 8.1**)

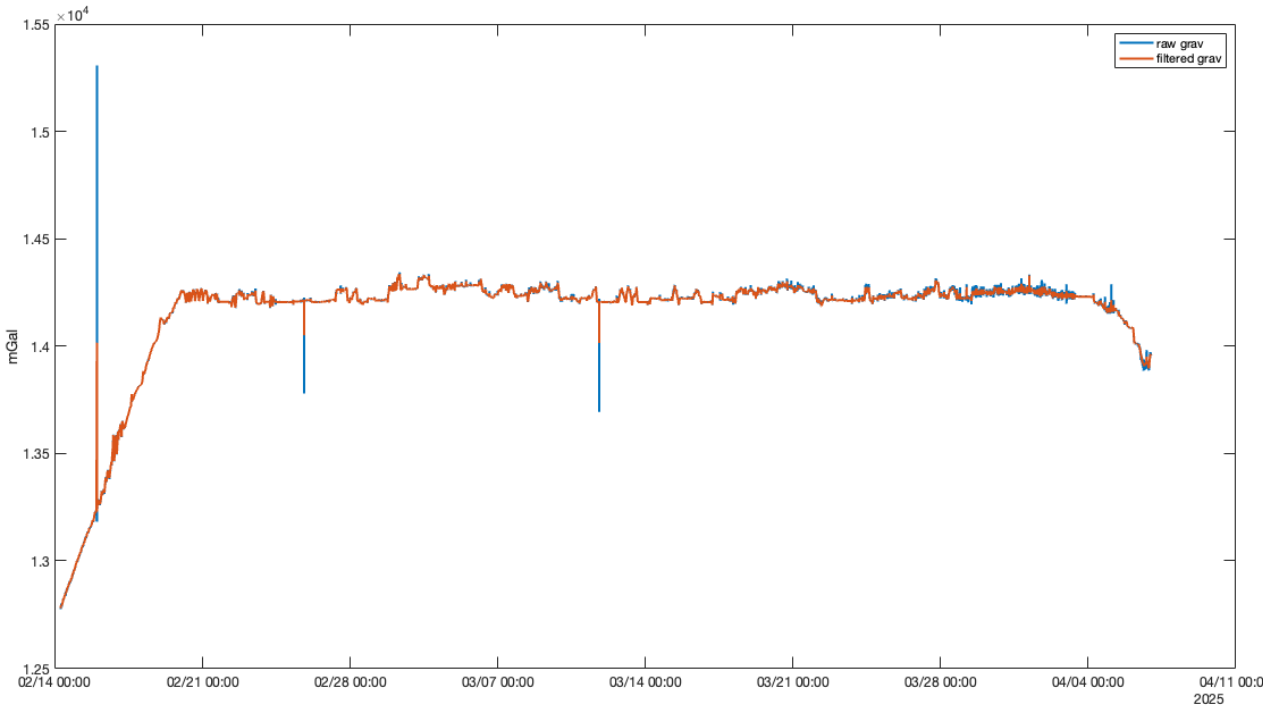

Figure 8.1: Raw gravity data (blue line) and band-pass filtered data (orange line) time series.

9. Sea Surface Magnetometer

Jonas Preine

9.1 Overview

Magnetic field data were collected during the cruise using a Marine Magnetics SeaSpy magnetometer. The SeaSpy1 is an Overhauser system that operates on the nuclear spin resonance principle, allowing total field measurements with a precision of 0.01 nT. The sensor was towed astern (**Fig. 9.1**). The tow cable was deployed and recovered using a winch provided by USAP, mounted on the first upper deck on the port side. The winch was powered by a ship-supplied three-phase 208 V source.

The deck cable was routed to a junction box in the Marine Technician Shop, near the stairway. From there, data were transmitted to the dry lab, where they were collected with a serial cable on a Lenovo ThinkPad T14 running Windows 11 and Marine Magnetics' "BOB" software. This laptop was also connected to the ship's GPS system. GPS and magnetometer data were logged at a baud rate of 9600, with GPS data recorded on COM5 and magnetometer data on COM3. Readings were sampled at a rate of one per second with a precision. GPS navigation was recorded at the same interval, with the "BOB" software applying a layback correction of 304 meters. All timestamps were set to Universal Coordinated Time (UTC).

Data processing involved parsing the daily raw magnetometer files and merging them with the ship's Seapath navigation data. The final files were saved in ASCII format.

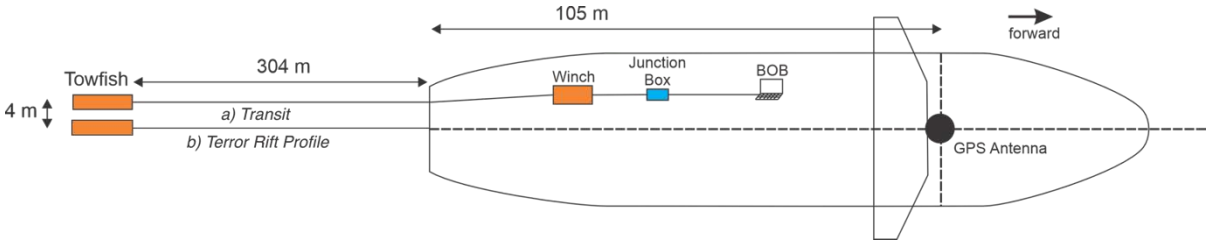

Figure 9.1: Overview of the acquisition setup of surface-towed magnetometer during the transit from New Zealand's EEZ to the survey area in the Ross Sea (a) and during the profile crossing the Terror Rift Axis (b).

9.2 Operations

During Expedition NBP25-01, we collected surface-towed magnetometer data during the transit from New Zealand's Exclusive Economic Zone (EEZ) to the Ross Sea. The magnetometer was deployed on February 14th at 07:19 UTC and recovered on February 20th at 02:03 UTC (**Fig. 9.2**). Data recording was briefly interrupted on February 18th at 02:28 UTC for five minutes due to a crash of the recording laptop. Throughout the transit, the sensor was towed 304 meters behind the vessel, with the tow point located 105 meters aft of the GPS antenna's 0000 origin and offset by 4 meters to port (**Fig. 9.1**). A plot of the measured magnetic data during the transit is shown in **Figure 9.3**.

On February 21st, we redeployed the magnetometer along a WSW–ENE profile crossing the Terror Rift axis (**Fig. 9.2**). Due to prevailing ice conditions, we adjusted the tow geometry by relocating the tie-off point to the center of the stern (**Fig. 9.1**), thereby eliminating the previous along-axis offset (**Fig. 9.4**).

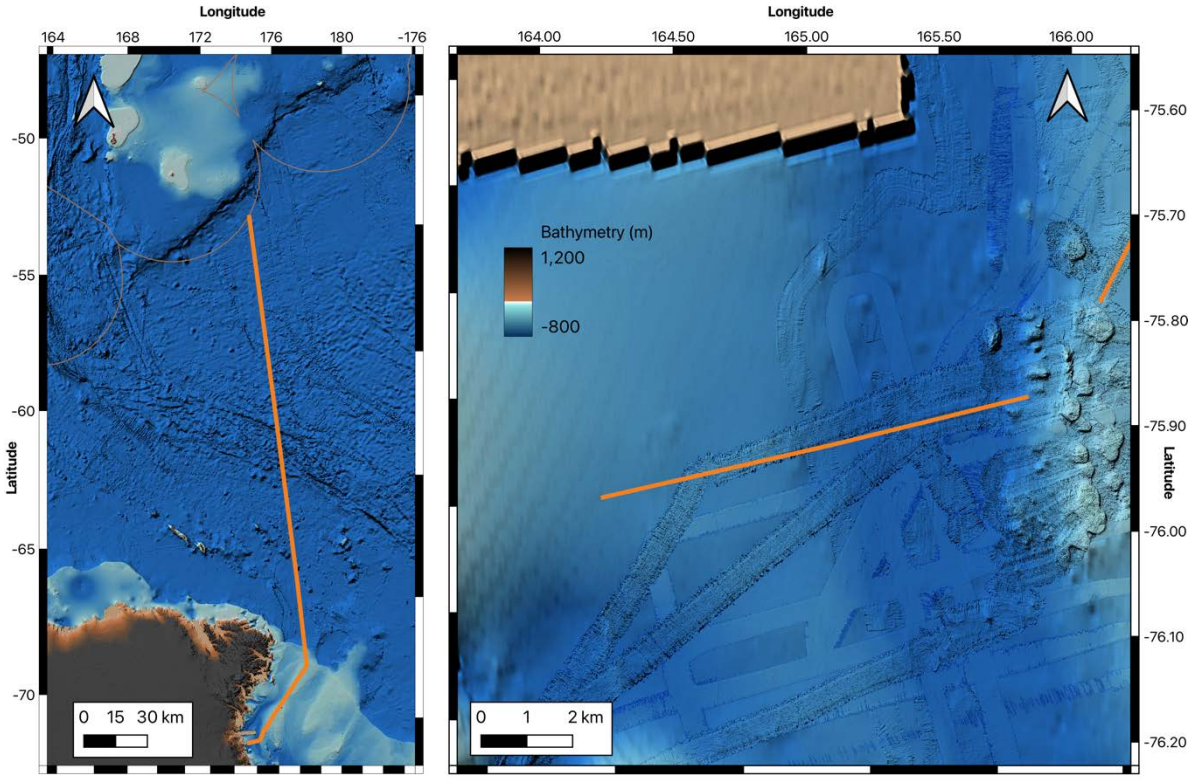

Figure 9.2: Overview of two profiles measured during Expedition NBP25-01. Left panel shows the transit profile from New Zealand's EEZ to the survey area in the Ross Sea. Right panel shows the profile measured across the Terror Rift axis.

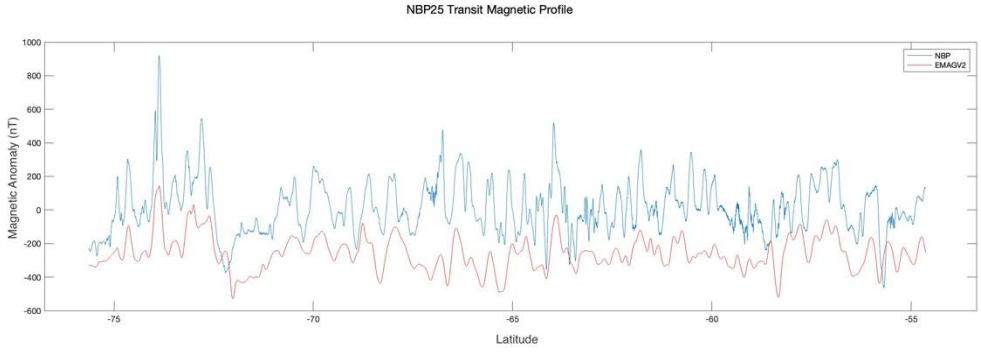

Figure 9.3: Plot of the measured total magnetic field along the transit profile after removal for the international geomagnetic reference field. For comparison, we plot a parallel profile extracted from the Earth Magnetic Anomaly Grid 2 (EMAG2) field. For location, see **Figure 9.2**.

Figure 9.4: Photos of the magnetometer tow cable being towed from center line during the profile crossing the terror rift axis (**Fig 9.2**).

10. Dredge Sampling

Carole Berthod, Kurt Panter, Mathilde Cannat, Dan Wildrick, Jacquelyn Kalemba, Katherine Shanks, Hila Shooter

10.1 Overview

The G-82-N dredging operations carried out during the NBP25-01 campaign successfully sampled seamounts in six regions - Flapjack Field, Davey Bank, Aurora Bank, Beaufort Bank, Channel Group and surrounding Franklin Island. A total of 50 dredges were completed on a total of 35 separate volcanic edifices with only one unsuccessful dredge haul (i.e., no material recovered). The total weight of material recovered by dredging, including the accompanying mud, dropstones (Ice Rafted Debris - IRD) and biology, was 7,130 kilograms (15,719 pounds). Volcanic lithologies recovered include lava fragments and volcanoclastic material that comprise agglomerate, breccia, tuff and bombs. Compositionally, samples are basaltic with abundant olivine +/- pyroxene +/- amphibole +/- plagioclase. In addition, mantle xenoliths (peridotite and amphibolite) were sampled at most seamounts.

10.2 Introduction

Rock samples will provide in situ evidence of materials that compose the seafloor and heat source. Distribution of lithology and age will allow us to map out the distribution of heat source in the past and possibly the present. Age determination of volcanic materials is critical to evaluate any chronological link among these seafloor features in the western Ross Sea that facilitate the generation of volcanic islands and seamounts, rift/fault activities, and grounded ice (time).

Compositional data on volcanic rocks (i.e., minerals present, major, and trace element concentrations) will allow better characterization of the Terror Rift Volcanic Field. Compositional data along with age will be used to evaluate possible effects of glacioisostasy on volcanism. The recovery of fresh and relatively unfractionated basaltic materials will also be used to help evaluate magma origins and to better constrain compositions of mantle sources that have facilitated the Erebus Volcanic Province.

10.3 Strategy

To achieve these objectives, several areas have been targeted (**Fig. 10.1**):

- A first zone north of the Terror Rift: includes flat-topped mounds - *Flapjack Field*. Previously, only one dredge was carried out on a flat top seamount (Lee et al. 2015) in this area. This dredge yielded an age at 0.46 and 0.41 (+/-0.03) Ma. The aim of our dredging work during this campaign was therefore to determine the nature and composition of the edifices identified during previous campaigns and edifices discovering in the new high-resolution bathymetry from this expedition.
- Further south of Flapjack Field, a large edifice, named *Davey Bank*, displays an elongated N-S morphology. A dozen dredges were carried out on this 40 x 10 km edifice, including profiles on various neighboring isolated edifices, and sampling of lower and upper units.

- In previous studies, the southern part of the *Aurora Bank* has been sampled and dated at 3,778 ± 0.039 to 4,153 ± 0.03 Ma (Rilling et al. 2009). Dredging on this expedition was therefore carried out in the northern part of the edifice.
- *Beaufort Island* (1.972 ± 0.046 and 1.941 ± 0.035 Ma, Rilling et al. 2009) and *Beaufort Bank* are located between Aurora Bank and Ross Sea Island. The unknown Beaufort Bank, located east to the of Beaufort Island, was the site of 3 dredges.
- Several recent and ancient submarine volcanic edifices lie to the north, east and south of *Franklin Island* and have been dredge during previous campaigns (0.132 ± 0.026 to 8.55 ± 0.078 Ma, Rilling et al. 2009). We conducted multiple dredges in this area, spanning from the *Coco Channel* site south of Franklin Island to *Potter Peak* North of Franklin Island.

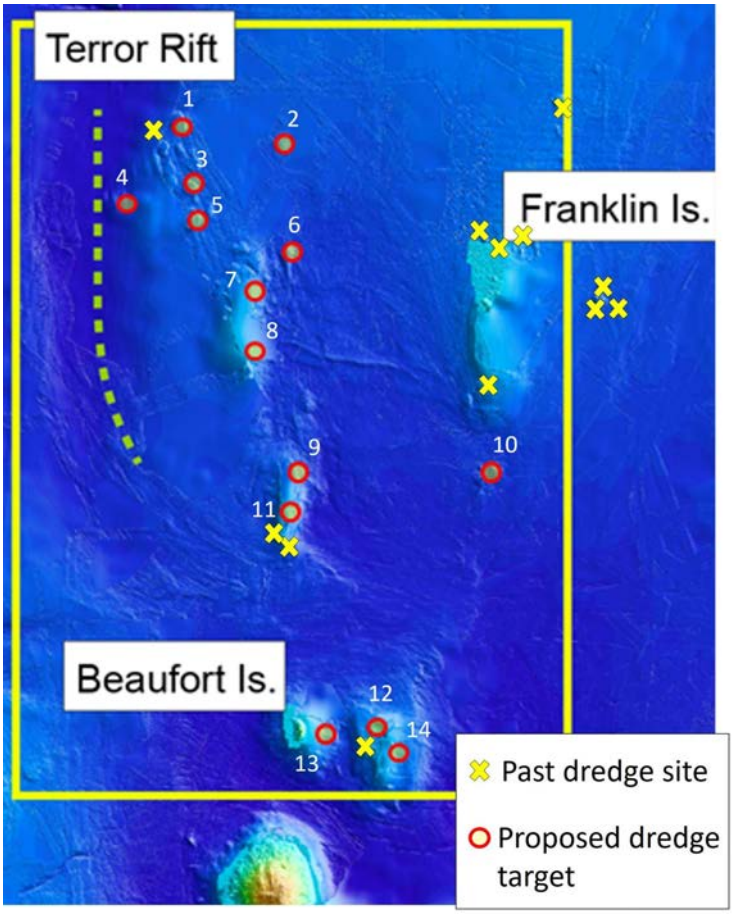

Figure 10.1: Targets selected for dredging during Expedition NBP25-01. Also shown are dredges from past expeditions (Rilling et al., 2009; Lee et al., 2015).

10.4 Methods

10.4.1 Equipment

Tension Member: 3x19 9/16” trawl wire spooled on Markey DUSH-9-11 Deep Sea Trawl Winch.

10.4.2 Termination: Swivel

Two different dredges were used during cruise NBP-2501. While the dimensions of the dredge mouths were approximately the same, the rigging configurations varied slightly.

MARSSAM Dredge (**Fig. 10.2**): In the MARSSAM setup, the termination was shackled to the recovery chain, which was in turn shackled to a ¼" rope threaded through the chain bag. This configuration allowed for manual retrieval in case the shear pin in the weak link failed under tension. Additionally, the termination was independently shackled to the main weak link, which was connected to a master link. From this master link, one set of bridle chains was attached to the dredge mouth via hammer links. A second shackle from the master link connected a side weak link to another shackle, which secured the second set of bridle chains. Each set of bridle chains referred to those mounted on the short sides of the rectangular dredge mouth. The bridle chains in this configuration were 8 feet in length.

USAP Dredge (**Fig. 10.2**, also known as the "Hila special"): In this configuration, the termination was shackled to a pear ring, which was then shackled to a ⅜" recovery wire. This wire was attached to the base of the chain bag to allow retrieval if the weak link failed. The pear ring also held a shackle that connected the main weak link to another shackle leading to a master link. The master link was fitted with four hammer links, each retaining one bridle chain.

The main difference between the MARSSAM and USAP dredges lies in the attachment of the side weak links: the MARSSAM dredge used a single side link connecting the tops of two bridle chains, while the USAP dredge employed two side links, each connected to the bottom of separate bridle chains. This difference is largely preferential and only affects the selection of the shear pin strength used in the side weak links. In both configurations, it is expected that the shear pin in the main weak link would be the first to fail under excessive tension. The bridle chains for the USAP dredge measured approximately 5.5 feet in length.

10.4.3 Mouth of dredge

In reference to the MARSSAM dredge, all four bridle chains were shackled to holes in the corners at the top side of the dredge mouth. The net and chain bag were shackled to the holes in the perimeter of the bottom of the mouth of the dredge. The MARSSAM dredge mouth was constructed from ½" steel stock.

The USAP dredge, as noted previously, utilized two "side" weak links on the bottom ends of two bridle chains. The other set of bridle chains was shackled directly to the dredge mouth in the same fashion as the MARSSAM dredge. The net and chain bag were also shackled to the mouth of the dredge in the same fashion as the MARSSAM dredge. The USAP dredge mouth was constructed from ¾" steel stock.

10.4.4 Chain bag and net

At the bottom of the MARSSAM dredge mouth, 32 holes were spaced evenly along the perimeter. From each hole, a 6-foot length of ¼" grade 30 chain was suspended vertically using small shackles. These shackles also secured the upper edge of the internal net lining the chain bag. To interconnect the vertical chains, ¼" quick links were used horizontally. The internal net was intentionally made slightly longer than the chain bag and cinched shut at the bottom using seine twine, ensuring that the net fit entirely within the chain bag while leaving some space above the cod-end when cinched. The chain bag itself was closed by weaving a length of ¼" wire rope—

terminated with thimbles at both ends—through the lowest row of vertical chains and fastening it with a small shackle to form a cod-end. Upon recovery, the wire rope was disconnected and the seine twine was cut to release the dredge's contents.

In comparison, the USAP dredge employed a heavier-duty setup. It used ½" vertical chains suspended from 32 holes along the perimeter of the dredge mouth. These larger chains accommodated ¼" chain links woven horizontally through them. To prevent the vertical chains from sliding along the horizontal links, ¼" lap links were inserted between each vertical length. The net used in the USAP dredge had a mesh size similar to that of the MARSSAM dredge, but was constructed from a thicker, more durable material. Instead of being cinched with seine twine, the net was secured by weaving a line through the shackles attached to its mesh and then cinching it closed using a daisy chain-style trawl net knot. The chain bag was sealed not with wire rope, but with pear rings attached to its bottom edge. A line was threaded through these pear rings and likewise cinched using a trawl net knot. After recovery, both knots could be released to empty the dredge.

Overall, the USAP dredge featured a more robust chain bag and net design. Its total weight was approximately 1000 lb, compared to the MARSSAM dredge's 500 lb, a difference attributed primarily to the chain bag construction and the thicker dredge mouth.

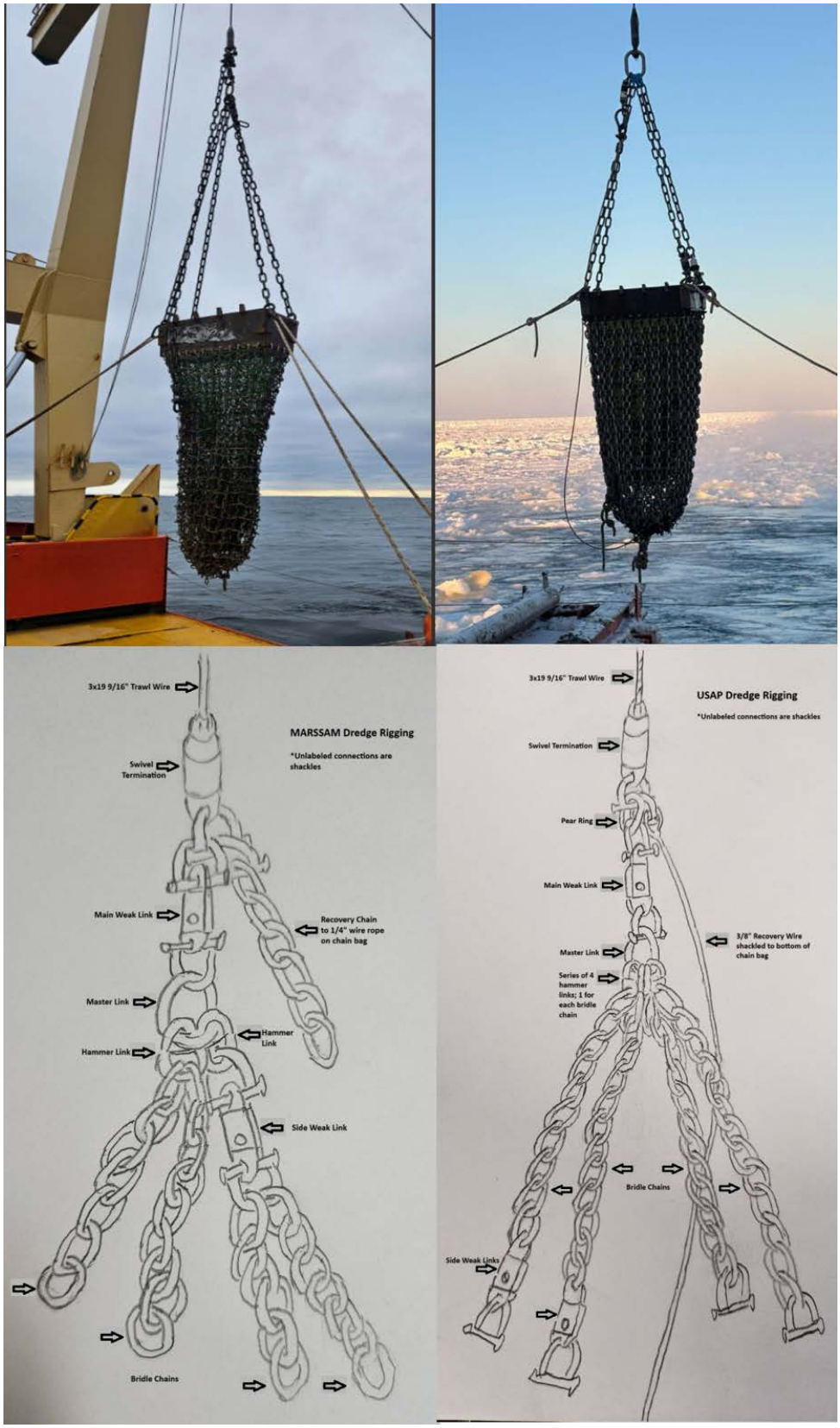

Figure 10.2: Photos of the MARSSAM Dredge (left) and the USAP Dredge (right) with drawings highlighting the differences in the weak links (MARSSAM Dredge left; USAP Dredge right). Drawing: D. Wildrick.

10.4.5. Preparation

Dredging preparation primarily involved identifying the deployment location, desired depth, and topographic profile, along with selecting the appropriate dredge for the operation. Several key factors were considered to optimize the dredging profile within the study area:

- Bathymetric data were acquired using multibeam surveys, supplemented by TowCam imagery when available. Slope angle and reflectivity maps helped refine the target sampling area.
- To maximize dredging efficiency, preferred profiles included smooth, continuous slopes—from base to crest—without significant breaks. This allowed the dredge to remain properly oriented and maintain consistent contact with the seafloor, minimizing the risk of premature emptying. In some cases, however, dredging was also successful on nearly flat terrain where only minor elevation differences (a few meters) existed.
- Meteorological conditions played a critical role in planning. Vessel alignment with prevailing currents, ice drift, and wind direction was essential, enabling the ship to face into these forces and thereby simplifying maneuvering during dredging. Given how rapidly weather and sea ice conditions could change, final adjustments were sometimes necessary upon arrival at the site.
- To define the length of the seabed section to be sampled, both the starting and ending coordinates of the target zone were fixed in advance. This allowed the ship's captain to plan the dredging trajectory according to real-time conditions.
- Before deployment, the dredge was thoroughly cleaned by the crew to ensure no residual rock fragments remained lodged in the metal mesh, which could compromise the integrity of the sample.

10.5 Dredging operation

10.5.1 Dredge Notes

During Expedition NBP-25-01, passive dredging was selected as the preferred sampling method. Although more time-consuming than active dredging, passive dredging is generally considered safer—particularly in regions like the Ross Sea, where the seafloor composition is less well known.

10.5.2 Pre-deployment procedure and considerations:

The ship's ability to orient along a desired feature during dredging is influenced by wind and swell conditions. Prior to deployment, the scientists responsible for site selection consulted with the bridge to determine the range of feasible headings under current conditions. Based on this information, a suitable track line was selected along the target feature.

Essential details to relay to the dredge technician included the start and end depths of the track line, as well as its total length—typically around 1000 meters, though this was adjusted depending on site constraints. These variables enabled the technician to calculate the appropriate shear pin break strength, which is based on the amount of wire that needs to be paid out. This, in turn, depended on the seafloor depths at the start and end of the track, the length of the track line, and the elevation change along it.

Additional factors influencing shear pin selection include the seafloor profile—whether steep or flat—and sea state. Steep slopes increased the risk of the dredge catching on outcrops, which can generate dangerously high tension. Likewise, significant swell could cause rapid fluctuations in tension, sometimes varying by several thousand pounds per heave.

10.5.3 Water column to seafloor, and along track line

The dredge was lowered through the water column to approximately 30 meters above the seafloor. At that point, the vessel began moving along the predetermined track line at a target speed of 1.0 knot. Once the ship approached this speed, the winch operator began paying out wire at a corresponding rate—approximately 30 meters per minute, which closely matches 1 knot. Initiating forward motion before the dredge reached the seafloor helped ensure that the chain bag and dredge mouth would contact the bottom in an optimal orientation.

Bottom contact was identified by monitoring the winch tension graph: a noticeable drop in tension, followed by a decrease in amplitude, typically indicated that the dredge had made contact with the seafloor.

The amount of wire paid out during the tow was calculated based on the seafloor depth at the start of the track line, the depth at the end, the total track length, and the elevation change along the line. For instance, if the depth at the start was 500 m, the end depth was 400 m, and the track line was 500 m long, then a total of 900 m of wire would be paid out. This ensured that the dredge was not actively pulled by the ship—i.e., active dredging—but rather dragged passively along the seafloor. In practice, a margin of ±20–50 meters from the calculated payout was acceptable. The rationale was that once the dredge was resting on the seafloor and the ship was moving, the cable laid flat along the bottom, forming a roughly vertical segment up to the ship. If slightly less cable was paid out, the angle would decrease but typically not enough to lift or pull the dredge. Conversely, excess wire extended recovery time without offering a substantial advantage.

Wire scope ratios—the ratio of wire out to seafloor depth—also influenced dredging efficiency. For steeper slopes, a scope of 1.2 to 1.3:1 is generally considered optimal. On flatter terrain, however, these ratios may change, and in passive dredging, it is common that parts of the track fall outside the ideal scope range. It remains uncertain how deviations from the “ideal” wire scope affect rock recovery, though some successful hauls have occurred under suboptimal conditions.

10.5.4 Upon completion of track line

Once the amount of wire out was less than the seafloor depth and the tension graph indicated that the dredge had left the bottom, the dredge was recovered at the speed that the ship was comfortable with. In general, this turned out to be 30 meters per minute.

10.5.5. Operations during Expedition NBP25-01

To increase time efficiency, dredge paths were kept to modest lengths relative to “normal” 1000 m-1500 m track lines. Track lines between 350 m and 600 m were the norm. The combination of shallow depths along chosen track lines, and shortened track line lengths, relative to having

deeper depths, and longer track line lengths, allowed for better time efficiency per dredge evolution.

10.5.6 Notes regarding failed dredge deployment on NBP-25-01

During one deployment, a miscommunication occurred between the bridge and the aft control room. The aft control team believed, based on a radio transmission, that the vessel had reached the agreed-upon speed of 1 knot. Acting on this assumption, wire payout began. However, the ship's speed-over-ground (SOG) display in the aft control room is known to fluctuate significantly and is unreliable at low speeds, making it difficult to confirm whether the ship had actually started moving.

Subsequently, the tension graph indicated that the dredge had contacted the seafloor. At that moment, the bridge radioed aft control to ask whether the vessel should begin moving along the transect—revealing that the ship had not yet started its forward motion. It is hypothesized that the dredge reached the bottom before the vessel was underway, preventing the dredge from being laid out in the proper orientation for effective rock collection.

Upon recovery, the bridle chains and chain bag were found tangled around the teeth at the top of the dredge mouth. This configuration suggests that the dredge did not settle on the seafloor as intended. Had the ship been moving at the moment of seafloor contact, this entanglement—and the likely failure to collect samples—would probably have been avoided.

10.6 Sample Recovery and Sorting

10.6.1 Sieving and cleaning

Before the dredge was brought on deck, the working area was thoroughly cleaned to remove any remaining material from previous deployments, thereby minimizing the risk of sample contamination. Once the dredge was secured above deck, it was carefully emptied.

An initial sieving and rinsing of the dredged material was conducted, followed by photographic documentation of the bulk sample—both within the dredge and after the rocks were placed on deck. These photographs serve as a valuable reference for approximating the stratigraphy of the collected material, with the earliest samples (retrieved at the start of the dredge path) likely found at the base of the chain bag, and the latest samples (retrieved near the end) nearer the top.

10.6.2 Sorting

A preliminary sorting process was conducted on the deck to select the most representative and atypical sample types, focusing on both common and distinct varieties. The sorting was based on characteristics such as the presence of lava and/or pyroclastic materials.

For lava samples, the following features were noted:

- Lava texture (pillows, cord, lobes, prisms, slabs)

- Presence of glassy rims, crystals, enclaves, ferruginous deposits, and traces of gas or hydrothermal sublimates
- Variation in vesicularity (size, shape, and quantity of vesicles)

For pyroclastic products, the sorting focused on:

- Bombs, lapilli, ash, and different juvenile textures (vitreous, vesicular, dense)
- Various types of non-juvenile fragments
- Identification of datable ancient biological samples, such as corals
- Enclaves and crystals present within the samples
- Fragile breccias or samples set aside for preservation

Following the initial sorting, a more detailed secondary sorting was conducted:

- All fragments were reviewed to determine which would not be retained for further analysis
- Morphological refinement of the sorting categories was completed
- Enclaves were searched for, with additional sawing and breaking of non-preserved samples, if necessary
- Samples were sawn to further examine textures, identify mineral presence, and uncover enclaves, as well as to prepare materials for total rock analysis and thin/thick section preparation
- Detailed descriptions of the various sample types were recorded, using a magnifying glass or binocular microscope when necessary
- Descriptions were documented in the log book for future reference
- Friable pyroclastic breccias were carefully conditioned to preserve their integrity

10.7 Rocks description

The characteristics of dredge samples were systematically recorded following a standard protocol:

- Sample Identification: The first section of the log includes essential identification details such as the cruise name, dredge number, sample number, total weight of the dredge, and the weight of each individual sample. This ensures proper labeling and traceability of samples from each dredge.
- Physical Description: A detailed description of the sample's physical characteristics was recorded, beginning with the classification of the sample (lava, breccia, drop-stone/erratic, xenolith) and, if volcanic, the amount of glass present.
- Textural Characteristics: The textural features of volcanic samples were described, including the overall texture (e.g., porphyritic, vesicular, massive, banded) and the nature

of the groundmass (e.g., fine-coarse grained, aphanitic). In the case of volcaniclastic samples, the size, angularity of clasts, type of lithics, and the characteristics of the inter-clast matrix were also recorded.

- Alteration Details: A crucial part of the logging process involves noting any alterations present in the sample. This includes identifying manganese coatings, oxidized rinds, and any alterations of minerals or groundmass, which may provide insights into the sample's history.
- Compositional Characteristics: The compositional properties were recorded, including the volume percentage of crystals, identification of mineral types, and details on the size and shape of crystals (e.g., anhedral, euhedral, subhedral).
- Vesicular Samples: For vesicular samples, detailed descriptions of the vesicles were noted, including their volume, shape, size, and the nature of any material filling the vesicles.
- Modal Rock Description: A summary of the overall texture and mineralogy was then provided, presenting a modal rock description. For example, a description might read, "Porphyritic, non-vesicular basalt with 15% phenocrysts of olivine, pyroxene, and plagioclase in an aphanitic groundmass."
- Additional Notes and Priority Analysis: Finally, any other relevant observations were recorded, and a priority analysis was assigned. This analysis ensures that rocks are flagged for further examination in areas such as geochronology, geochemistry, and preparation for thin or thick section analysis (e.g., for EMPA).
- Protocol Consistency: This logging protocol was applied consistently to each rock sample to maintain standardization and ensure detailed, systematic documentation.

10.8 Labelling

The photographs taken during the dredging process were carefully documented, including images at the scale of the dredge, as well as close-ups of individual sample types. Each photograph was labeled with the corresponding sample number and scale for easy identification. After collection, each sample was individually bagged and assigned a unique reference number (e.g., NBP25-01-DR01-G1, NBP25-01-DR01-G2, etc.). These reference numbers were clearly displayed on a label, which was then protected by a small plastic bag to ensure that it remained intact. Additionally, each sample was given an international nomenclature number to maintain consistent identification across various scientific platforms and databases (**Fig. 10.3**).

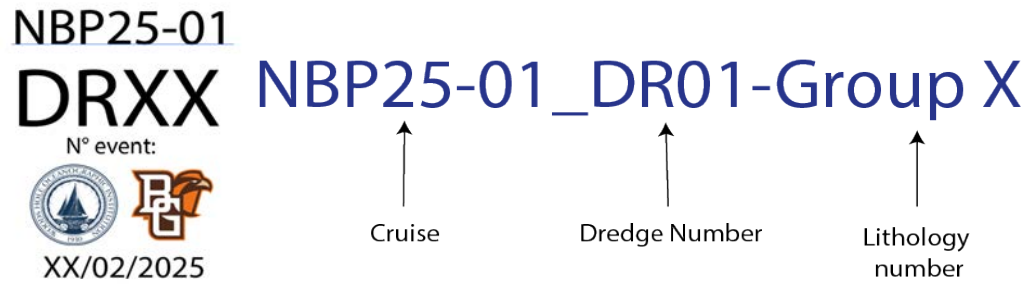

Figure 10.3: Label to be used to photograph the dredged rocks on the deck (Upper left). Label to be used to archive the sorted samples (right and bottom).

10.9 Preliminary Results

During the NBP25-01 cruise, 50 dredges have been performed on the two branches of the Terror Rift (**Fig. 10.4**).

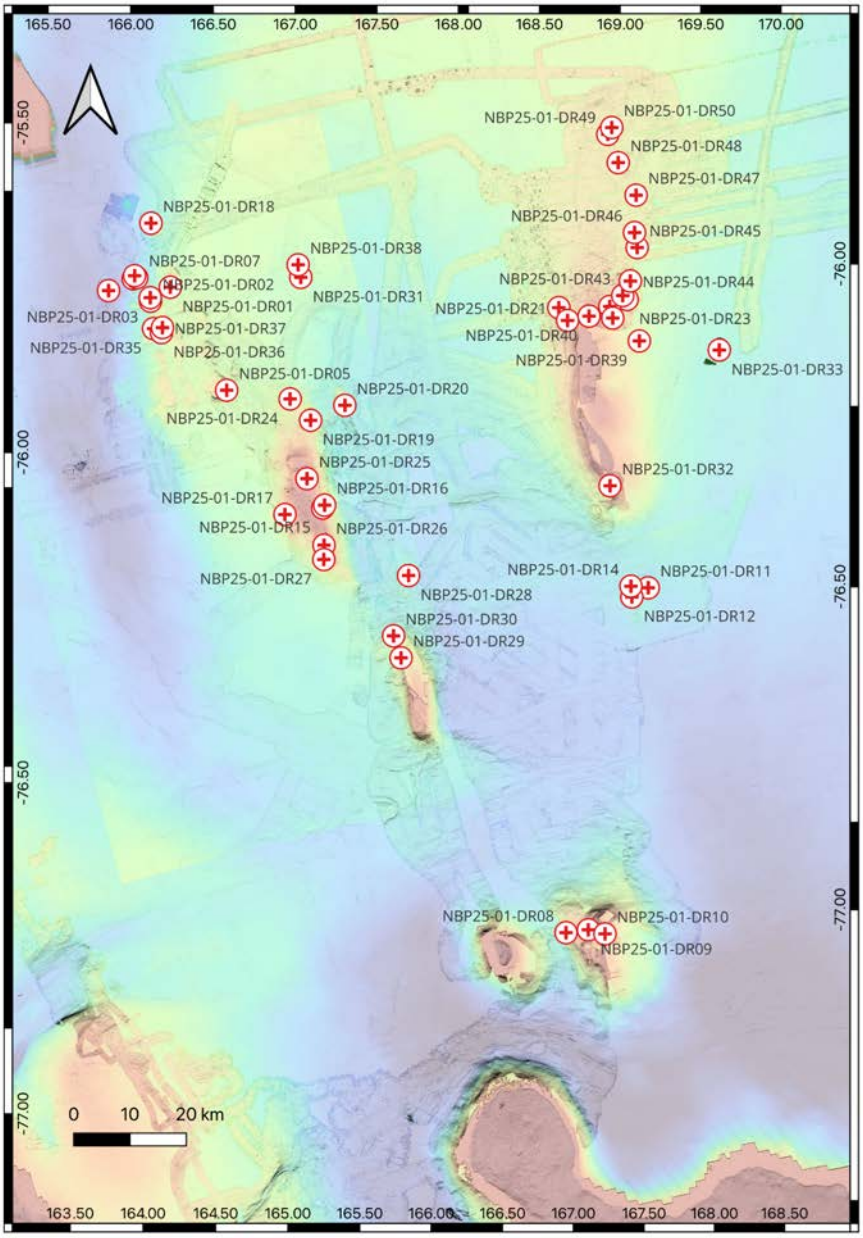

Figure 10.4: Location of dredges performed during Expedition NBP25-01.

10.9.1 DR01

Flat-top seamount (named Nomad, **Fig. 10.5**), located in the northern part of the Flapjack Field, was dredged on February 22nd. Dredged samples are mainly greenish-gray fine-grained breccia and erratics. We also found fragments of vesicular lava (**Fig. 10.5**) which may contain mantle xenoliths and armored bombs made of ash and lapilli with olivine and pyroxene crystals.

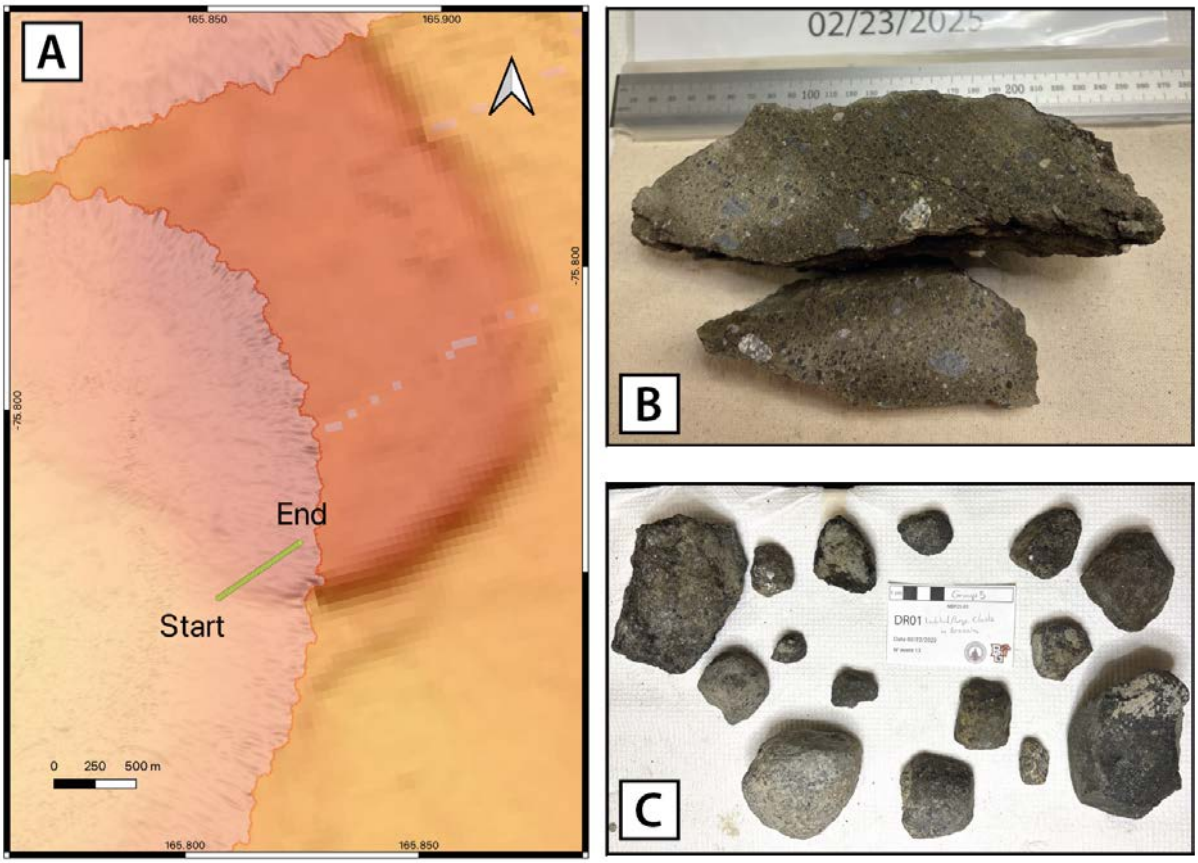

Figure 10.5: a) DR01 performed on the Nomad seamount in the Flapjack field. b) breccia and c) volcanic clasts collected.

10.9.2 DR02

Two dredges were realized on the Squid Ridge on February 22nd (**Fig. 10.6**). Squid Ridge is an elongated volcanic edifice with a steep relief. The first dredge, performed on the lower platform, collected highly altered and oxidized breccia with angular and blocky clasts. Olivine, clinopyroxene and amphibole crystals have been sorted. Dredge DR02 also collected lapilli-ash deposits on which fine grains of glass and minerals have been identified.

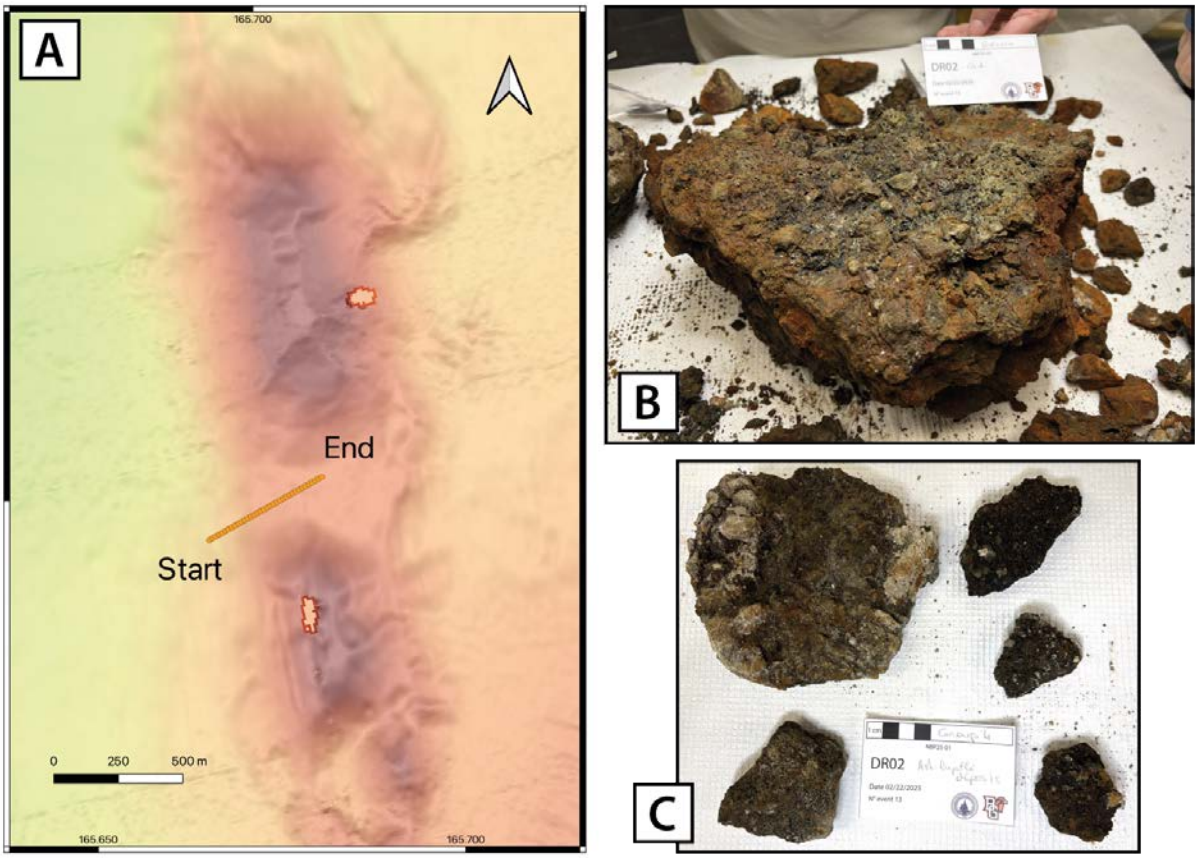

Figure 10.6: a) DR02 performed on the lower platform of Squid ridge edifice. b) breccia and c) lapilli-ash deposits collected.

10.9.3 DR03

The second dredge on Squid Ridge was performed on the main edifice on February 22nd (**Fig. 10.7**). The dredge collected glassy amphibole-bearing lava and bombs containing peridotite xenoliths. Other lava samples collected show light and dark-colored portions that appear mingled. Also breccia was recovered that contains matrix-supported angular to subround clasts of glass and crystals (amphibole, olivine). In addition, DR03 dredge recovered a large amount of round and lumpy 'cauliflower-shaped' lava. This dredge had very few erratics.

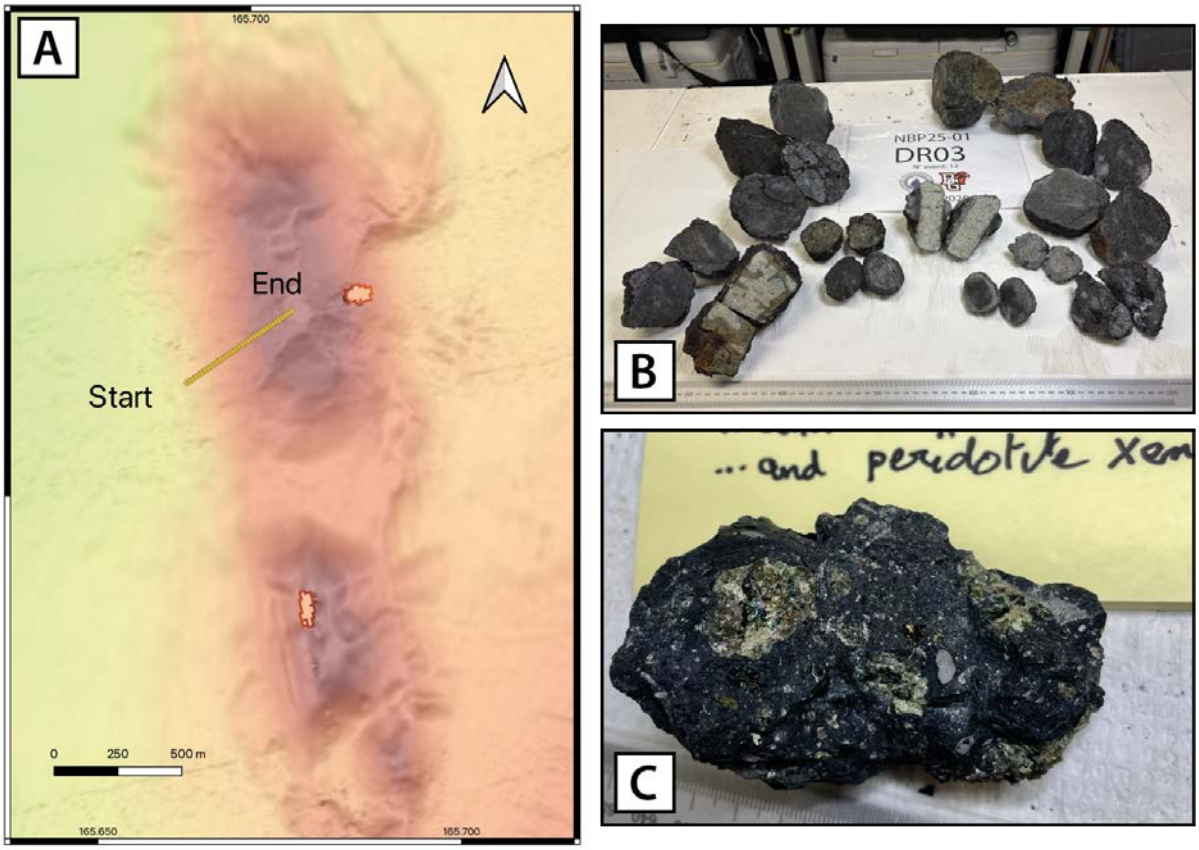

Figure 10.7: a) DR03, the second dredge performed on Squid Ridge on the main edifice. b) cut samples of breccia, lava a bomb with xenoliths and c) xenolith-bearing lava.

10.9.4 DR04

DR04 was conducted on Feather Top seamount (**Fig. 10.8**) on February 22nd. The dredge track included a portion of the lower relief flat-top on which the steep ridge of Feather Top sits. DR04 recovered an agglomerate with ash-lapilli sized clasts composed of vesicular glass and crystals of olivine and pyroxene and some mantle xenoliths were identified. Also collected was a red-orange oxidized crust with a muddy matrix with a surface with burrows(?).

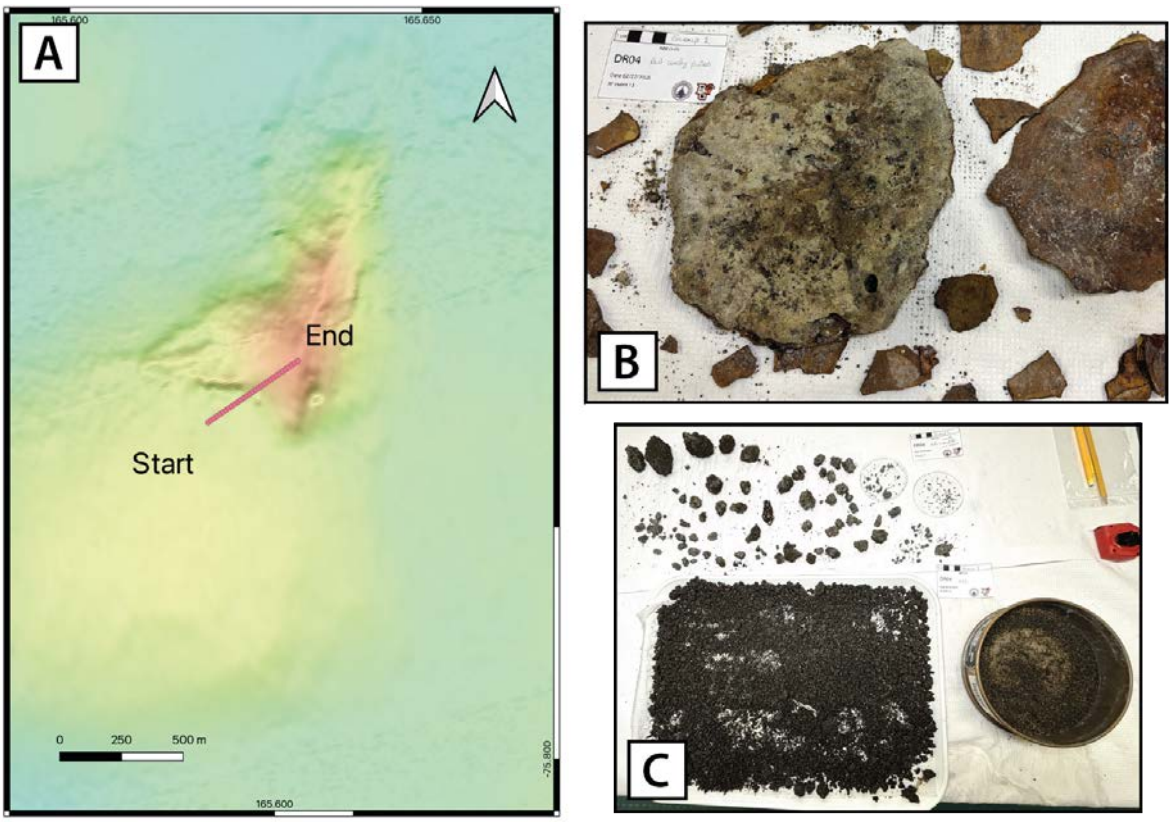

Figure 10.8: a) DR04, conducted on Feather Top includes low-relief portion at base. b) oxidized crust with burrows(?). c) agglomerate fragments and smaller fractions.

10.9.5 DR05

In the southern portion of the Flapjack Field, the flat-top Hoto kēiki (**Fig. 10.09**) was dredged on February 27th. Dredged samples consist of fine-grained ash and fine-grained matrix-supported tuff breccia with clasts of non-vesicular angular glass, olivine crystals and no lithics. DR05 recovered a small amount of vesicular lava and a few erratics.

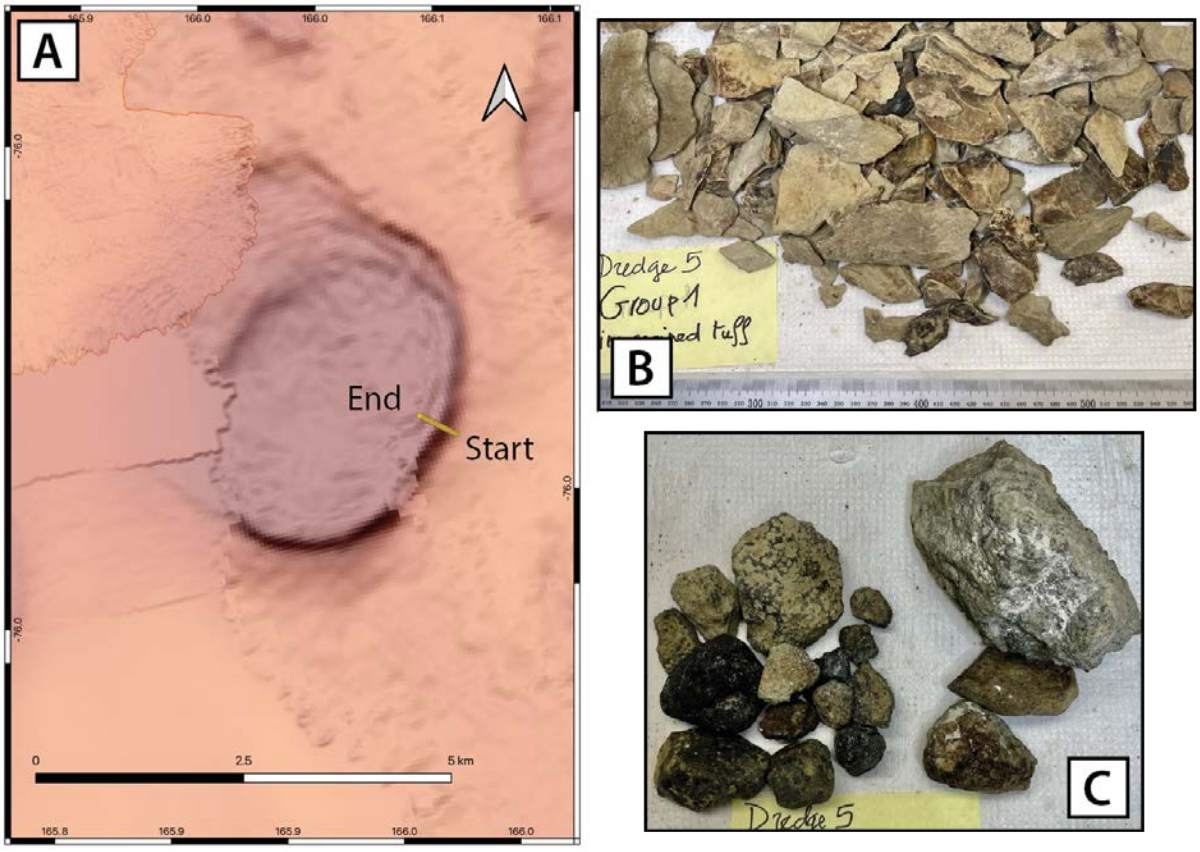

Figure 10.9: a) DR05, performed on steeper SE side of Hoto kēiki flat-top seamount. b) fine grained (ash) hyalotuff. c) breccia and lava samples collected.

10.9.6 DR06

Dredge DR06 took place on February 27th to the west of the Flapjack Field and further into the Terror Rift on a prominent ridge that is named Mittlekind (**Fig. 10.10**). Recovered from this dredge is scoria and clast-supported ash-lapilli breccia containing glass and minerals of olivine, pyroxene and amphibole. Peridotite xenoliths are identified. DR06 also collected a diverse suite of erratics that include granitoids, shale, schist and consolidated diamictite.

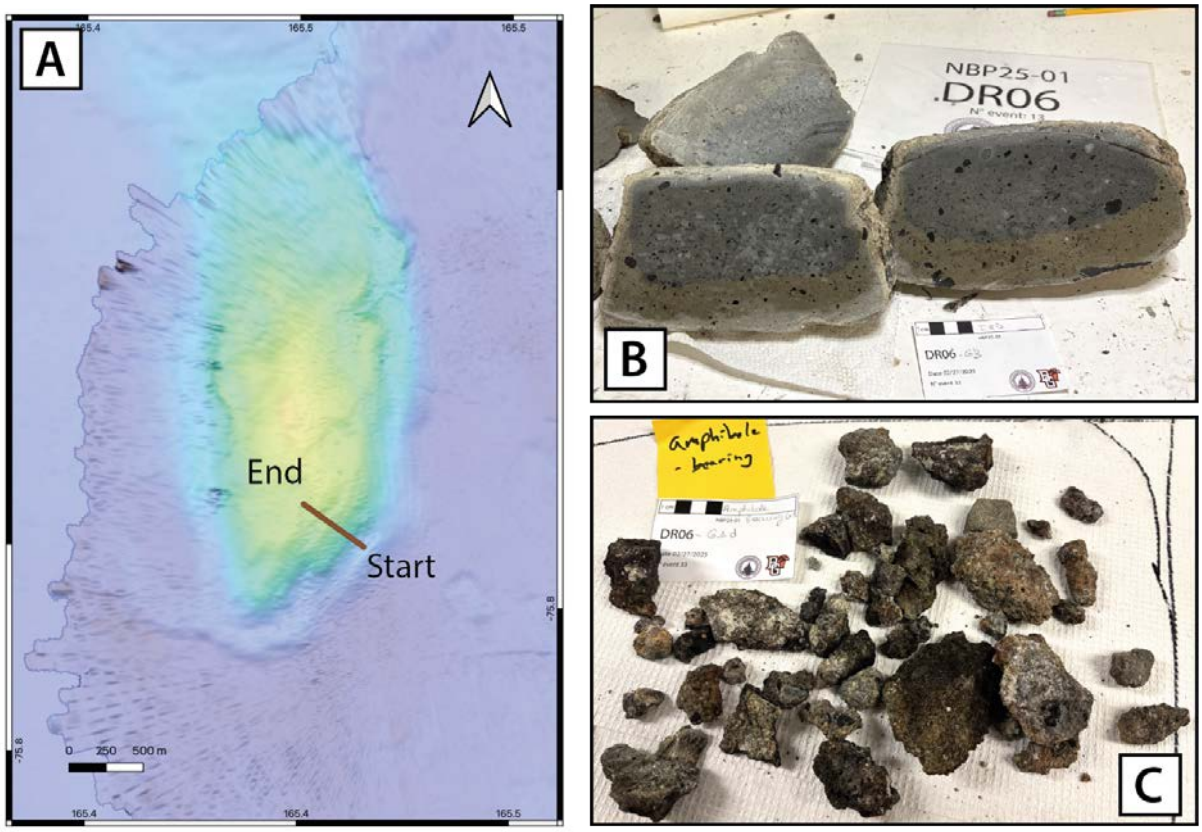

Figure 10.10: a) DR06 performed on Mittlekind Ridge. b) cut boulder of a diamictite erratic with alteration rind. c) amphibole-bearing ash-lapilli breccia, scoria, agglomerate (all pyroclastic).

10.9.7 DR07

Returning to Feather Top (**Fig. 10.11**) on February 28th the second dredge on this seamount yielded red and highly oxidized volcanic 'crust' (lava or tephra) and breccia. Also recovered were a few small erratics.

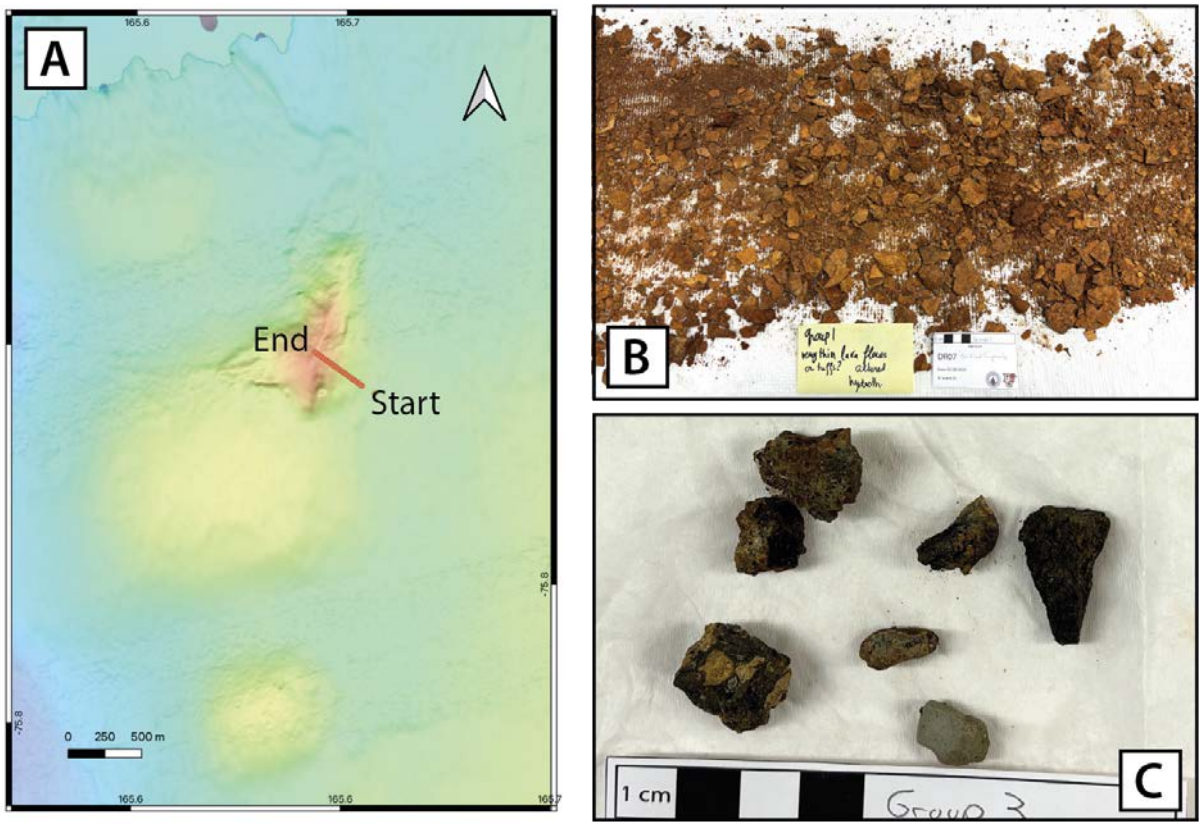

Figure 10.11: a) DR07, second dredge on Feather Top (refer to DR04). b) red, hydrothermally altered volcanic material near the start of dredge at base. c) lava clasts from breccia.

10.9.8 DR08

On March 3rd dredging was conducted on Beaufort Bank in the southern region of the Terror Rift Volcanic Field (**Fig. 10.12**). The first of 3 dredges, DR08 was near the base of the edifice and recovered dark gray, moderately vesicular to massive, porphyritic lava with phenocrysts of pyroxene and feldspar (minor olivine). The lava also contains peridotite xenoliths. In addition, the dredge contains reddish-brown scoria with phenocrysts of pyroxene and amphibole in a glassy groundmass. A relatively smaller amount of lava and breccia was also recovered. No erratics.

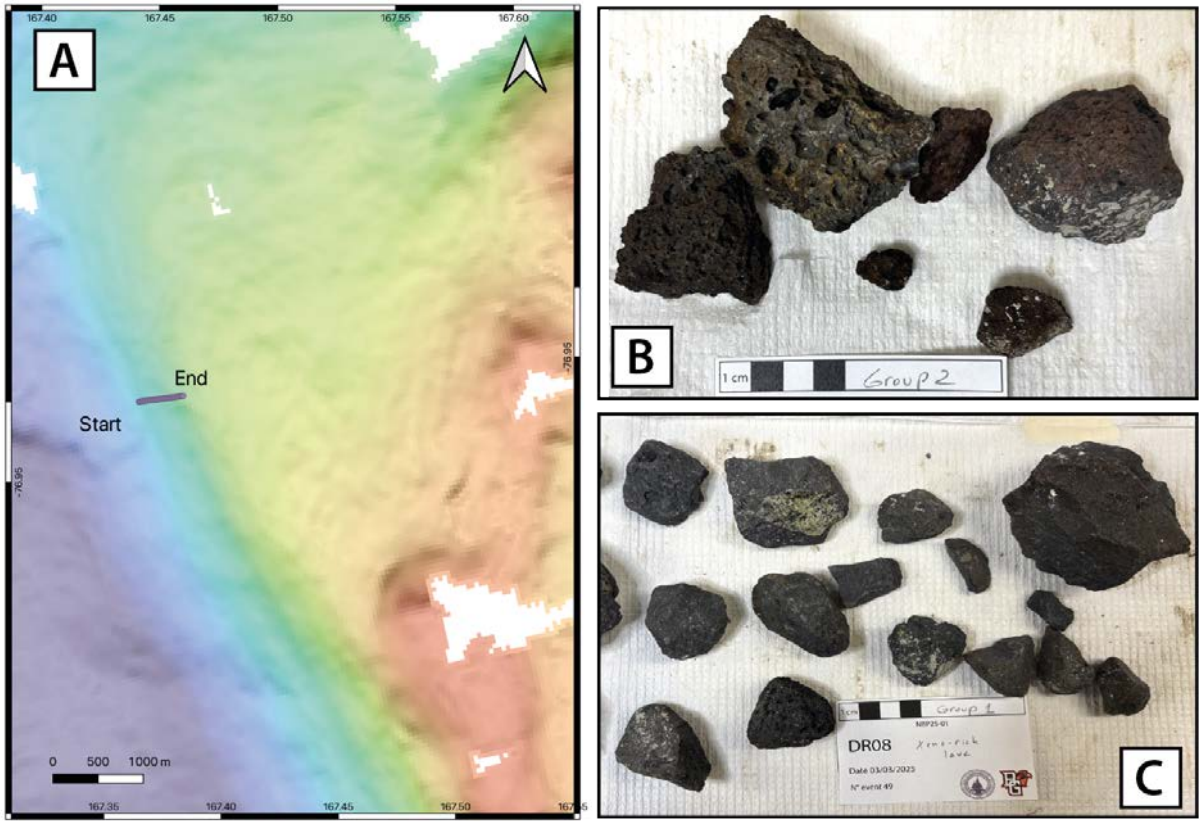

Figure 10.12: a) DR08, conducted near the base of Beaufort Bank' western flank. b) scoria with phenocrysts of amphibole and pyroxene. c) mantle xenolith-bearing lava.

10.9.9 DR09

The second dredge on Beaufort Bank on the same day (March 3rd) was taken mid-way up the edifice (**Fig. 10.13**). The most abundant lithology is a brownish-red, clast-supported, monolithic breccia containing glassy, coarse-ash to fine-lapilli clasts. In addition, grayish-brown, massive to vesicular lava with sparse phenocrysts of olivine, pyroxene and feldspar is recovered. Amphibole and glass were separated from finer unsorted sample fragments and several small peridotite xenoliths are found. DR09 dredge contained one erratic; a boulder-sized diorite fragment.

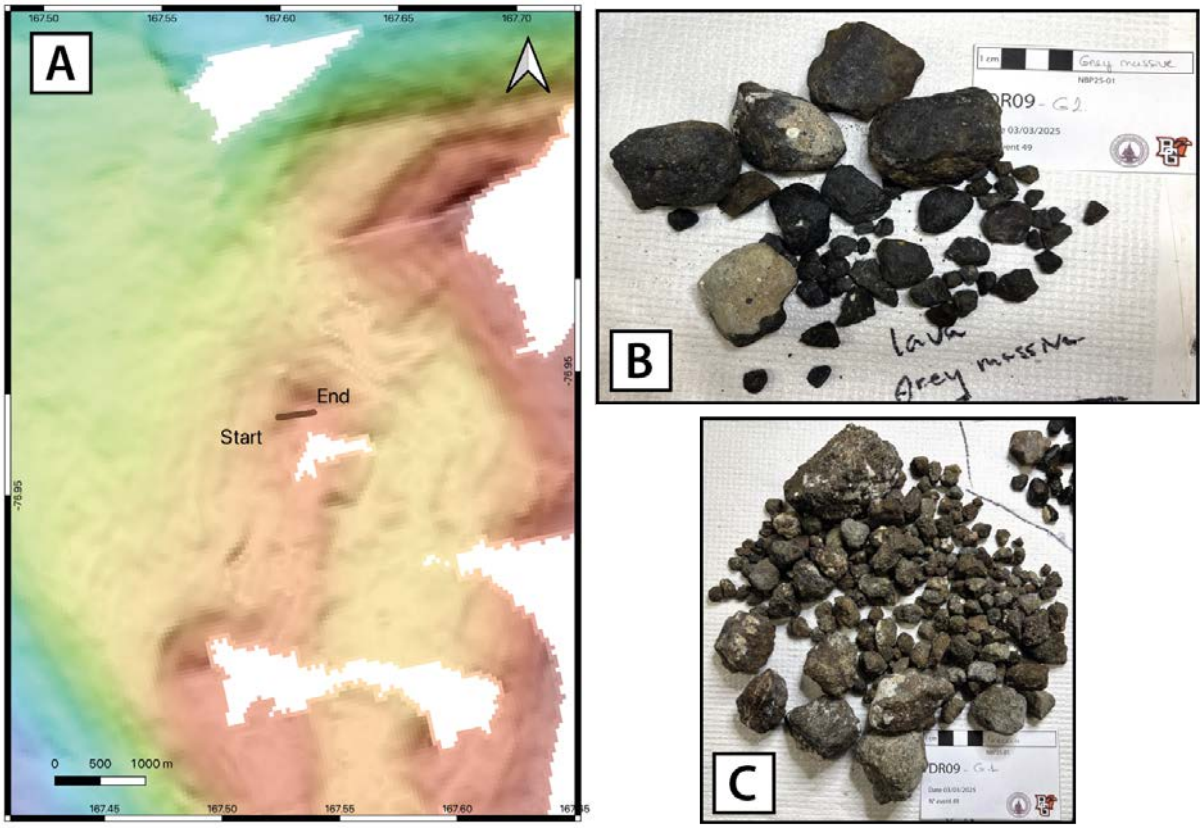

Figure 10.13: a) DR09 was performed mid-way up the western flank of Beaufort Bank. b) massive to coarsely vesiculated lava. c) monolithic breccia.

10.9.10 DR10

The third dredge on Beaufort Bank, also on March 3rd, was near the top of the edifice (**Fig. 10.14**). Recovered in DR10 was a very small amount of gray to black, variably vesicular mafic lava. Mostly subround to round fragments, one contains amphibole and one shows glacial striations.

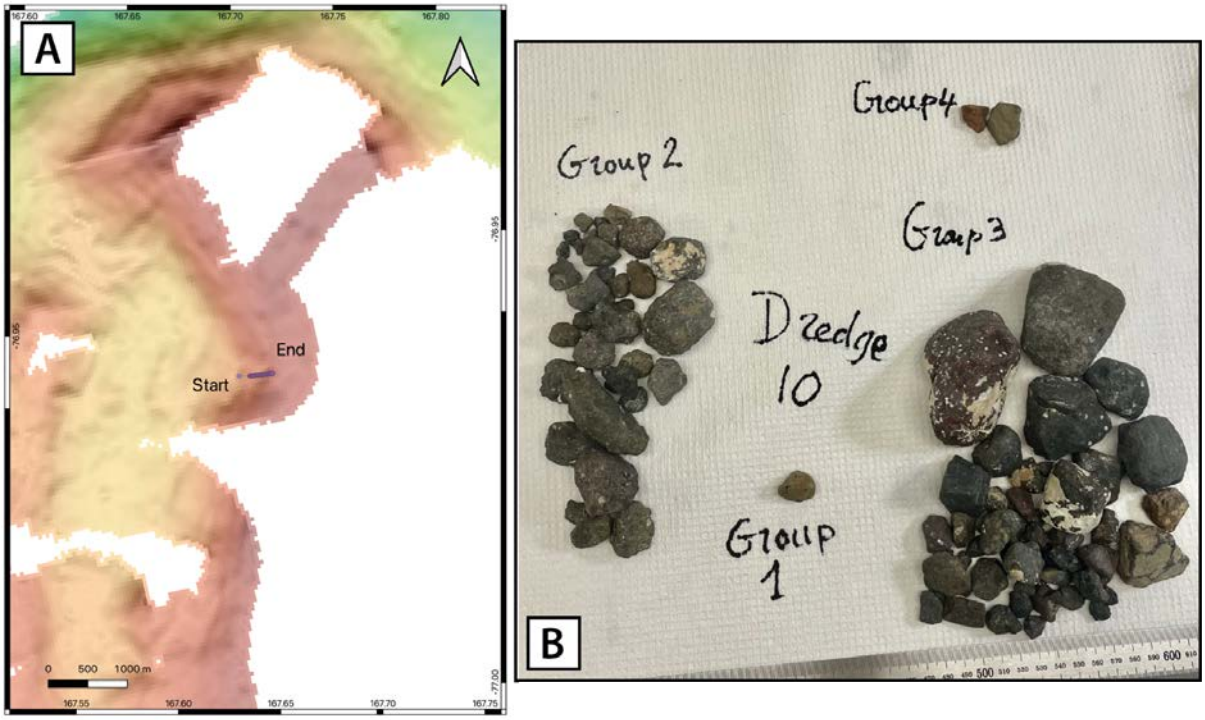

Figure 10.14: a) DR10 was conducted on the upper western flank of Beaufort Bank. b) shows all samples collected that includes breccia, lava and lithics.

10.9.11 DR11

Dredge DR11 took place on seamount N°5 within the Channel Group south of Franklin Island (**Fig. 10.15**) on March 5th. Samples recovered include reddish-gray variably vesicular lava with phenocrysts of olivine and amphibole. About half-dozen lava samples contain peridotite (mantle xenoliths). In addition, the dredge contains yellowish-gray to brown, matrix-supported breccia with monolithic lapilli-sized, non-vesicular clasts. DR11 also recovered brownish to dark gray monolithic agglutinated lapilli consisting of angular, crystal-poor clasts. Two erratics are identified.

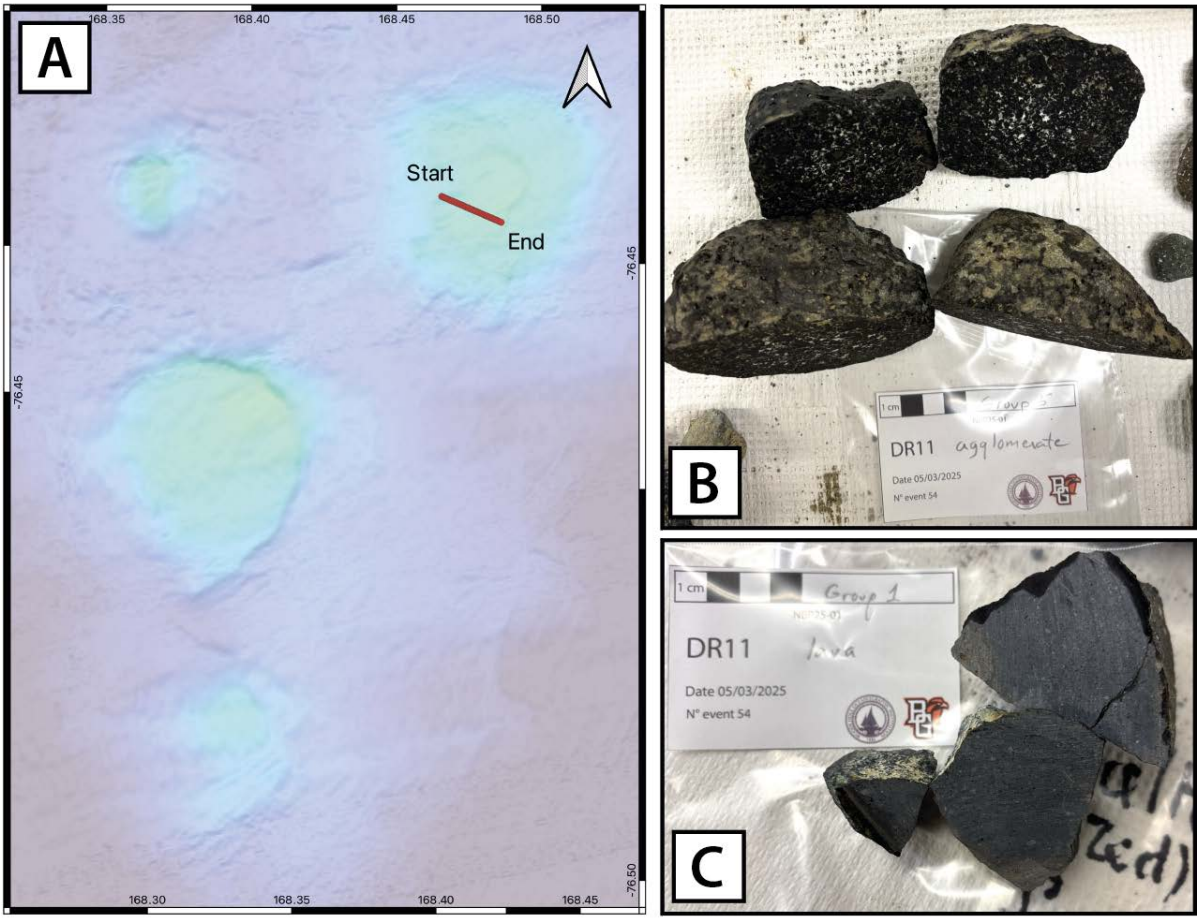

Figure 10.15: a) DR11, was performed on the N°5 seamount, part of the Channel Group. b) cut pieces of ash-lapilli agglomerate. c) cut pieces of amphibole- and xenolith-bearing lava.

10.9.12 DR12

Due to technical difficulties no material was recovered from this dredge, which was attempted on Mademoiselle seamount in the Channel Group.

10.9.13 DR13

On March 5th the Mademoiselle seamount (a flat-top morphology) in the Channel Group was dredged successfully (**Fig. 10.16**). DR13 recovered grayish-black agglutinated ash and lapilli-ash, greenish-brown to reddish-brown, monolithic breccia and brownish-gray to reddish-gray scoria. Clasts within lapilli-ash agglomerate and within breccia are vesicular while in the finer-grained, poorly consolidated ash are less vesicular, glassy and blocky. In addition, DR13 recovered dark gray to greenish-gray to reddish, poorly vesicular lava within which two peridotite xenoliths were identified.

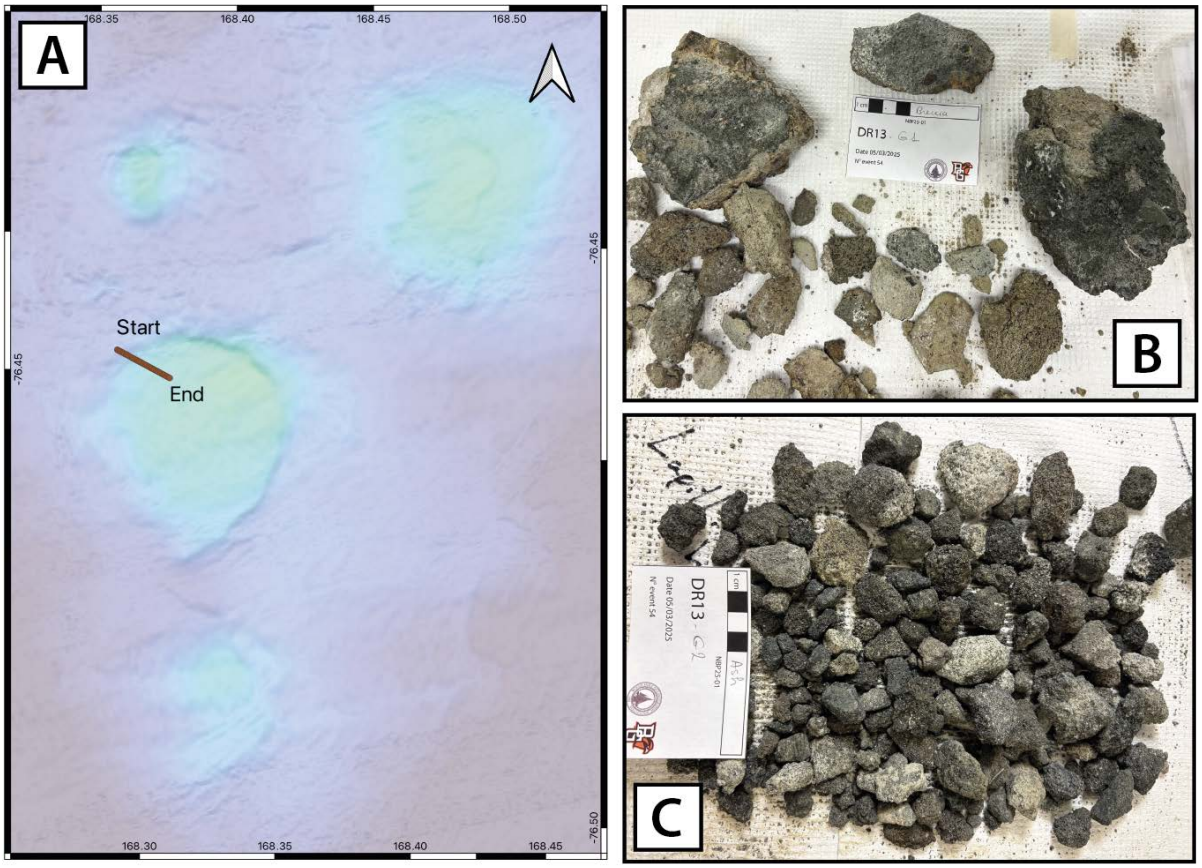

Figure 10.16: a) DR13 was taken on Mademoiselle flat-top seamount in the Channel Island Group. b) breccia with matrix supported volcanic clasts. c) agglomerate made up of fine to medium ash.

10.9.14 DR14

A third volcanic edifice within the Channel Group was dredged on March 5th. This volcanic cone lies to the north of the 'Mademoiselle' flat-top seamount and appears to intersect the channel (**Fig. 10.17**). Dredged samples consist of indurated and agglutinated ash and lapilli-ash deposit fragments. DR14 also recovered light gray to reddish-gray breccia containing angular to subrounded vesicular and blocky lava clasts. Some of these breccia and lava clasts display a greater degree of weathering. A few samples are vesicular to massive angular lava containing amphibole crystals and mantle xenoliths. Three IRD samples are identified.

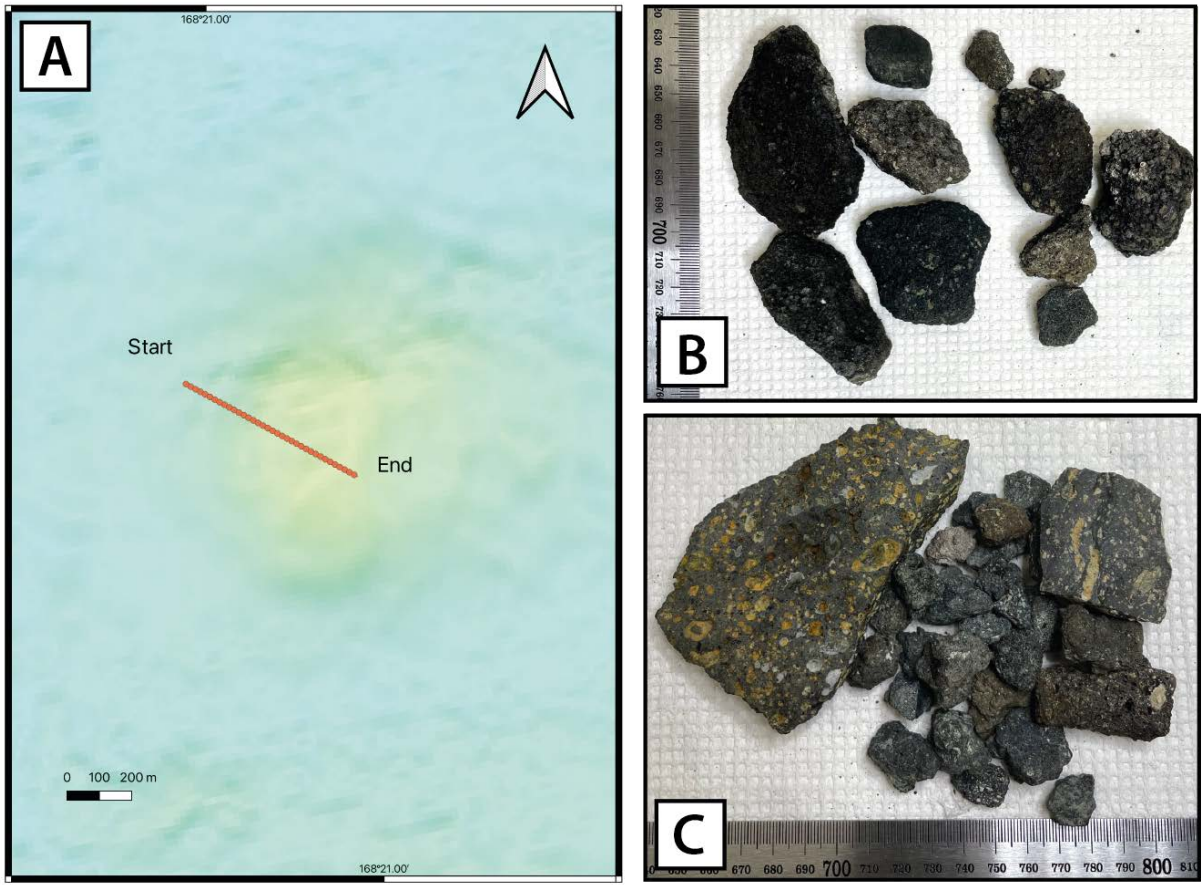

Figure 10.17: a) DR14 taken on Coco seamount was the last site dredged in the Channel Group. b) agglomerate made up of lapilli. c) vesicular lava containing amphibole.

10.9.15 DR15

DR15 took place on March 9th on the eastern flank of Davey Bank (**Fig. 10.18**). Samples recovered include light gray and friable matrix-supported breccia. Clasts in this monolithic breccia consist of millimetric to centimetric volcanic fragments. DR15 also sampled highly vesicular and aphanitic angular scoria, angular to subrounded lava fragments containing feldspar phenocrysts, crystalline groundmass and few mantle xenoliths and glass.

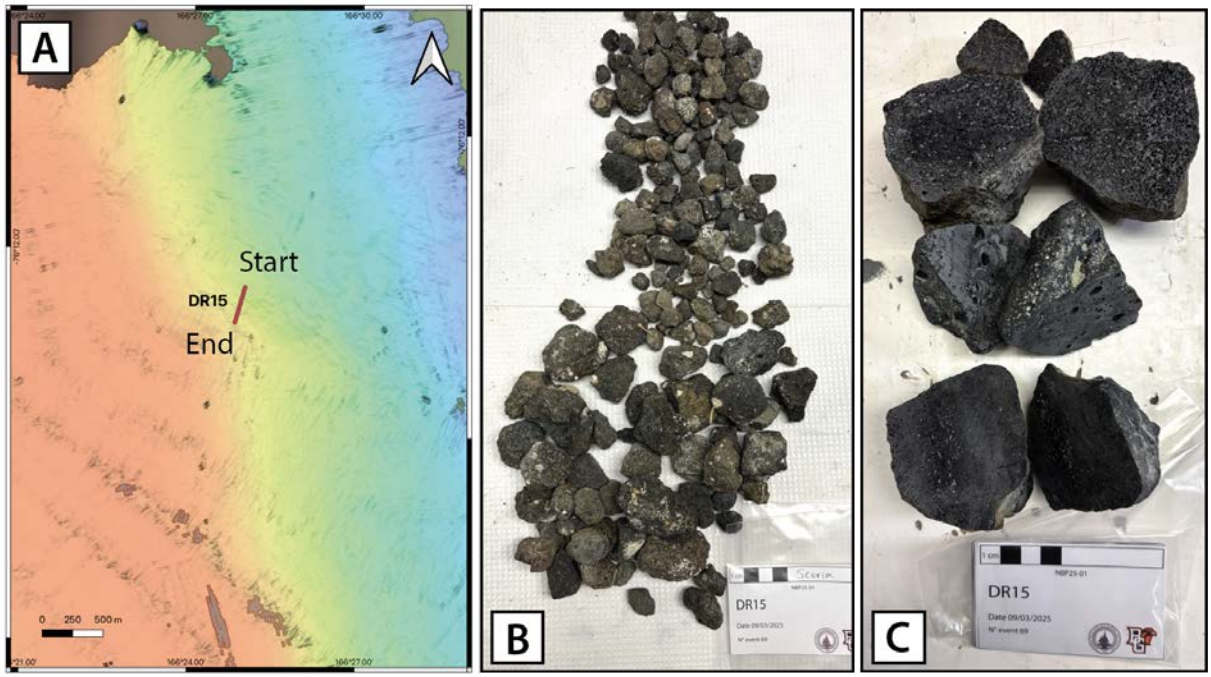

Figure 10.18: a) DR15 was conducted on the east flank of Davey Bank. b) scoria with aphanitic groundmass. c) split samples of lava and breccia.

10.9.16 DR16

Rocks were collected by dredging on the southeastern slopes of Davey Bank on March 9th (**Fig. 10.19**). Poor recovery yielded small quantities of breccia and lava. Lava recovered from DR16 consists of dark gray, massive to highly vesicular lithologies with microcrystalline groundmass. Samples of breccia are light brownish-red to gray, matrix-supported, containing round to subround, moderately vesicular, monolithic clasts. A total of 2-3 erratics, one schist, is identified.

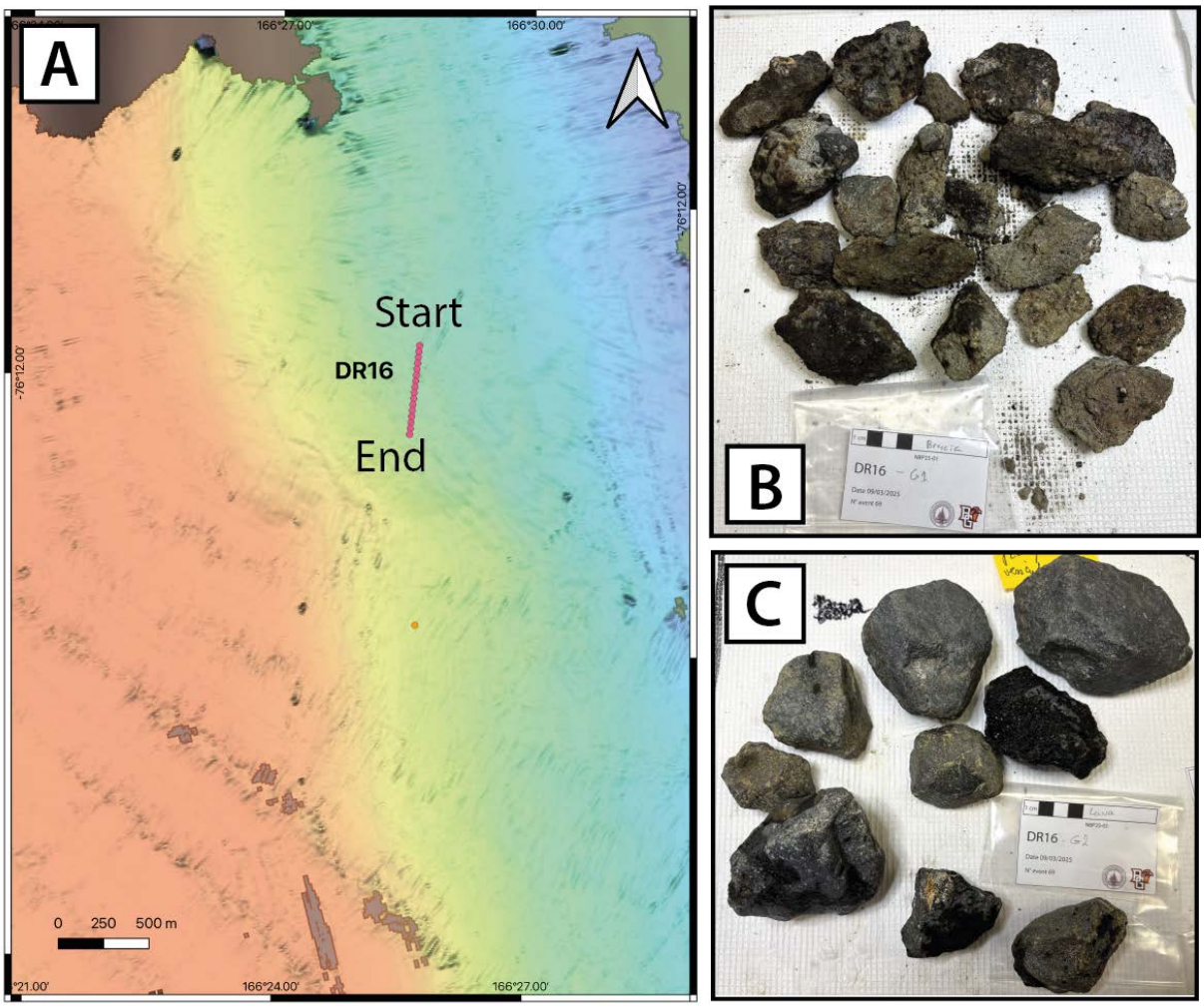

Figure 10.19: a) DR16 was undertaken on the SE flank of Davey Bank. b) monolithic breccia with clasts supported by matrix. c) lava with microcrystalline groundmass.

10.9.17 DR17

A third dredge on the Davey Bank, also on March 9th, was on its western flank (**Fig. 10.20**). As the dredge was carried out in bad weather, its exact location could not be determined. DR17 collected yellowish-brown matrix-supported breccia with massive to vesicular volcanic clasts and minerals. Isolated lava samples were also recovered. Lava samples consist of centimetric to pluricentimetric massive to highly vesicular (scoriacious) fragments with plagioclase phenocryst and microcrystalline groundmass. Few IRD showing striations (schist, granitoids and maybe some volcanic) have been recovered.

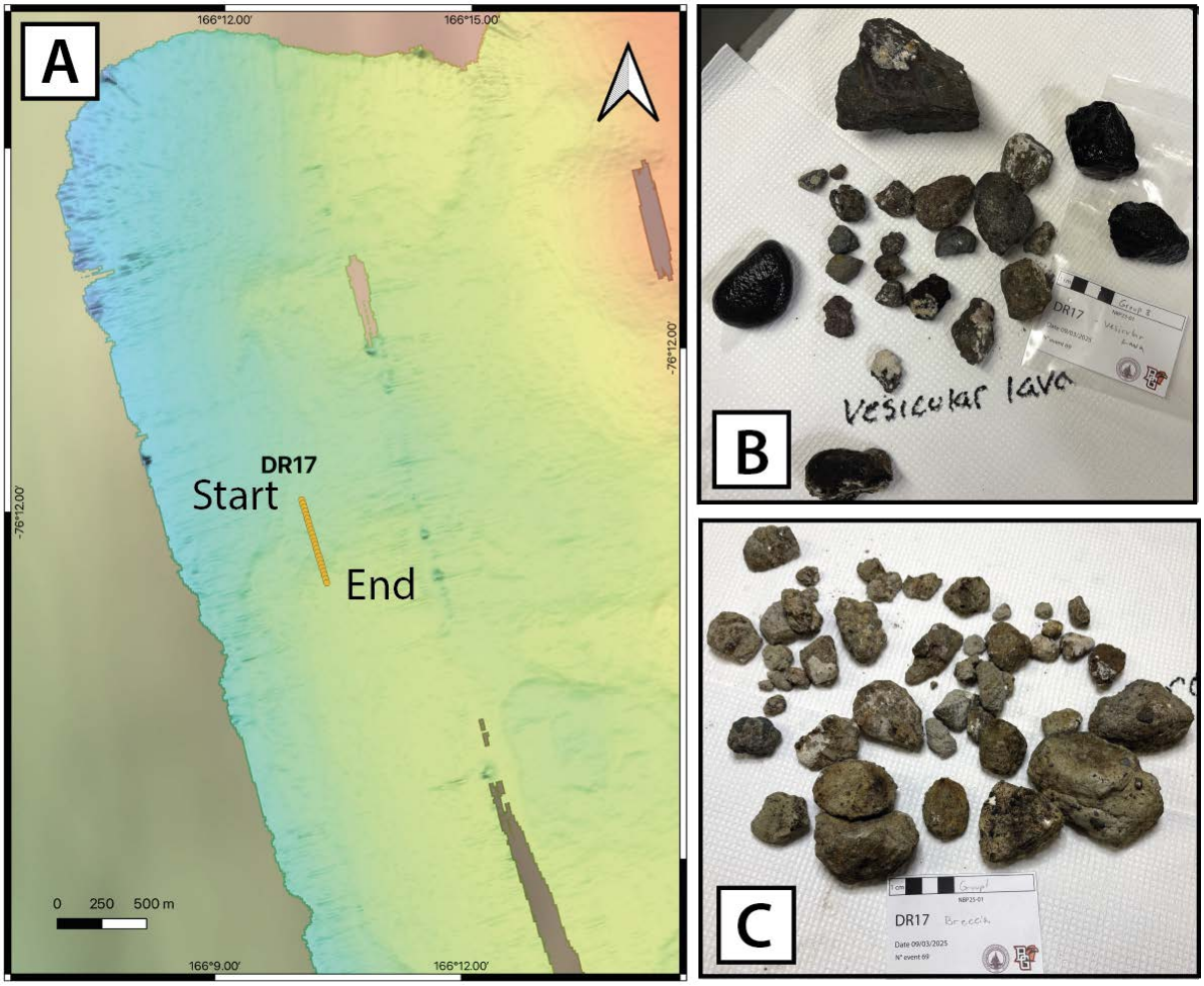

Figure 10.20: a) DR17 was conducted on Davey Bank west flank. b) vesicular lava with phenocrysts of plagioclase. c) breccia with both massive and vesicular matrix-supported clasts.

10.9.18 DR18

DR18 was performed on the Galette seamount (flat-top) in the northern portion of the Flapjack Field (**Fig. 10.21**) on March 11th. Yellow to brownish-gray, matrix-supported, heterolithic breccia was recovered. Clasts within the breccia are angular to subround and mostly volcanic (crystalline, glassy and poorly vesicular matrices) but some granitoid clasts are identified within the breccia. Peridotite xenoliths are identified in some of the clasts and other clasts are crystal-rich with amphibole, olivine, pyroxene and feldspar. Also included in the dredge haul are a small number (10-12) of agglomerates of ash-lapilli. Granitoid erratics also make up a small proportion recovered and minerals and small fragments of granitoids were loose from the breccia and separated.

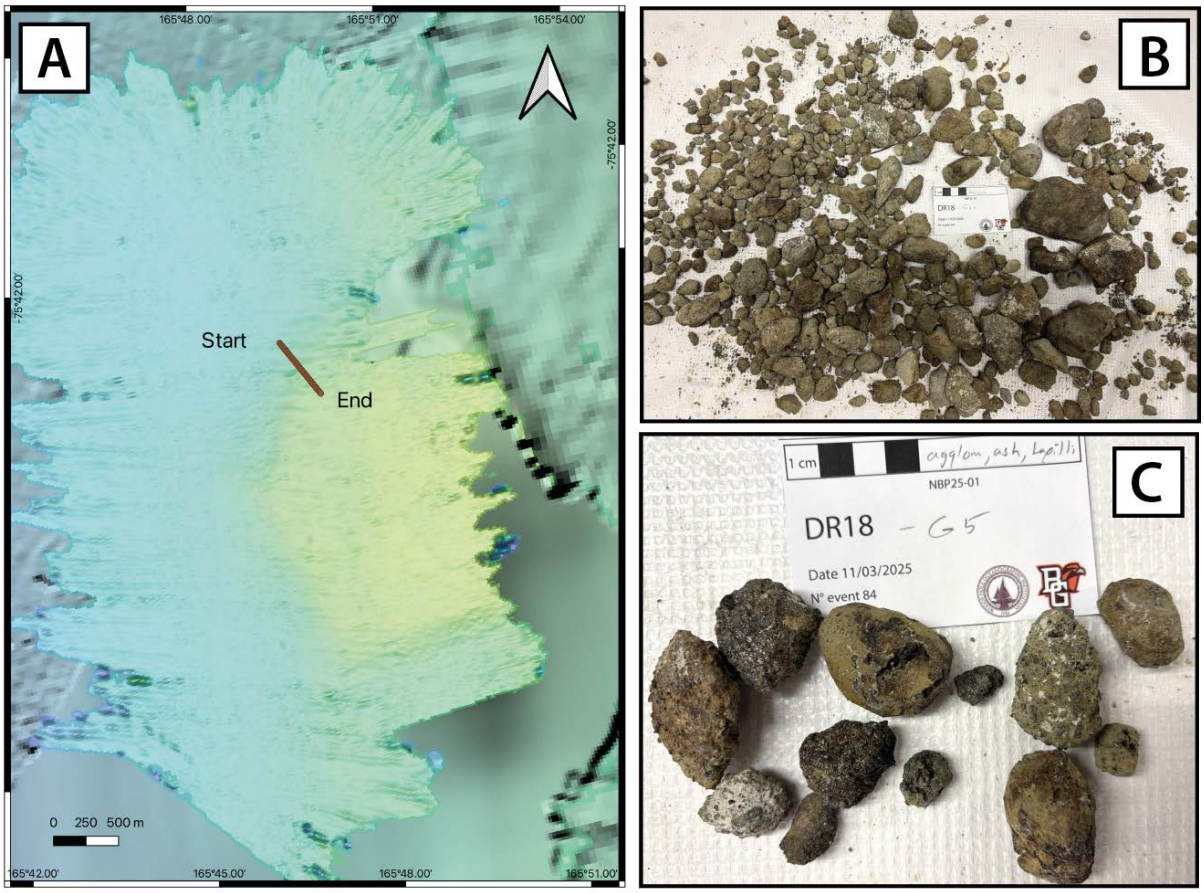

Figure 10.21: a) DR18 occurred in the northern part of the Flapjack Field on a flat-top seamount named Galette. b) breccia with mostly volcanic clasts but also granitoids. c) ash-lapilli agglomerate.

10.9.19 DR19

A flat-top seamount located in the northern part on Davey Bank was dredged on March 18th (**Fig. 10.22**). The collected samples are xenolith-bearing lava, pyroclasts and breccia. Some lava

mingling is observed. Pyroclast deposits consist of agglutinated ash and lapilli. The matrix supported breccia contains glass and may be layered. Lava fragments in breccia or isolated are mostly vesicular and contain olivine and pyroxene crystals.

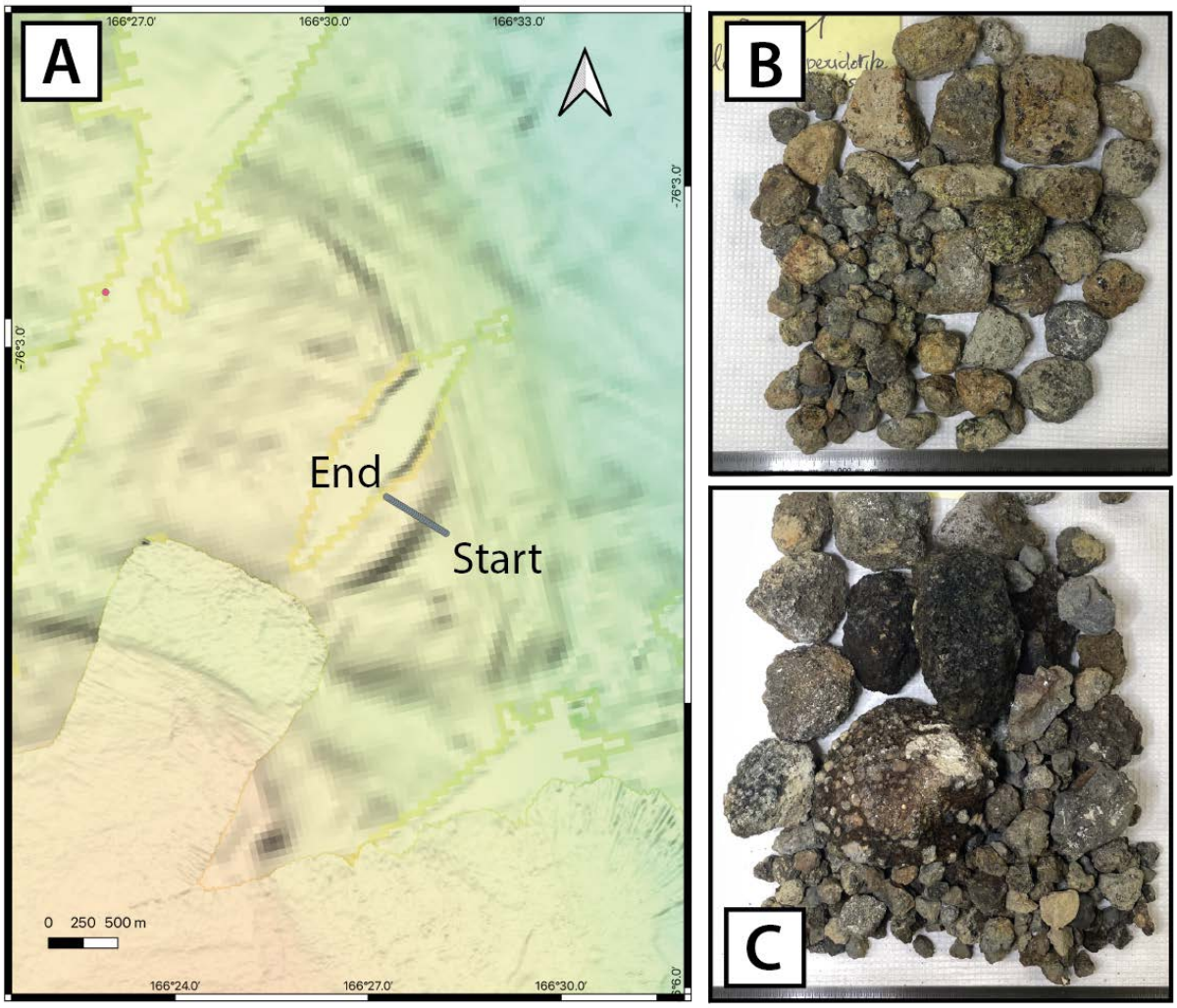

Figure 10.22: a) DR19 was undertaken on a flat-top seamount immediately north of Davey Bank and named Biscuit. b) agglomerate and bombs containing xenoliths. c) agglomerate with bomb pieces(?).

10.9.20 DR20

The Attenuator seamount is an isolated edifice to the northeast of Davey Bank (**Fig. 10.23**) and was dredged on March 18th. Most of the lithologies recovered from this seamount are lava and consist of light gray to beige to dark gray and are both massive and vesicular. They are mostly coated with mud, which is strongly adhered and obscures surfaces. DR20 also recovered a few agglomerates which are greenish-gray and contain angular clasts that are coarse ash to lapilli in size. Small, single samples include one that contains a large amphibole (xenocryst?) and a vesicular lava with an altered peridotite inclusion. No erratics were found in this dredge.

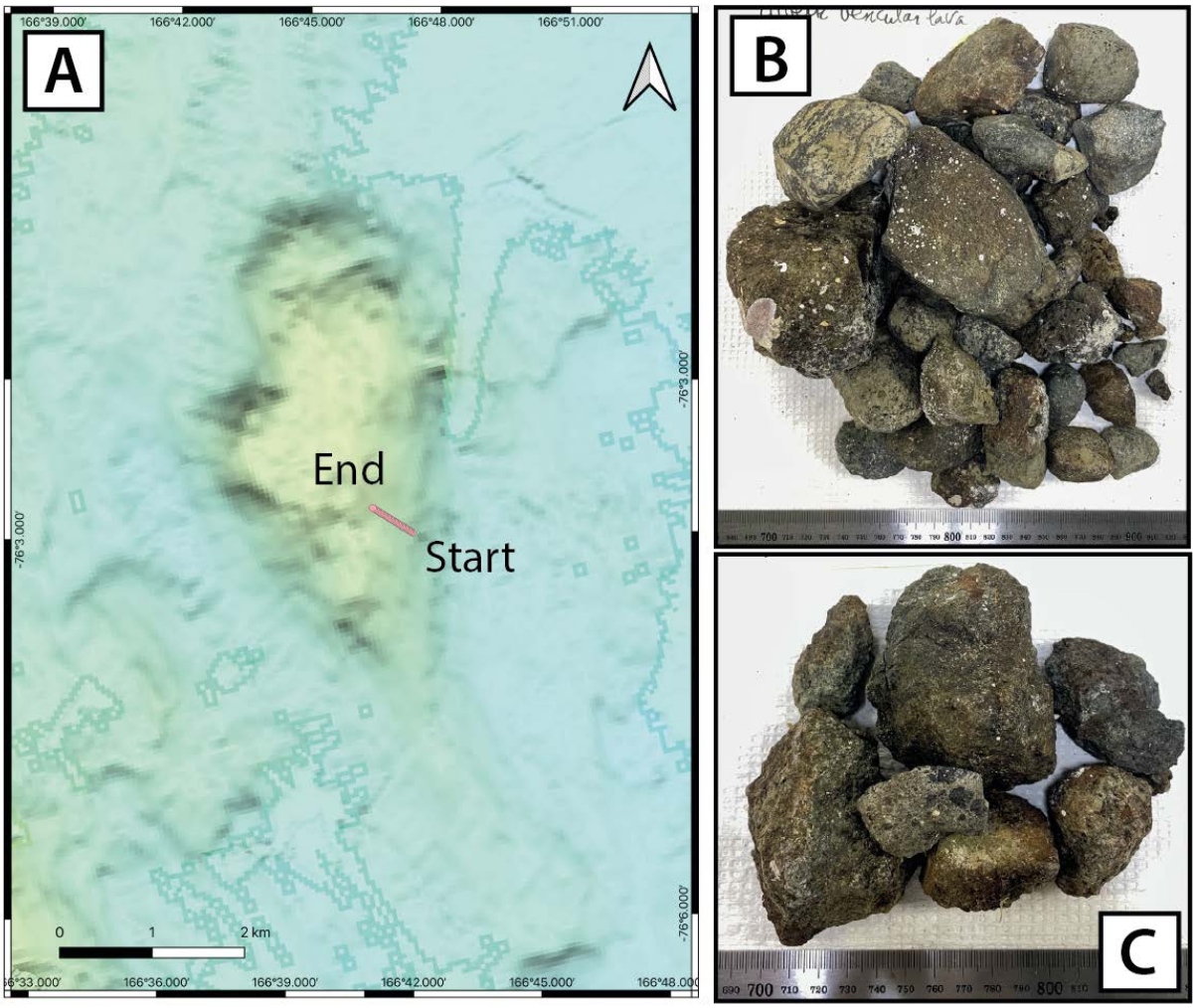

Figure 10.23: a) DR20 was taken on an isolated edifice to the northeast of Davey Bank named Attenuator. b) Vesicular lava fragments. c) Greenish-gray agglomerates containing coarse ash to lapilli.

10.9.21 DR21

A small seamount north of Franklin Island adjacent to the pockmark field (**Fig. 10.24**) was dredged on March 18th. Dark gray to beige, matrix supported breccia contains glass and vesicular clasts. Also sampled are agglomerates with ash to lapilli-size agglutinated fragments. Smaller samples of agglomerates appear to have fresh(er) glass. Dark gray lava samples vary from poorly vesicular to vesicular and a xenolith (peridotite?) is identified in one sample. Lava fragments have abundant coral coating their surfaces. One piece is very fine grained and may be intrusive (erratic?).

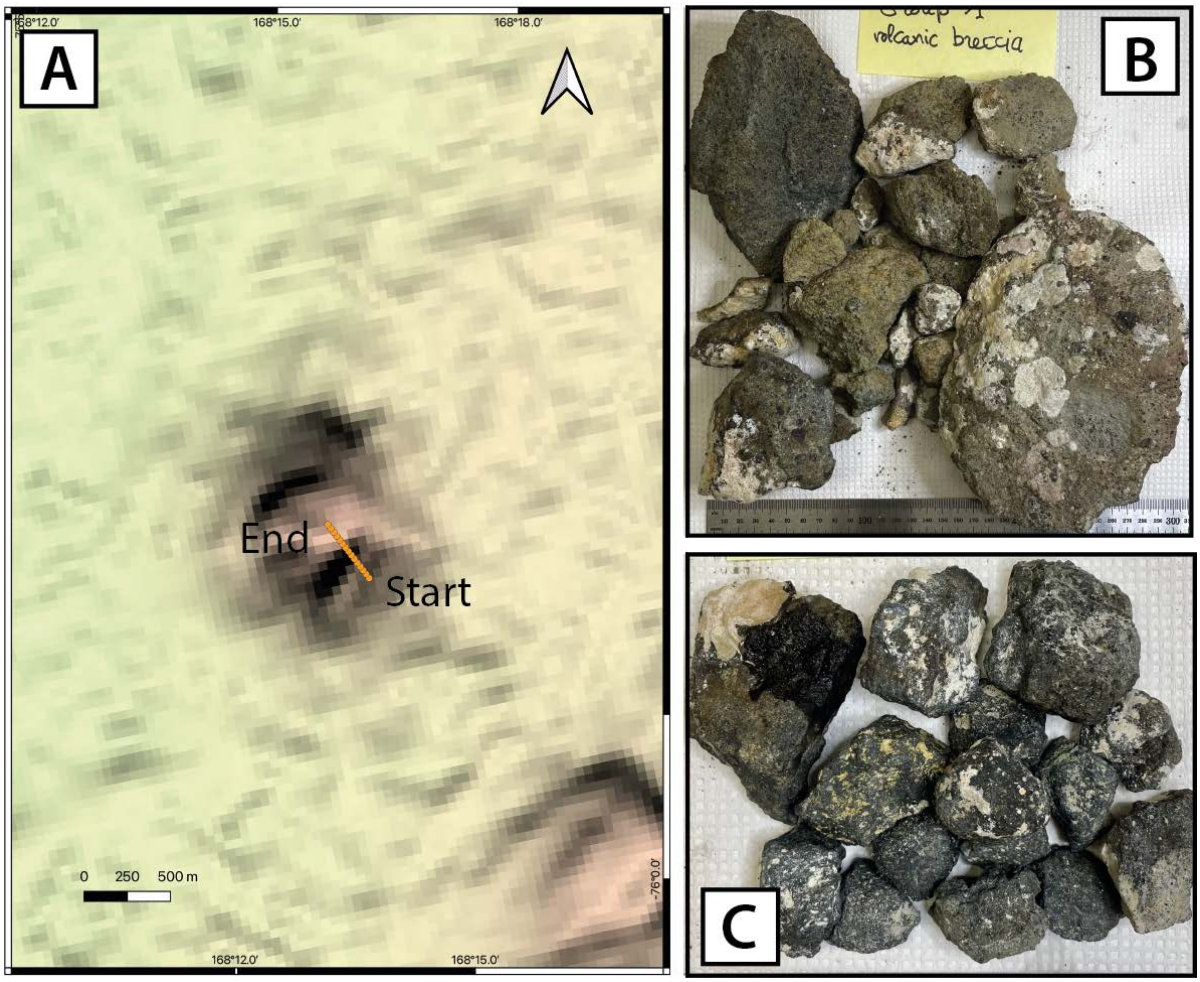

Figure 10.24: a) DR21 was performed on a small seamount north of Franklin Island and just east of the pockmark field. b) breccia with vesicular clasts supported by matrix. c) vesicular lava.

10.9.22 DR22

DR22 is from another small seamount to the east of DR21 (**Fig. 10.25**) and was dredged on March 19th. A small amount of material was recovered from this dredge and consists of a few breccia fragments that have matrix-supported angular, glassy clasts and amphibole is identified in one of the samples. An equally small number of lava fragments are gray to black massive to vesicular and one is olivine-rich. Dark gray rounded lava fragments are more abundant and are moderately vesicular, aphanitic to porphyritic with phenocrysts of olivine. Many samples are coated with coral.

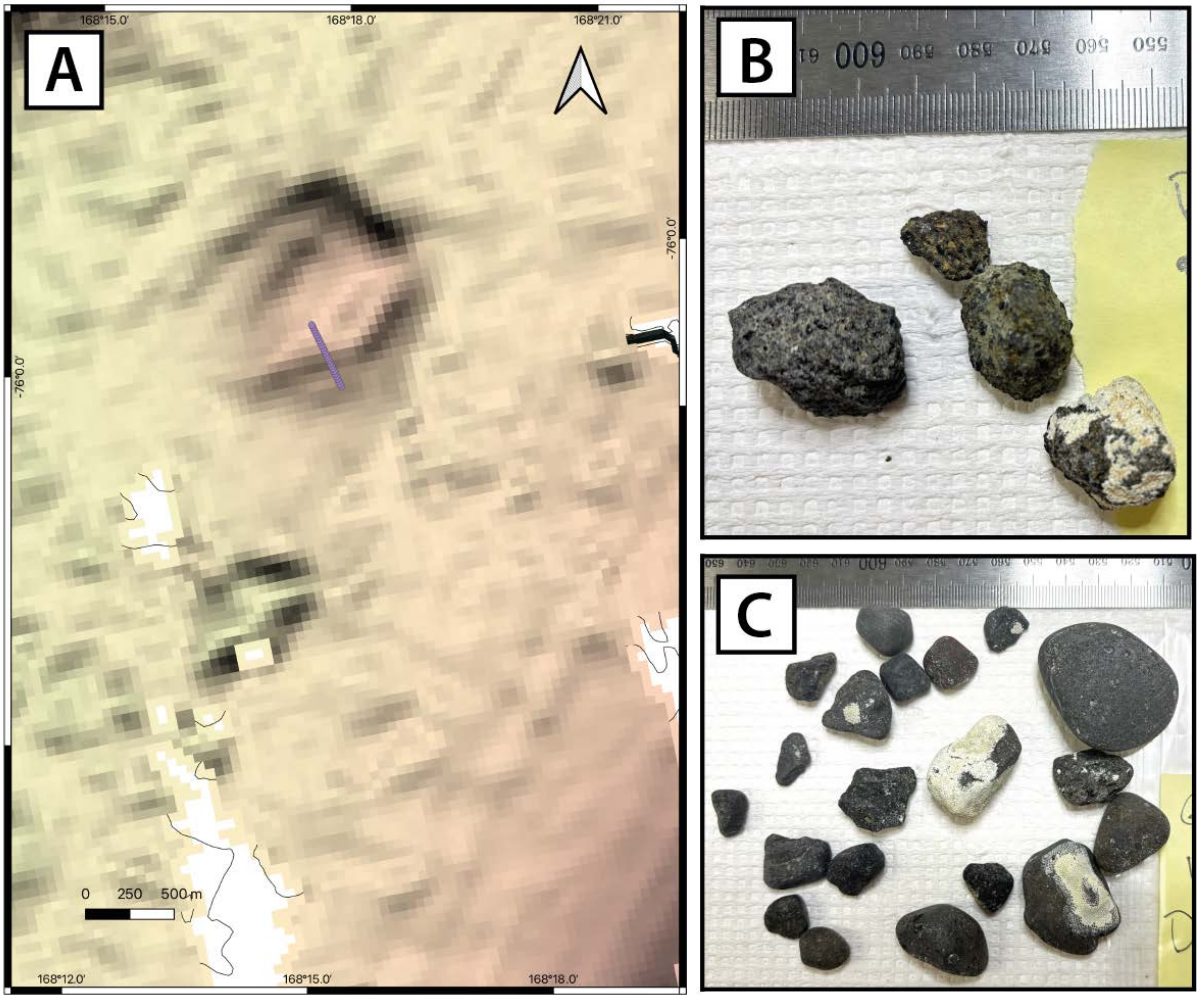

Figure 10.25: a) DR22 was sampled on small seamount north of Franklin Island and just SE of pockmark field. b) breccia with matrix-supported glassy clasts. c) round lava samples with olivine phenocrysts.

10.9.23 DR23

DR23 was performed on a fault scarp to the northeast of Franklin island (**Fig. 10.26**). Most of the lithologies recovered from this seamount are breccia. Matrix- to clast-supported breccia contains millimetric to centimetric blocky volcanic clasts. Fragments are coated by corals and mud. Lava fragments are round to angular in shape and show a large range of vesicularity.

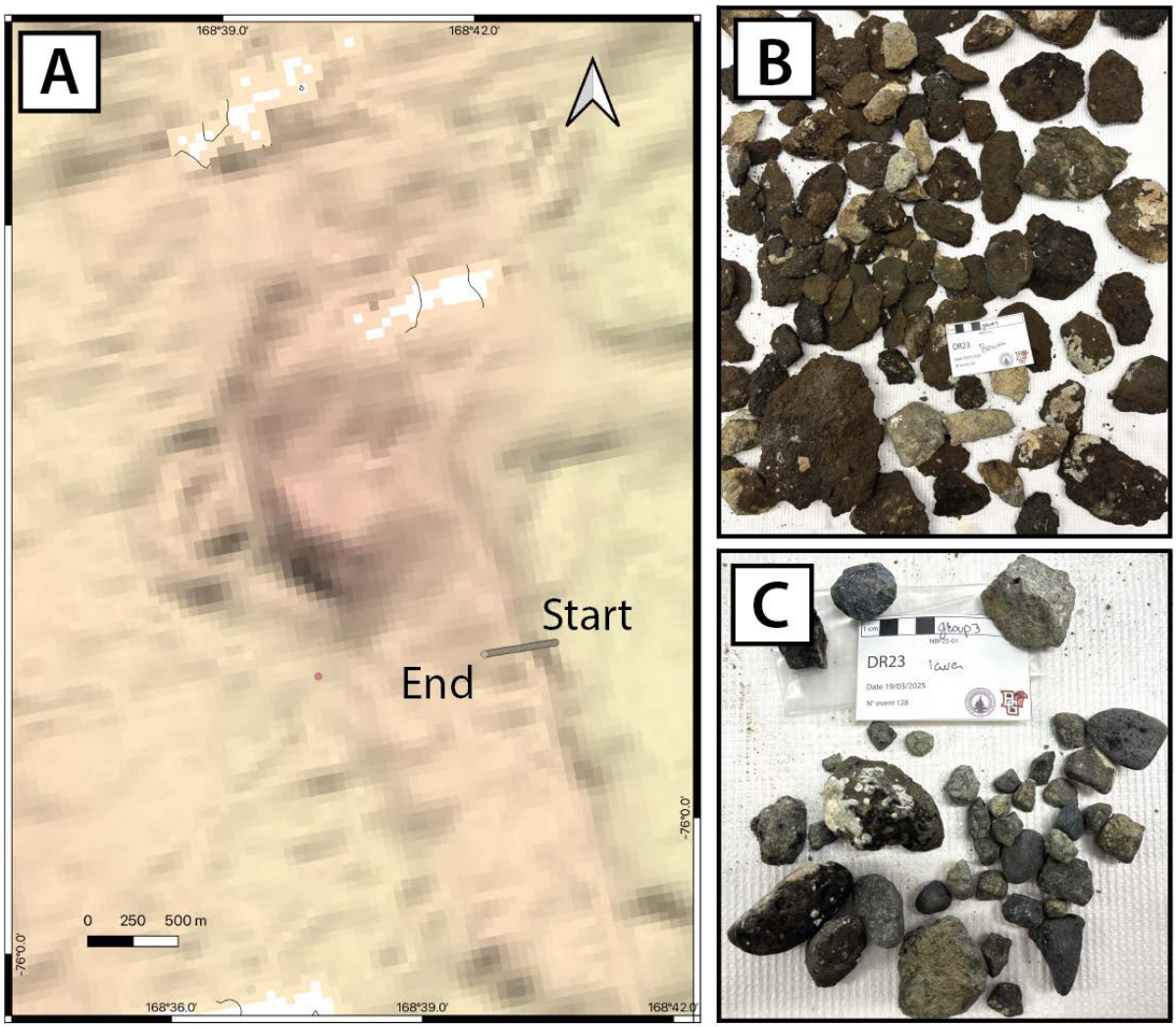

Figure 10.26: a) DR23 was performed on a fault scarp NNE of Franklin Island. b) breccia, matrix-supported to clast-supported. c) vesicular to non-vesicular lava.

10.9.24 DR24

Davey Bank's northernmost seamount (Pumpkin) was dredged on March 20th (**Fig. 10.27**). Most of the lithologies recovered from this seamount are beige to green matrix-supported breccia with centimetric volcanic clasts. Lava fragments display a large range of vesicularity from blocky to highly vesicular textures. Small fragments of fine-grained breccia show layering. Some IRD/erratics were collected.

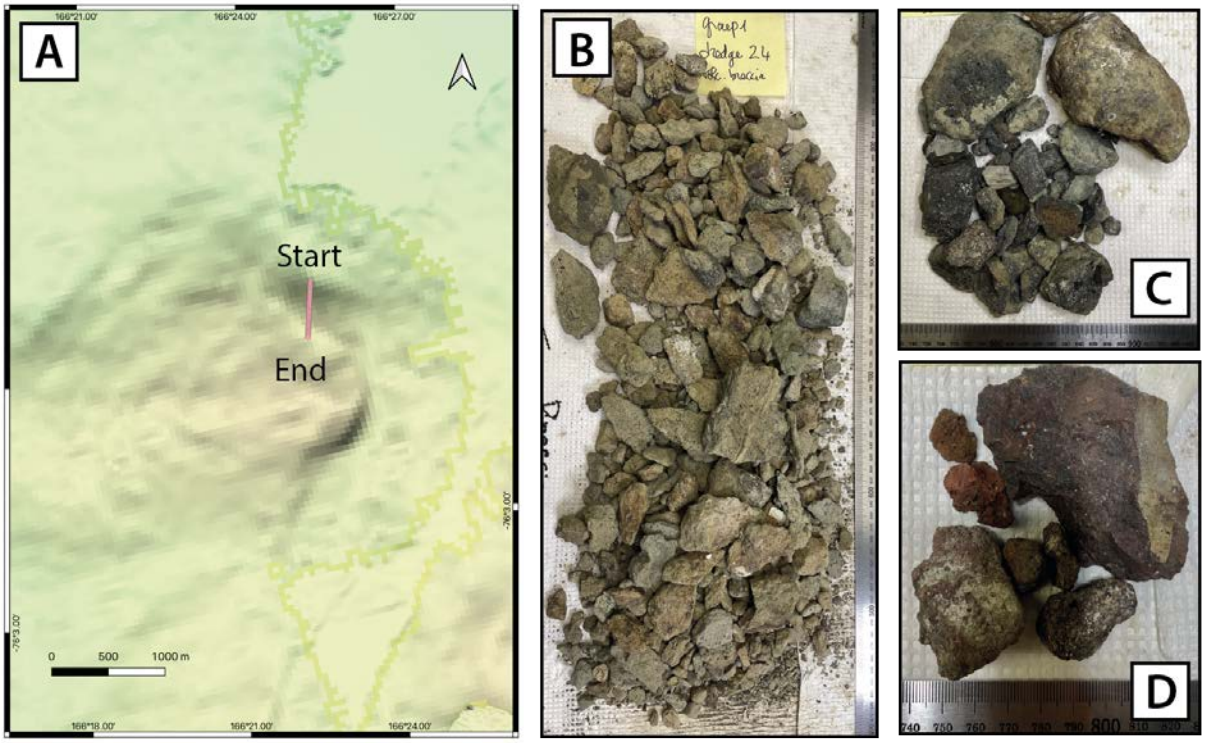

Figure 10.27: a) DR24 was conducted on the Pumpkin seamount on north end of Davey Bank. b) breccia with matrix-supported clasts. c) vesicular lava. d) lava and breccia.

10.9.25 DR25

The top of Davey Bank (Mt Petit, **Fig. 10.28**) was dredged on March 20th. The dredge haul consists mostly of lava. The lava ranges from dark gray to black, finely vesicular to non-vesicular (i.e., massive), with crystalline to glassy groundmass. Also recovered are breccia, possibly agglomerate fragments containing angular clasts. Erratics consist of granitoids and rounded massive lava (which could be primary).

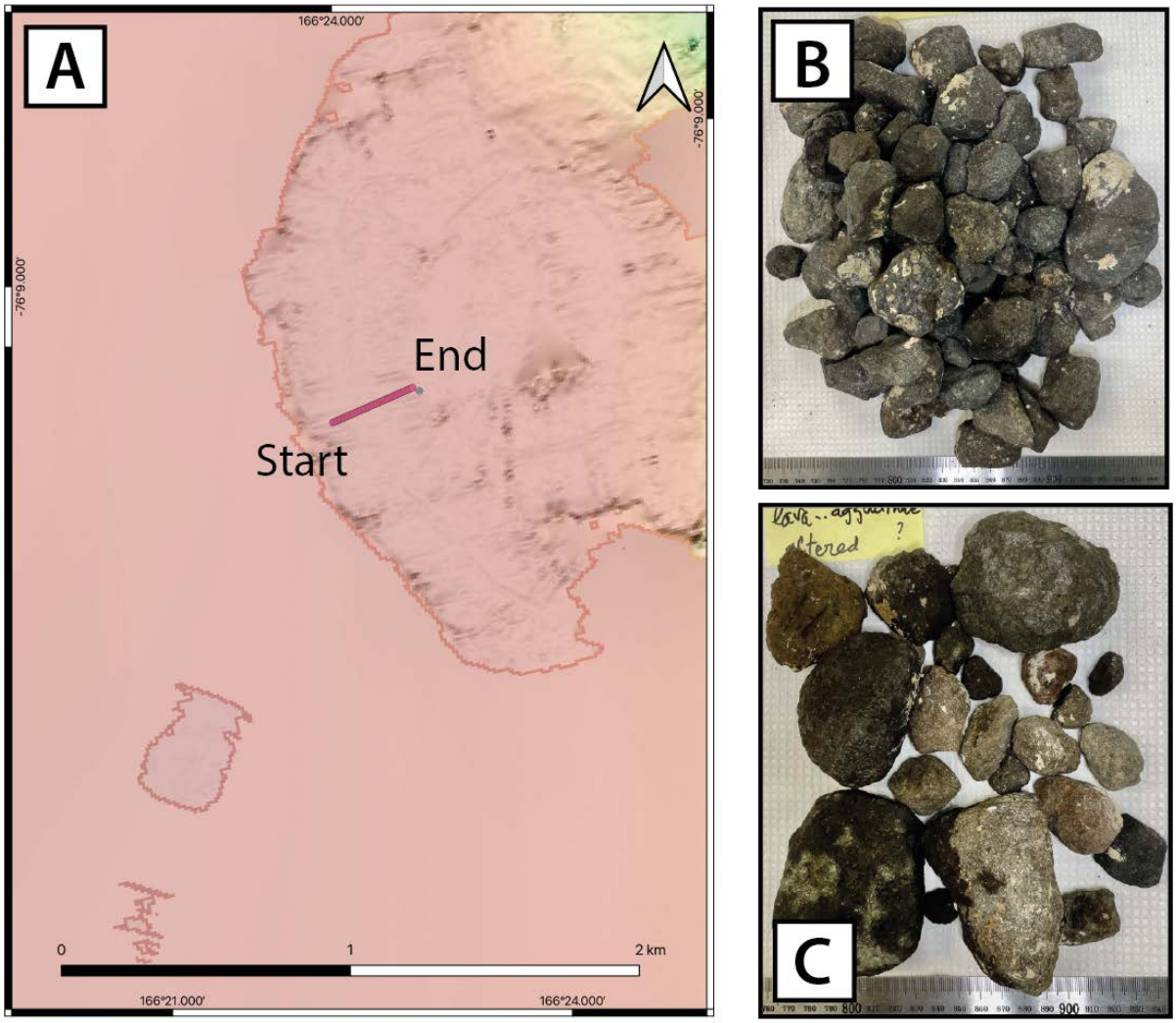

Figure 10.28: a) DR25 is a site on top of Davey Bank - Mt. Petit. b) vesicular lava. c) agglomerate.

10.9.26 DR26

DR26 was performed on the southwest part of the Davey Bank on March 20th (**Fig. 10.29**). Dredged samples include angular massive to vesicular lava. Some fragments display variable degrees of weathering and are coated by corals.

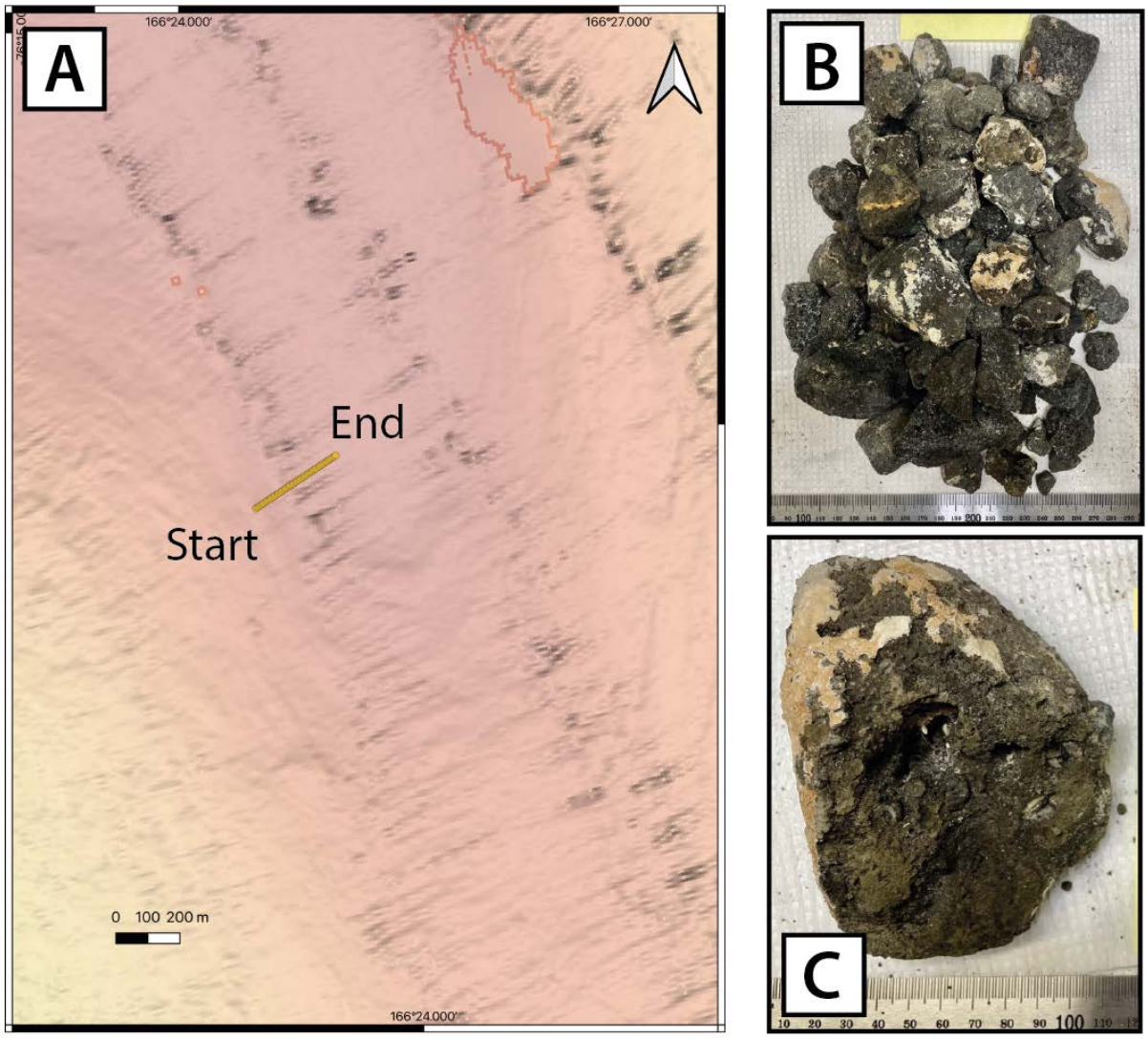

Figure 10.29: a) DR26 was conducted on the southwestern flank of Davey Bank. b) coral covered vesicular lava. c) agglomerate with large vug.

10.9.27 DR27

This dredge was taken on Davey Bank's lower southwestern flank on March 20th (**Fig. 10.30**). Both fine and coarse breccia samples occur. Breccia is dark brownish-gray, with matrix-supported clasts that are glassy, micro-porphyritic (olivine, pyroxene, feldspar?) and moderately vesicular. One piece contains abundant amphibole. Another sample contains a large vug/cavity. Many of the fine breccia fragments have brown-yellow coating (palagonite?) and the darker coarser breccia is friable and appears less altered. In addition, DR27 contains scoria and scoriaceous lava with some fragments showing bands of vesicles. Others have micro-phenocrysts of olivine and pyroxene. Lava fragments also constitute the dredge haul and are dark gray-brown, moderately vesicular with micro-phenocrysts of feldspar.

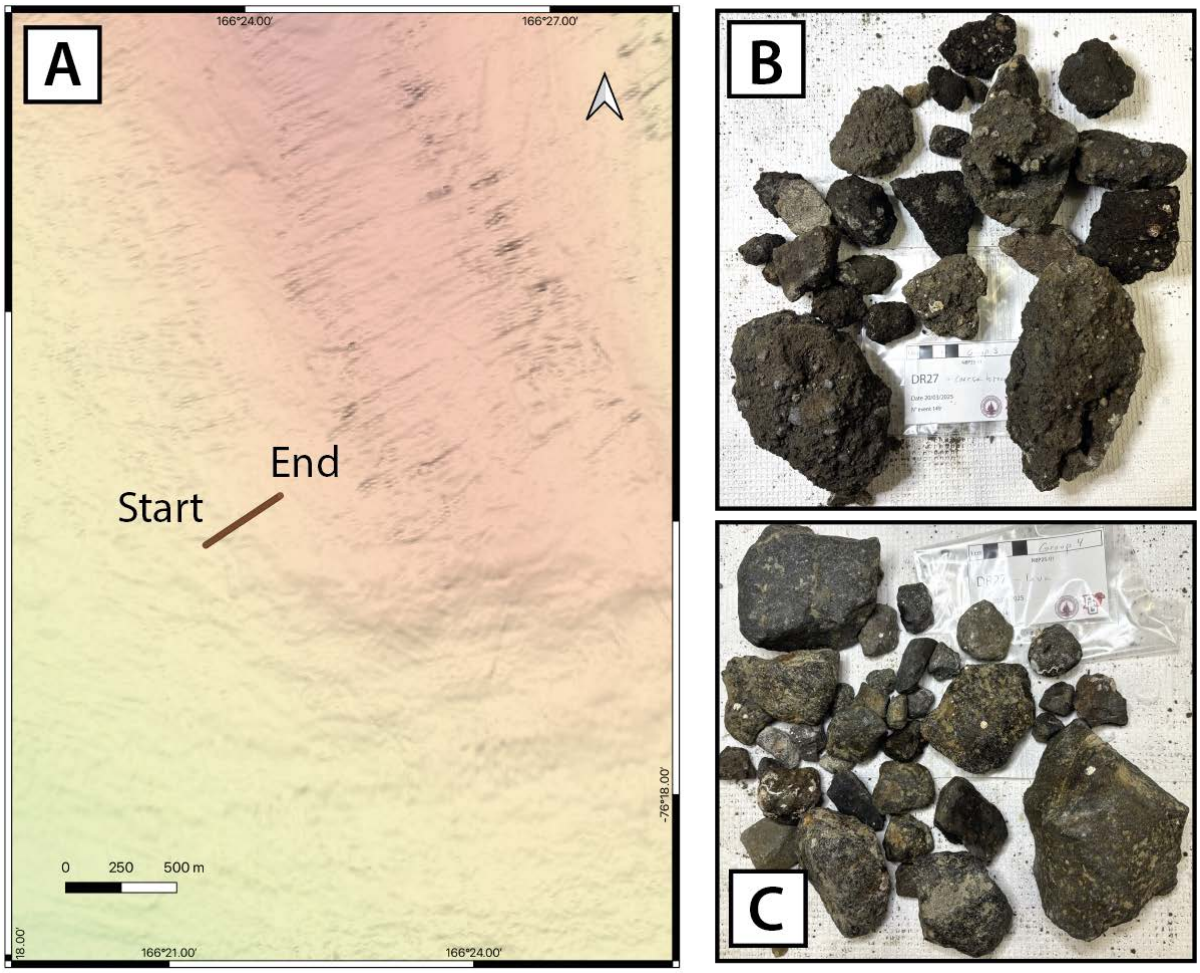

Figure 10.30: a) DR27 was also taken on the southwestern flank of Davey Bank but lower. b) coarse breccia. c) moderately vesicular lava.

10.9.28 DR28

DR28 is from an isolated seamount, Conquest, located to the east of Davey Bank's southern end (**Fig. 10.31**) and was sampled on March 21st. There was a small amount of volcanic material in this dredge and it consists of a small assortment of gray to dark gray to black lava, breccia and agglomerate. The lava varies from non-vesicular to vesicular with aphanitic groundmass. The agglomerate is monolithic and clasts are vesicular. A small xenolith in one sample and amphibole in a separate sample are identified.

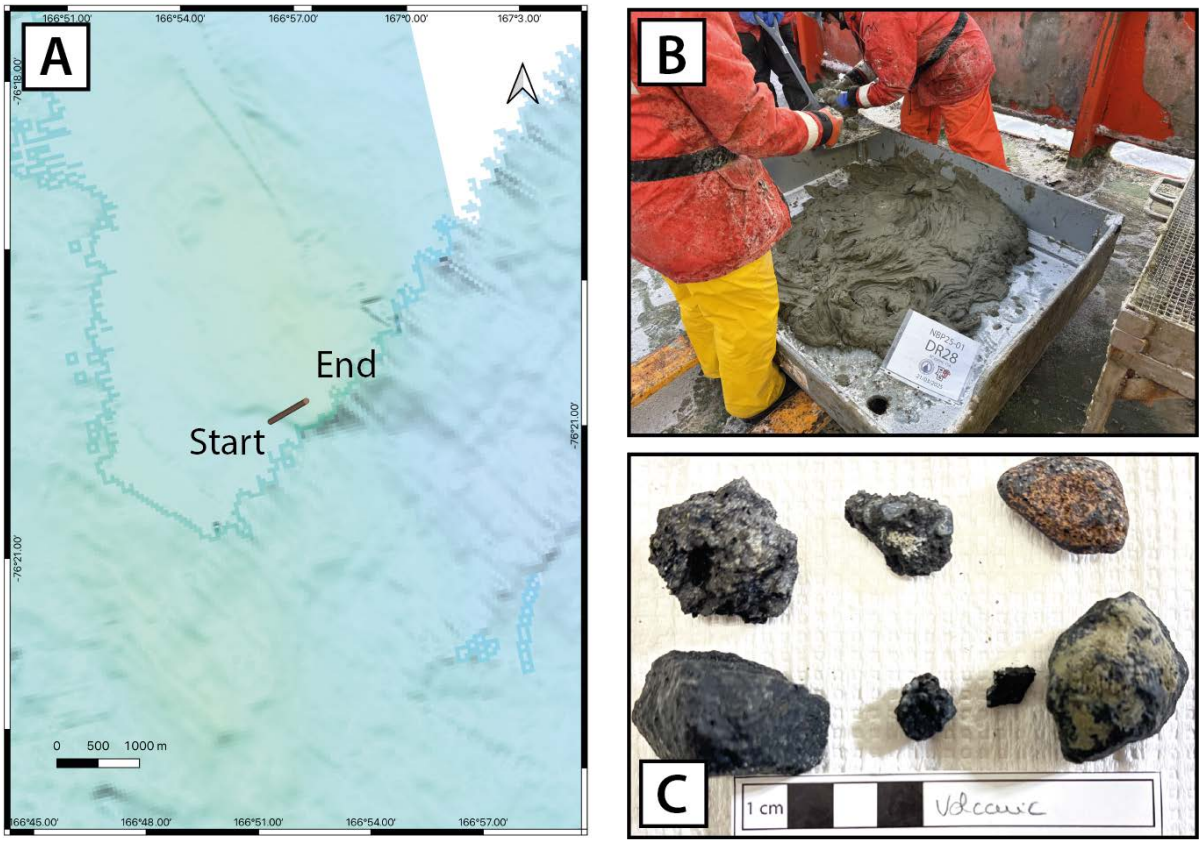

Figure 10.31: a) DR28 was taken on the Conquest seamount. b) the DR28 dredge collected a large quantity of mud and only a small amount of volcanic material, c) assortment of gray to dark gray to black lava, breccia and agglomerate.

10.9.29 DR29

DR29 was conducted on the upper part of Aurora Bank on March 21 (**Fig. 10.32**). The collected samples include matrix-supported breccia with subrounded volcanic clasts (some glassy) and agglutinated ash and lapilli. A large variety of lava (from massive to vesicular and banded) have also been recovered. Some fragments contain amphibole crystals.

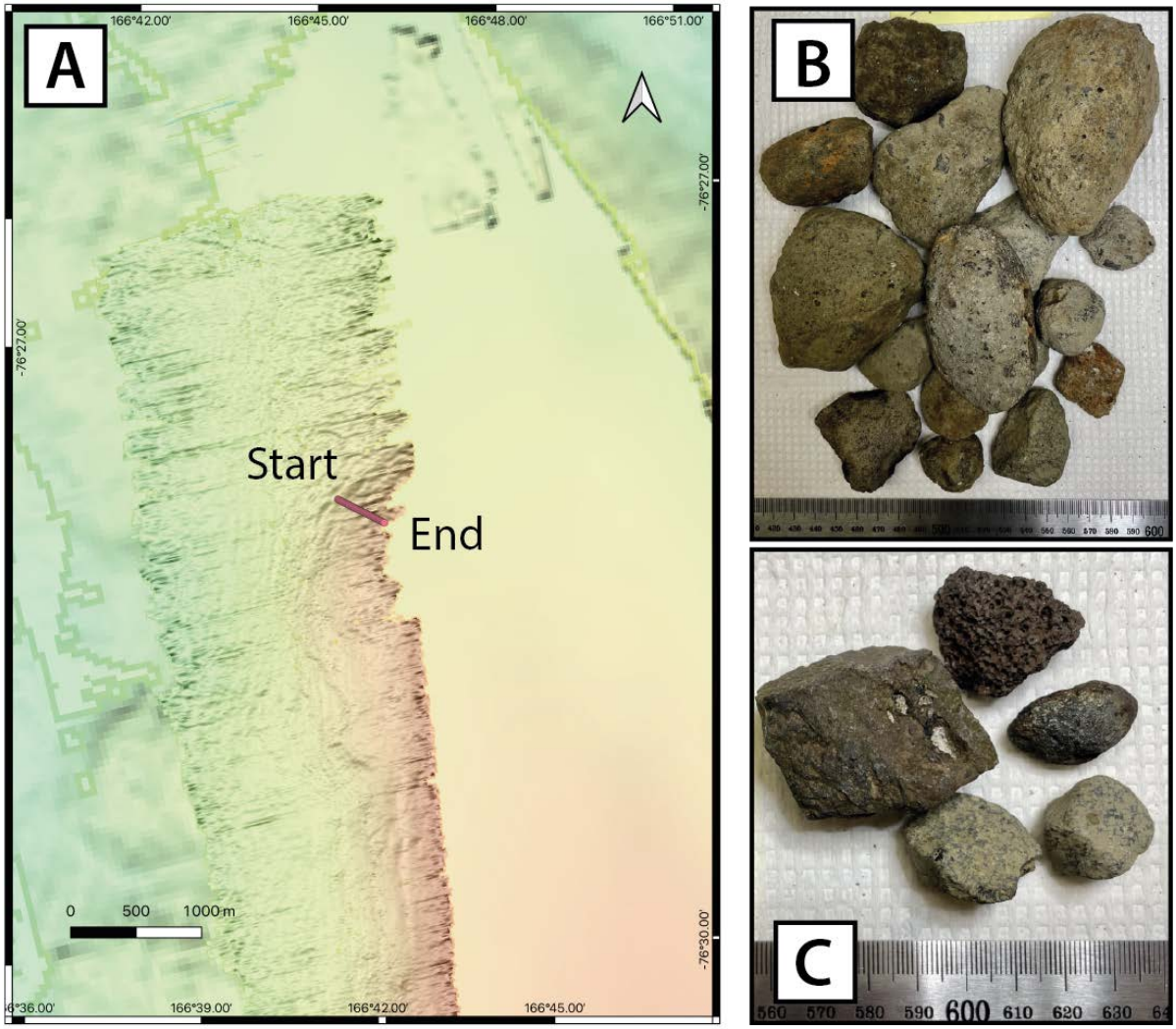

Figure 10.32: a) DR29 is the first dredge conducted on the upper part of Aurora Bank. b) Matrix-supported breccia with subrounded volcanic clasts (some glassy), c) massive to vesicular lava fragments recovered.

10.9.30 DR30

On March 21st the northwest tip of Aurora Bank was dredged (**Fig. 10.33**). Materials recovered are breccia, agglomerate and lava. The agglomerate consists of 4 samples, one large (9x7cm) that contains dark, finely vesicular fragments with olivine crystals. The breccia is multi-colored (beige, gray, green and red) and clasts are supported by a glass-rich matrix. Clasts are round to subround and mostly less than 2mm is size. Some layering defined by grain size is noted. Lava is dark gray to red and vesicular with amphibole and glass identified in the largest sample. In addition, a dark gray to black, fine grained, non-vesicular, 20x20cm sample, contains abundant xenoliths including a very coarse grained peridotite. This sample is considered to be shallow, subvolcanic intrusion. Erratics consist of seven pieces of granitoid, diorite, schist and a sedimentary rock (?).

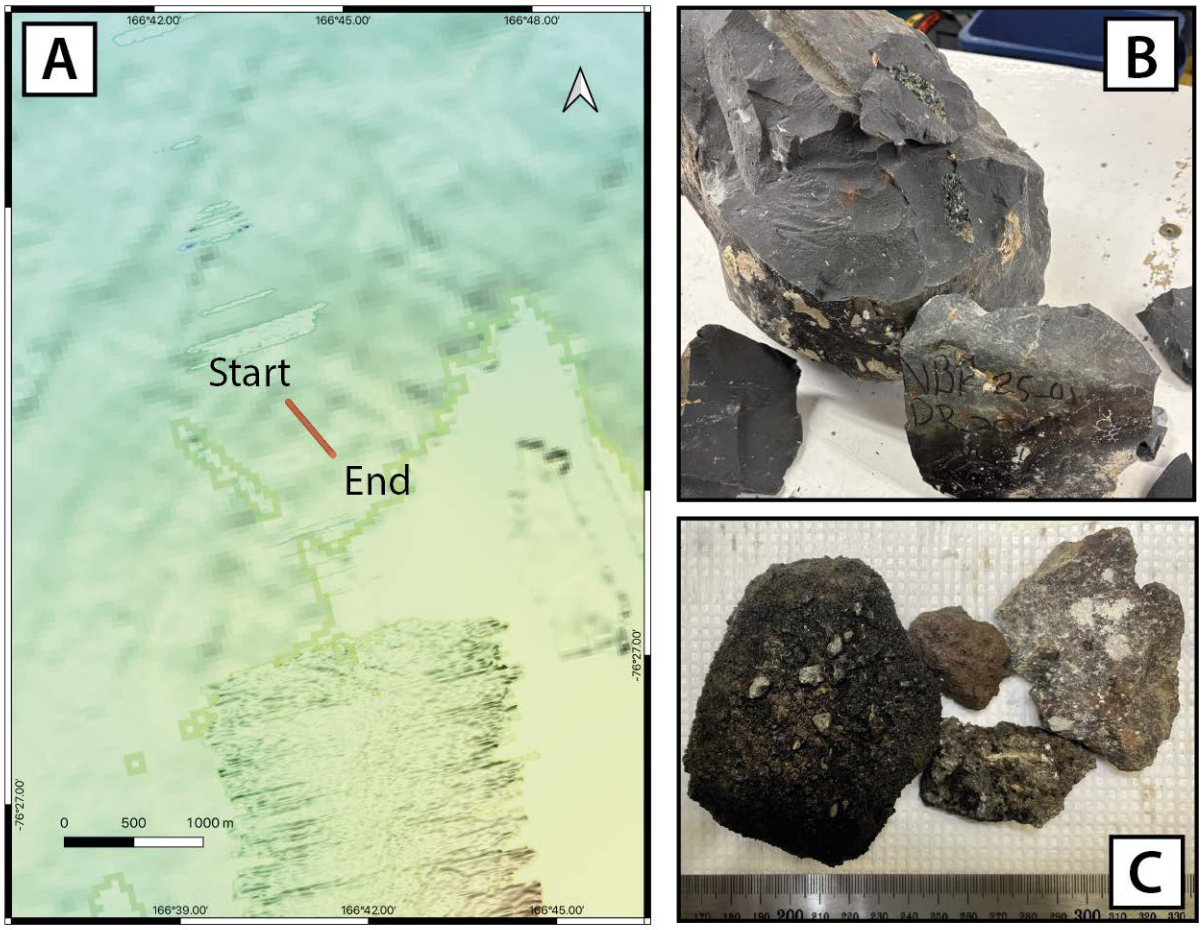

Figure 10.33: a) DR30 was performed on the northwest tip of Aurora Bank. b) Large block of xenolith-bearing lava. c) Agglomerate ash and lapilli.

10.9.31 DR31

Dredge DR31 sampled a seamount on March 21st, named Vagabond, located 19 km east of Flapjack Field (**Fig. 10.34**). Collected samples include matrix-supported breccia with millitmetric, subangular clasts, agglomerate ash and lapilli, xenolith-bearing lava, IRD and mudstone fragments. Clasts in breccia consist of subangular granitoid and volcanics, mostly vesicular, fragments. Importantly, one fragment of breccia contains a large vesicle (2 - 3 cm in size). Agglomerated ash consists of dark brown and black ash and olivine crystals. Black ash is highly vesicular.

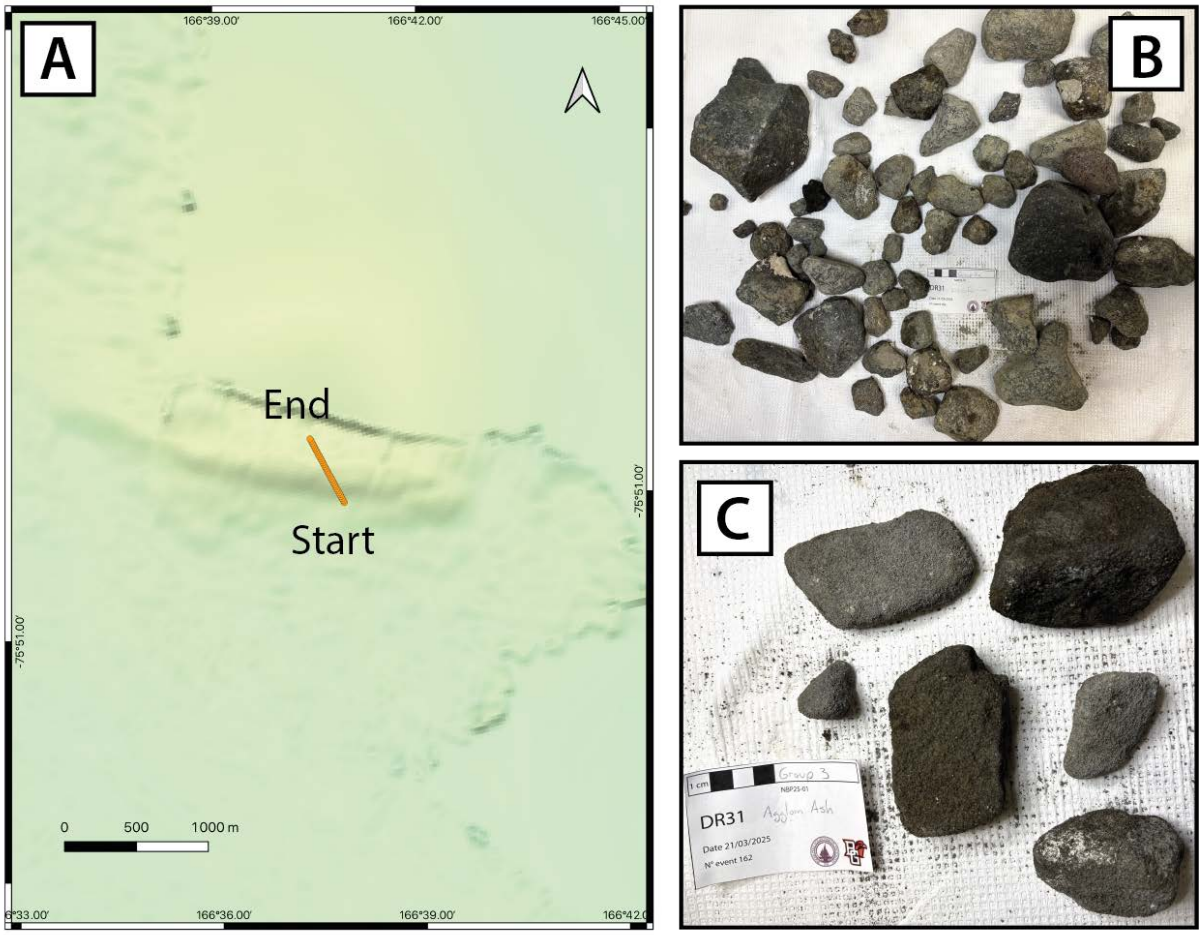

Figure 10.34: a) DR31 occurred on the Vagabond seamount, 20 km east of Flapjack Field. b) Fragments of vesicular lava and c) Crystal-rich agglomerate ash.

10.9.32 DR32

Dredge DR32 recovered samples from the Baby Banksy Baby Bank (**Fig. 10.35**) located south of Franklin Island on March 27. Samples collected include lava fragments, breccia, coarse ash agglomerate, and vesicular bomb. Greenish-gray to yellowish-gray breccia is matrix supported with mostly blocky non-vesicular clasts and contains olivine, amphibole and glass. Other samples contain abundant amphibole and peridotite xenoliths in lava and agglomerate fragments.

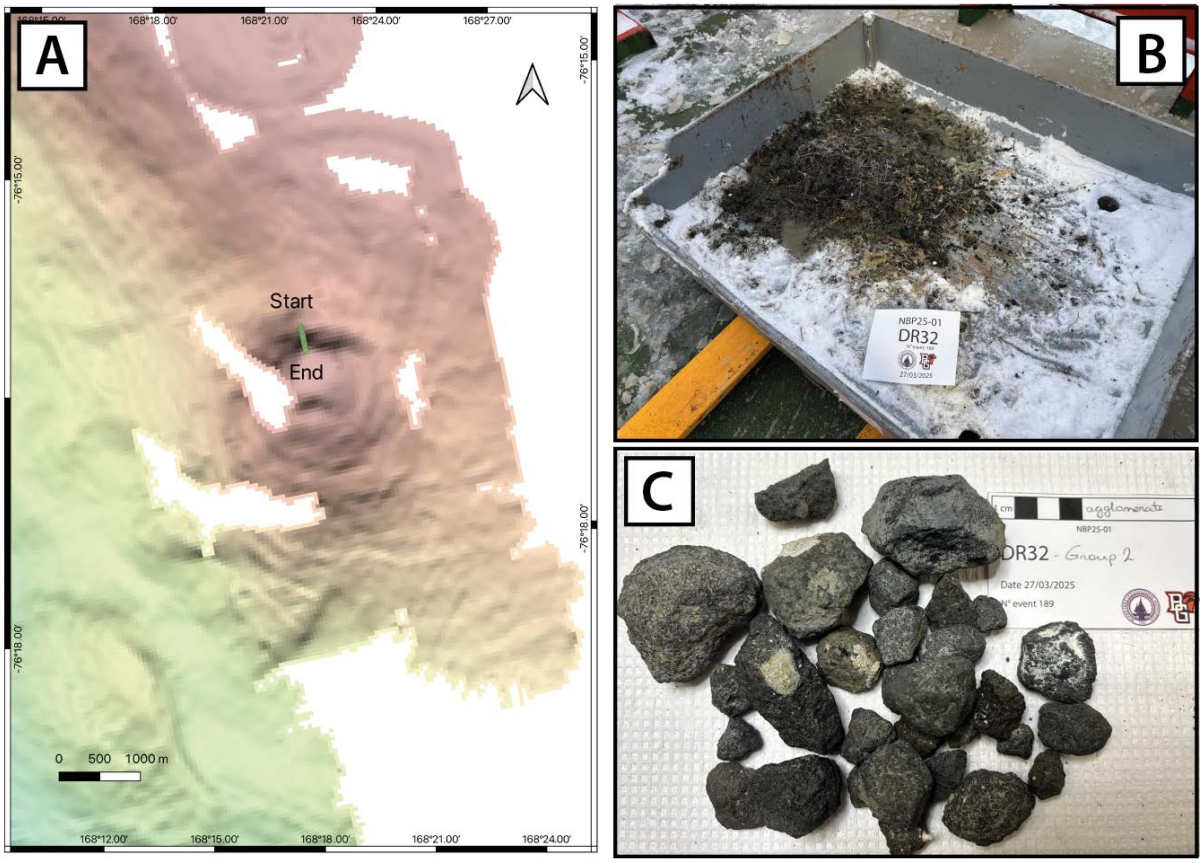

Figure 10.35: a) DR32 trackline on Baby Banksy Baby Bank south of Franklin Island. b) dredge haul (unsorted). c) green-ish gray, coarse ash agglomerate fragments.

10.9.33 DR33

Dredge DR33 occurred on March 27th with samples collected from Weasley Peak (**Fig. 10.36**), a prominent seamount east of Franklin Island. The dredge haul recovered fragments of breccia and agglomerate. The brownish-red breccia varies from clast- to matrix-supported and clasts are angular to subround within an altered matrix that contains olivine, amphibole and glass. The agglomerate consists of coarse ash that ranges from aphanitic-glassy but minerals are present (amphibole and plagioclase). It is important to note that cut breccia samples contain agglomerate cores.

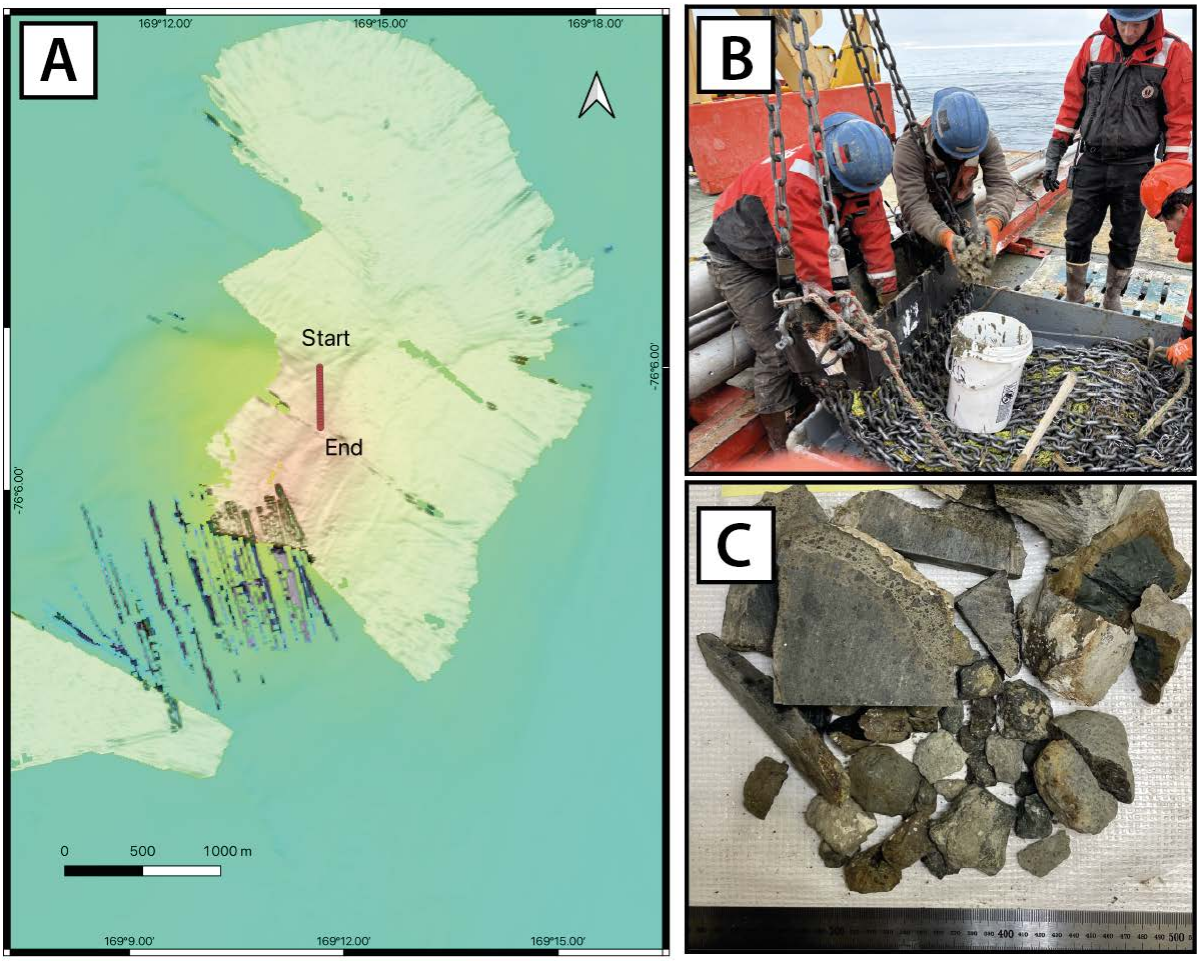

Figure 10.36: a) DR33 was performed on Weasley Peak, east of Franklin Island on March 27. b) dredge with rocks lodged at the top.

10.9.34 DR34

Dredge DR34 was conducted on Feather Top seamount (**Fig. 10.37**) west of the Flapjack Field. Materials that were recovered include agglomerate, xenolith-cored bombs and glass-rich fragments, likely outer rinds on bombs. In addition, are fragments of a red, fine-grained (clay-silt) and finely laminated 'crust'. Brownish-red agglomerates that consist of blocky and glassy ash to coarse lapilli with olivine and amphibole. Importantly, the agglomerate is also xenolith-rich with peridotite and amphibolite cores of glassy bomb fragments that are up to 10 cm long-axis. Peridotite xenoliths are altered-oxidized.

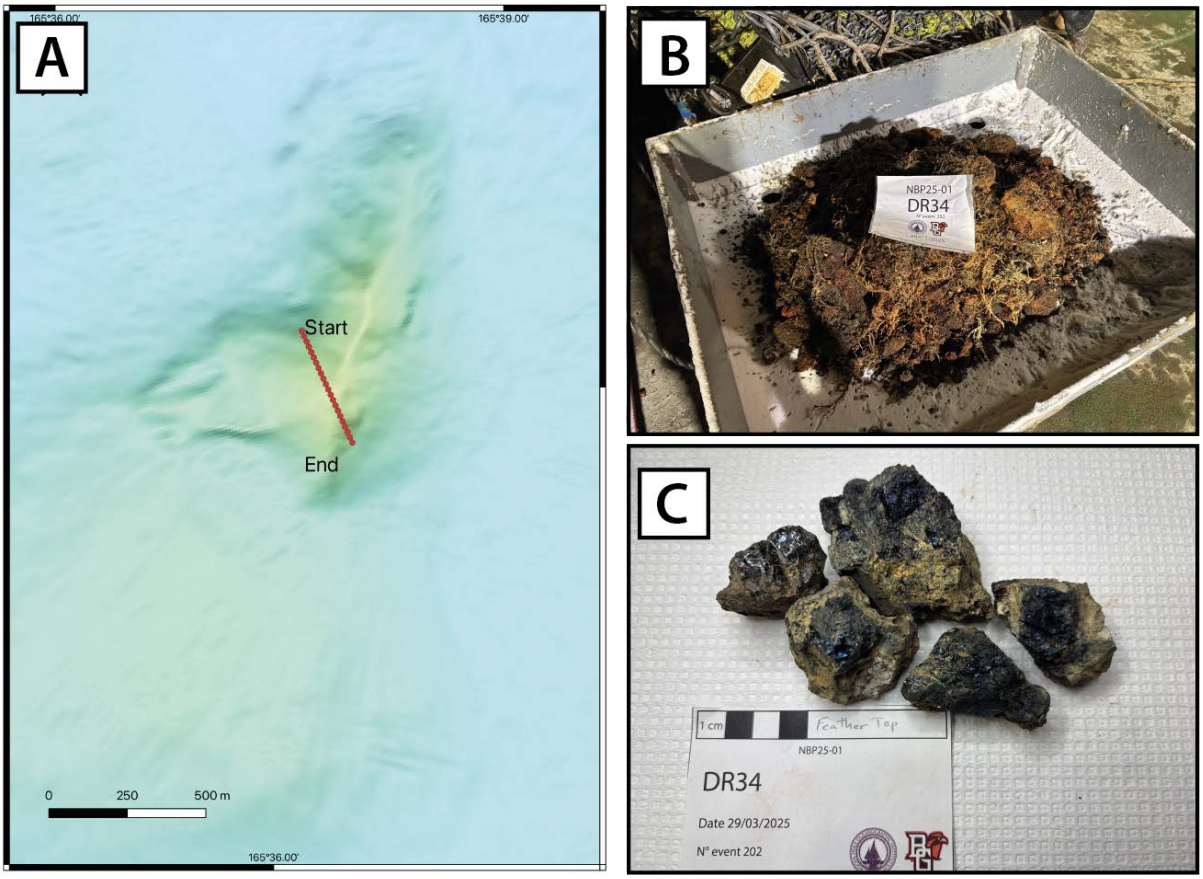

Figure 10.37: a) DR34 was conducted on Feather Top seamount on March 29th. b) dredge haul (unsorted) with abundant biology - sponge, coral. c) black, iridescent glass fragments.

10.9.35 DR35

Dredge DR35 occurred samples on the top of Pfannkuchen flat-top seamount on March 29, located in the Flapjack Field (**Fig. 10.38**). Collected samples were breccia, lava fragments, bombs and IRD (erratics). The dark gray to reddish-brown breccia consists of matrix-supported clasts, which are angular to subangular and blocky. The breccia matrix is crystal-rich containing olivine, amphibole and pyroxene and includes mantle xenoliths (peridotite). The lava recovered is dark gray to black, massive to poorly vesicular and porphyritic with phenocrysts of olivine and pyroxene. Amphibole is found in one fragment. Bombs are black to dark gray and highly vesicular with unfilled round vesicles and phenocrysts of olivine and pyroxene. Presence of xenoliths. Erratics are granite and fine-grained intrusives.

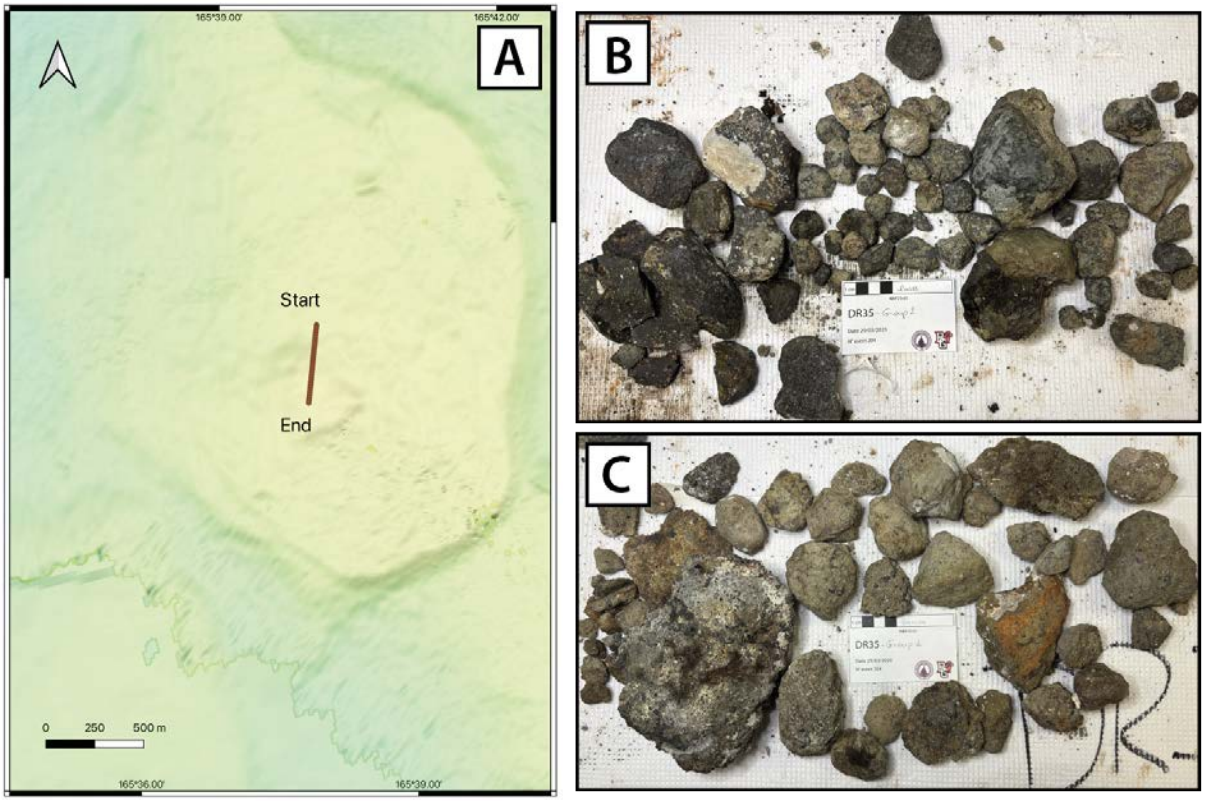

Figure 10.38: a) DR35 occurred on summit of Pfannkuchen flat-top in Flapjack Field. b) Lava fragments. c) breccia fragments.

10.9.36 DR36

Dredge DR36 recovered samples close to DR35 on Baby Pfannkuchen (**Fig. 10.39**) in the Flapjack Field on March 29th. A small amount of material was recovered from this dredge and consists of breccia, breccia clasts and several small granitoids (lithics or erratics?). The breccia is dark brown to black, matrix supported and contains some lithic (granitoid) clasts. Lava clasts, considered to be from breccia, are blocky, non-vesicular and porphyritic (minerals not identified).

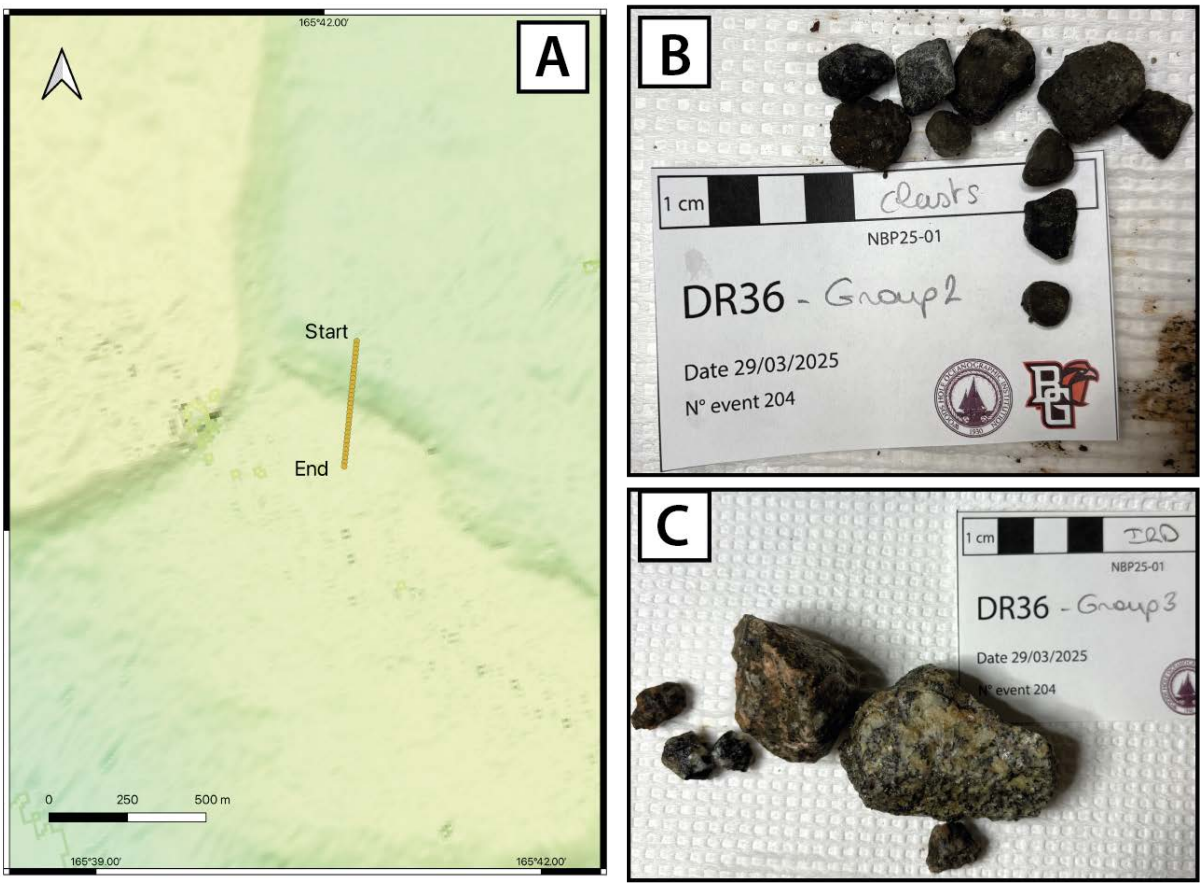

Figure 10.39: a) DR36 on Baby Pfannkuchen in Flapjack Field. b) lava clasts from breccia. c) granitoid erratics but possibly lithic clasts from breccia.

10.9.37 DR37

Dredge DR37 was performed on the seafloor In Between flat-tops on the eastern side of Pfannkuchen (**Fig. 10.40**) on March 30th. Collected a total of 3 small samples that are considered to be IRDs - granitoid, fine-grained rock (intrusive or volcanic?) and a mud clast.

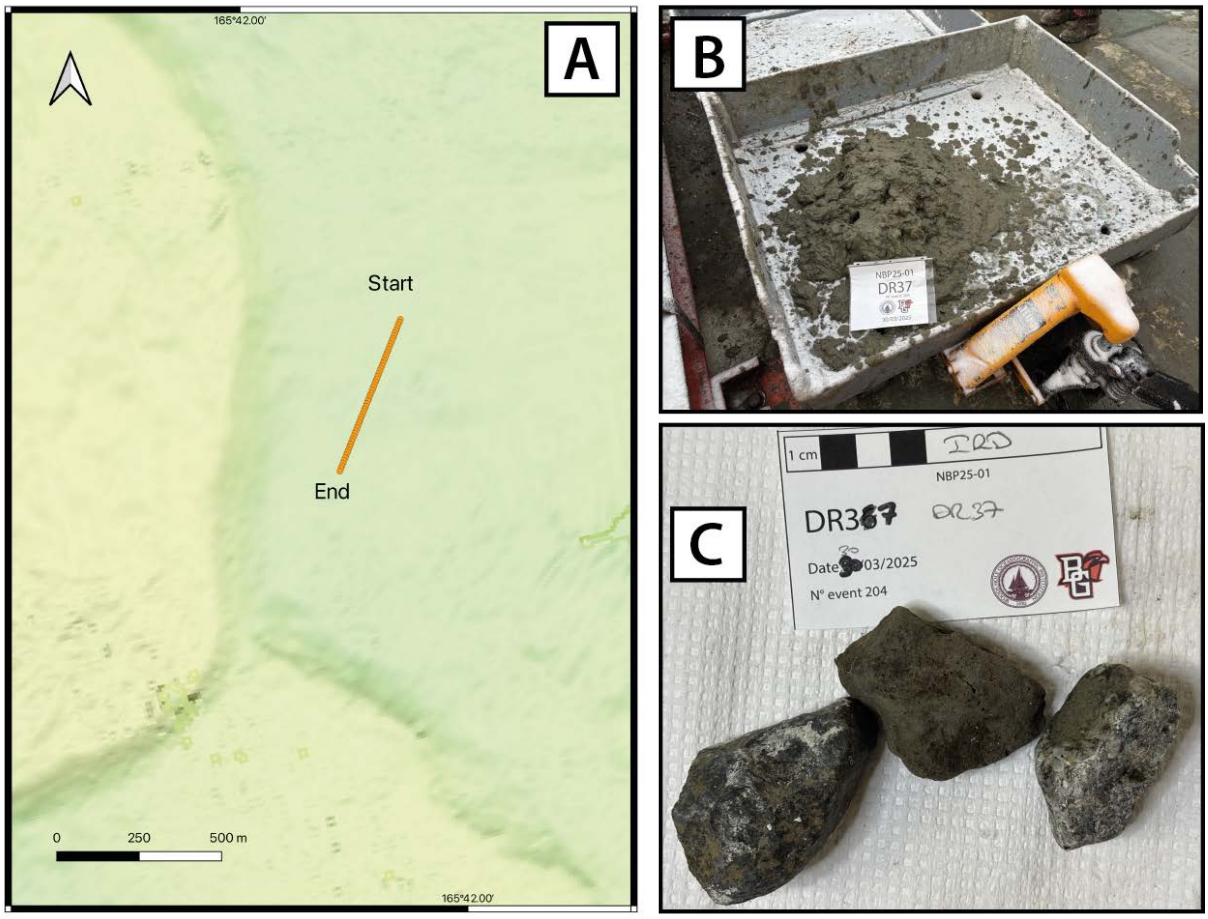

Figure 10.40: a) DR37 on seafloor In Between flat-tops on eastern side of Pfannkuchen. b) dredge haul (unsorted). c) total rock samples recovered - 3 IRDs.

10.9.38 DR38

Dredge DR38 was conducted on Vagabond seamount (**Fig. 10.41**), isolated and east of Flapjack Field on March 30. A small amount of material was collected consisting of vesicular to mildly vesicular lava and breccia. Some of the breccia is clast supported and maybe agglomerate. All clasts are volcanic. Note a Smith Mac was performed on this seamount and recovered sand-pebble sized volcanic material from surface.

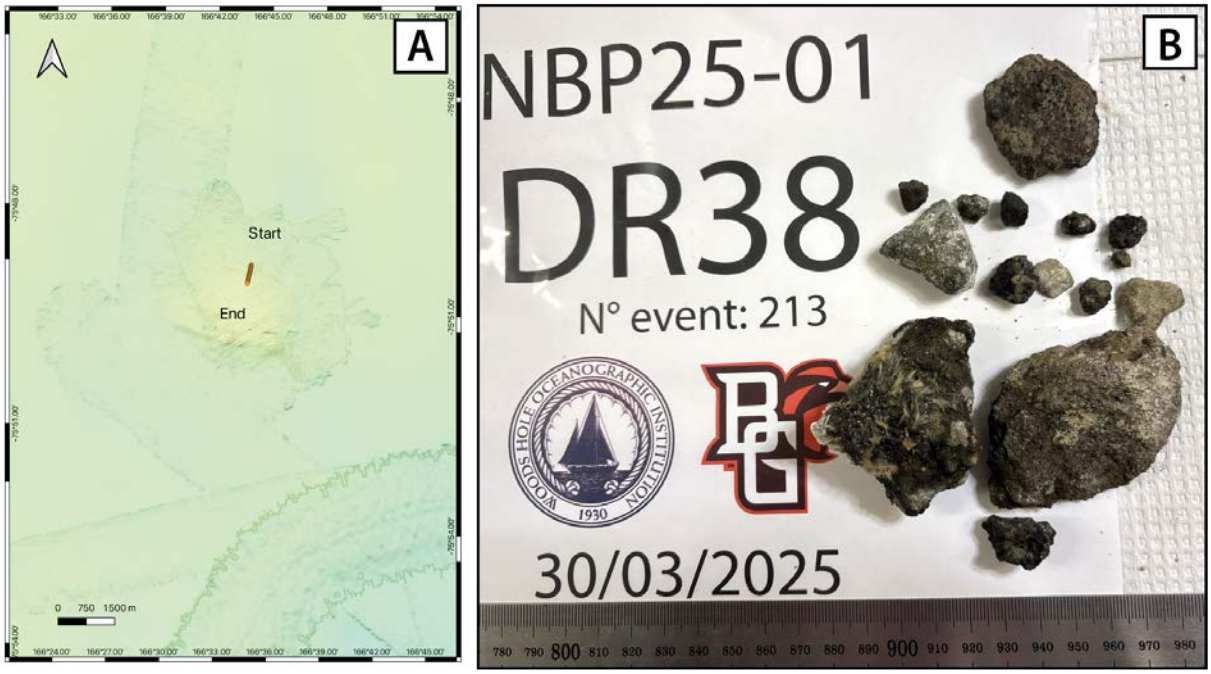

Figure 10.41: a) DR38 trackline on Vagabond seamount east of Flapjack Field. b) total material collected consisting of lava and breccia.

10.9.39 DR39

Dredge DR39 was performed on the Merope seamount (**Fig. 10.42**) east of Franklin Island on March 30. Samples collected include breccia, agglomerate, scoria, massive lava and xenolith-bearing fragments. Breccia is brownish-gray and fragments are tabular containing volcanic clasts (matrix-supported), glass and minerals - olivine and pyroxene. Agglomerate is dark gray to black, clast-supported and clasts are micro-vesicular. Lava recovered include highly vesicular (scoriaceous) round to subrounded samples and others are massive and microcrystalline with phenocrysts of amphibole, olivine and pyroxene. Many are covered by coral.

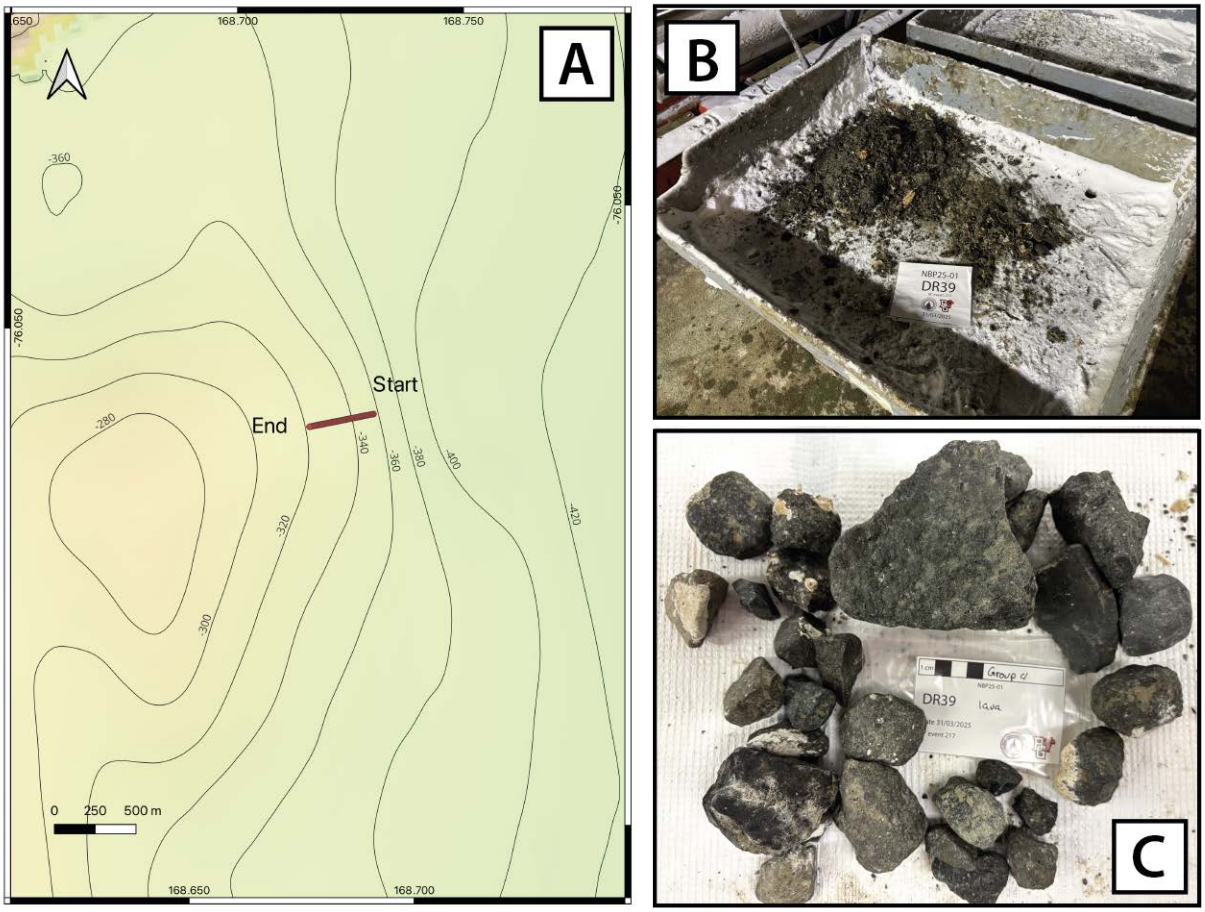

Figure 10.42: a) DR39 trackline on Merope seamount NE of Franklin Island. b) dredge haul (unsorted). c) Lava, aphanitic to microcrystalline.

10.9.40 DR40

Dredge DR40 was conducted on the Electra seamount (**Fig. 10.43**) NNE of Franklin Island on A. The samples recovered are breccia and agglomerate, lava, xenolith-bearing fragments and erratics. Breccia is gray-black, matrix-supported clasts that include angular and vesicular pieces in some fragments. Glass, olivine, amphibole and pyroxene are identified. Agglomerate is amphibole-rich and includes larger lava fragments that show gray fluidal areas considered to be mingled magma. Lava varies from vesicular to massive and aphanitic to microcrystalline with phenocrysts of olivine, amphibole and pyroxene (?). Both lava and agglomerate contain xenoliths (peridotite and amphibolite). Erratics included rounded vesicular lava and other igneous rocks.

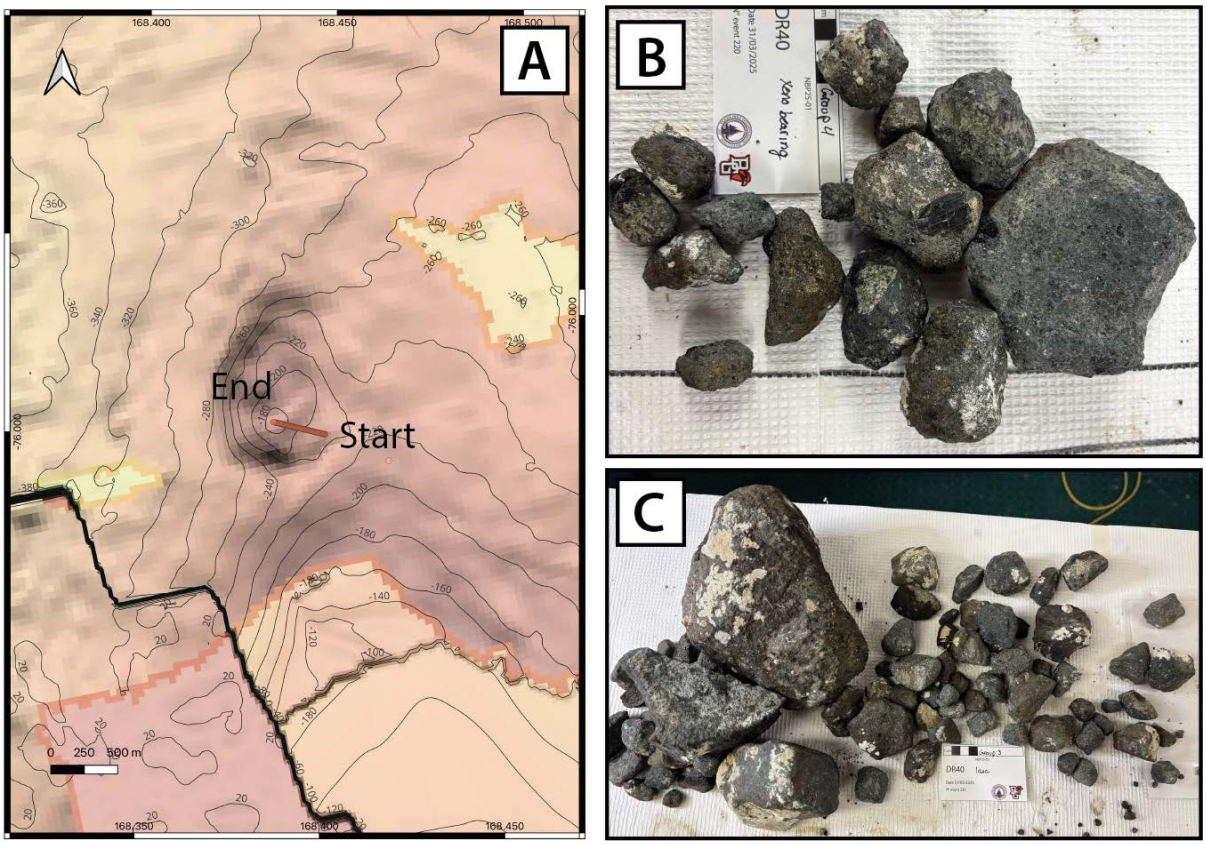

Figure 10.43: a) DR40 trackline on Electra seamount NNE of Franklin Island. b) Xenolith-bearing fragments of lava and agglomerate. c) lava fragments.

10.9.41 DR41

Dredge DR41 occurred at Celaine seamount (**Fig. 10.44**) north of Franklin Island on April 1st. The dredged samples consist of breccia, agglomerates, and both vesicular and non-vesicular lava. The breccia is light gray to brown, matrix supported, with clasts that consist of vesicular to blocky material that is subangular. Glass is identified. Agglomerate is dark gray to black, clast supported. Clasts display a large range in vesicularity. Glass and unidentified minerals are noted. Lava is light gray to dark gray to brown, non-vesicular to mildly vesicular with millimetric vesicles with filled vesicles, groundmass is crystal-rich. In at least one sample, amphibole, olivine, and feldspar were identified. Vesicular lava is light to dark gray. Vesicle sizes are millimeter to centimeter and aphanitic. Some coral coatings and adhered breccia are identified in samples.

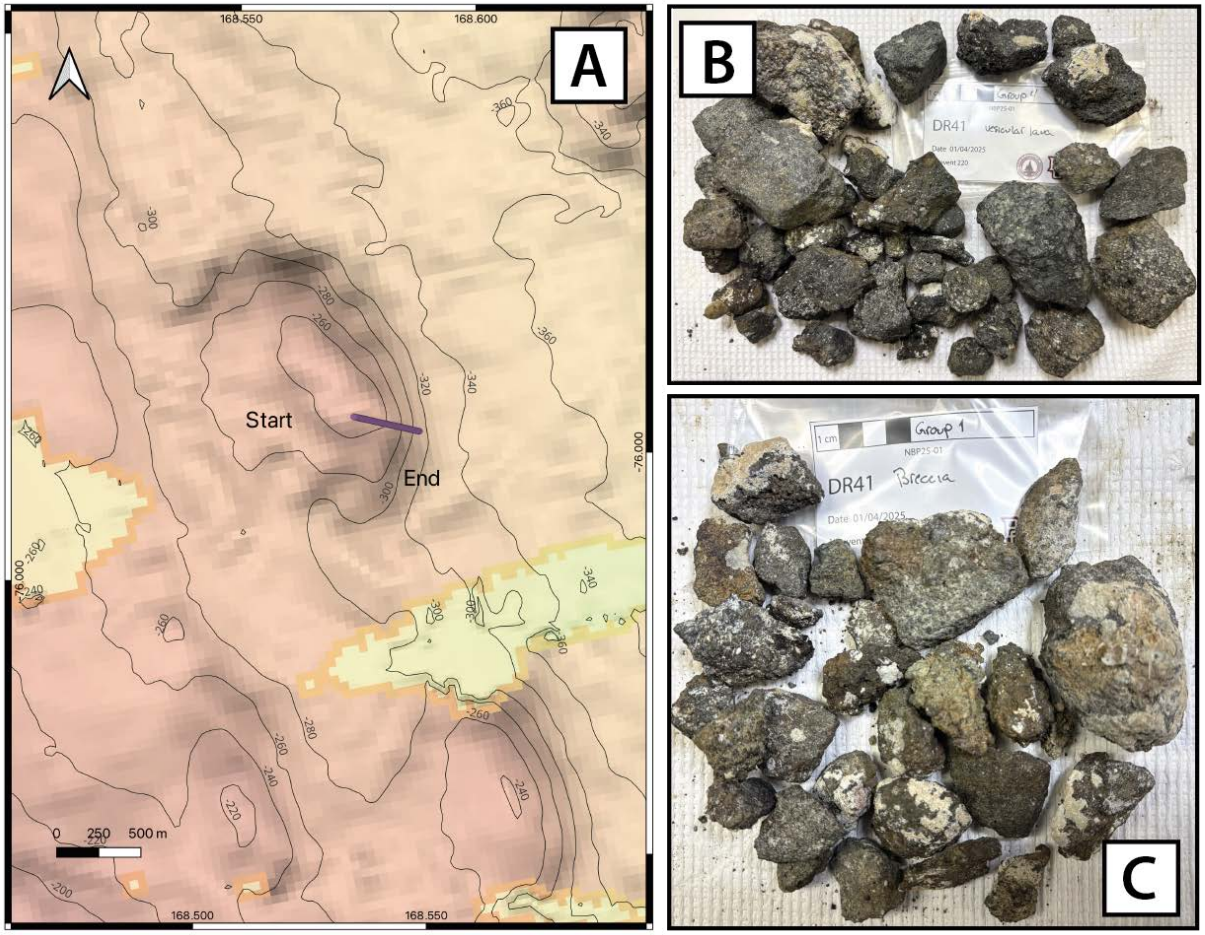

Figure 10.44: a) DR41 trackline on Celaine seamount N of Franklin Island. b) vesicular lava c) breccia fragments

10.9.42 DR42

Dredge DR42 was performed at Alcyone seamount (**Fig. 10.45**) north of Franklin Island on April 1st. The samples recovered consist of breccia, agglomerates, and both vesicular and non-vesicular lava. The breccia is light gray to brown, matrix supported, with rouded to subrouded clasts. Glass is identified. Agglomerate is dark gray to black, clast supported ash to lapilli in size, and range in vesicularity. Glass is also identified. Aphanitic vesicular lava light to black, consist of millimetric to centimetric vesicleswith some filled vesicles. Some coral and breccia are identified on samples. Lava is light gray to dark gray to brown, non-vesicular to mildly vesicular with millimetric vesicles, some are filled. Groundmass is aphanitic and glassy.

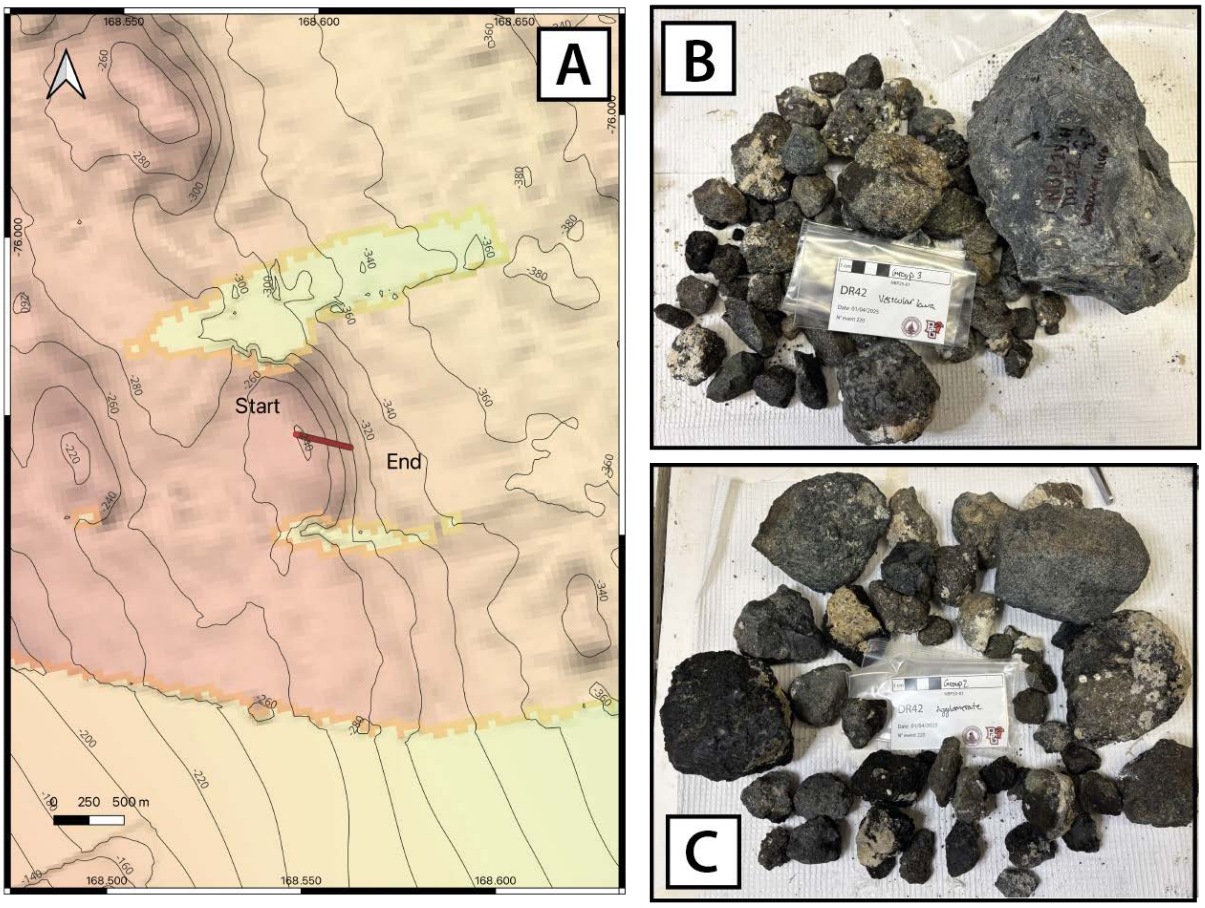

Figure 10.45: a) DR42 trackline on Alcyone seamount north of Franklin Island. b) vesicular lava c) agglomerate fragments.

10.9.43 DR43

Dredge DR43 was conducted at Taygeta seamount (**Fig. 10.46**) north of Franklin Island on April 1st. The samples recovered consist of breccia, agglomerates, and both vesicular and non-vesicular lava, and erratics. The breccia is light gray to black, matrix supported, with clasts that are subrounded. Vesicular and non-vesicular lava is identified. Agglomerate is dark gray to black, clast-supported with clasts that are ash to bomb in size and range in vesicularity. Glass is identified. Lava is light gray to dark gray and has inclusions of light gray areas that may be a separate composition, indicating mingled magmas. Groundmass is microcrystalline. Glass is identified. Vesicular lava is light to black, highly vesicular with some vesicles filled with secondary material. Vesicles are millimeter to centimeter in size. Groundmass is aphanitic. Reddened material ("Iron deposit") includes some agglomerate and other samples are platy and layered. Five erratics range from microcrystalline to aphanitic but mostly coral covered.

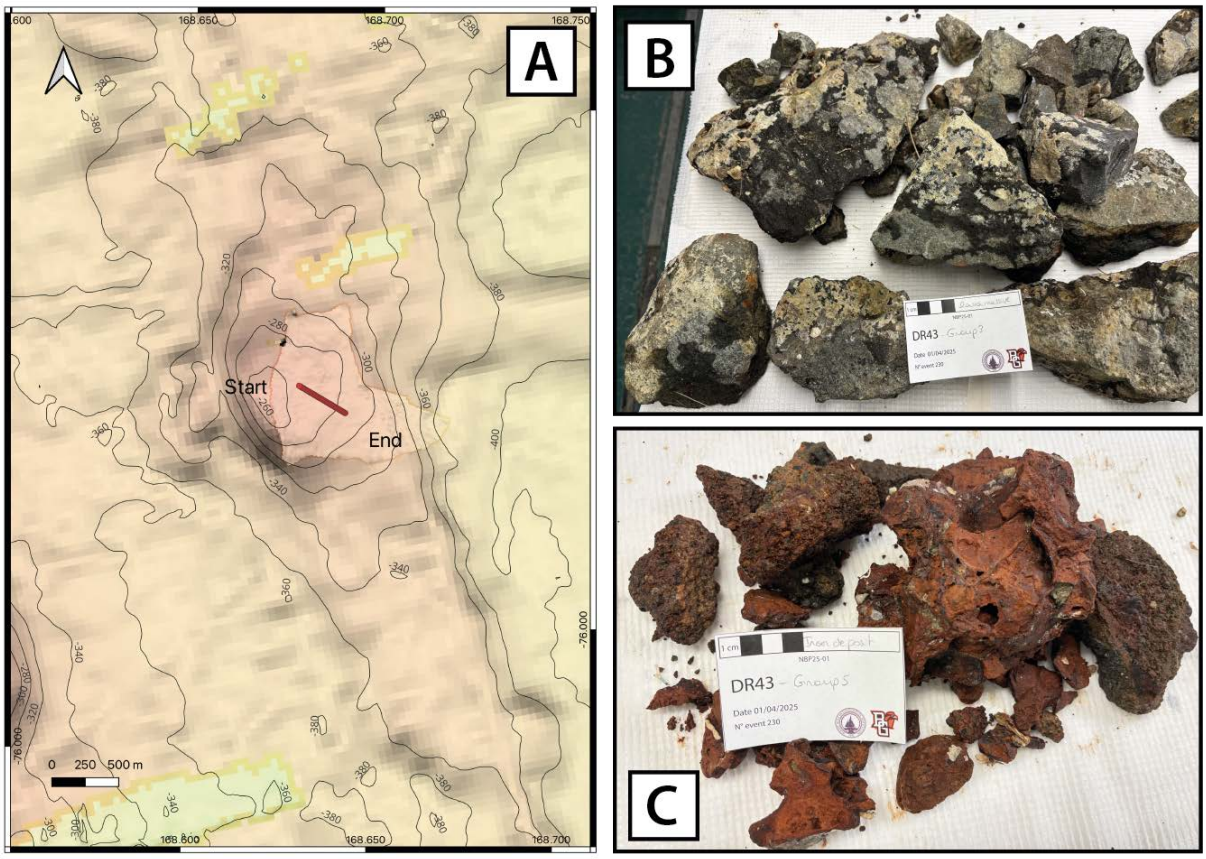

Figure 10.46: a) DR43 performed on Taygeta seamount north of Franklin Island. b) lava fragments c) iron deposit fragments.

10.9.44 DR44

Dredge DR44 was conducted at Alcyone seamount (**Fig. 10.47**) northeast of Franklin Island on April 2sd. The samples recovered consist of breccia, agglomerates, lava, and erratics. The breccia is light brown to greenish gray, matrix supported that contains fine grain mud, with clasts

that are subrounded and monolithic with some being blocky and some vesicular, millimetric clasts. Glass is identified. Agglomerate is dark brown to black, clast supported, ash to fine ash in size, and clasts range in vesicularity. Agglomerates also show subtle laminations. We note the presence of glass, olivine, and amphibole. Lava is brownish to black, non-vesicular to mildly vesicular, some adhered with breccia and large glassy fragments. Many lava fragments are mud and coral covered. Erratics consist of very fine grained sedimentary to aphanitic volcanics several with glacial striations.

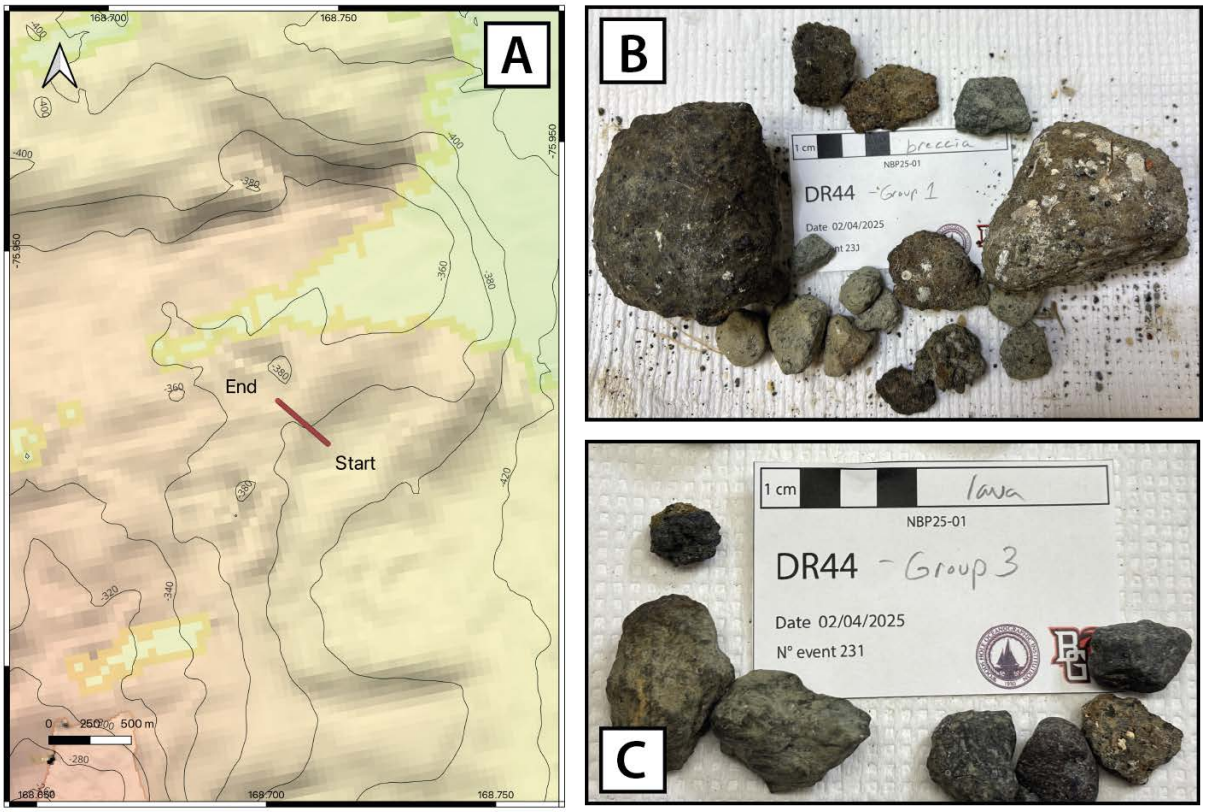

Figure 10.47: a) DR44 trackline on Alcyone seamount NNE of Franklin Island. b) breccia fragments. c) lava fragments.

10.9.45 DR45

Dredge DR45 was conducted at Alpha-Centauri A seamount (**Fig. 10.48**) northeast of Franklin Island on April 2. Five samples were recovered all less than 6 cm x 5 cm in size. Two samples are heterolithic breccia/conglomerate, matrix-supported, with millimetric sized rounded granite and angular volcanic fragments. One sample shows glacial striations.

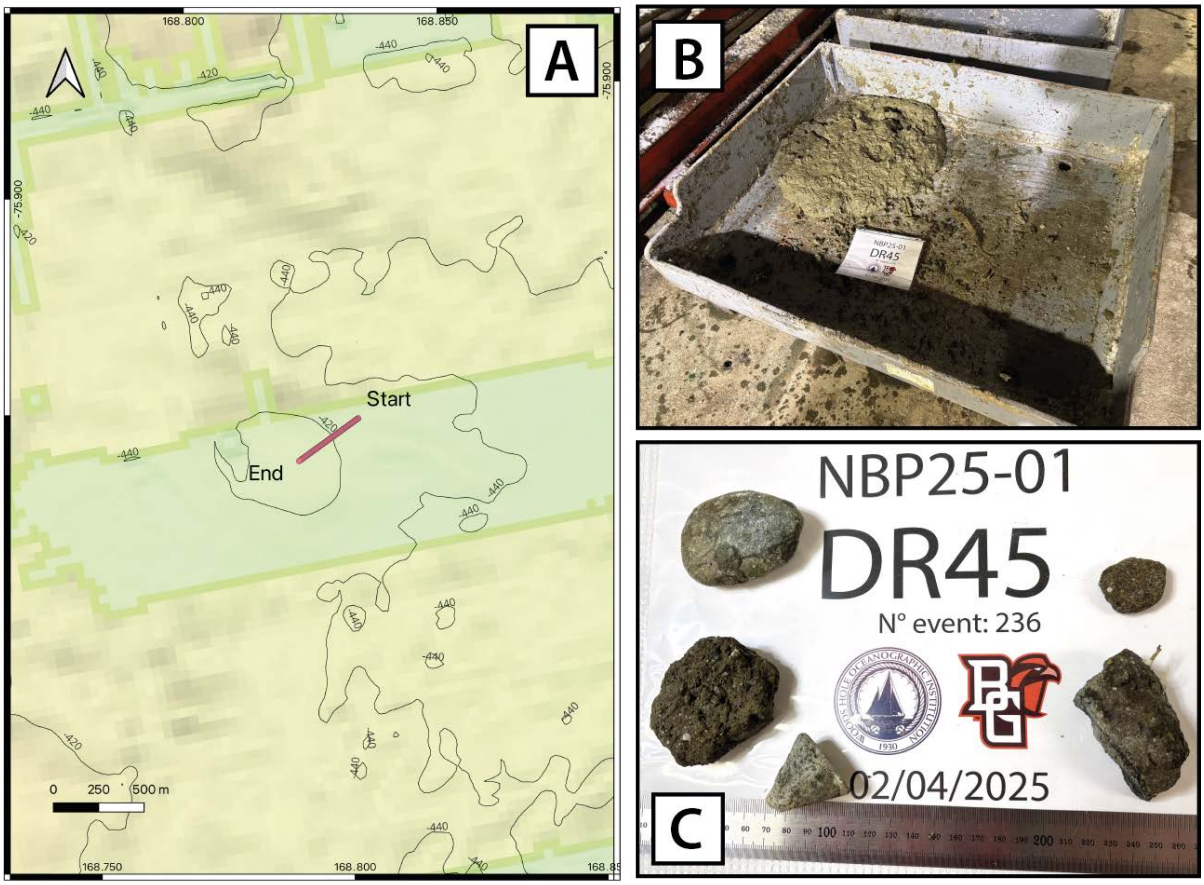

Figure 10.48: a) DR45 trackline on Alpha-Centauri A seamount NNE of Franklin Island. b) dredge on deck c) samples obtained

10.9.46 DR46

Dredge DR46 was conducted at Alpha-Centauri B seamount (**Fig. 10.49**) northeast of Franklin Island on April 2. The samples recovered consist of lava. Lava is light gray and non-vesicular. Three samples are angular, two samples are subround, and one sample is platy.

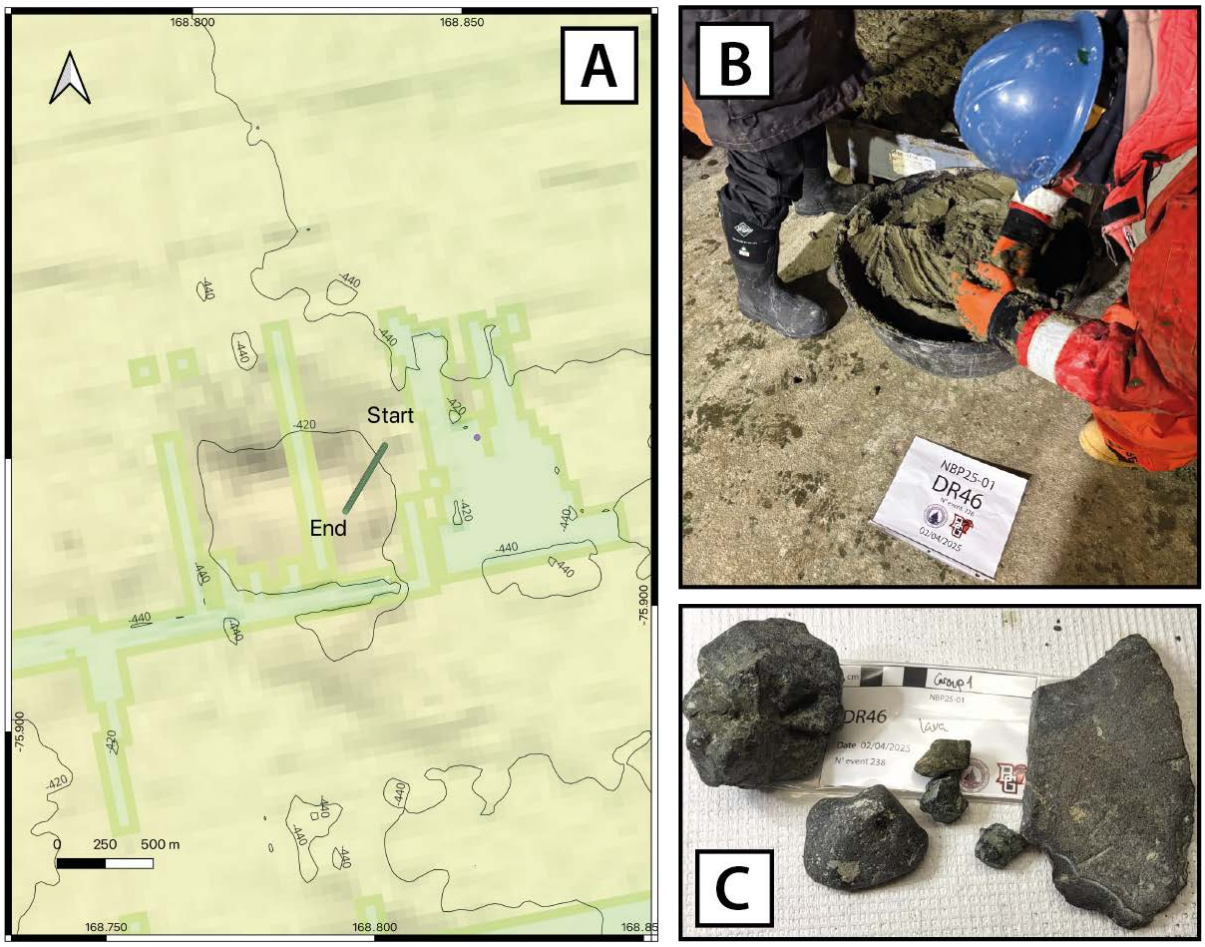

Figure 10.49: a) DR46 trackline on Alpha-Centauri B seamount NNE of Franklin Island. b) dredge being sorted c) lava fragments.

10.9.47 DR47

Dredge DR47 was conducted at Proxima-Centauri B seamount (**Fig. 10.50**) northeast of Franklin island on April 2. The samples recovered consist of breccia and erratics. The breccia is light gray to brown, matrix-supported with clasts that are vesicular to non-vesicular-blocky and centimetric in size. Lithics are identified. One sample of granite is recovered.

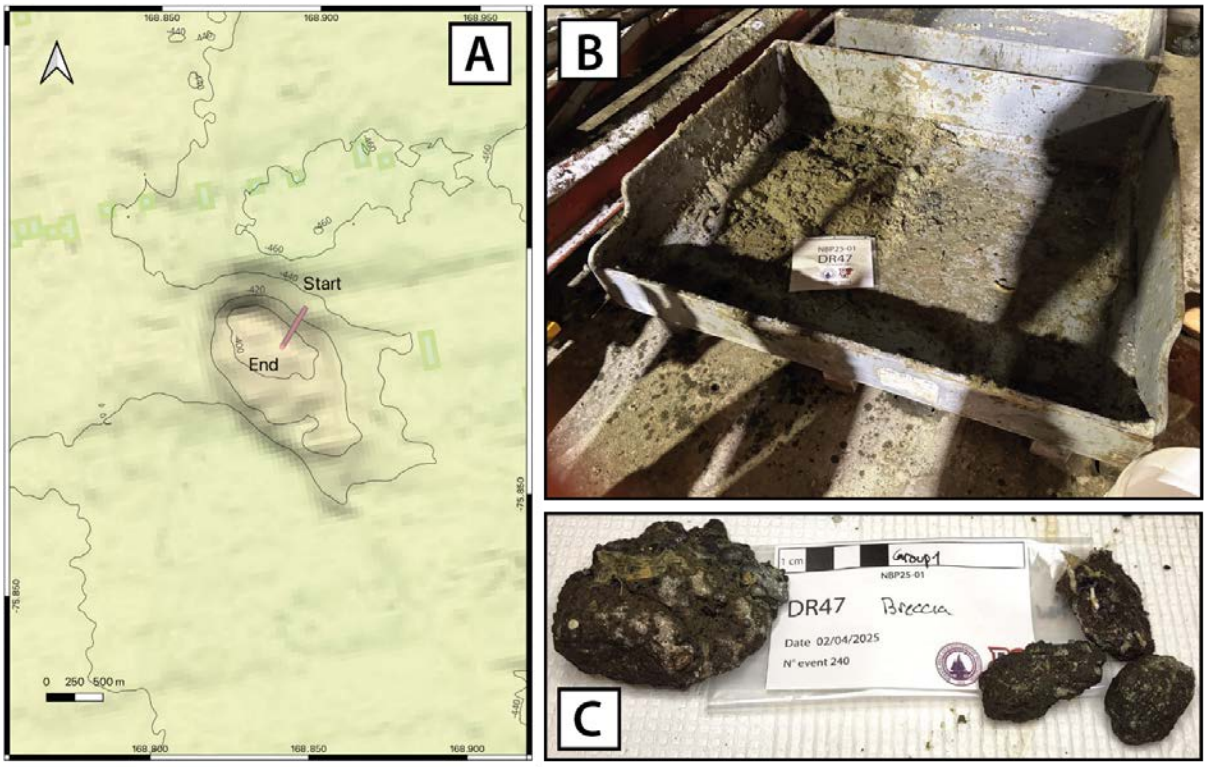

Figure 10.50: a) DR47 trackline on Proxima-Centauri B seamount NNE of Franklin Island. b) dredge on deck c) breccia fragments

10.9.48 DR48

Dredge DR48 was conducted at End-Is-Near seamount (**Fig. 10.51**) northeast of Franklin island on April 2. The samples recovered consist of breccia, agglomerates, and lava. The breccia is gray to brown, matrix-supported with clasts that are vesicular to non-vesicular-blocky and subangular. Glass is identified. Agglomerate is dark gray to black, clast supported, lapilli in size, and has an agglutinated texture. Glass and olivine are identified. Lava is light gray to dark gray, non-vesicular to mildly vesicular with microcrystalline to aphanitic groundmass. Lava fragments are angular to subround.

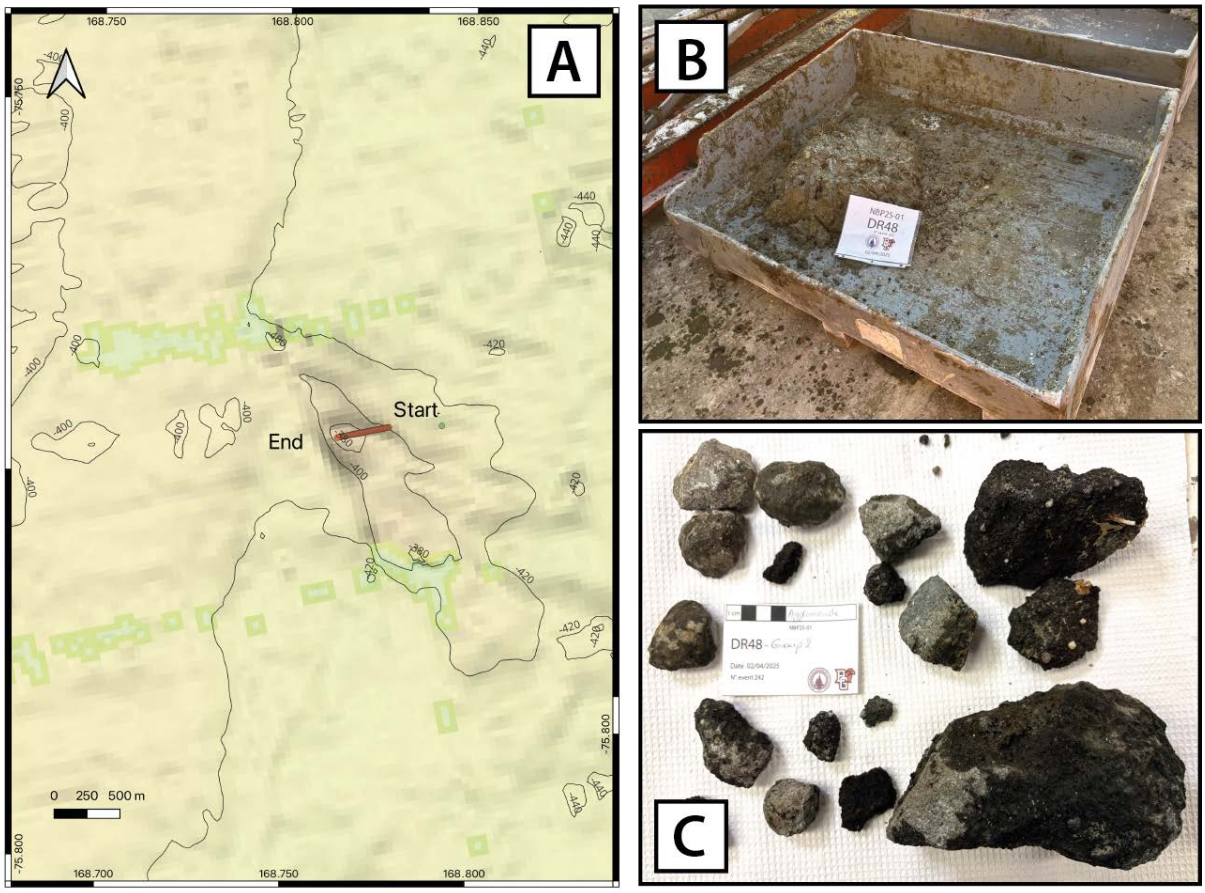

Figure 10.51: a) DR48 trackline on End-Is-Near seamount NNE of Franklin Island. b) dredge on deck. c) agglomerate fragments.

10.9.49 DR49

Dredge DR49 was conducted on the southern edifice of Potter Peak seamount (**Fig. 10.52**) on April 2. The recovered samples consist of breccia, agglomerates, lava, and IRDs. The breccia is brownish yellow, matrix-supported monolithic with clasts that are angular to subround and millimeter to centimeter in size. Agglomerate is brownish gray to black, clast-supported, ash to lapilli size, and blocky to vesicular. Olivine is identified. Lava is light gray to dark gray to reddish, non-vesicular to mildly vesicular with aphanitic to microcrystalline groundmass. Samples are angular to subround. Olivine phenocrysts are identified. Two angular to subround granitoids are recovered.

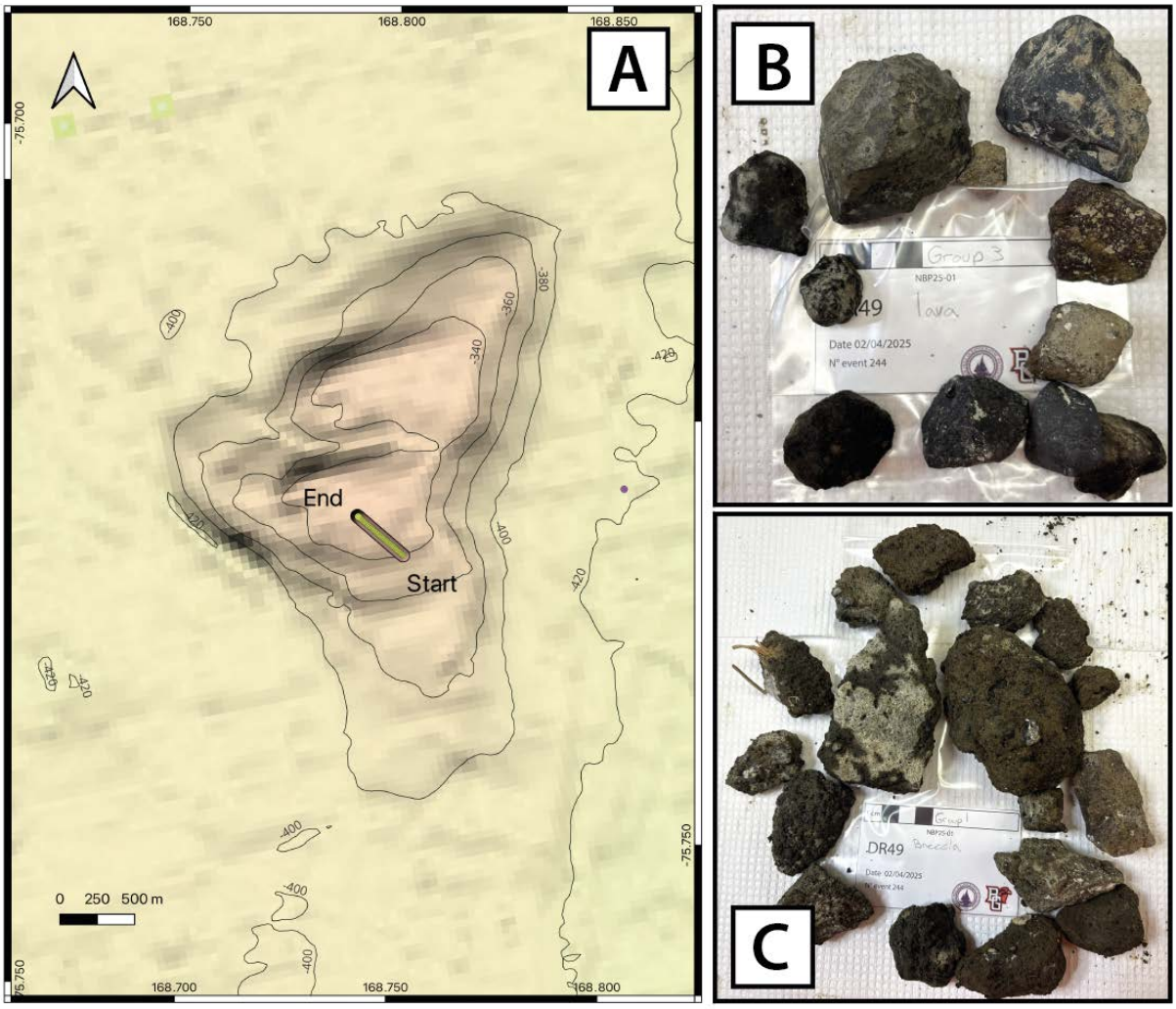

Figure 10.52: a) DR49 trackline on Potter Peak seamount S side of Potter Peak. b) lava fragments. c) breccia fragments.

10.9.50 DR50

Dredge DR50 was conducted on the northern edifice of Potter Peak seamount (**Fig. 10.53**) on April 3. The samples recovered consist of breccia, lava, agglomerates, and IRDs. The breccia is dark brownish green, matrix supported, with clasts that are volcanic and lithics. Clasts are angular to subround and millimeter in size. Lava is dark gray, non-vesicular with one sample being vesicular and possibly a bomb. Agglomerate is black, clast-supported with angular clasts that are non-vesicular- blocky to vesicular and millimetric in size.

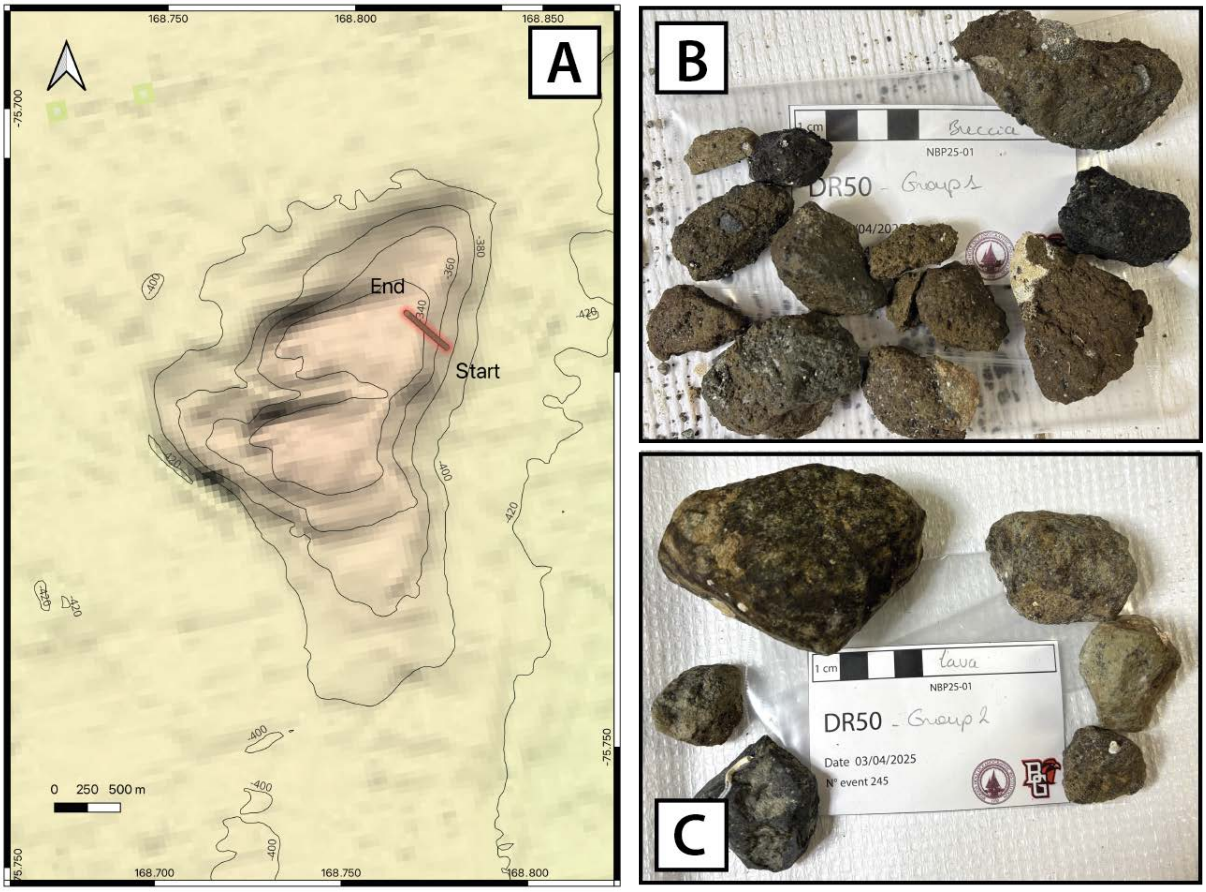

Figure 10.53: a) DR50 trackline on Potter Peak seamount N side of Potter Peak. b) breccia fragments c) lava fragments

10.10 Metadata

FID	NumPrel	Cruise	Date start dredge in water	Time TU start dredge in water	Date end dredge on deck	Time TU end dredge onboard	Total Time h:mm	Lat_start_dredging	Long_start_dredging	Depth_dredge_on	Lat_End_dredging	Long_End_dredging	Depth_dredge_off	Lenght	Site	Weight (kg)
1	NBP25-01-DR01	NBP25-01	22/02/2025	15:50:00	22/02/2025	17:29:00	1:39	-75°48.744	165°49.37	-514	-75°48.664	165°50.27	-462	480	Nomad seamount	400
2	NBP25-01-DR02	NBP25-01	22/02/2025	18:35:00	22/02/2025	20:01:00	1:26	-75°49.566	165°40.63	-572	-75°49.519	165°40.36	-497	410	Squid rifge (lower part)	100
3	NBP25-01-DR03	NBP25-01	22/02/2025	21:10:00	22/02/2025	22:07:00	0:57	-75°49.24	165°40.87	-546	-75°49.175	165°41.59	-375	500	Squi ridge, east flank	200
4	NBP25-01-DR04	NBP25-01	22/02/2025	23:51:00	23/02/2025	01:24:00	1:27	-75°47.109	165°36.284	-634	-75°47.029	165°37.181	-504	400	Flat Top seamount and Feather top (TC_007)	20
5	NBP25-01-DR05	NBP25-01	27/02/2025	16:36:00	27/02/2025	18:58:00	2:22	-75°59.47	166°0.891	-490	-75°59.34	166°0.245	-413	500	Flat Top seamount (TC_003)	200
6	NBP25-01-DR06	NBP25-01	27/02/2025	21:17:00	27/02/2025	23:00:00	1:43	-75°47.61	165°25.959	-792	-75°47.46	165°25.44	-663	500	Mittel kind seamount	300
7	NBP25-01-DR07	NBP25-01	28/02/2025	00:14:00	28/02/2025	01:50:00	1:36	-75°47.097	165°37.737	-645	-75°46.988	165°37.363	-523	300	East flank of feather top	50
8	NBP25-01-DR08	NBP25-01	03/03/2025	06:38:00	03/03/2025	08:03:00	1:25	-76°56.703	167°24.366	-466	-76°56.724	167°25.416	-396	480	Lower part of Beaufort Bank (West flank)	150
9	NBP25-01-DR09	NBP25-01	03/03/2025	08:44:00	03/03/2025	09:42:00	0:58	-76°56.892	167°33.769	-228	-76°56.907	167°34.519	-199	340	Edifice on Beaufort Bank	400
10	NBP25-01-DR10	NBP25-01	03/03/2025	10:28:00	03/03/2025	11:15:00	0:47	-76°57.612	167°40.235	-188	-76°57.625	167°40.925	-140	480	Top of Beaufort Bank	400
11	NBP25-01-DR11	NBP25-01	05/03/2025	09:46:00	05/03/2025	11:45:00	1:59	-76°26.48	168°27.04	-602	-76°26.72	168°28.15	-590	600	N°5 seamount on the coco channel site	80
12	NBP25-01-DR12	NBP25-01	05/03/2025	12:30:00	05/03/2025	14:16:00	1:46	Failed							Mademoiselle flat top seamount on the coco channel site	
13	NBP25-01-DR13	NBP25-01	05/03/2025	14:46:00	05/03/2025	16:30:00	1:44	-76°27.012	168°19.81	-660	-76°27.21	168°20.84	-608	600	Mademoiselle flat top seamount on the coco channel site	100
14	NBP25-01-DR14	NBP25-01	05/03/2025	17:21:00	05/03/2025	19:07:00	1:46	-76°26.003	168°20.33	-659	-76°26.157	168°21.09	-609	600	Coco seamount on the coco channel site	80
15	NBP25-01-DR15	NBP25-01	09/03/2025	03:41:00	09/03/2025	04:29:00	0:48	-76°12.425	166°26.665	-278	-76°12.551	166°26.360	-243	300	Upper part of the East flank of Davey Bank	150
16	NBP25-01-DR16	NBP25-01	09/03/2025	05:36:00	09/03/2025	06:49:00	1:13	-76°12.204	166°27.661	-372	-76°12.434	166°27.284	-343	500	Lower part of the East flank of Davey Bank	30
17	NBP25-01-DR17	NBP25-01	09/03/2025	08:25:00	09/03/2025	09:56:00	1:31	-76°12.172	166°11.476	-357	-76°12.430	166°11.533	-319	500	Lava flow (?) West flank of Davey Bank	30
18	NBP25-01-DR18	NBP25-01	11/03/2025	09:12:00	11/03/2025	10:50:00	1:38	-75°42.449	165°48.162	-667	-75°42.691	165°48.618	-554	500	Flat top seamount north to Flapjack field	100
19	NBP25-01-DR19	NBP25-01	18/03/2025	12:57:00	18/03/2025	14:23:00	1:26	-76°4.112	166°30.08	-440	-76°3.967	166°29.439	-408	500	Flat top North of Davey Bank	200
20	NBP25-01-DR20	NBP25-01	18/03/2025	16:06:00	18/03/2025	17:33:00	1:27	-76°3.486	166°44.55	-577	-76°3.389'	166°44.051	-555	320	Attenuetor Seamount	150
21	NBP25-01-DR21	NBP25-01	18/03/2025	22:56:00	19/03/2025	00:01:00	1:05	-75°58.882	168°14.632	-321	-75°58.762	168°14.390	-272	270	Seamount North Franklin Island	100
22	NBP25-01-DR22	NBP25-01	19/03/2025	00:54:00	19/03/2025	01:45:00	0:51	-76°0.237	168°16.98	-321	-76°0.034	168°16.56	-294	600	Seamount North Franklin Island	300
23	NBP25-01-DR23	NBP25-01	19/03/2025	04:16:00	19/03/2025	05:19:00	1:03	-75°59.413	168°41.437	-382	-75°59.40	168°40.59	-328	380	Fault North Franklin Island	250
24	NBP25-01-DR24	NBP25-01	20/03/2025	00:39:00	20/03/2025	02:08:00	1:29	-76°1.7	166°24.22	-514	-76°1.988	166°23.76	-470	500	North Davey Bank	250

25	NBP25-01-DR25	NBP25-01	20/03/2025	12:51	20/03/2025	13:27:00	0:36	-76°9.382'	166°23.304	-126	-76°9.366'	166°23.675	-127	170	Mont Petit, Davey Bank	150
26	NBP25-01-DR26	NBP25-01	20/03/2025	15:57:00	20/03/2025	16:46:00	0:49	-76°15.867	166°23.706	-186	-76°15.819	166°24.268	-147	255	South Davey Bank	300
27	NBP25-01-DR27	NBP25-01	20/03/2025	18:16:00	20/03/2025	19:23:00	1:07	-76°17.17	166°22.30	-387	-76°17.094	166°23.057	-347	350	South Davey Bank	200
28	NBP25-01-DR28	NBP25-01	21/03/2025	03:00:00	21/03/2025	04:31:00	1:31	-76°20.5	166°53.81	-650	-76°20.472	166°54.561	-631	475	Conquest seamount, East of Davey Bank	250
29	NBP25-01-DR29	NBP25-01	21/03/2025	06:30:00	21/03/2025	07:42:00	1:12	-76°27.9	166°43.33	-409	-76°28.018	166°43.950	-347	350	Aurora Bank, top	200
30	NBP25-01-DR30	NBP25-01	21/03/2025	09:07:00	21/03/2025	10:43:00	1:36	-76°25.72	166°42.42	-556	-76°25.951	166°43.124	-544	450	Aurora Bank, base	100
31	NBP25-01-DR31	NBP25-01	21/03/2025	18:19:00	21/03/2025	19:53:00	1:34	-75°50.784	166°39.244	-514	-75°50.598	166°39.040	-470	380	Vagadond seamount	350
32	NBP25-01-DR32	NBP25-01	27/03/2025	20:16:00	27/03/2025	21:11:00	0:55	-76°16.319	168°20.238	-193	-76°16.449	168°20.234	-149	275	Seamount South of Franklin Island	100
33	NBP25-01-DR33	NBP25-01	28/03/2025	02:22:00	28/03/2025	03:25:00	1:03	-76°5.77	169°13.165	-413	-76°5.939	169°13.066	-344	375	Seamount East of Franklin Island	150
34	NBP25-01-DR34	NBP25-01	29/03/2025	08:34:00	29/03/2025	10:10:00	1:36	-75°46.86	165°37.11	-600	-75°47.04	165°37.199	-500	350	West flank of Feather top	300
35	NBP25-01-DR35	NBP25-01	29/03/2025	20:24:00	29/03/2025	21:38:00	1:14	-75°52.14	165°39.1567	-443	-75°52.393	165°38.81	-432	400	Pfannkuchen flat top seamount	5
36	NBP25-01-DR36	NBP25-01	29/03/2025	23:02:00	29/03/2025	00:27:00	1:25	-75°52.693	165°41.737	-528	-75°52.93	165°41.46	-476	500	Baby pfannkuchen flat top seamount	10
37	NBP25-01-DR37	NBP25-01	30/03/2025	01:36:00	30/03/2025	03:20:00	1:44	-75°52.255	165°42.595	-526	-75°52.5161	165°41.725'	-526	600	In between	50
38	NBP25-01-DR38	NBP25-01	30/03/2025	21:33:00	30/03/2025	22:56:00	1:23	75°49.577	166°39.3640	-500	-75°49.679	66°39.042	?	?	Vagadond seamount	10
39	NBP25-01-DR39	NBP25-01	31/03/2025	10:41:00	31/03/2025	11:44:00	1:03	-76°3.485	168°42.9633	-377	-76°3.4875	68°41.858	-320	500	Merope Seamount	50
40	NBP25-01-DR40	NBP25-01	31/03/2025	21:01:00	31/03/2025	21:52:00	0:51	-76°0.245	168°25.564	-208	-76°0.13	168°24.73	-175	390	Electra seamount	200
41	NBP25-01-DR41	NBP25-01	01/04/2025	00:18:00	01/04/2025	01:16:00	0:58	75°59.745	168°34.2665	-311	-75°59.60	168°33.57	-255	370	Celaire seamount	80
42	NBP25-01-DR42	NBP25-01	01/04/2025	03:39:00	01/04/2025	04:58:00	1:19	-76°0.8647	168°34.4931	-313	-76°0.8647	68°34.493'	-250	360	Alcyone seamount	100
43	NBP25-01-DR43	NBP25-01	01/04/2025	20:19:00	01/04/2025	21:23:00	1:04	-75°58.976	168°40.054	-281	-75°58.8756	68°39.224	-255	420	Taygeta seamount	150
44	NBP25-01-DR44	NBP25-01	02/04/2025	01:43:00	02/04/2025	03:04:00	1:21	75°57.771	168°44.083	-387	-75°57.575	68°43.457	368	460	Asterope seamount	5
45	NBP25-01-DR45	NBP25-01	02/04/2025	08:38:00	02/04/2025	09:46:00	1:08	-75°54.81	168°49.2	-426	-75°54.86	168°48.2	405	440	Alpha-Centaury A	30
46	NBP25-01-DR46	NBP25-01	02/04/2025	11:31:00	02/04/2025	12:49:00	1:18	75°53.365	168°49.3198	-420	-75°53.5648	68°48.559	395	510	Alpha-Centaury B	80
47	NBP25-01-DR47	NBP25-01	02/04/2025	15:46:00	02/04/2025	17:01:00	1:15	75°49.939	168°52.7099	-428	-75°50.1172	68°52.087	-383	470	Proxima-Centaury	20
48	NBP25-01-DR48	NBP25-01	02/04/2025	19:27:00	02/04/2025	20:32:00	1:05	-75°46.60	168°48.36	-402	-75°46.6048	68°47.378	-369	455	End is Near Seamount	80
49	NBP25-01-DR49	NBP25-01	02/04/2025	22:22:00	02/04/2025	23:27:00	1:05	75°43.796	168°46.5227	-336	-75°43.6195	68°45.943	-316	420	Potter Peak, south	80
50	NBP25-01-DR50	NBP25-01	03/04/2025	00:48:00	03/04/2025	01:53:00	1:12	75°43.235	168°48.5371	-375	-75°43.0693	68°48.097	-328	380	Potter Peak, nroth	40

10.11 Inventory

NBP25-01-G82-N

Rock samples for hand carry to BGSU by Kurt Panter (PI), Jacquelyn Kalemba, Katherine Shanks, Ann Beck

DR#	Sample groups (“special”)	Final Sample Selection	T.S. billet	chem chip	Location	Wt (lbs)
01	G1,SS,G3	G1,G3, seps for G1	Yes	No	Pfannkuchen (flapjack)	0.5
03	G1-3,G5, seps & cut bomb	G1-3,G5, seps	No	No	Squid Ridge (flapjack)	1.5
04	G1, seps	G1, seps	No	No	Feather Top (flapjack)	0.5
05	G1+ash, seps, SS,G2	G1,G2	No	No	Hotto Keki (flapjack)	1
06	G1a,b,c, G2, amph seps	G1a,G1c,G2	Yes	Yes	Mittel Kind (flapjack)	1
11	G1,G2,G3,G5	G1	Yes	Yes	No5 (channel)	1
13	G1,SS,G2,G3, seps	G2,G5, seps	Yes	Yes	Mademoiselle (channel)	0.5
14	G1,G2,G5,G7,olivine	G2	No	No	CoCo (channel)	<0.5
15	G1-4	G4	Yes	Yes	Davey Bank (east flank)	<0.5
16	G2	G2	Yes	Yes	Davey Bank (east flank)	<0.5
17	G1,G2.G3	G3	Yes	Yes	Davey Bank (west flank)	<0.5
18	G1a SS, G4,G3, spes	seps	Yes	Yes	Galette (flapjack)	0.5

19	G1,G3 _SS, G5, seps	G1,G3, SS and spes	Yes	Yes	Biscuit (Davey Bank flat-top)	1
20	G1, G4, seps	G1, G4, seps	Yes	Yes	Attenuator	0.5
24	G1,G3,G4 +SS	G3,G4	Yes	Yes	Davey Bank (north)	0.5
25	G1, G2,G4	G2,G4	Yes	Yes	Mt. Petit (Davey Bank)	1
26	G1,G2	G1,G2	Yes	Yes	Davey Bank (SW middle)	0.5
27	G1,G2,G3,G4	G2-4	Yes	Yes	Davey Bank (NE tip)	2.5
30	G2-4	G4	Yes	Yes	Aurora Bank (NE tip)	1.5
34	-	G#,G4	No	No	Feather Top	1
35	-	9 samples unlabeled	No	No	Pfannkuchen	1
36	-	G1,G2,G3	No	No	Baby Pfannkuchen	<0.5
Smear powders & glass slides			-	-	-	<0.5
SmithMac #8		1.5 samples	No	No	Smith-Mac summit	<0.5

11. Coring

Carole Berthod, Masako Tominaga, Kurt Panter, Jonas Preine, Jyun-Nai Wu

11.1 Overview

The aim of the coring was to sample part of the series of volcaniclastic deposits at the foot of the active Erebus volcano, in order to date and identify the nature of these deposits, and to produce a timeline of the recent volcanic explosive activity of Mt. Erebus.

With this objective in mind, we carried out a Chirp acoustic survey in the Lewis Bay, north of the Mt. Erebus (**Fig. 11.1**) to locate zones characterized by significant sediment accumulation (**Fig. 11.2**). Two zones, with 6 – 10m of sediments, have been selected to performed 2.5 m gravity cores.

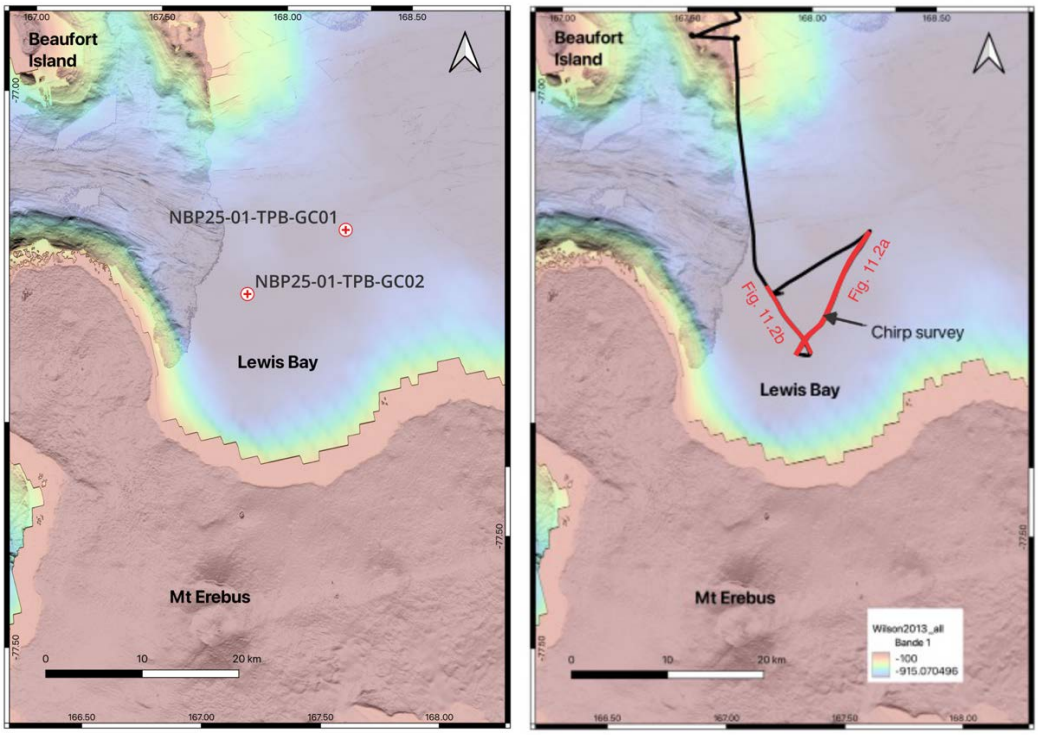

Figure 11.1: Morphological map of Lewis Bay. Left panel shows locations of the two coring sites north of Mt. Erebus. Right panel shows location of the Chirp Echosounder profiles used to identify two areas with a significant sediment unit (**Fig. 11.2**).

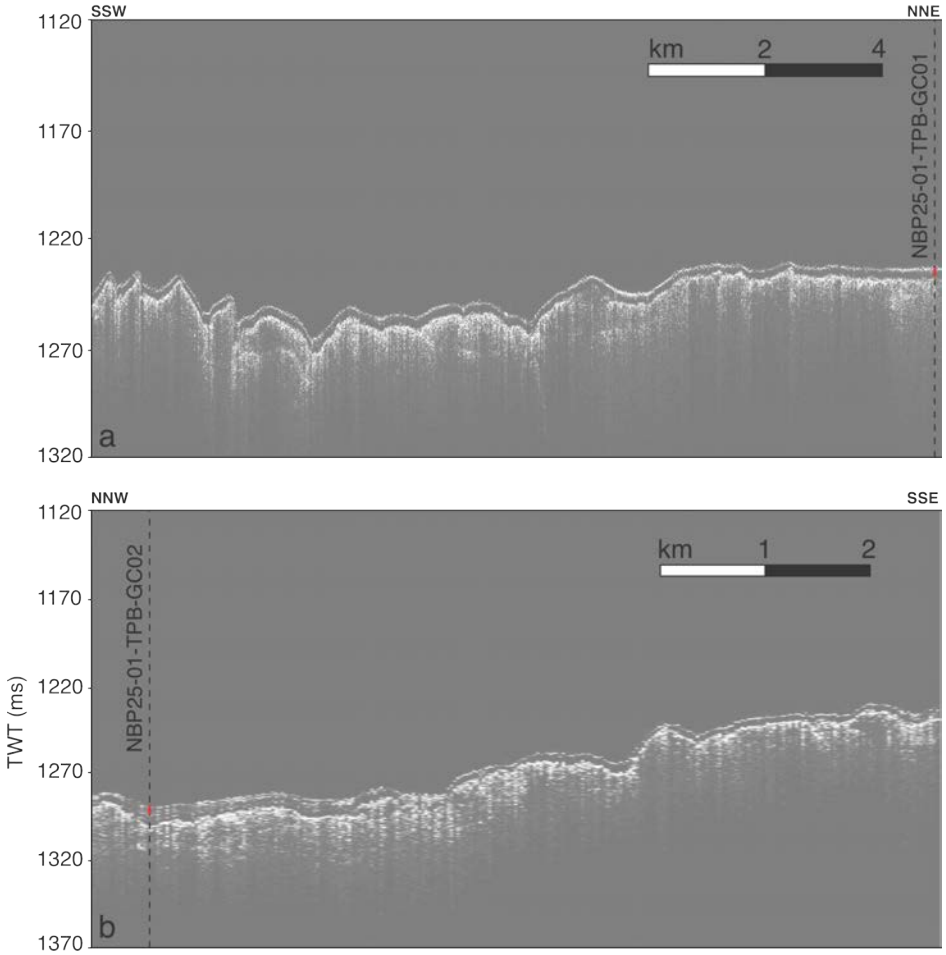

Figure 11.2: Chirp profiles crossing the two coring locations. For locations, see **Figure 11.1**. TWT: Two-way-travel time.

11.2 Gravity coring

Gravity corers are tools used for taking samples of sediment located on the seafloor. The gravity corer comprises a weight of up to 2500 pounds fitted to an assembly of steel tubes which is tipped with a cutter bit to ensure penetration into the sediment. The corer was deployed on the starboard side. The gravity corer is lowered to approximately 30 meters above the seafloor. Once clearance is confirmed with the bridge, it is released and descends at a controlled speed of 30 meters per minute, penetrating the sediment under its own weight. Recovery begins at a slower pace—10 meters per minute—until the corer is completely free from the seafloor. It is then hoisted back on deck at a standard retrieval speed of 30 meters per minute.

The coring operations, realized on the March 2nd, recovered two cores (**Tab. 11.1**), 111 cm (NBP25-01-TPB-GC01) and 135 cm long (NBP25-01-TPB-GC02). Two bags containing the core catcher have been archived.

Table 11.1: Summary table of core samples collected during the NBP25-01 cruise.

Cruise Name	Date Collected	Time collected	Latitude	Longitude	Water Depth	Tube lenght (cm)	Core lenght (cm)	recovery rate (%)	Recovery Method
NBP25-01	2/3/25	*14:12*	*-77.1932*	*168.046°*	*885*	*250*	*111*	*44.4*	*Gravity core*
NBP25-01	2/3/25	*17:32*	*-77.2312°*	*167.5917°*	*928*	*250*	135	*54*	*Gravity core*

11.3 Curation

The two collected cores remained unopened to enable physical property measurements to be conducted on intact, continuous sections.

12. Smith Mac Grabber

Carole Berthod, Kurt Panter, Katherine Shanks, Jacquelyn Kalemba,

12.1 Overview

To target the biology imaged on the Feather Top seamount and following the loss of an epibenthic SLED device, the decision was made to use the Smith-Mac grab sampler to collect biology and discrete sediment samples from the seafloor. These grab samplers are known for their durability, reliability, and operational simplicity.

12.1 Operations

The impact of the Smith-Mac's foot plates on the seafloor triggers the release of heavy-duty springs that rapidly force the bucket jaws to clamp shut into the bottom sediment (**Fig. 12.1**). This forceful, quick action ensures penetration even in stiff sediment. On retrieval, the lifting force of the wire closes the jaws and holds them tightly shut until the sampler is recovered to the deck.

The Smith Mac was deployed at 20 meters per minute up to 30 meters above the seafloor. After checking with the bridge, the Smith Mac is released and descends at a controlled speed of 15 meters per minute. Extraction from the seafloor is carried out slowly at a rate of 5 m/min, followed by a faster recovery phase at 20 m/min

Figure 12.1: Left: recovery of the Smith Mac grabber. Right: recovery of the sample on the back deck.

12.1 Collected rocks

During the NBP25-01 cruise, 8 Smith-Mac were performed (**Tab. 12.1**).

Table 12.1: Smith-Mac locations

Event #	method	date	GMT	Lat	Long	Depth (m)
198	Smith-Mac	March 29, 2025	01:48	-75° 47.05	165° 37.21	530
198	Smith-Mac	March 29, 2025	03:50	-75° 47.01	165° 37.51	610
198	Smith-Mac	March 29, 2025	05:30	-75° 47.08	165° 38.28	680
206	Smith-Mac	March 30, 2025	07:25	-75° 53.07	165° 39.54	530
212	Smith-Mac	March 30, 2025	19:42	-75° 49.9312	166° 38.5867	468
219	Smith-Mac	March 30, 2025	19:45	-76° 0.23421	168° 24.6606	180
227	Smith-Mac	April 1, 2025	10:15	-76° 0.05870	168° 0.7039	300
248	Smith-Mac	April 3, 2025	10:06	-76° 39.25	169° 3.80	400

Smith-Mac sampling was mainly carried out for the team of biologists. However, during these operations, a number of rocks were collected. The descriptions are given below:

- **Smith-Mac on Baby Pfannkuchen, March 29, Event #198**

Brownish-gray to red breccia with lava clasts
Breccia is matrix supported
Clasts are angular to subangular
Clasts are mostly millimetric with several larger clasts (centrimetric)
Clasts are glassy and non-vesicular
Some fragments show layering mostly emphasized by color (i.e. rusty bands) but also by subtle grain size differences
IRDs – 3 samples, one is a granitoid + 1 feldspar crystal

- **Smith-Mac on Vagabond seamount, March 30, Event #212**

Sand to pebble sized volcanic material (round)
Minerals separates from fine-grained fraction = 2 olivine, 2 pyroxene, 5 feldspar grains.

- **Smith-Mac on Smith-Mac seamount, April 3, Event #248**

  1 cm fragment collected + millimetric clasts
  Matrix supported with dark subangular clasts
  Clasts are volcanic and seem blocky

13. References

1. An, M., Wiens, D. A., Zhao, Y., Feng, M., Nyblade, A., Kanao, M., Li, Yuansheng, Al. Magi, and J.-J. Lévêque (2015). Temperature, lithosphere-asthenosphere boundary, and heat flux beneath the Antarctic Plate inferred from seismic velocities. Journal of Geophysical Research: Solid Earth, 120(12), 8720–8742. doi:10.1002/2015JB011917
2. Anderson, J. B., Conway, H., Bart, P. J., Witus, A. E., Greenwood, S. L., McKay, R. M., Hall, B. L., R. P. Ackert, K. Licht, M. Jacokbsson, and J. O. Stone (2014). Ross Sea paleo-ice sheet drainage and deglacial history during and since the LGM. Reconstruction of Antarctic Ice Sheet Deglaciation (RAISED), 100, 31–54. doi:10.1016/j.quascirev.2013.08.020
3. ANTOSTRAT Project, 1995; Seismic stratigraphic atlas of the Ross Sea, Antarctica, in Geology and Seismic Stratigraphy of the Antarctic Margin, Antarct. Res. Ser., vol. 68, edited by A. K. Cooper, P. F. Barker, and G. Brancolini, 22 plates, AGU, Washington D. C.
4. Berg, J. H., Moscati, R. J., and Herz, D. L. (1989). A petrologic geotherm from a continental rift in Antarctica. Earth and Planetary Science Letters, 93(1), 98–108. doi:10.1016/0012-821X(89)90187-8.
5. Blackman, D.K., Von Herzen, R.P. and Lawver, L.A., 1987. Heat flow and tectonics in the western Ross Sea, Antarctica.
6. Busetti, M., Geletti, R., Civile, D., Sauli, C., Brancatelli, G., Forlin, E., Accettella, D., Savonuzzi, L.B., De Santis, L., Vesnaver, A. and Cova, A. (2024). Geophysical evidence of a large occurrence of mud volcanoes associated with gas plumbing system in the Ross Sea (Antarctica). Geoscience Frontiers, 15(1), p.101727.
7. Davis, E. E. and H. Elderfield (2005), Hydrogeology of the Oceanic Lithosphere, Cambridge University Press.,726 pages.
8. Della Vedova, B., Pellis, G., and Lawver, L.A. (1992), Heat flow and active tectonics of the western Ross Sea, in Yoshida, Y., Kaminuma, K., and Shiraishi, K., eds., Proceedings of the 6th ISSUES: Saitama, Japan, p. 627–637.
9. Fisher, A. T., Becker, K. (1991). Heat flow, hydrothermal circulation and basalt intrusions in the Guaymas Basin, Gulf of California. Earth and Planetary Science Letters, 103(1), 84–99. doi:10.1016/0012-821X(91)90152-8.
10. German, C., Yoerger, D. R., Jakuba, M., Shank, T., Langmuir, C. H., & Nakamura, K. ichi. (2008). Hydrothermal exploration with the Autonomous Benthic Explorer. *Deep-Sea Research Part I: Oceanographic Research Papers*, *55*(2), 203–219. https://doi.org/10.1016/j.dsr.2007.11.004
11. Giustiniani, M.; Tinivella, U.; Sauli, C.; Della Vedova, B. 2017, Distribution of the gas hydrate stability in the Ross Sea, Antarctica. Andean Geology 45 (1): 78-86. doi:http://dx.doi.org/10.5027/andgeoV45n1-2989.
12. Goldsby, D. L., Kohlstedt, D. L. (2001). Superplastic deformation of ice: Experimental observations. Journal of Geophysical Research: Solid Earth, 106(B6), 11017–11030. doi:10.1029/2000JB900336.
13. Gradstein, F. M., Ogg, J. G., Schmitz, M. D., Ogg, G. M. (Eds.). (2020). Chapter 14 - Geomathematics. In Geologic Time Scale 2020 (pp. 401–439). Elsevier. doi:10.1016/B978-0-12-824360-2.00014-0.
14. Greenwood, S. L., Simkins, L. M., Halberstadt, A. R. W., Prothro, L. O., Anderson, J. B. (2018). Holocene reconfiguration and readvance of the East Antarctic Ice Sheet. Nature Communications, 9(1), 3176. doi:10.1038/s41467-018-05625-3.

15. Gueriot, D., Chedru, J., Daniel, S., & Maillard, E. (2000). The patch test: a comprehensive calibration tool for multibeam echosounders. In *OCEANS 2000 MTS/IEEE Conference and Exhibition. Conference Proceedings (Cat. No. 00CH37158)* (Vol. 3, pp. 1655-1661). IEEE.
16. Halberstadt, A. R. W., 2016, Paleo-Ice Stream Behavior: Retreat Scenarios and Changing Controls in the Ross Sea, Antarctica. MS Thesis, Rice University. https://hdl.handle.net/1911/96244.
17. Hall, J. M., 2006, Structural evolution of the Terror Rift, western Ross Sea, Antarctica: Interpretation from 2D reflection seismic, Master's thesis, The Ohio State Univ., Columbus, Ohio.
18. Hall, J., T. Wilson, and S. Henrys, 2007, U.S. Geological Survey and The National Academies; USGS OFR-2007-1047, Short Research Paper 108; doi:10.3133/of2007-1047.srp108.
19. Hartmann, A. and H. W. Villinger (2002). "Inversion of marine heat flow measurements by expansion of the temperature decay function." Geophysical Journal International 148(3): 628–636.
20. Hyndman, R. D., et al. (1979). "The measurement of marine geothermal heat flow by a multipenetration probe with digital acoustic telemetry and insitu thermal conductivity." Marine Geophysical Research 4(2): 181–205.
21. Lawver, L.A., Davis, M.B., and Wilson, T.J., and shipboard scientific party, 2007, Neotectonic and other features of the Victoria Land Basin, Antarctica, interpreted from multibeam bathymetry data, in Cooper, C.K., Raymond, C.R., and ISAES Editorial Team eds., Antarctica: A Keystone in a Changing World—Online Proceedings of the 10th International Symposium on Antarctic Earth Sciences: U.S. Geol. Survey Open-File Report 2007-1047, Extended Abstract 017.
22. Lawver, L., Lee, J., Kim, Y., Davey, F. (2012). Flat-topped mounds in western Ross Sea: Carbonate mounds or subglacial volcanic features? Geosphere, 8(3), 645–653. doi:10.1130/GES00766.1.
23. Lee, J. I., McKay, R. M., Golledge, N. R., Yoon, H. I., Yoo, K.-C., Kim, H. J., Hong, J. K. (2017). Widespread persistence of expanded East Antarctic glaciers in the southwest Ross Sea during the last deglaciation. Geology, 45(5), 403–406. doi:10.1130/G38715.1
24. Lee, M. J., Lee, J. I., Kim, T. H., Lee, J., Nagao, K. (2015). Age, geochemistry and Sr-Nd-Pb isotopic compositions of alkali volcanic rocks from Mt. Melbourne and the western Ross Sea, Antarctica. Geosciences Journal, 19(4), 681–695. doi:10.1007/s12303-015-0061-y.
25. Lister, C.R.B., 1979. The pulse-probe method of conductivity measurement. *Geophysical Journal International*, *57*(2), pp.451-461.
26. MacGregor, J. A., Fahnestock, M. A., Catania, G. A., Aschwanden, A., Clow, G. D., Colgan, W. T., Gogineni, S. P., M. Morlighem, S. M. J. Nowiicki, J. D. Paden, S. F. Price, and H. Seroussi. (2016). A synthesis of the basal thermal state of the Greenland Ice Sheet. Journal of Geophysical Research: Earth Surface, 121(7), 1328–1350. doi:10.1002/2015JF003803.
27. Magee, W. R. and T. J. Wilson, 2010, Neogene fault and feeder dike patterns in the Western Ross Sea, American Geophys. Union, Fall Meeting, abstract #T21D-2203.
28. Magee, W. R., 2012, Magnitude of extension across the Central terror Rift, Antarctica: Structural interpretations and balanced cross sections, Master's thesis, Ohio State Univ., Columbus, Ohio.
29. Martos, Y. M., Catalán, M., Jordan, T. A., Golynsky, A., Golynsky, D., Eagles, G., Vaughan, D. G. (2017). Heat Flux Distribution of Antarctica Unveiled. Geophysical Research Letters, 44(22), 11,417-11,426. doi:10.1002/2017GL075609.

30. McKay, R., Golledge, N. R., Maas, S., Naish, T., Levy, R., Dunbar, G., Kuhn, G. (2016). Antarctic marine ice-sheet retreat in the Ross Sea during the early Holocene. Geology, 44(1), 7–10. doi:10.1130/G37315.1.
31. Morin, R. H., Williams, T., Henrys, S. A., Magens, D., Niessen, F., Hansaraj, D. (2010). Heat Flow and Hydrologic Characteristics at the AND-1B borehole, ANDRILL McMurdo Ice Shelf Project, Antarctica. Geosphere, 6(4), 370–378. doi:10.1130/GES00512.1.
32. Naish, T. R., R. D. Powell, R. H. Levy, and ANDRILL-MIS Science Team, 2007, Background to the ANDRILL McMurdo ice shelf project (Antarctica) and initial science volume, Terra Antarctica, 14, 121-130.
33. Naish, T., Powell, R., Levy, R., Wilson, G., Scherer, R., Talarico, F., Krissek, L., F. Niessen, M. Pompillo, T. Wilson, L. Carter, R. DeConto, P. Huybers, R. McKay, D. Pollard, J. Ross, D. Winter, P. Barrett, G. Browne, R. Cody, E. Cowen, J. Crampton, G. Dunbar, N. Dunbar, F. Florindo, C. Gebhardt, I. Graham, M. Hannah, D. Hansaraj, D. Harwood, D. Helling, S. Henrys, L. Hinnov, G. Kuhn, P. Kyle, A. Läufer, P. Maffioli, D. Magens, K. Mandernack, W. McIntosh, C. Miian, R. Morin, C. Ohneiser, T. Paulsen, D. Persico, I Raine, J. Reed, C. Riesselman, L. Sagnotti, D Schmitt, C Sjunneskog, P. Strong, M. Taviani, S. Vogel, T. Wilch, and T. Williams (2009). Obliquity-paced Pliocene West Antarctic ice sheet oscillations. Nature, 458(7236), 322–328. doi:10.1038/nature07867
34. Rilling, S., Mukasa, S., Wilson, T., Lawver, L., Hall, C. (2009). New determinations of 40Ar/39Ar isotopic ages and flow volumes for Cenozoic volcanism in the Terror Rift, Ross Sea, Antarctica. Journal of Geophysical Research: Solid Earth, 114(B12). doi:10.1029/2009JB006303.
35. Ryan, W. B. F., Carbotte, S. M., Coplan, J. O., O'Hara, S., Melkonian, A., Arko, R., R.A. Weissel, V. Ferrini, A. Goodwillie, F. Nitsche, J. Bonczkowski, and R. Zemsky (2009). Global Multi-Resolution Topography synthesis. Geochemistry, Geophysics, Geosystems, 10(3). doi:10.1029/2008GC002332.
36. Salvini, F., Brancolini, G., Busetti, M., Storti, F., Mazzarini, F., Coren, F. (1997). Cenozoic geodynamics of the Ross Sea region, Antarctica: Crustal extension, intraplate strike-slip faulting, and tectonic inheritance. Journal of Geophysical Research: Solid Earth, 102(B11), 24669–24696. doi:10.1029/97JB01643.
37. Schäfer, M., Gillet-Chaulet, F., Gladstone, R., Pettersson, R., A. Pohjola, V., Strozzi, T., Zwinger, T. (2014). Assessment of heat sources on the control of fast flow of Vestfonna ice cap, Svalbard. The Cryosphere, 8(5), 1951–1973. doi:10.5194/tc-8-1951-2014.
38. Schröder, H., Paulsen, T., Wonik, T. (2011). Thermal properties of the AND-2A borehole in the southern Victoria Land Basin, McMurdo Sound, Antarctica. Geosphere, 7(6), 1324–1330. doi:10.1130/GES00690.1.
39. Smellie, J. L., Martin, A. P. (2021). Chapter 5.2a Erebus Volcanic Province: volcanology. Geological Society, London, Memoirs, 55(1), 415. doi:10.1144/M55-2018-62.
40. Smellie, J. L., Rocchi, S. (2021). Chapter 5.1a Northern Victoria Land: volcanology. Geological Society, London, Memoirs, 55(1), 347. doi:10.1144/M55-2018-60.
41. Teske, A., de Beer, D., McKay, L. J., Tivey, M. K., Biddle, J. F., Hoer, D., K. G. Lloyd, M. A. Lever, H. Roy, D. B. Albert, H. P. Mendlovitz, and B. J. MacGregor (2016). The Guaymas Basin Hiking Guide to Hydrothermal Mounds, Chimneys, and Microbial Mats: Complex Seafloor Expressions of Subsurface Hydrothermal Circulation. Frontiers in Microbiology, 7. Retrieved from https://www.frontiersin.org/article/10.3389/fmicb.2016.00075.
42. Tivey, M. K. (2007). Generation of seafloor hydrothermal vent fluids and associated mineral deposits. *Oceanography*, *20* (SPL.ISS. 1), 50–65. https://doi.org/10.5670/oceanog.2007.80

43. Wilson, T. J., L. A. Lawver, S. A. Henrys, S. Mukasa, H. Horgan, M. Weiderspahn, M. Davis, J. Whittaker, A. Lowe, and M Watson, 2004, Cruise Report NBP040119 January to 18 February 2004-McMurdo Station to McMurdo Station, Ross Sea, Antarctica, sci. Rep. 2004/03, 79 pages., Inst. Geol. Nucl. Sci., Lower Hutt, New Zealand.